Programme co-funded by the EUROPEAN UNION

Clean ports - open doors

Final Report
ICME
Contract TR09.C1.01-02/298

Covering the reporting period from
01/12/2014 to 15/06/2015
Reporting Date
25/06/2015

Project coordinator: Prof.Dr.Kadir SEYHAN
Project website:www.icme-blacksea.eu

Prepared by DATAKENT Bilgisayar Yazılım Eğitim ve Satış Hizmetleri Ltd.Şti.

Trabzon 2015

Table of Contents

List of Figures

List of Tables

List of Pictures

1. General information about project

Black Seacross-borderproject, ICME, analysis the effects of sediment brought by Değirmendere on the port of Trabzonand its surroundings. Different scenarios and their effects will be investigated by using mathematical hydrodynamic model. Then, possible measures to be takenwill reveal. In order to establish correct model stated the monthly oceanographic measurement will be done at Değirmendere and harbors.This sampling will be carried out in astated time duration and the mathematical hydrodynamic models (mathematical models of spread of the pollutants, myocean result downscaling and sediment transport) and management scenarios for the Trabzon Port and Değirmendere area will be developed.

2. Trabzon Port

2.1. Location of Trabzon Port

Trabzon Port is located North between 40 57' 30"latitude, east of40 02' 30" north and longitude 41 06'36"latitude, east of 3925'00’ longitude. In other words, the lines drawn on the north direction from the light in the eastern Cape and the Western Cape are Narlık within the marine and coastal area bounded by adjacent Turkish territorial waters.

2.2. History of Trabzon port

Trabzon Port made by Pontus located in theBC117-119years, moved tothe area in which the current port is located. Harbor created by carving the rocks, the Ottoman Empire, it was began to be made by the commander Hasan Pasha, completed by Governor Mazha Pasha and taken into service in1903,Trabzon Port was one of the five major ports of the Ottoman Empire that date.

Picture 1. Historic view of Trabzon Port

The new port was started be built in 1946, completed in1954. In 80's port can not respond to the increasing ship traffic, therefore modernization of theport was taken to agenda. Moderinazitaion work was completed in1990. State-owned Trabzonport operations transferred to the private sector by way of privatization on 22 November2003..
Trabzon is located onthe historical Silk Road, a melting pot of languages, religions and culture center over the centuries, has a trade door to northern Russia and the Caucasus. Genoese, Venetians come and gonefrom this port; woolen fabrics, linen and silk goods they sell. In the Ottoman era inTrabzon, thanks to the port of Iran, Iraq, India, Russia, and has been the focal point of trade made the Caucasus.
Silk Road and Trabzon Port The date on which the wealth of the East for two thousand years later the caravan carrying the West Silk Road, which connects two continents and three sea basins. Beyond being a trade route linking Asia to Europe Silk Road, which provides the cultural exchange between civilizations. Starting from China divided into multiple routes of the Silk Road in Central Asia, Istanbul route was used as one of the major routes, the riches of the East to the West has passed through the port of Trabzon.

Trabzon with links to the world's largest sea was founded on the shores of the Black Sea, the largest inland sea, especially Iran, Iraq, Turkey and the Turkish Republic located at a strategic point at the beginning ofthe transit route. Trabzon Port plays a key role in connecting to all European and world markets of these countries

2.3. Technical Information on the Trabzon Port

Length of breakwaters at Trabzon port is given in the Following Table.

Table 1. Length of breakwaters at Trabzon port

Length of large breakwater	1,135 meters
Small breakwater length	440 meters
Secondary breakwater length	380 meters

2.4. Port Area

Ship handling and storage capacity of Trabzon port is shown in Table 2.

Table 2. Cargo handling and store capacity of Trabzon port

Total Quay Length (m)	Average Depth (m)	Handling Capacity (tons / year)	Ship Acceptance Capacity (pcs / year)	Storage Capacity (tons / year)
1525	2.5 - 10	3.839	2000	3.193

Lengths of each piers are given in Table 3.

Table 3. Length of piers at Trabzon port

Piers Name and ID	Length(m)	Depth (m)
Main Berth	400	9,5
General Cargo Berth	300	9,5
Container Berth	280	9,5
Mine Berth	290	11,5
RoRo Berth	25	10
Auxiliary Berth	200	3

2.5. Objectives

The oceanographic parameters will be measured with supplied equipment by the Contracting Authority for stated time duration, and raw datawill be reported in MS EXCEL as well as the results of the analysis of the data collected. Then, a mathematical model will be developed to investigate the hydrodynamic flow around Trabzon port and surroundings.The management strategies developed from the modeling results will reveal to minimize sediment accumulations in and around Trabzon Harbor.

3. Sampling Strategy

The first Samplings were done at 13 points with equipment supplied by Contracting Authority.Coordinates of the sampling stations are given in Table1 and shown in Figure 1.

Table 4. Coordinates of Sampling Stations and Depths

STATION	LONGITUDE (N)	LATITUDE (E)	DEPTH (m)
D1	41˚ 00' 38,63"	39˚ 46' 08,13"	34
D2	41˚ 00' 23,29"	39˚ 45' 40,13"	12
D3	41˚ 00' 14,51"	39˚ 45' 29,75"	2.5
D4	41˚ 00' 43,50"	39˚ 45' 46,39"	47
D5	41˚ 00' 30,24"	39˚ 45' 22,34"	35
D6	41˚ 00' 19,15"	39˚ 45' 20,90"	8
D7	41˚ 00' 19,18"	39˚ 45' 00"	10
D8	41˚ 00' 44,91"	39˚ 44' 48,35"	45
D9	41˚ 00' 45,98"	39˚ 44' 25,24"	40
D10	41˚ 00' 34"	39˚ 44' 17"	8.2
D11	41˚ 00' 24,60"	39˚ 44' 20,06"	10
D12	41˚ 00' 14,91"	39˚ 44' 28,59"	11
D13 (River enterence)	41˚ 00' 03,61"	39˚ 45' 25,58"	1

Figure 1. Sampling Stations

The first sampling of the following data was done at 13 stations.Aquadopp IM 300 current meter was used to measure currents and Sea Sun Tech. CTD 75 M multiparameter probe was used for oceanographic parameters. Picture of these two equipments are given in Picture 2.

Picture 2.CTD and current meterused in the sampling provided by the Project coordinator

Some pictures taken during the measurements were given in the following pictures.

Picture 3. Equipment and personnel conducted the measurements

Picture 4.During the Current measurements

Picture 5. During the CTD measurements (Note that A project research staff has joined all the samplings occations conducted)

Raw data is in the attached CD. Continuous data were measured for all oceanographic parameters.

Oceanographic parameters

- Pressure,
- Temperature,
- PH
- Conductivity,
- Turbidity,
- Salinity,
- Oxygen,
- Sound,
- Sigma,
- Current,
- DO.

Graphs for temperature, conductivity, salinity, versus depth (sigma) will be given for each stations and others will be given as raw data. Suspended sediment will be given at surface and maximum depth. Current speed and direction at surface, maximum depth and 2 more in between will be shown at each station points on google map given in Figure 1.

4. Meteorological Data

Precipitation and wind data were obtained from State Meteorological Office. However, wind measurements from land stations underestimate the magnitude of wind above sea surface. This is mainly due to differences in characteristics of the atmospheric planetary boundary layer over land and water. On the basis of theory discussed, wind speed over sea surface was found as

$$U_{sea} = 3.0(U_{land})^{0.67}$$

U_{sea}: Wind speed over sea surface (m/s)

U_{land}: Measured wind speed (m/s)

Table 5 shows the monthly and annual values for the most probable wind speed (Vmp), and the wind speed carrying maximum energy (VmaxE) at height of 10 m. and monthly average wind speed for Trabzon is given in Figure 2. (Akpınar,2012)

Table 5. Average monthly and annual values of the characteristic wind speeds at 10 m heights.

Months	Giresun		Ordu		Trabzon		Hopa	
	V_{mp}	V_{maxE}	V_{mp}	V_{maxE}	V_{mp}	V_{maxE}	V_{mp}	V_{maxE}
January	0.37	5.17	0.92	3.16	1.32	7.07	1.61	9.29
February	0.91	4.34	0.9	3.35	1.38	7.18	0.67	8.72
March	0.99	4.13	0.72	4.49	1.65	6.86	0.18	8.72
April	0.5	4.55	0.89	3.83	1.77	5.27	0.27	5.49
May	0.03	6.14	1.02	3.83	1.71	4.63	0.75	3.62
June	0.82	3.52	1.33	3.94	1.69	5.1	1.3	3.1
July	0.02	6.26	1.14	4.2	1.77	4.9	1.52	2.69
August	1.05	3.24	1.15	4.32	2.06	4.53	1.52	2.81
September	0.91	3.38	1.21	3.62	2.18	5.09	1.6	3.4
October	0.53	4.2	0.9	3.21	1.78	5.04	1	5.24
November	0.3	5.59	0.85	3.26	1.5	7.05	1.18	8.05
December	0.49	5.52	0.92	3.18	1.49	7.11	1.85	9.42
Annual	0.51	4.61	0.97	3.78	1.65	5.81	0.5	7.22

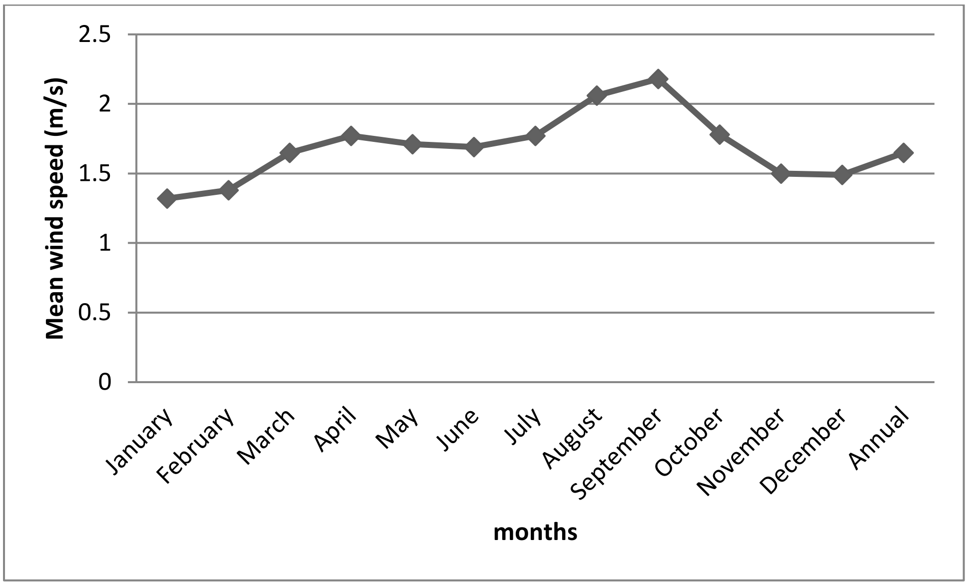

Figure 2. Mean monthly wind speed for Trabzon

Table 6. Meteorological data for Trabzon (DMI)between 1954 - 2013

TRABZON	Jan	Feb	March	Apr.	May	June	July	Aug.	Sep.	Oct.	Nov.	Dec.
	Average values (1954 - 2013)											
Average Temp. (°C)	7.4	7.3	8.6	11.8	16.0	20.4	23.2	23.4	20.3	16.5	12.7	9.6
Average Max. Temp. (°C)	10.9	11.0	12.1	15.5	19.1	23.5	26.2	26.7	23.8	20.1	16.5	13.2
Average Min. Temp. (°C)	4.7	4.4	5.5	8.8	12.9	17.1	20.1	20.4	17.3	13.6	9.8	6.7
Average Sun shine (h)	2.8	3.3	3.5	4.3	5.7	7.1	6.1	5.7	5.0	4.6	3.7	2.8
Average Number of Rainy Day	13.2	12.7	14.2	14.9	13.5	11.3	8.3	9.4	11.8	13.2	12.4	13.1
Average Total monthly precipitation (kg/m^2)	73.3	60.2	59.1	58.7	51.8	51.4	34.7	43.1	76.1	113.9	94.5	82.0
	Average Maximum and minimum Temperatures (1954 - 2013)											
Max.Temperature (°C)	25.2	28.2	35.2	37.6	37.8	35.9	37.0	34.8	33.2	32.7	30.3	26.4
Min. Temperature (°C)	-6.0	-6.1	-5.0	-2.0	5.4	9.2	13.5	13.8	8.5	3.4	0.6	-3.1

Analysis of the meteorological data showed that effective wind for Eastern Blacksea is NW.

Flux rates and sediment amount of Degirmendere was obtained from The General Directorate of State Hydraulic Works and given in Figure 3 and Table 7.

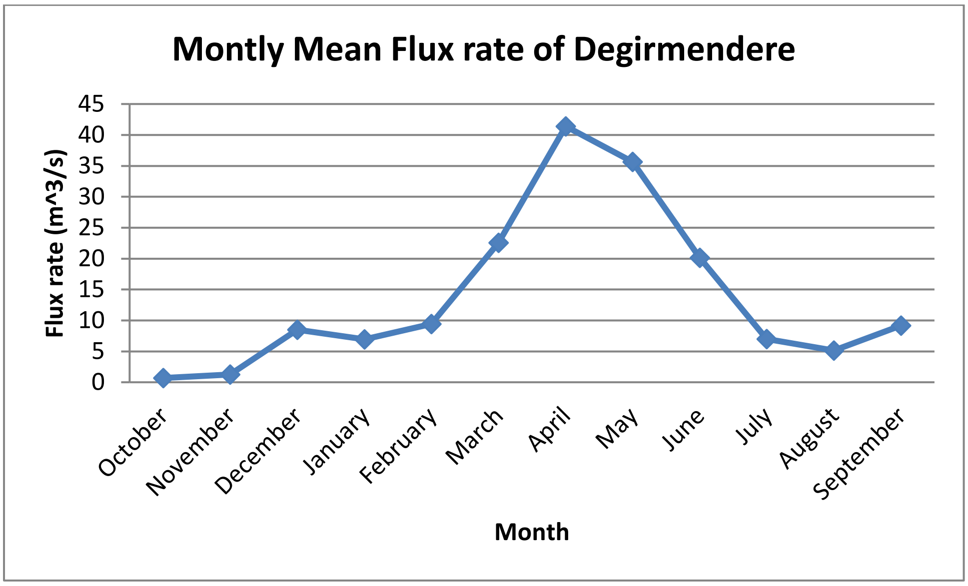

Figure 3. Montly flux rate of Degirmendere (DSI)

Table 7. Sediment amount measured from Değirmendere

Month	December	Jananuary	February	March	April	May	June	July
Sediment (mg/l)	346	181	381	216	427	489	385	274

5. MYOCEAN downscaling

Data for the Blacksea region were downscaled from MYOCEAN data and results were given in the following graphs

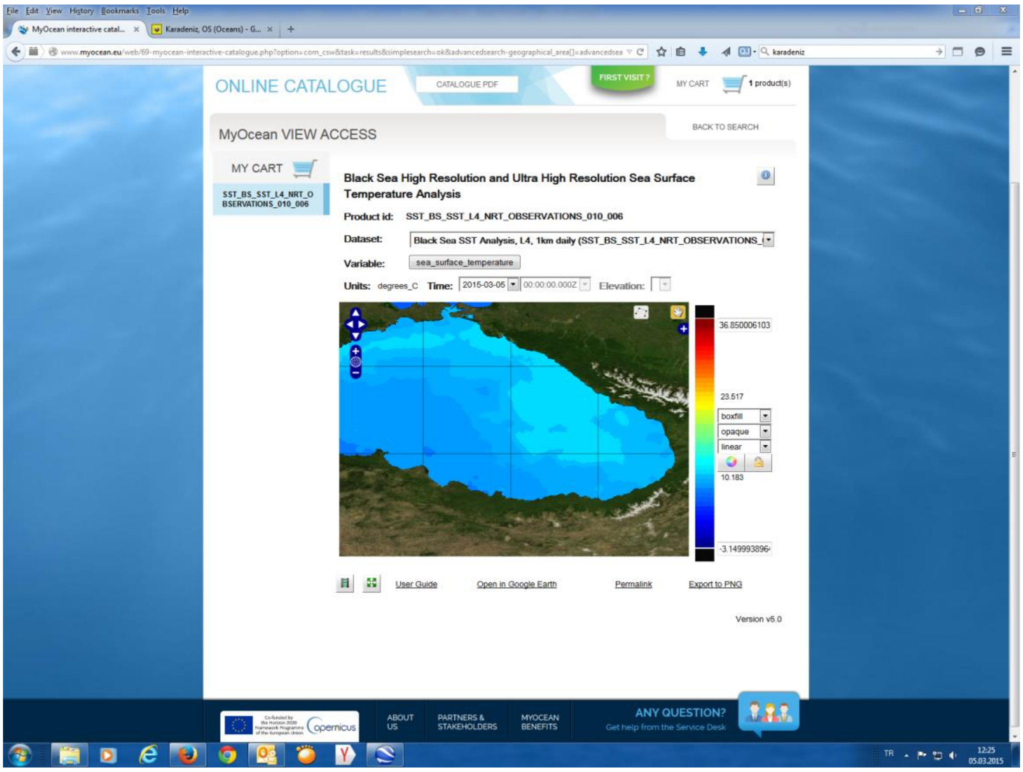

Figure 4. Downlaod page of MYOCEAN web site

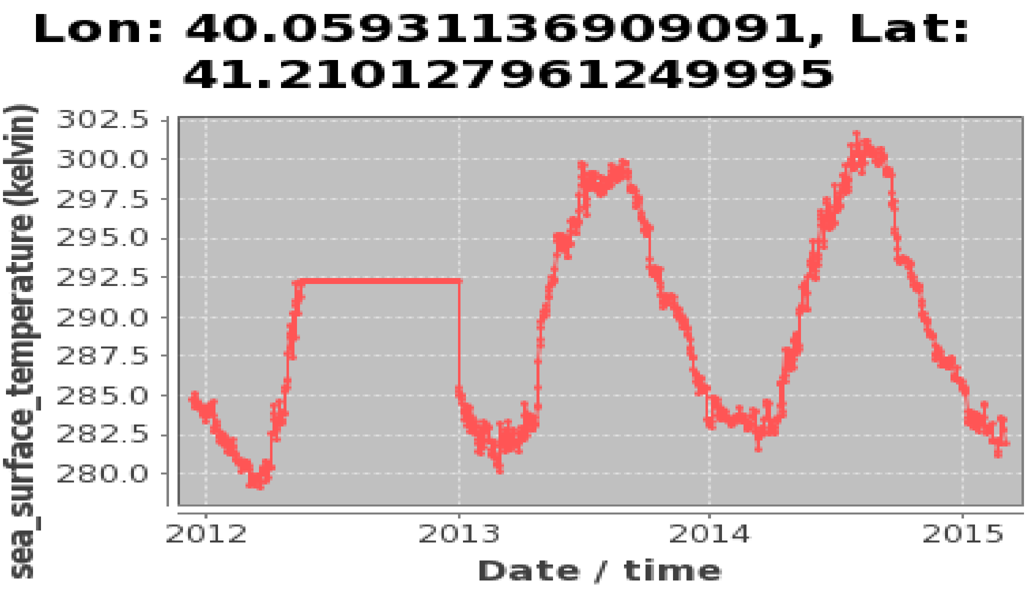

Figure 5. Sea surface temperature downscaled from myocean data set.

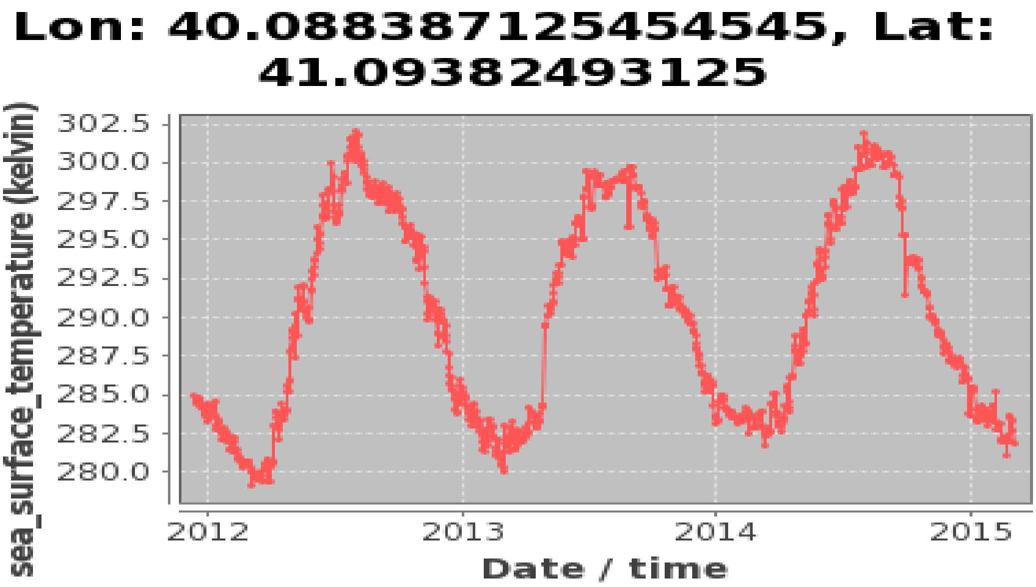

Figure 6. Sea surface temperature with 1km resolution downscaled from myocean data set.

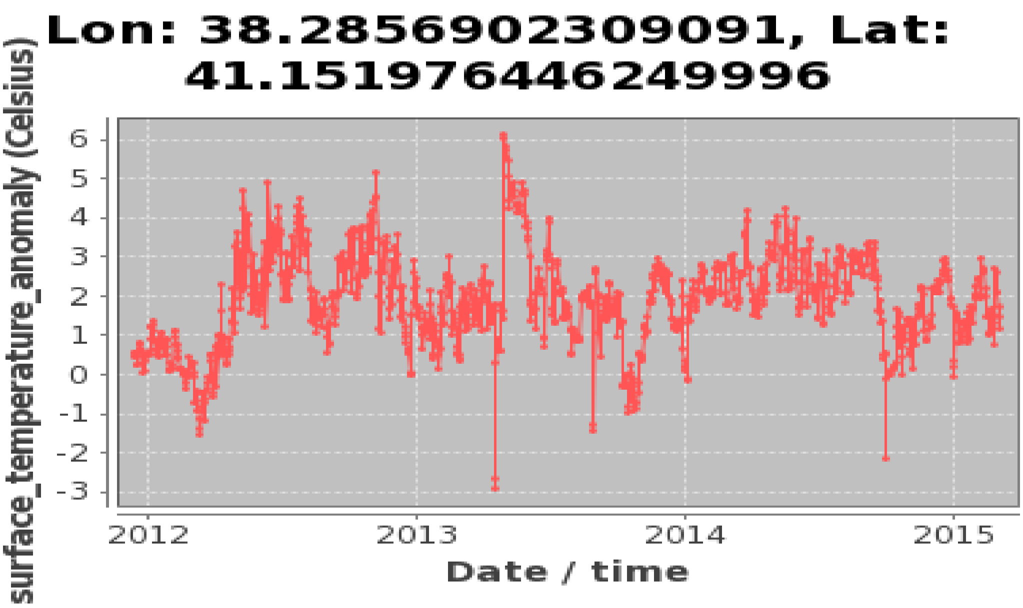

Figure 7. Sea surface temperature anomalies fort the Southeast Blacksea

6. Results of Sampling

6.1. Topography of the study area

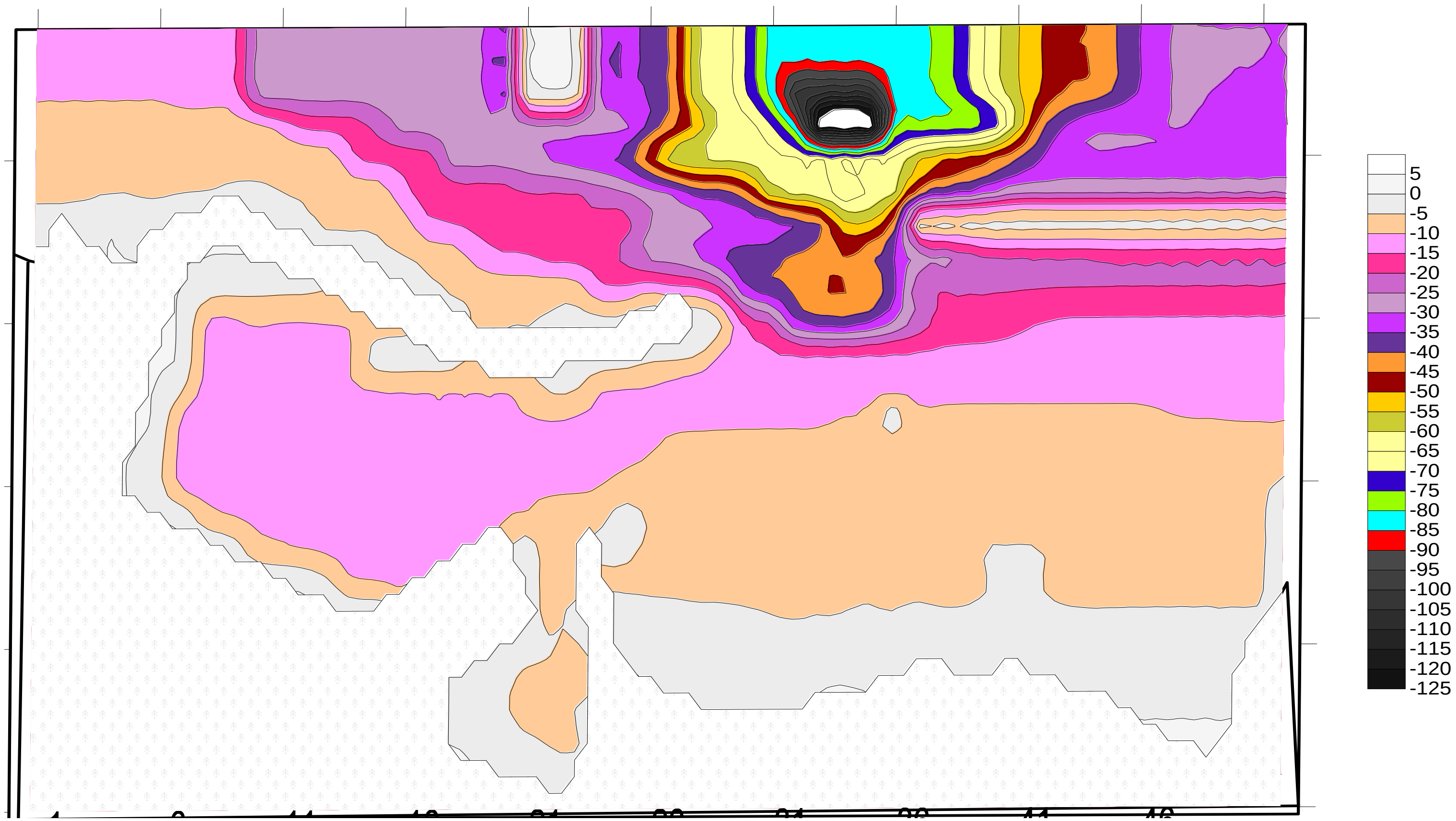

Figure 8. Topography of Trabzon port and Degirmendere area

6.2. Physical Properties of Seawater in the study area

6.2.1. CTD Measurements

CTD measurements were done on the following dates.

Month	First Measurement	Second measurement
December	28	--
January	4	25
February	6	22
March	7	28
April	11	26
May	3	30
June	6	

CTD graphs versus depth for each stations are given in below. Conductivity, Salinity and Temperature results for December are given in Figures 9 -20.

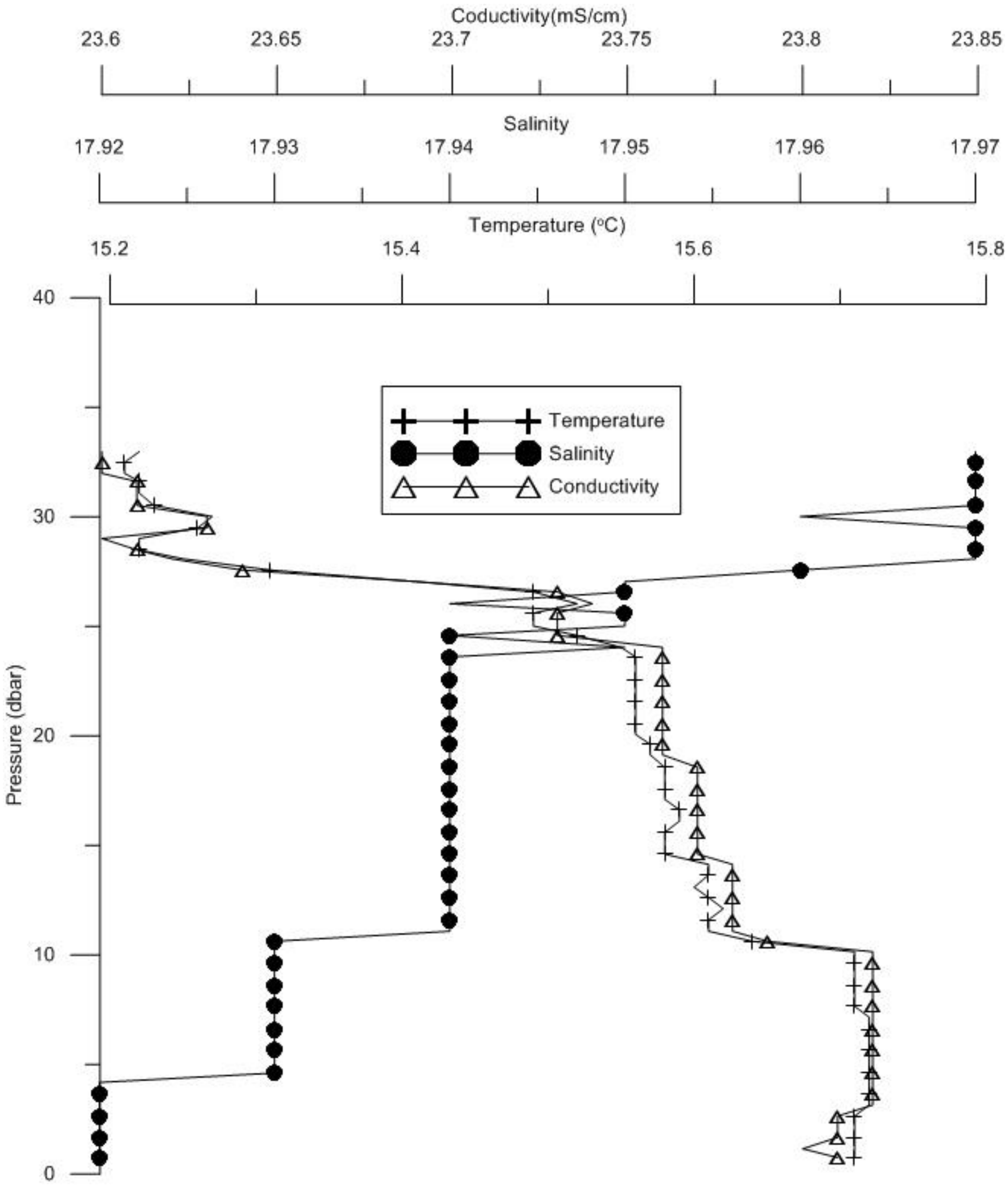

Figure 9. CTD from D1 Station for measurements in December 2014

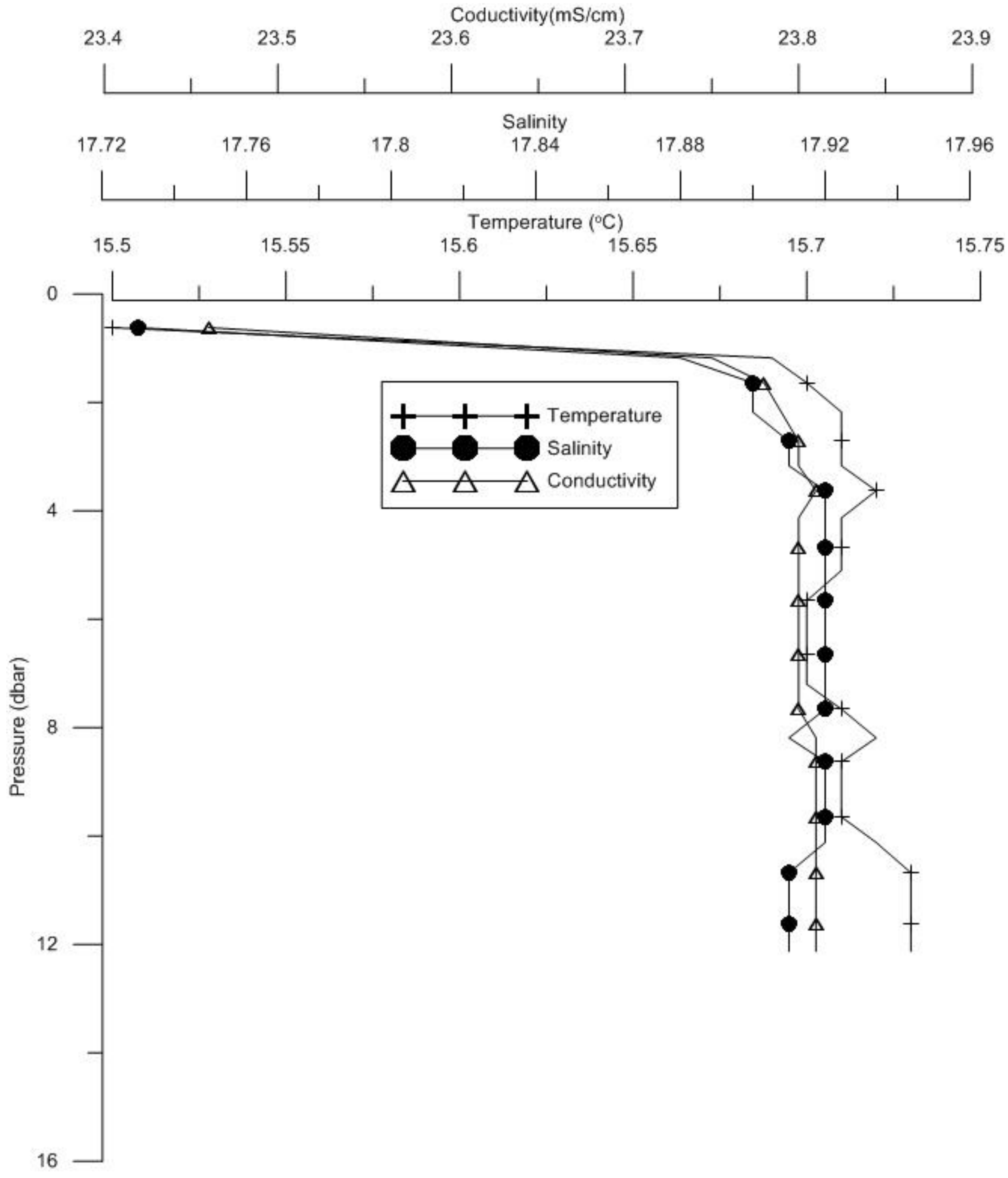

Figure 10. CTD from D2 Station for measurements in December2014

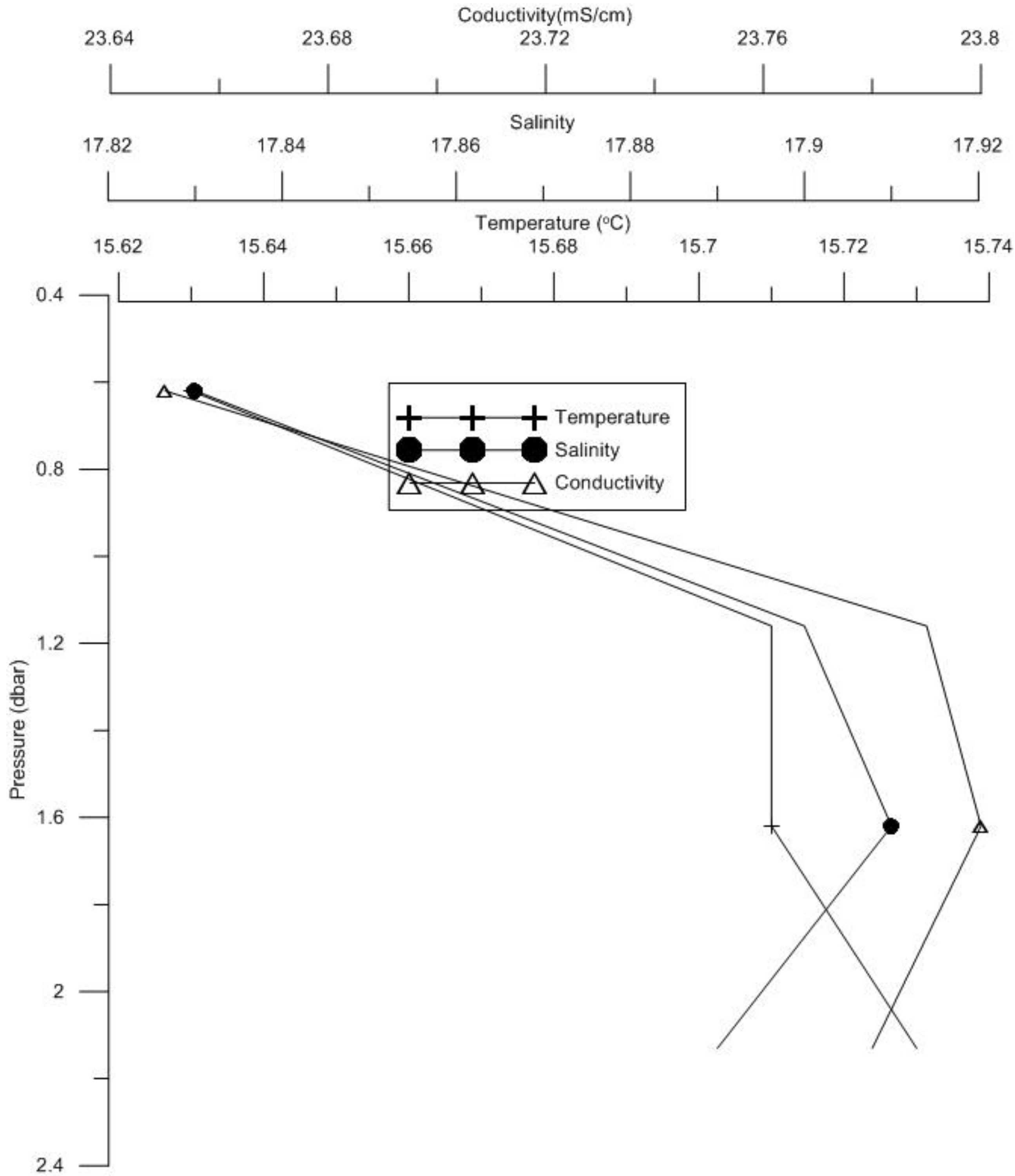

Figure 11. CTD from D3 Station for measurements in December2014

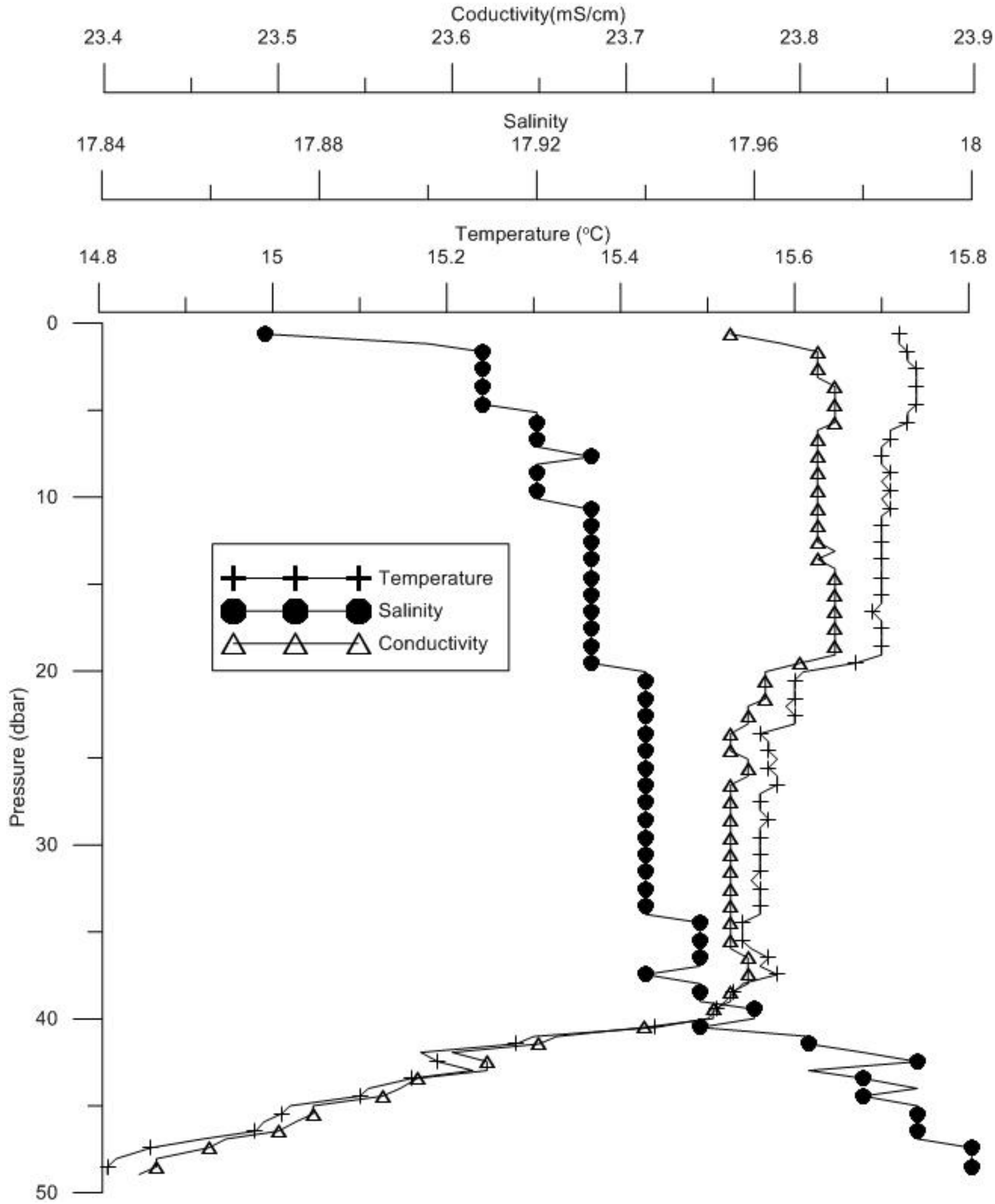

Figure 12.CTD from D4 Station for measurements in December2014

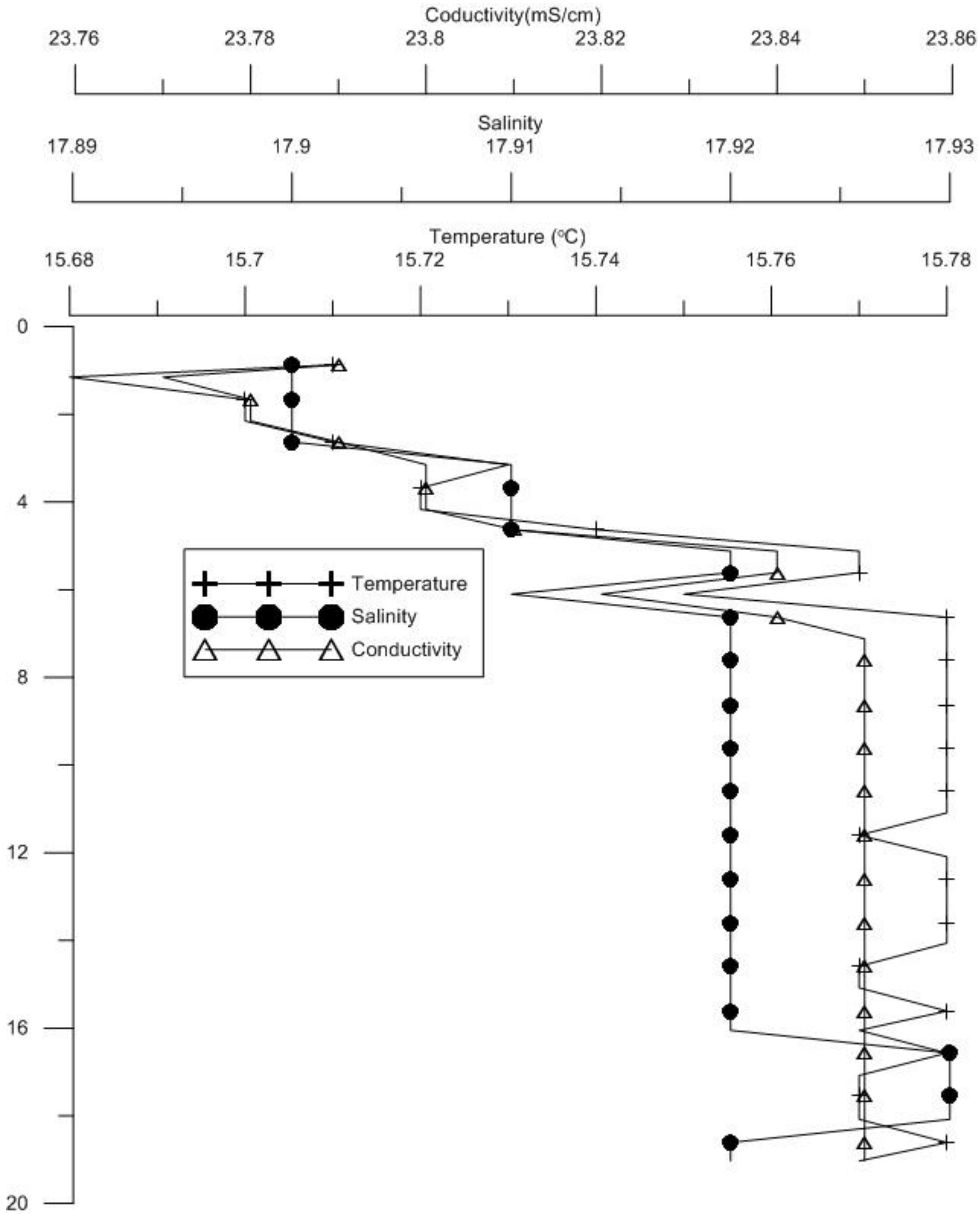

Figure 13. CTD from D5 Station for measurements in December2014

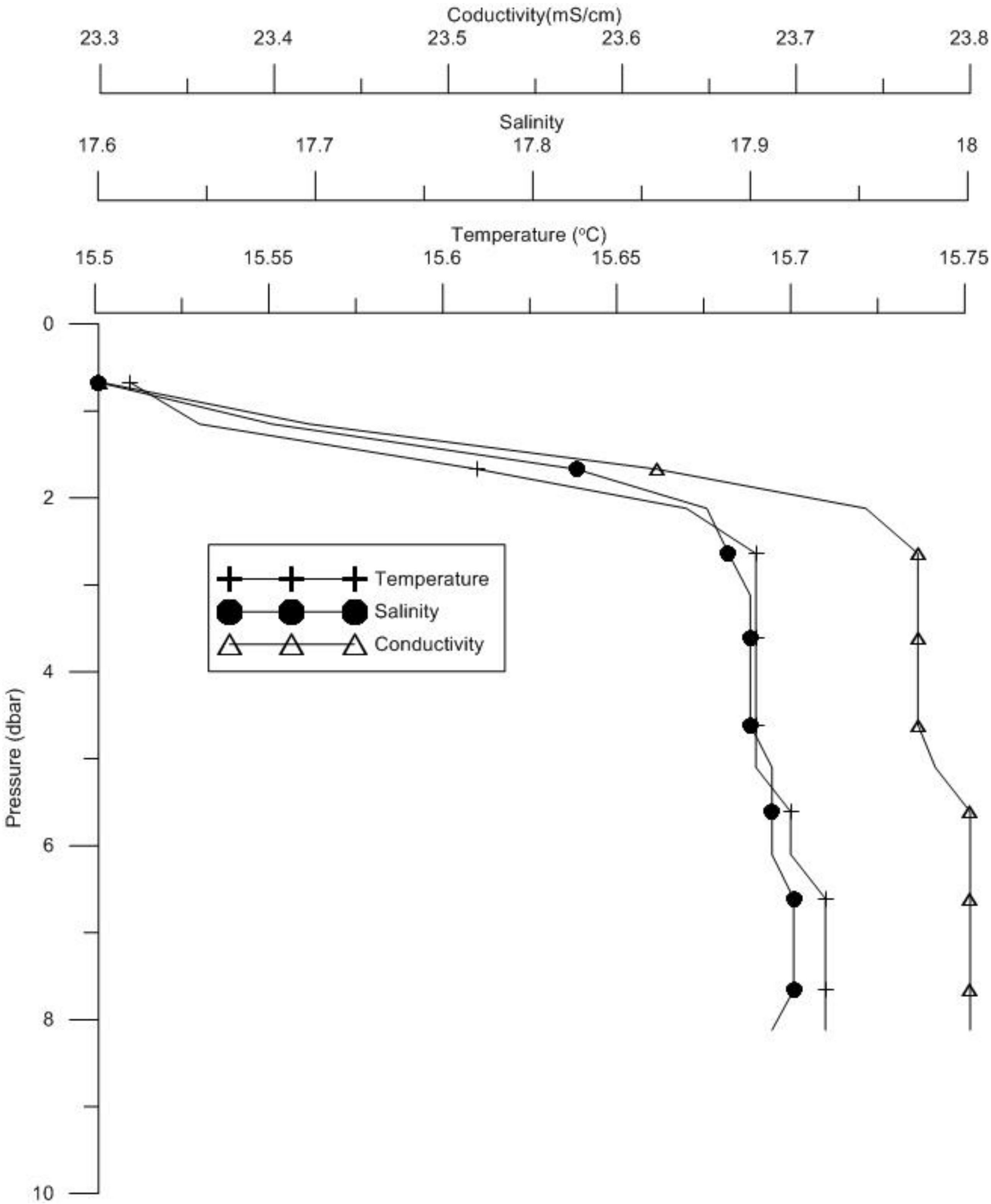

Figure 14. CTD from D6 Station for measurements in December2014

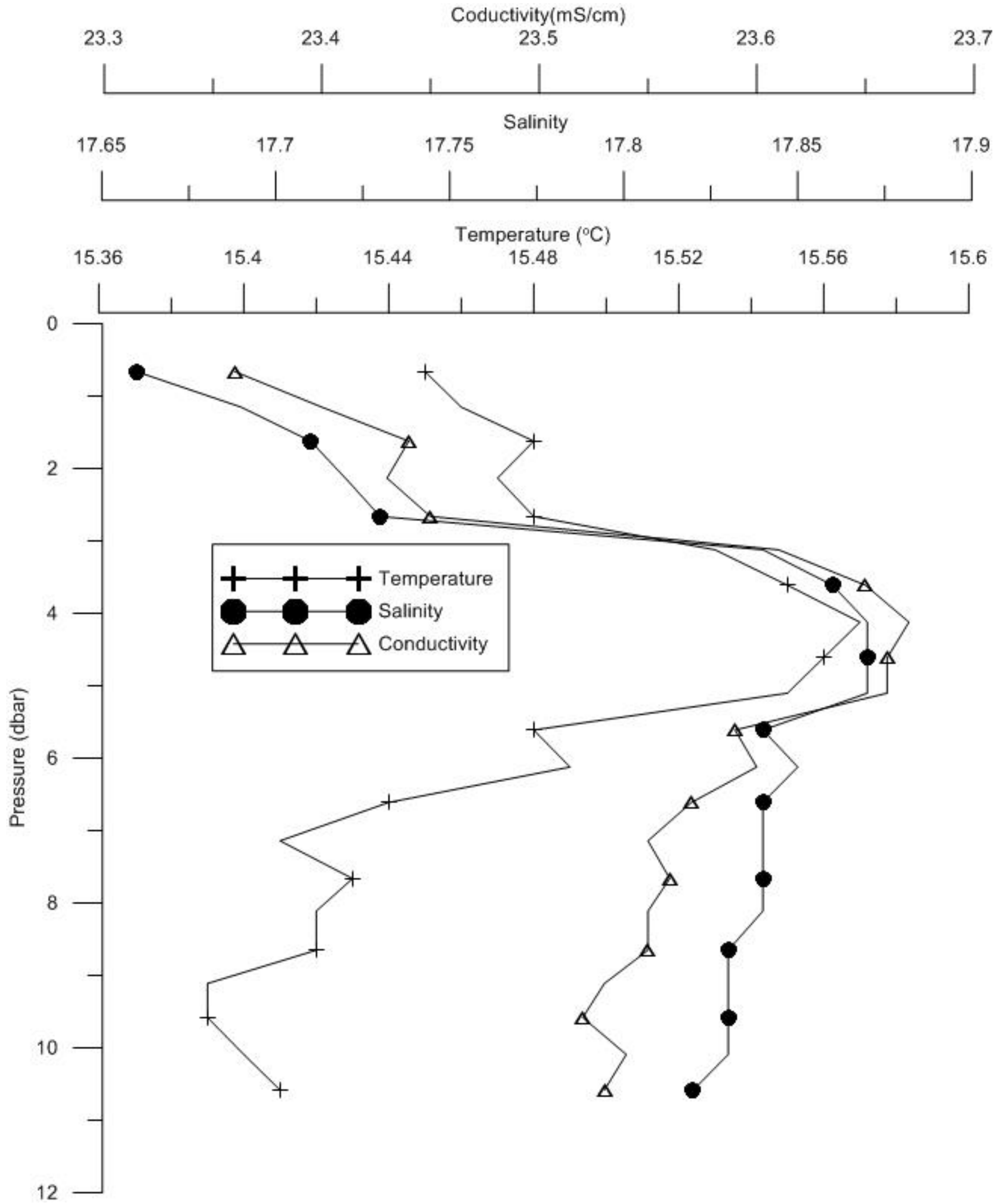

Figure 15. CTD from D7 Station for measurements in December2014

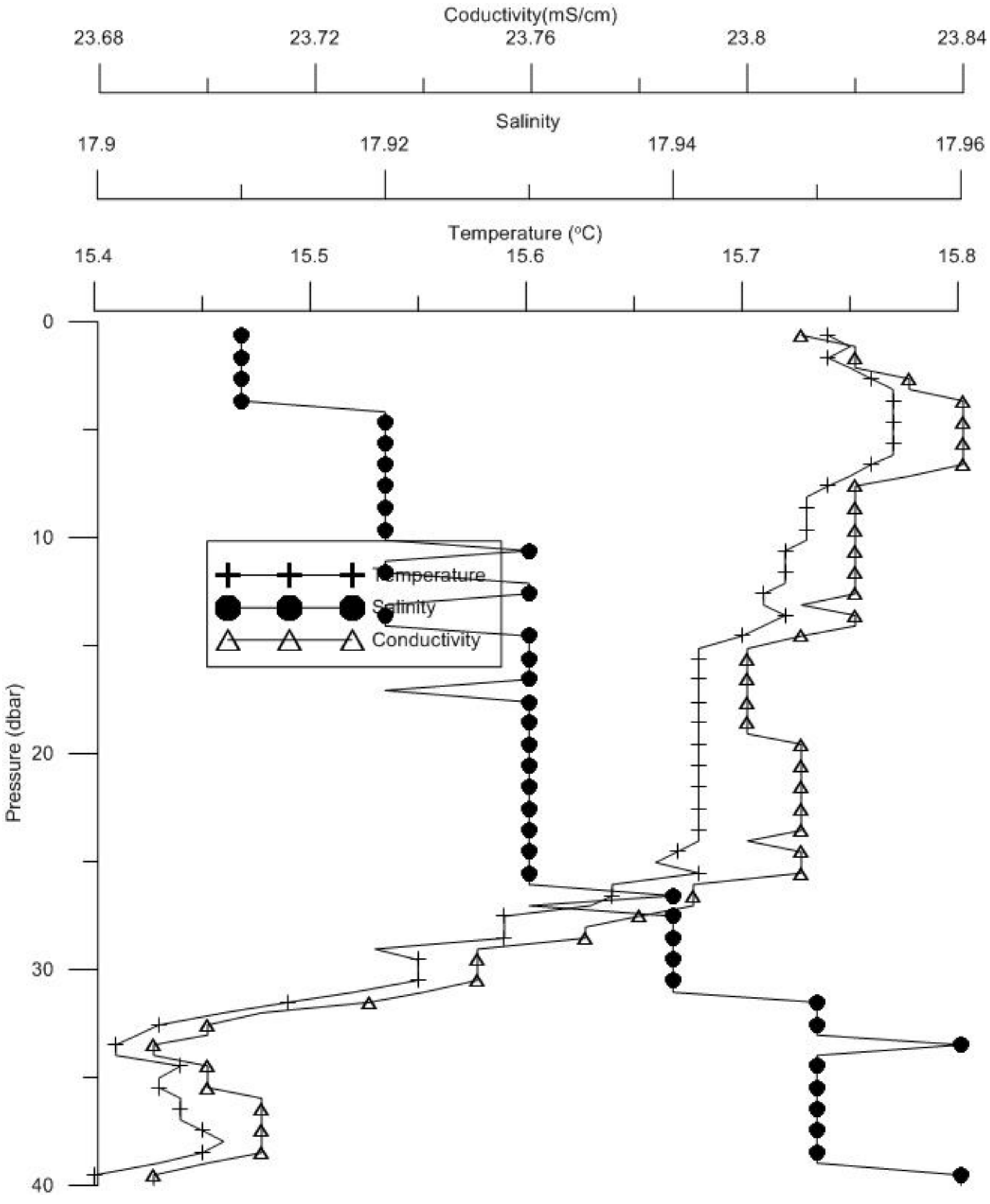

Figure 16.CTD from D8 Station for measurements in December2014

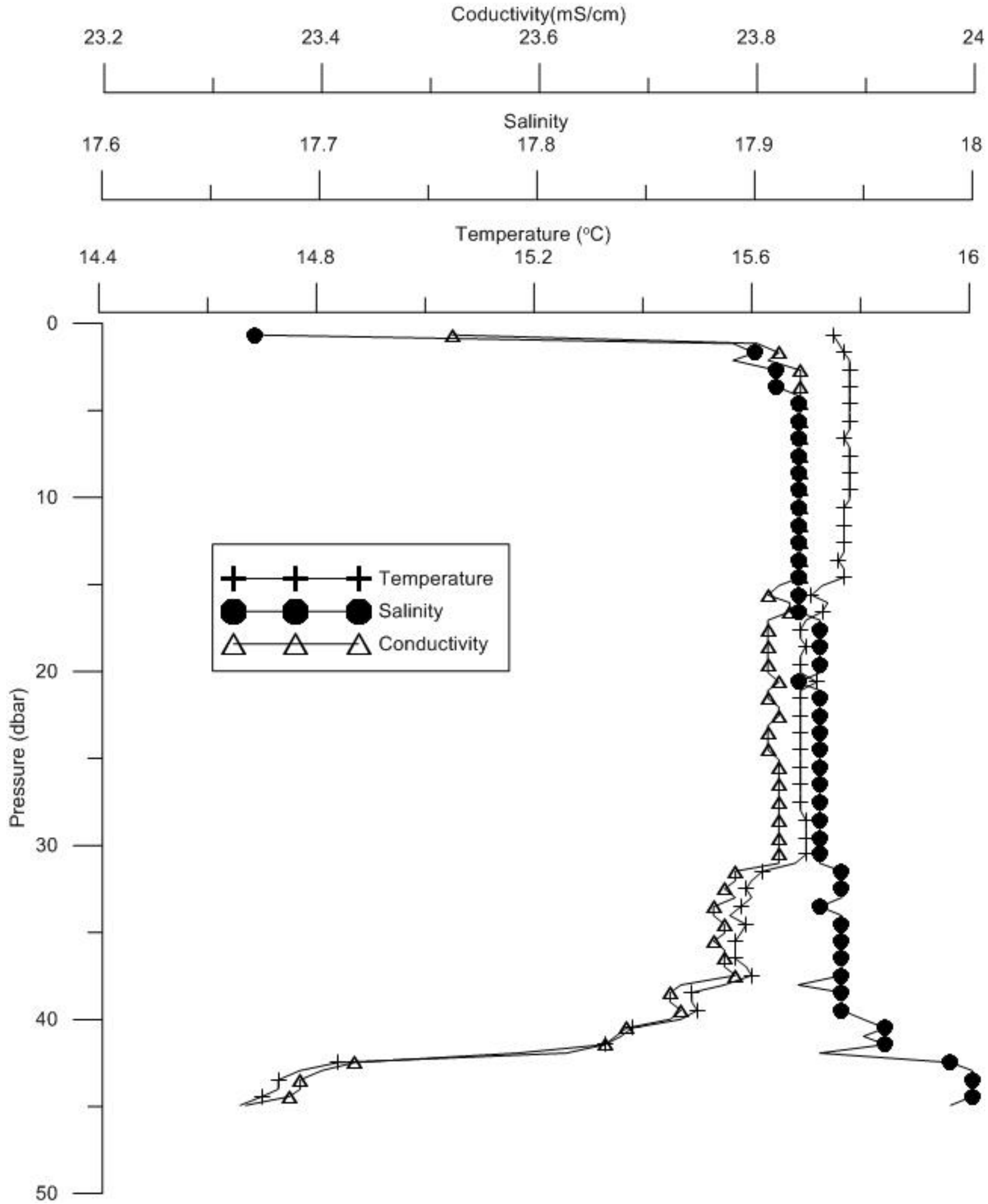

Figure 17.CTD from D9 Station for measurements in December2014

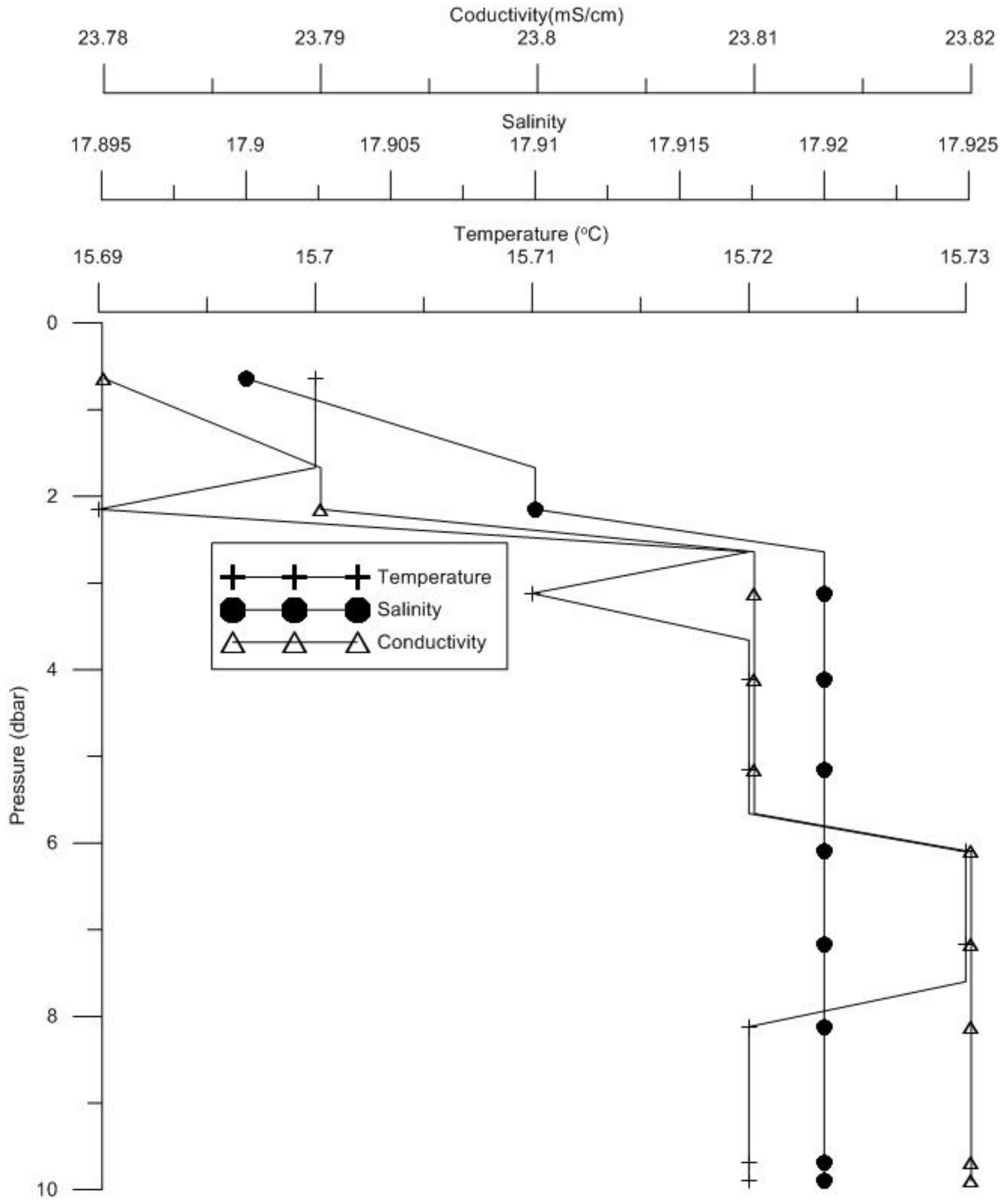

Figure 18.CTD from D10 Station for measurements in December2014

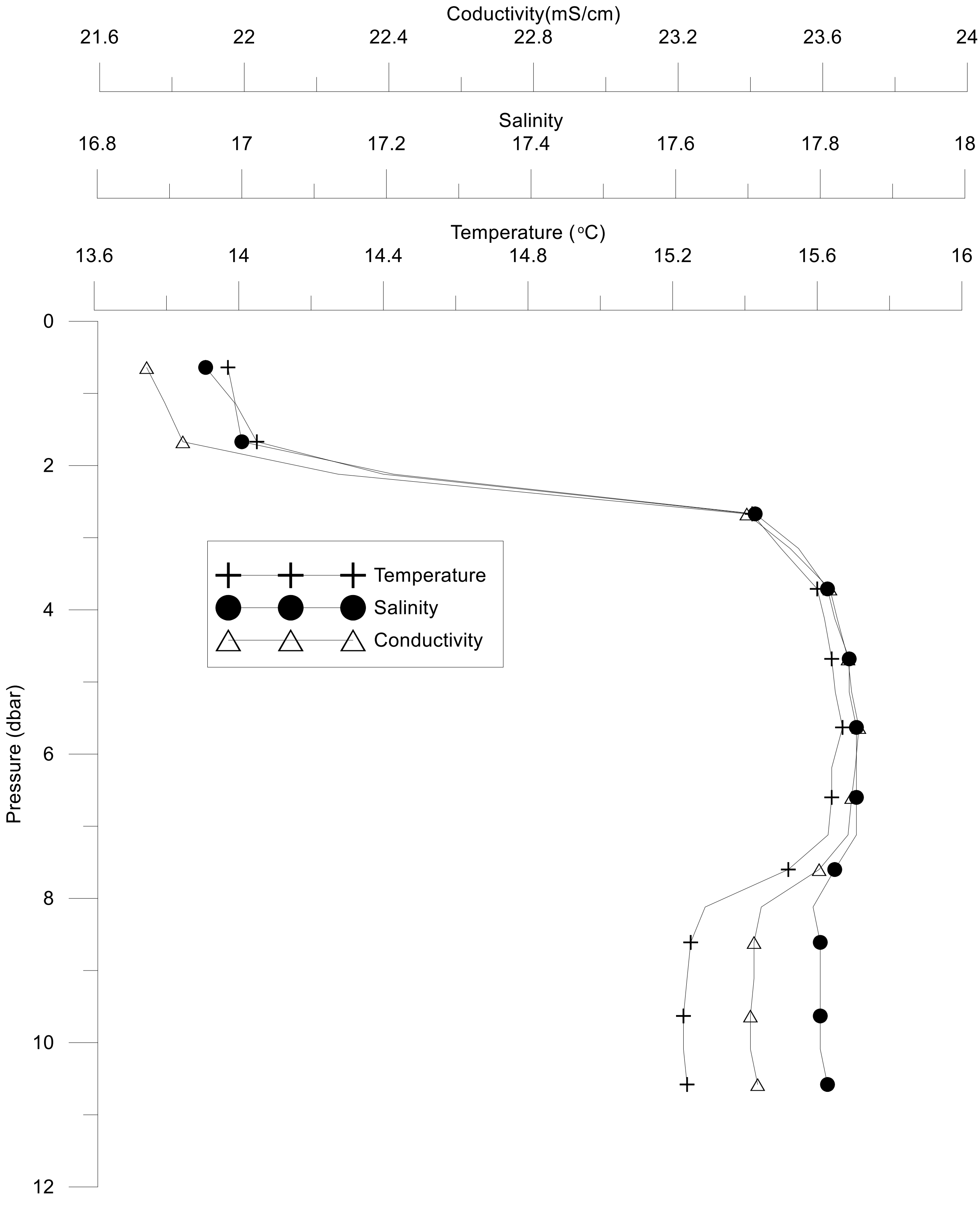

Figure 19.CTD from D11 Station for measurements in December2014

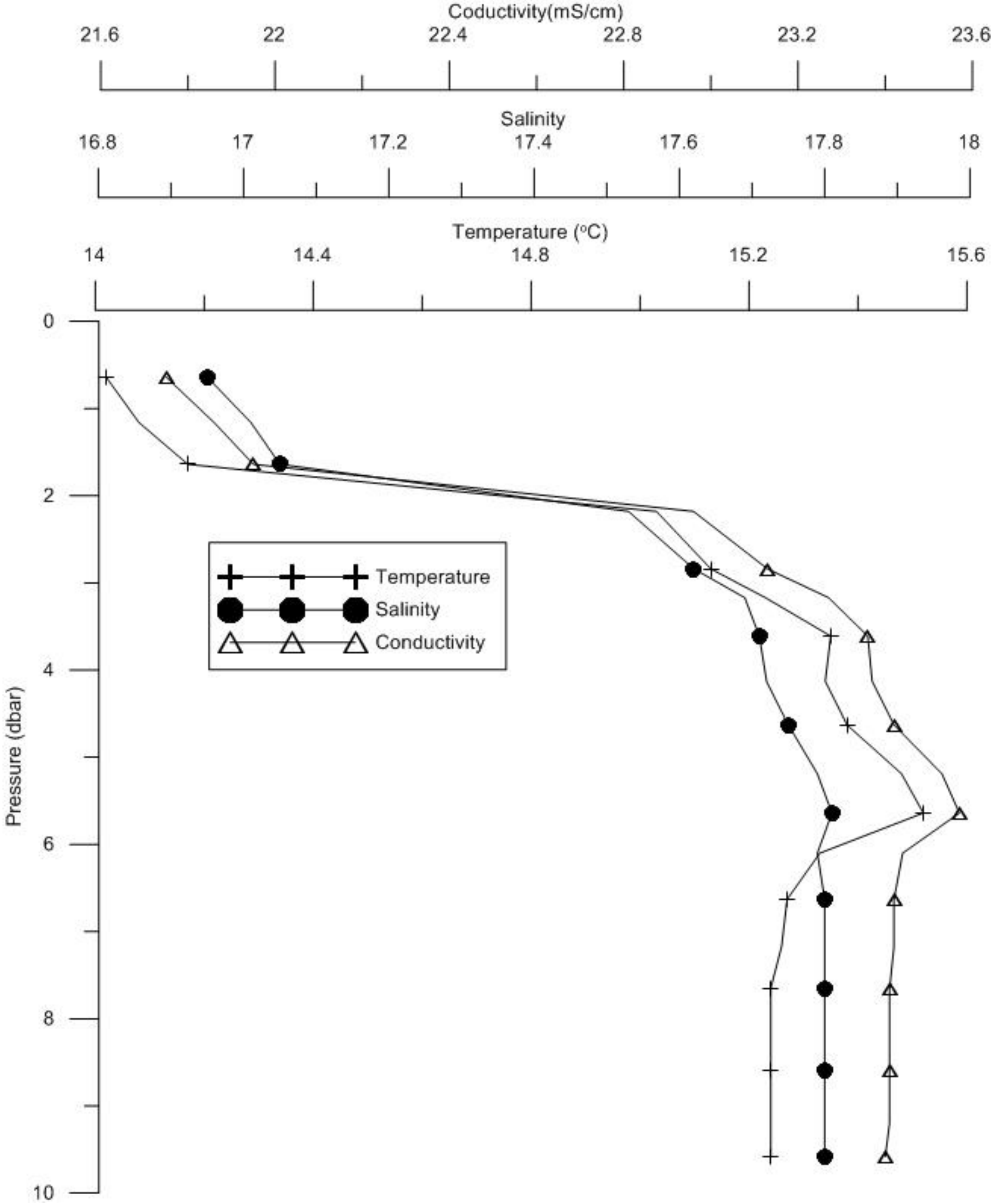

Figure 20.CTD from D12 Station for measurements in December2014

CTD graphs versus depth for each stations are given in the below. Conductivity, Salinity and Temperature results for the first period of January are given in Figures 21 -32.

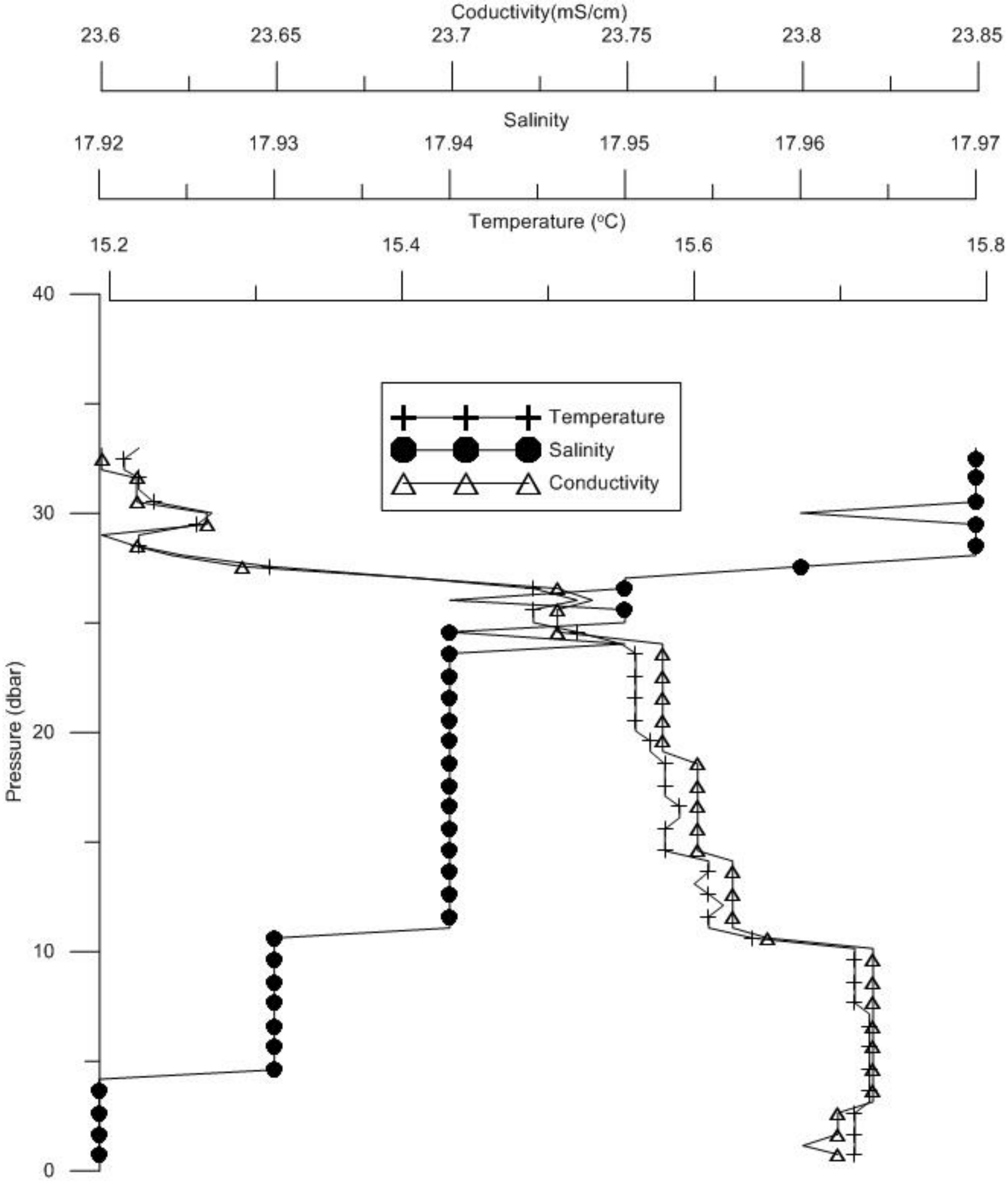

Figure 21. CTD from D1 Station for the first measurements in January2015

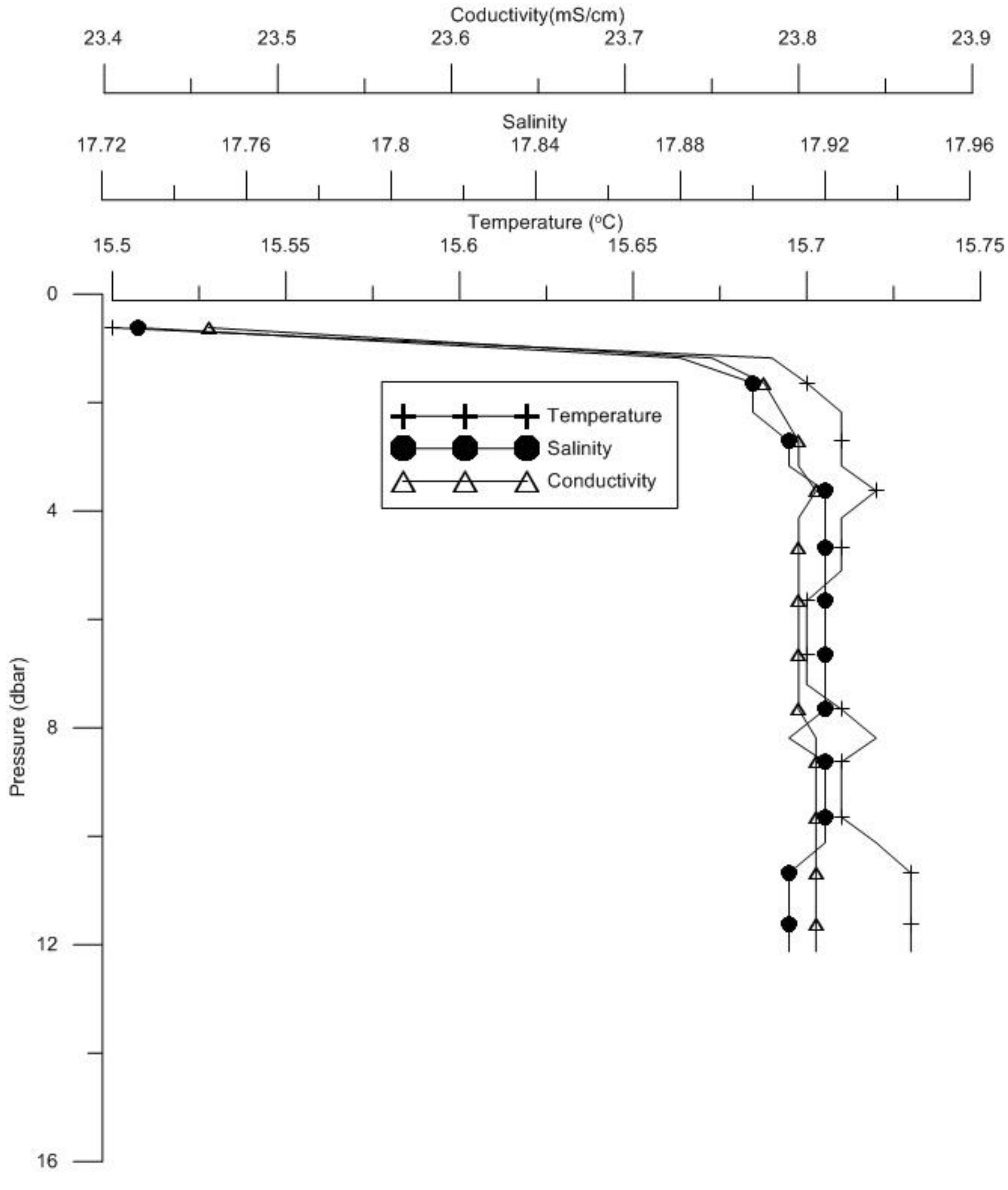

Figure 22.CTD from D2 Station for the first measurements in January2015

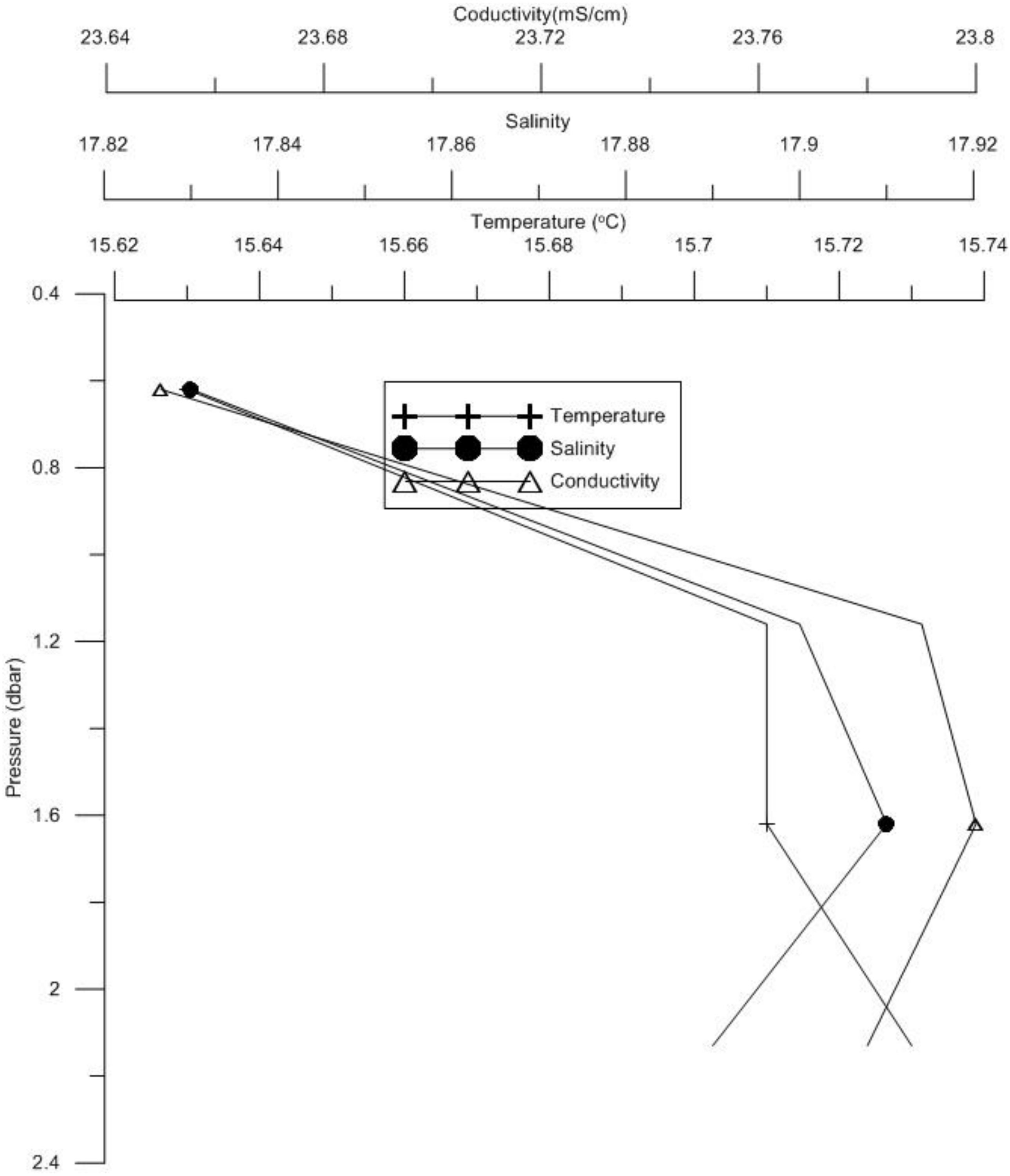

Figure 23.CTD from D3 Station for the first measurements in January2015

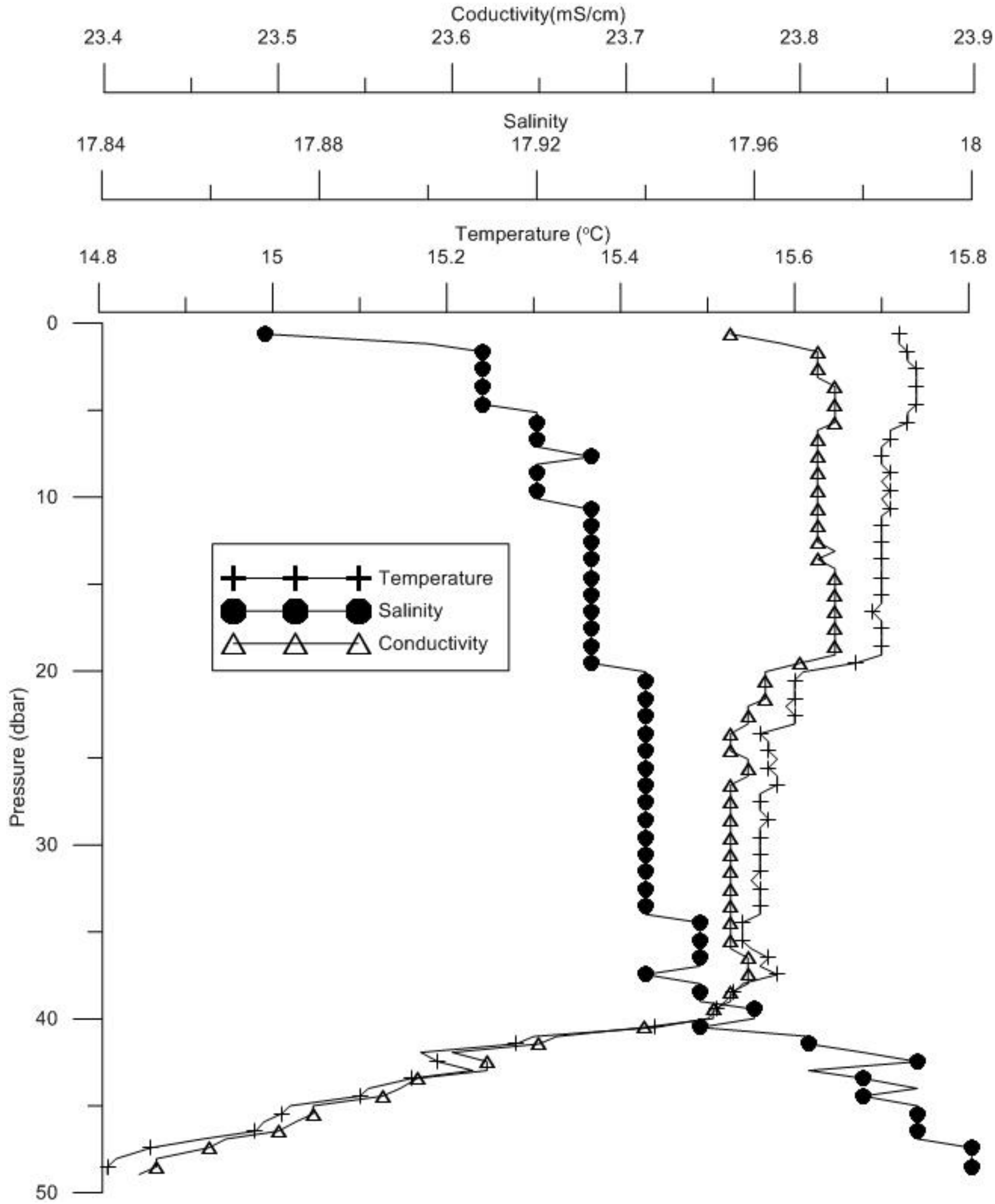

Figure 24.CTD from D4 Station for the first measurements in January2015

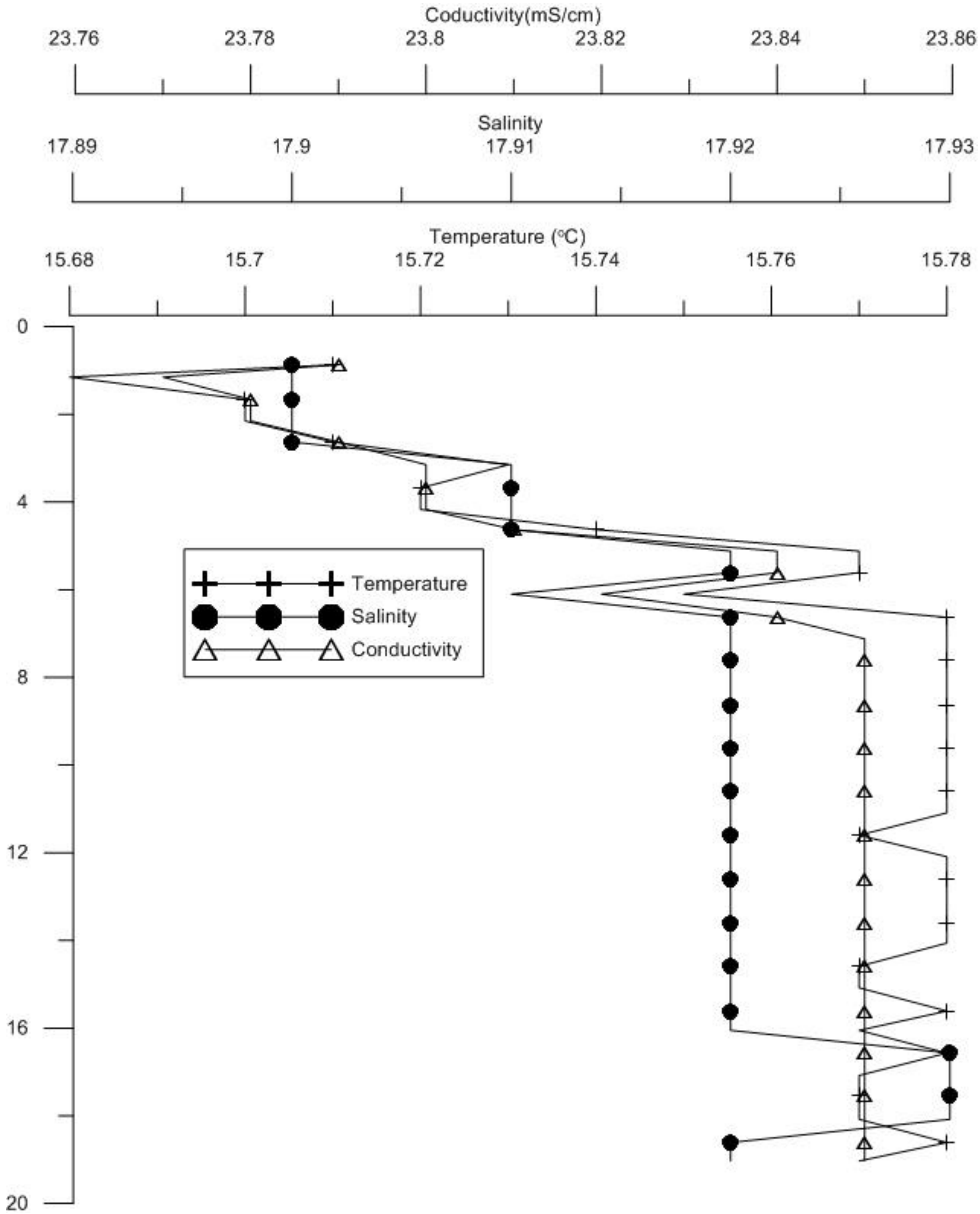

Figure 25.CTD from D5 Station for the first measurements in January2015

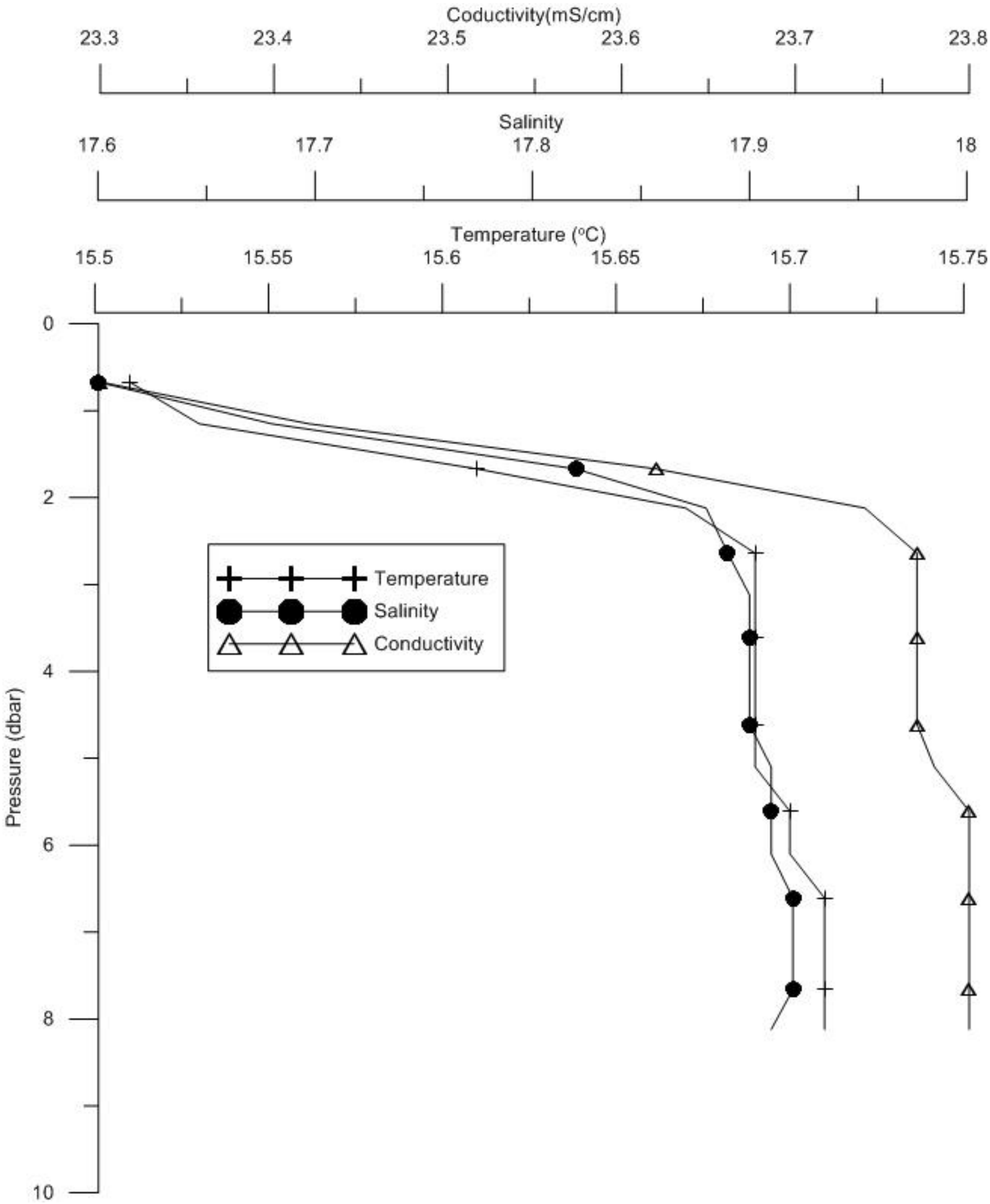

Figure 26.CTD from D6 Station for the first measurements in January2015

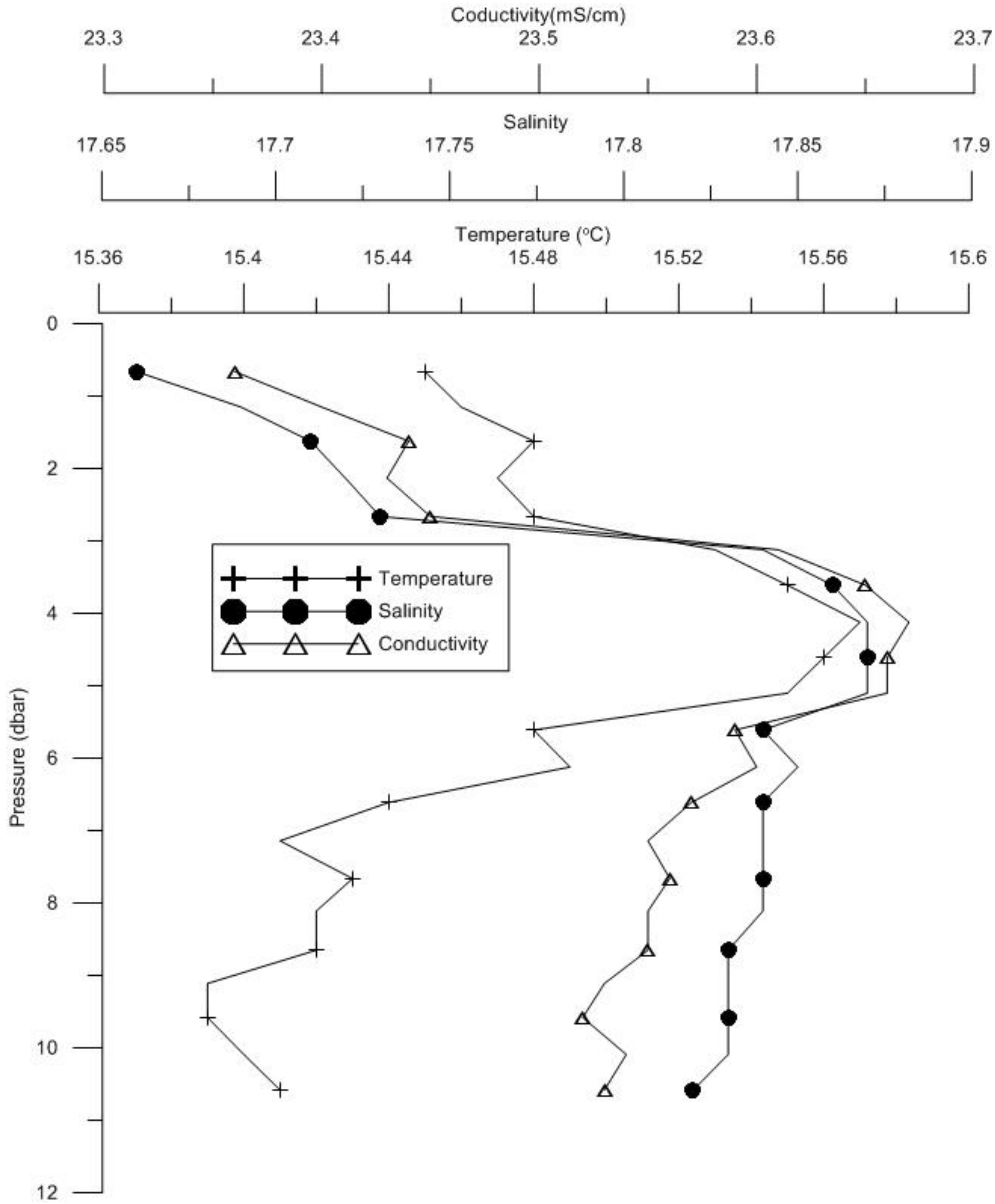

Figure 27.CTD from D7 Station for the first measurements in January2015

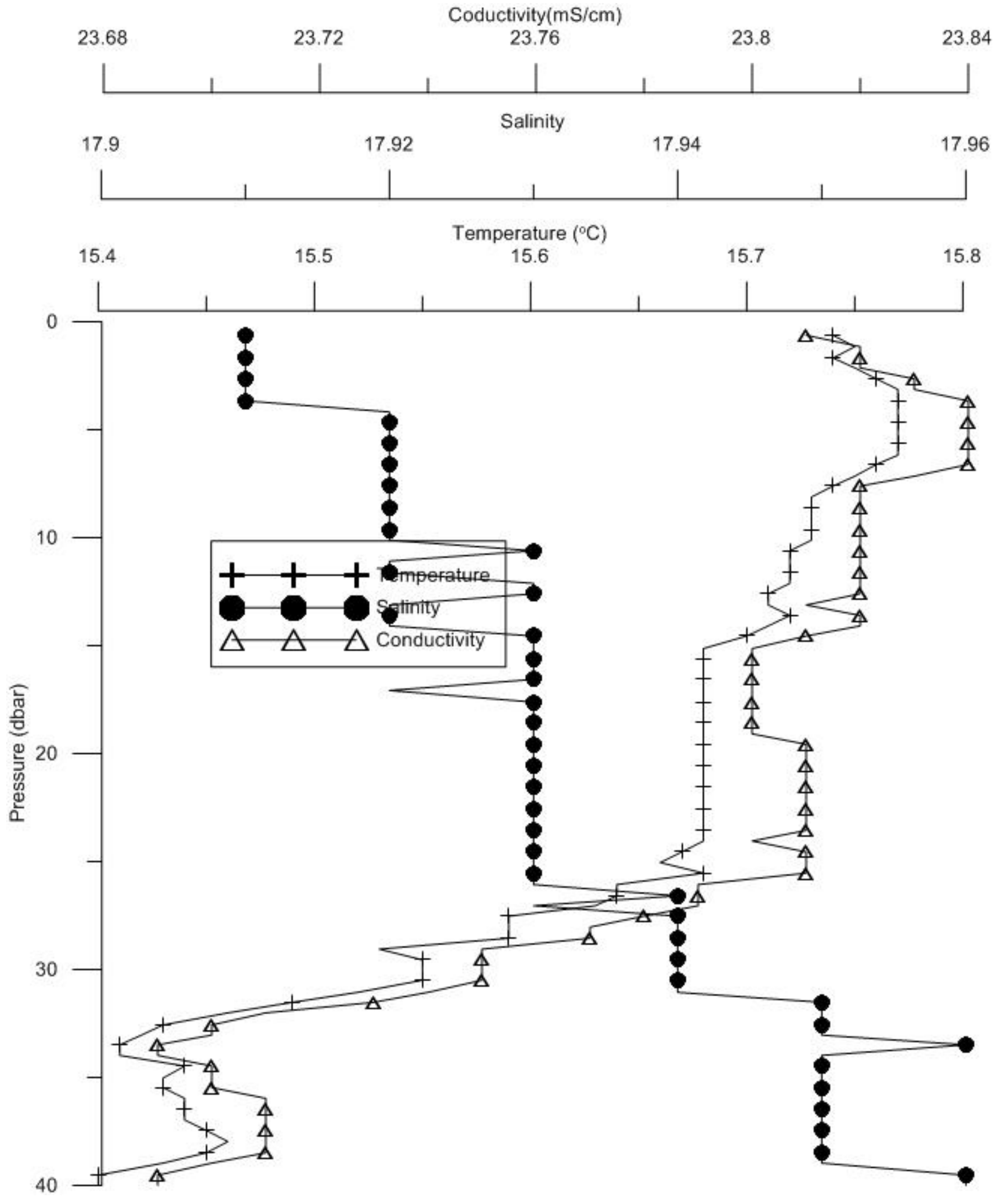

Figure 28.CTD from D8 Station for the first measurements in January2015

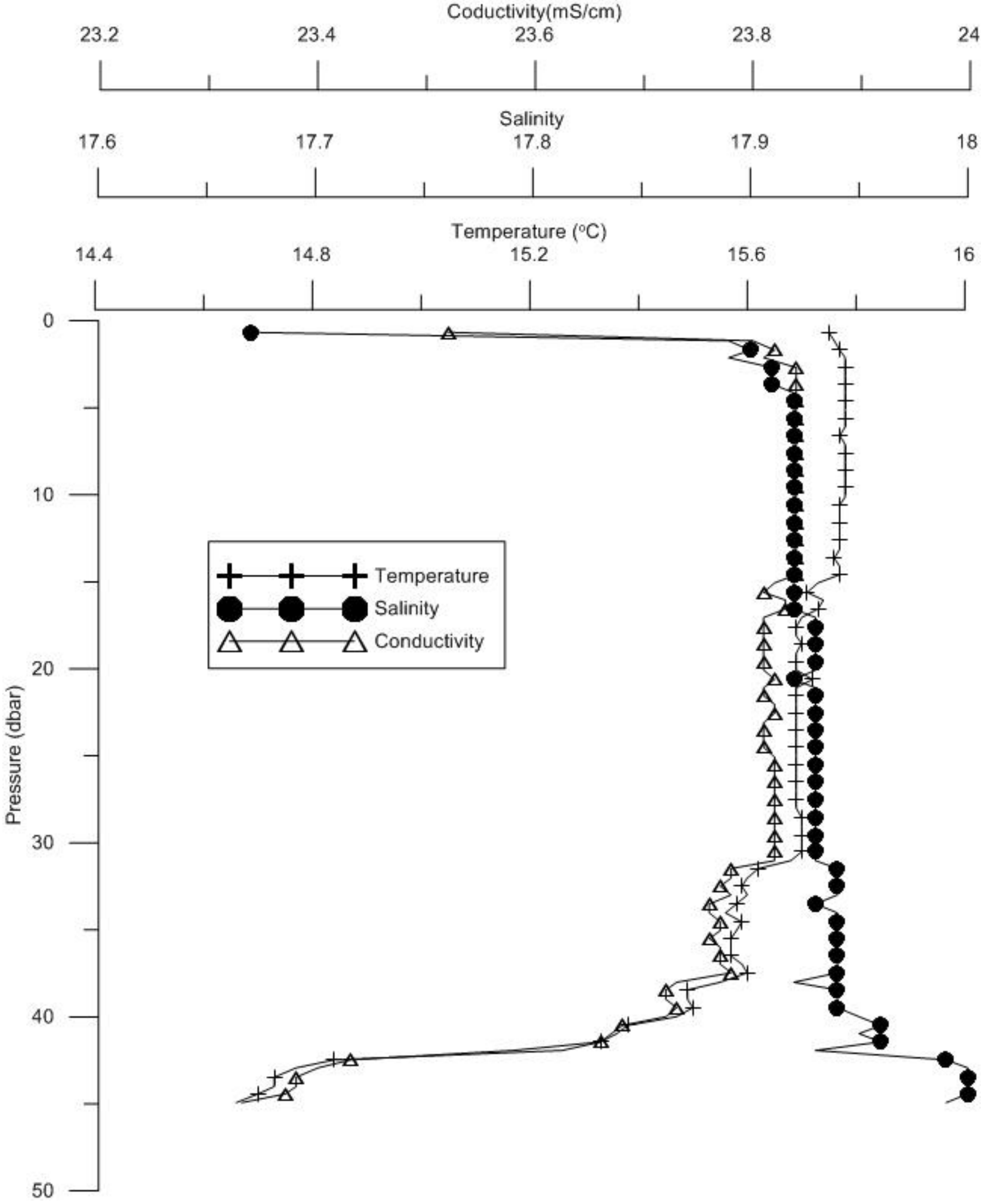

Figure 29.CTD from D9 Station for the first measurements in January2015

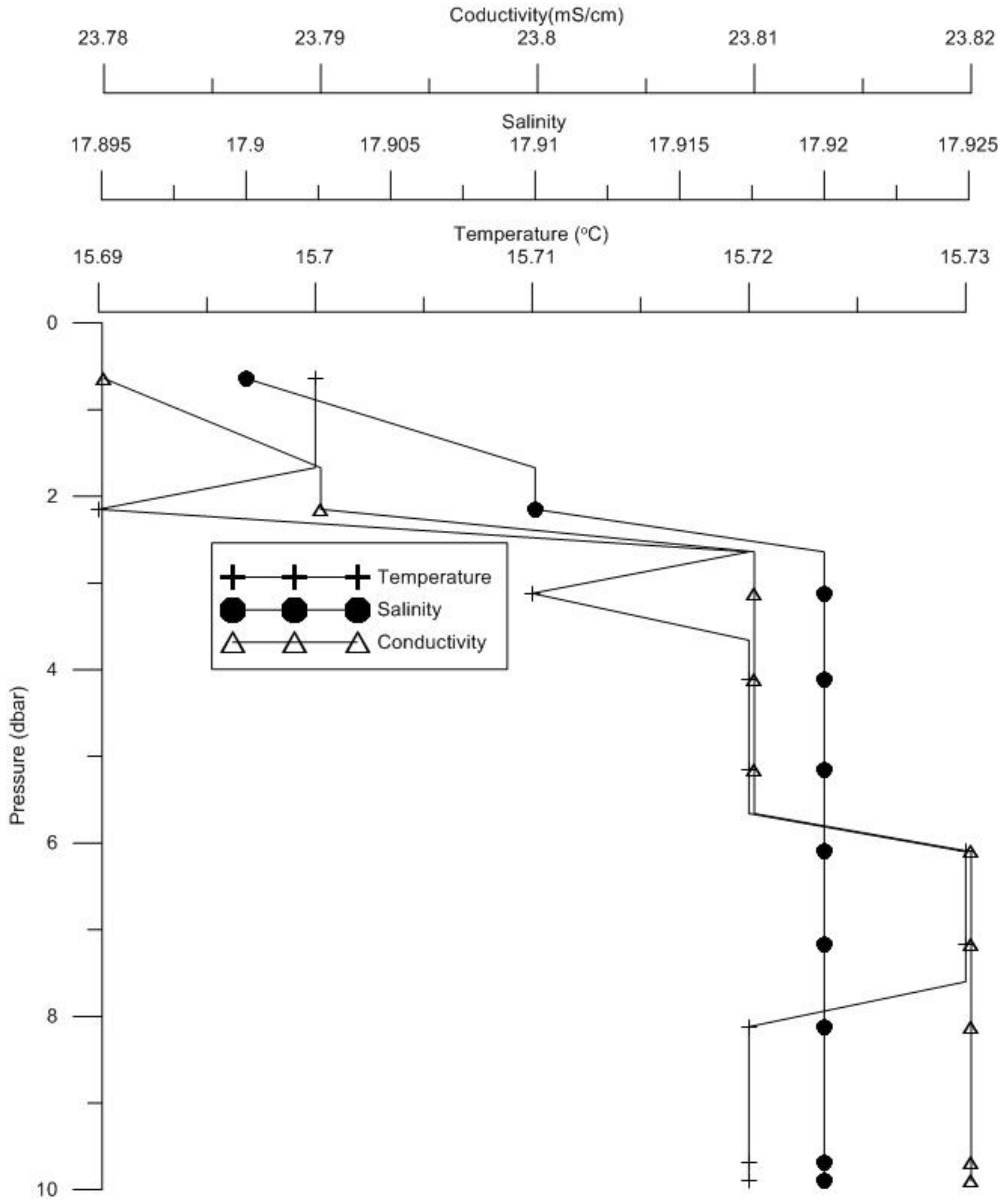

Figure 30.CTD from D10 Station for the first measurements in January2015

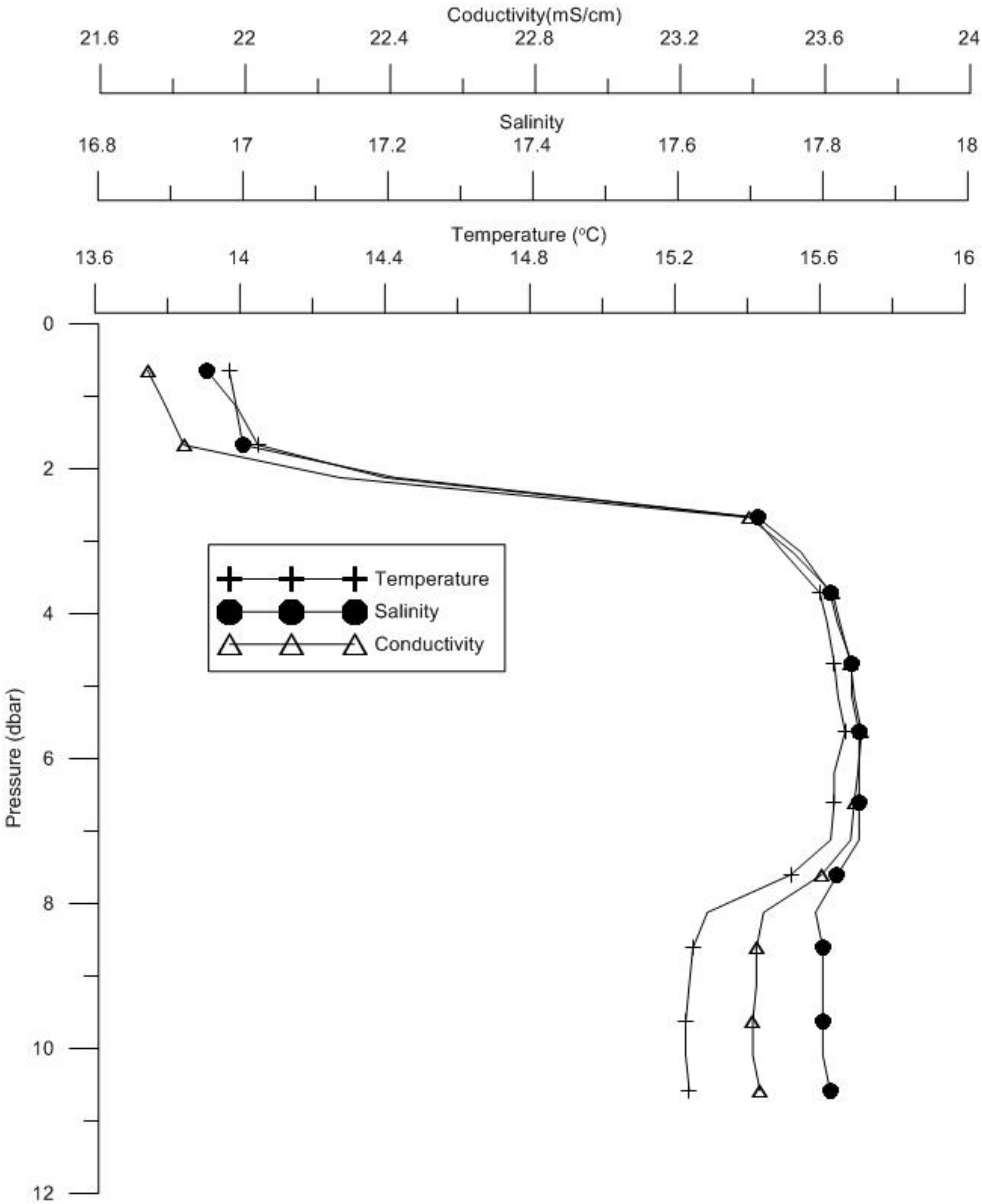

Figure 31.CTD from D11 Station for the first measurements in January2015

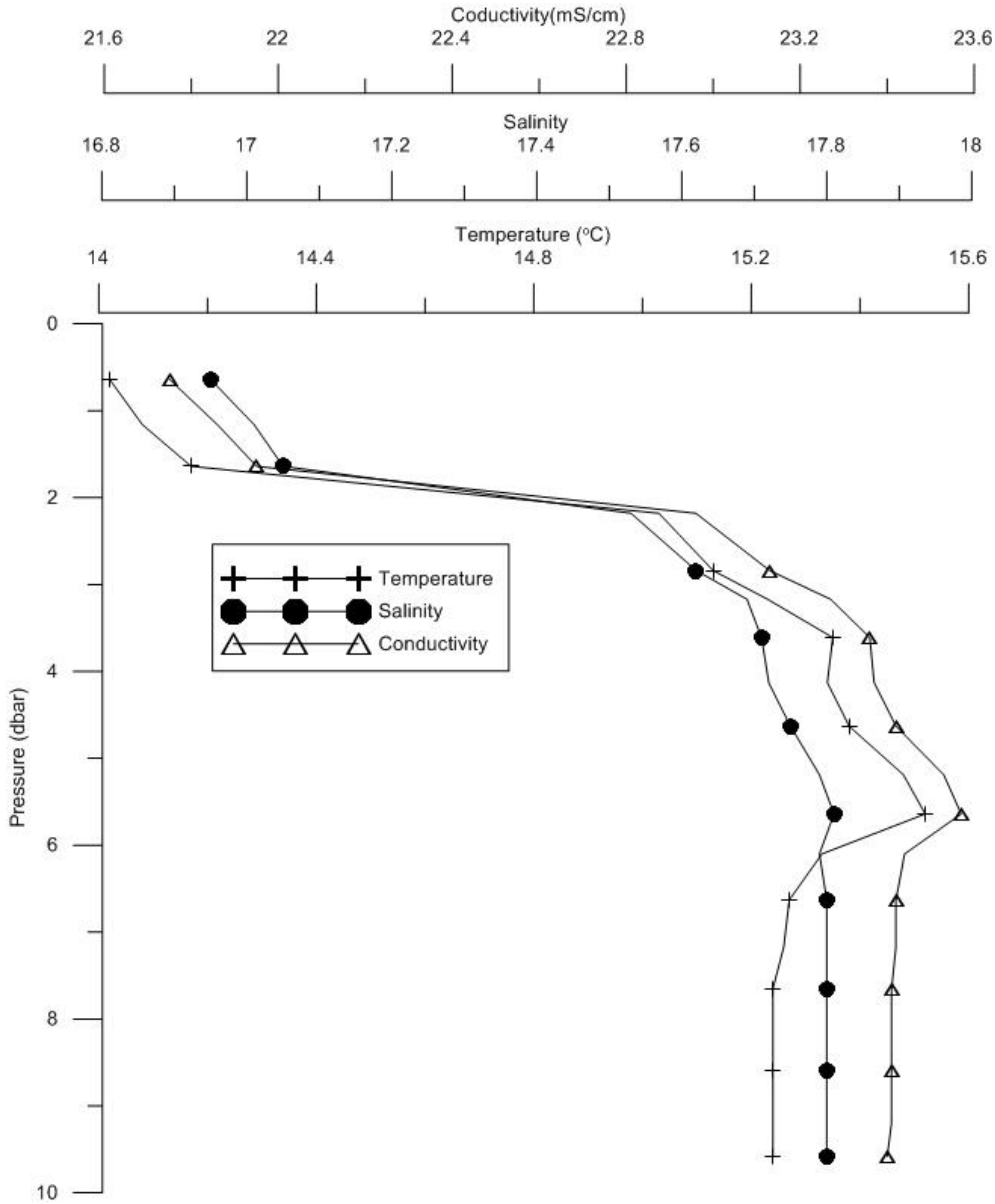

Figure 32.CTD from D12 Station for the first measurements in January2015

CTD graphs versus depth for each stations are given in the below. Conductivity, Salinity and Temperature results for the second period of January are given in Figures 33 -44.

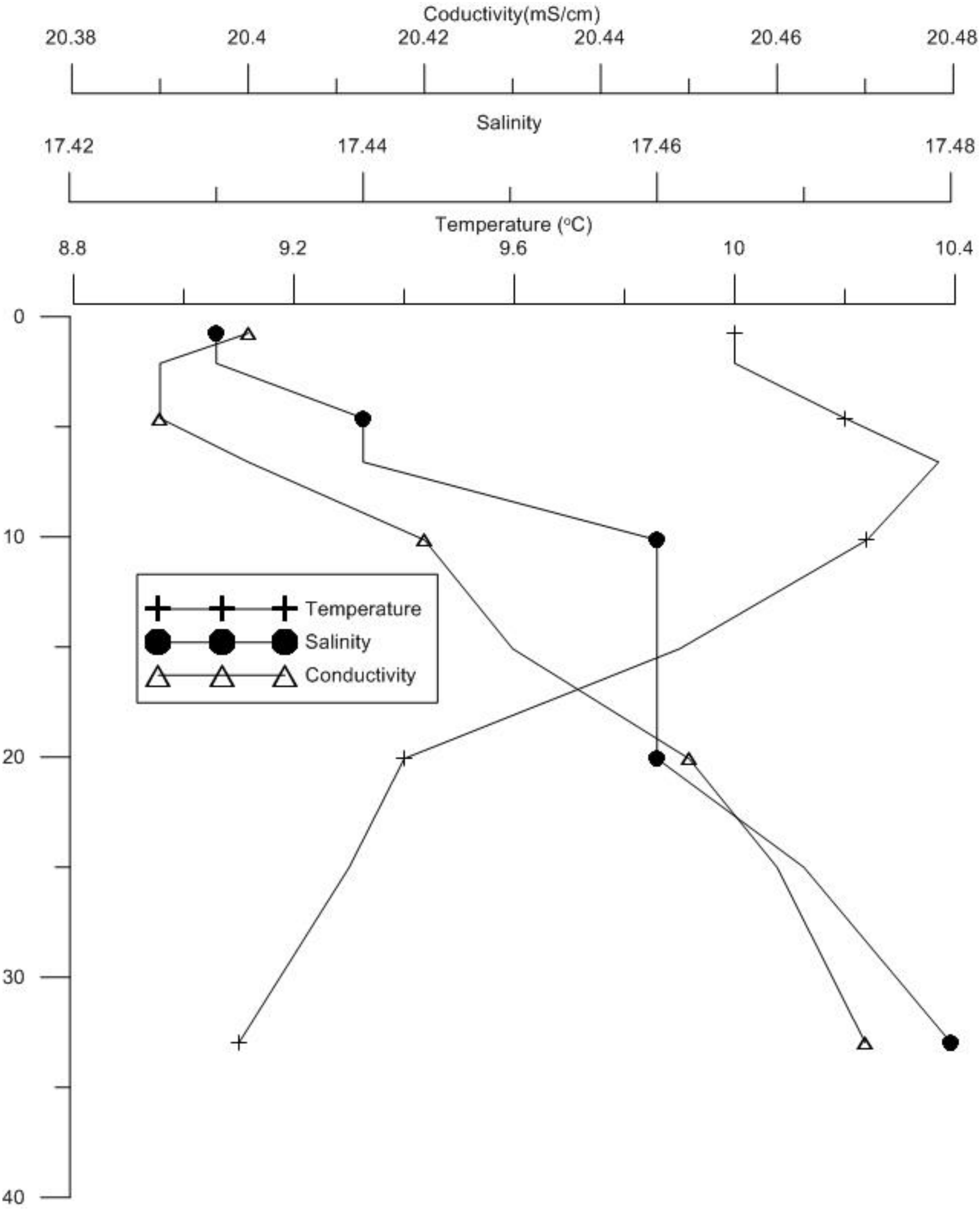

Figure 33. CTD from D1 Station for the second measurements in January2015

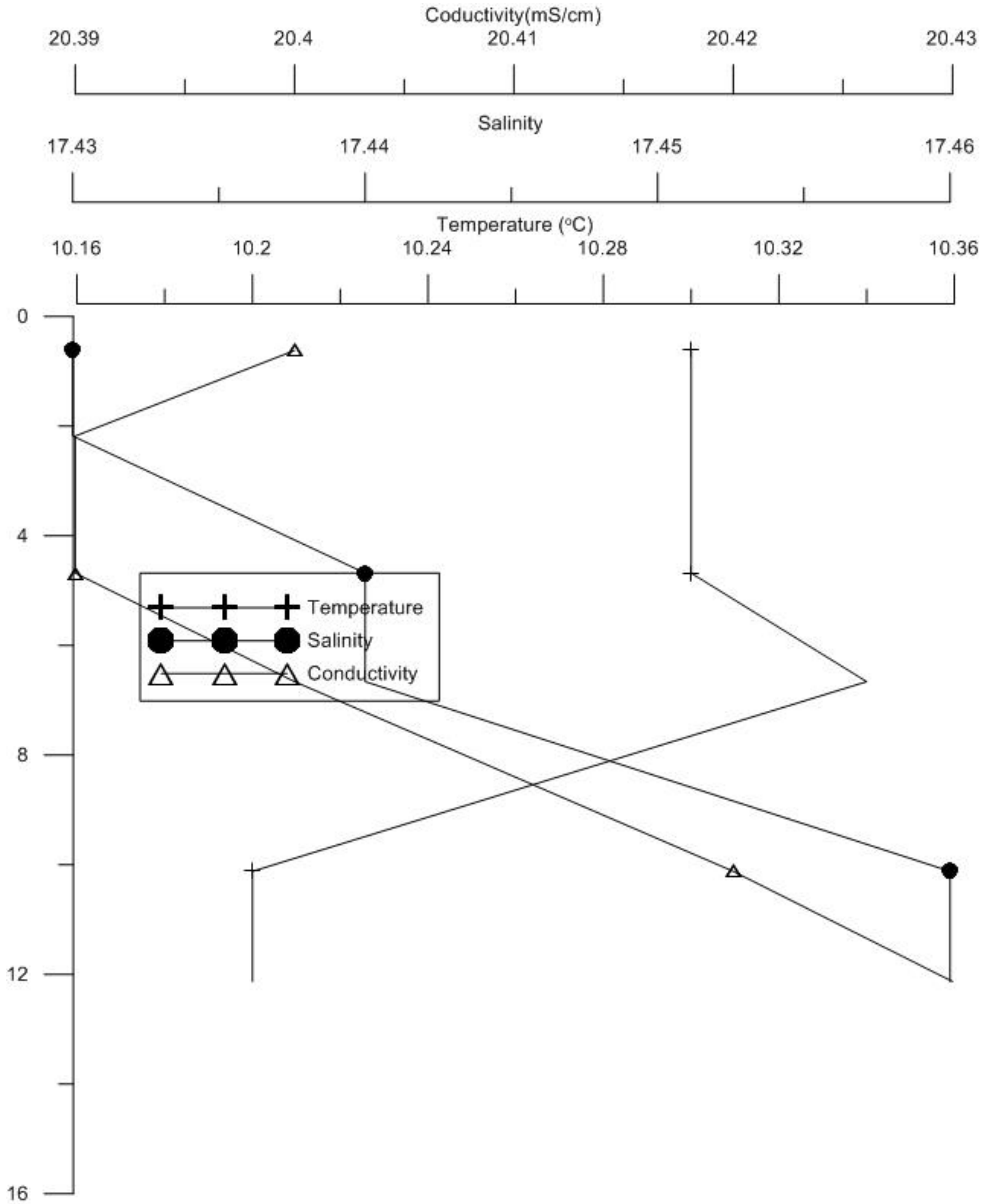

Figure 34.CTD from D2 Station for the second measurements in January2015

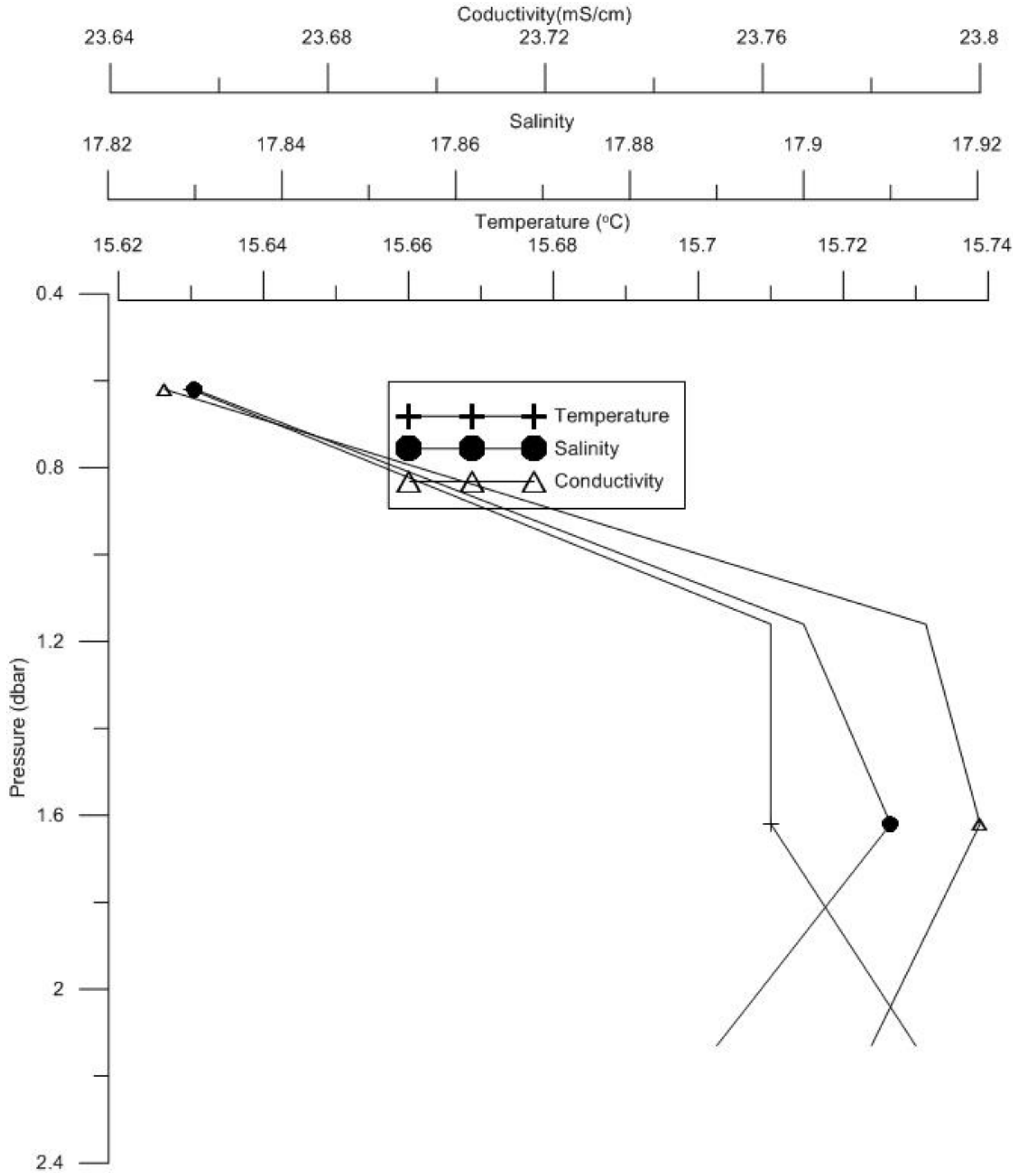

Figure 35.CTD from D3 Station for the second measurements in January2015

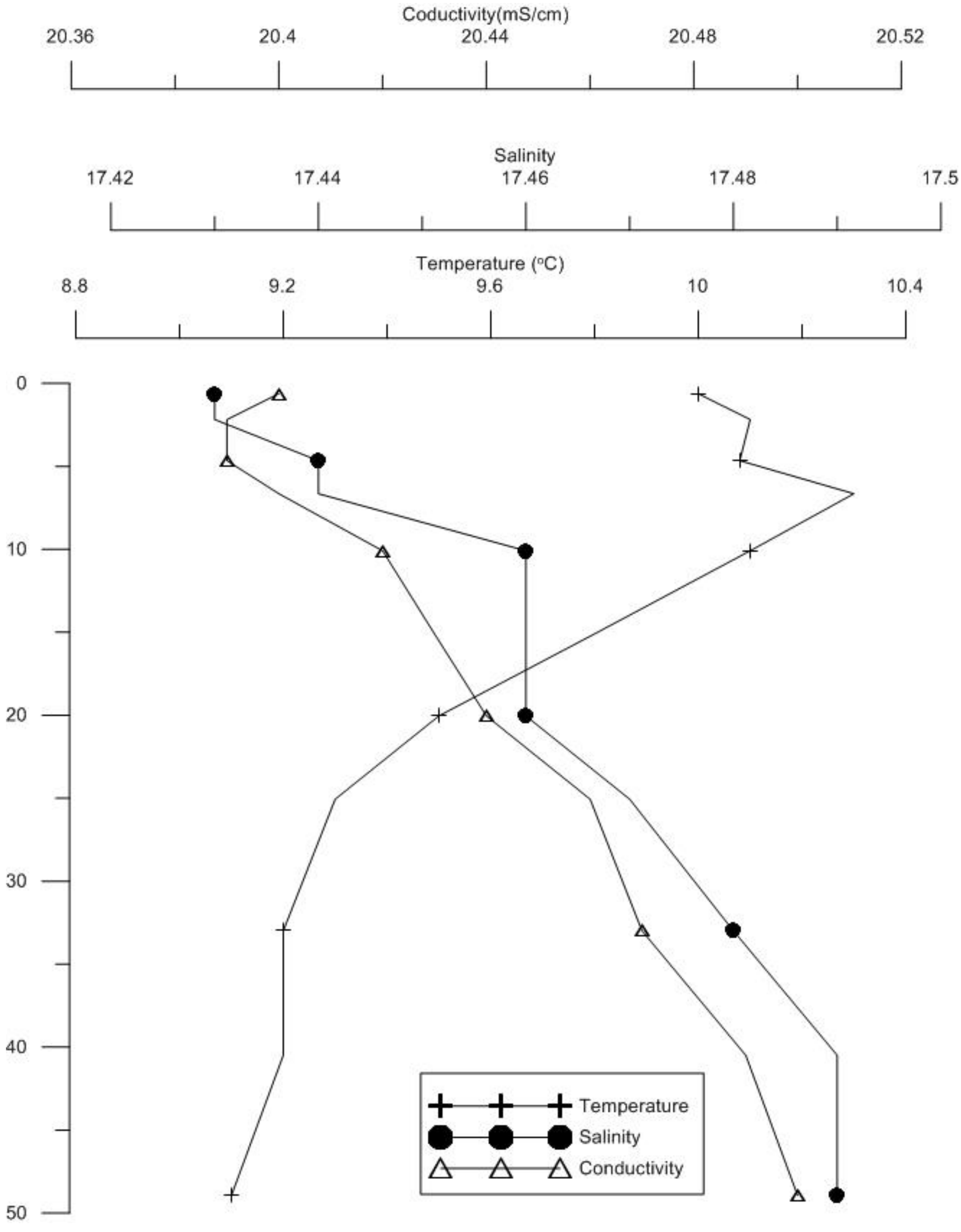

Figure 36.CTD from D4 Station for the second measurements in January2015

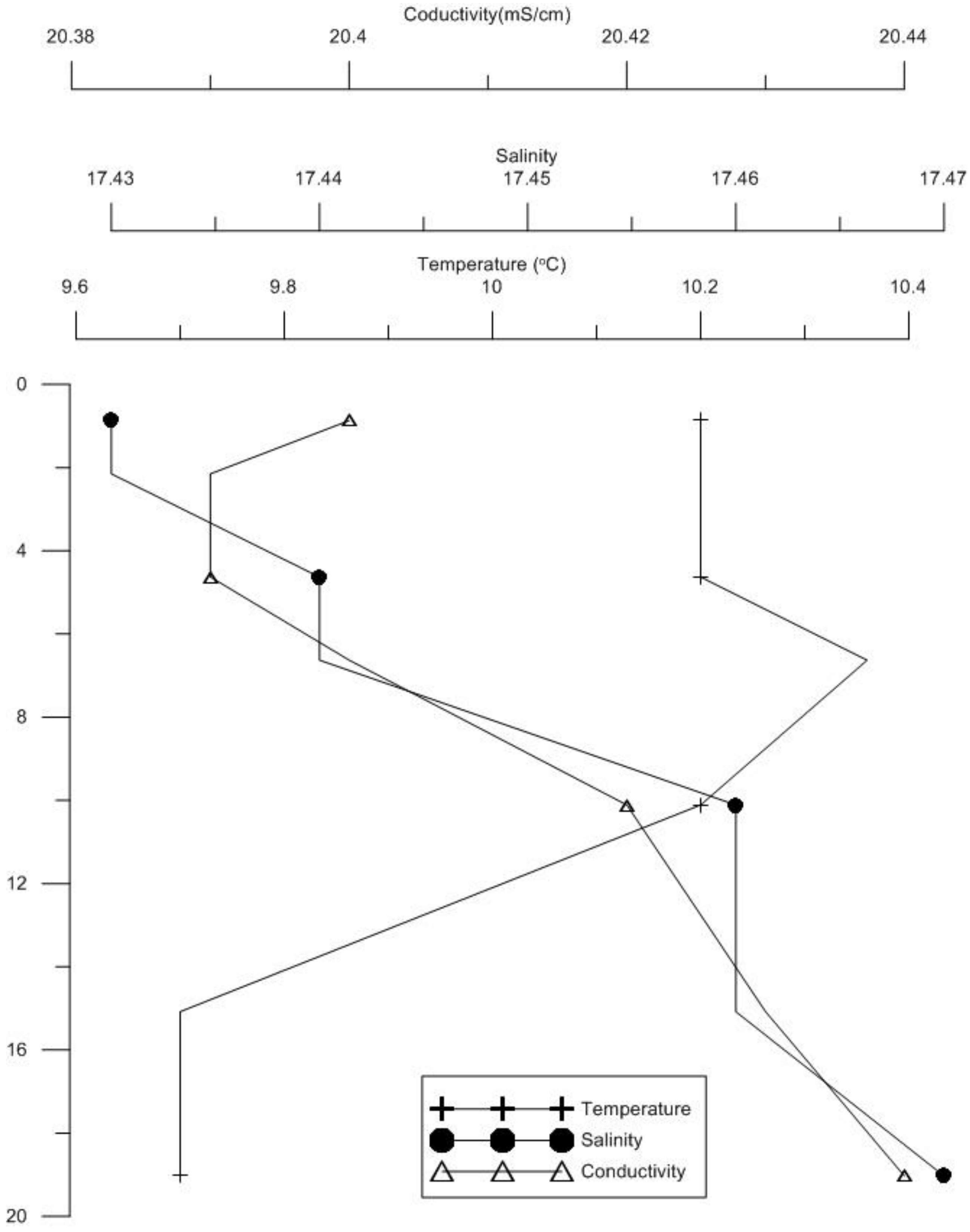

Figure 37.CTD from D5 Station for the second measurements in January2015

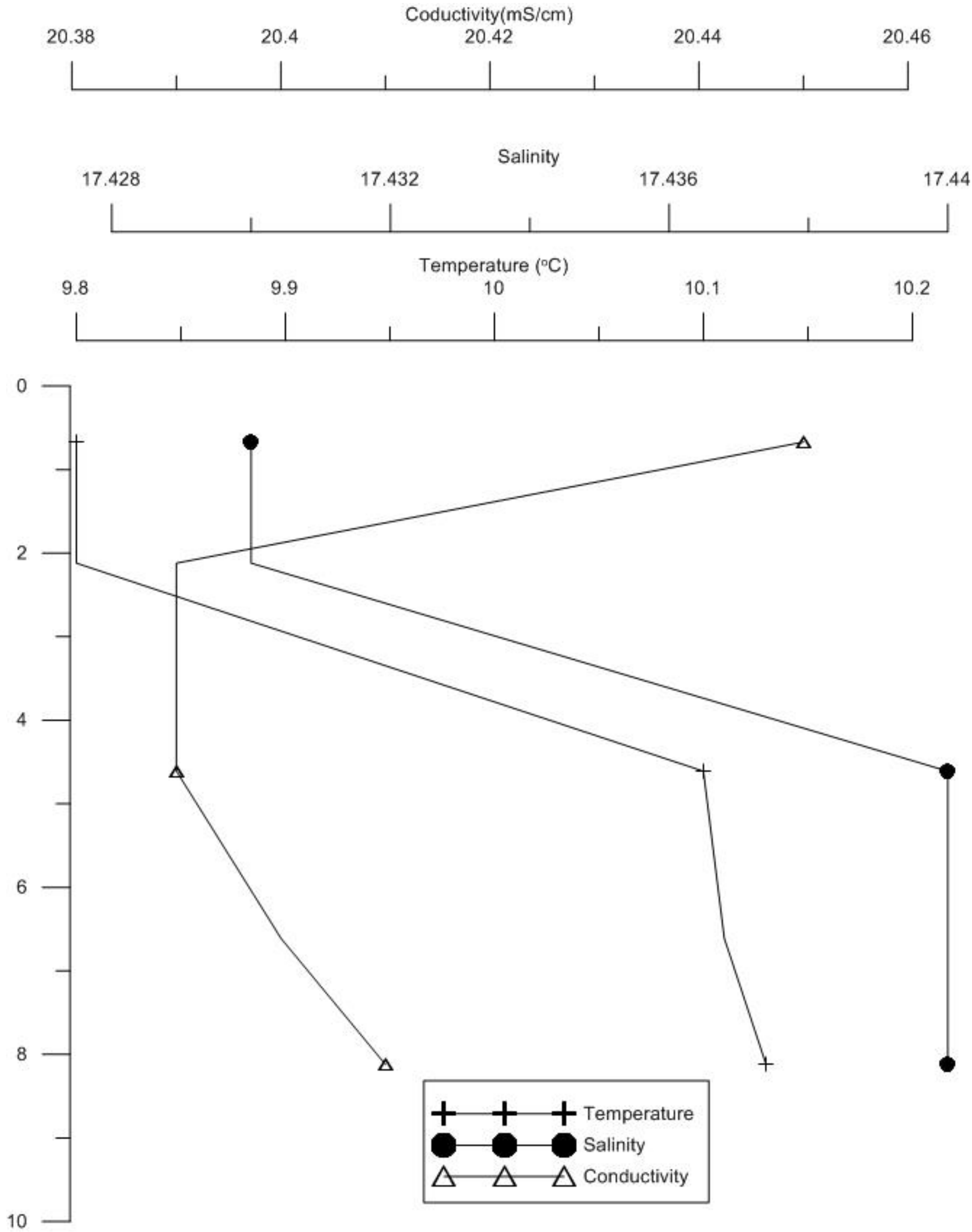

Figure 38.CTD from D6 Station for the second measurements in January2015

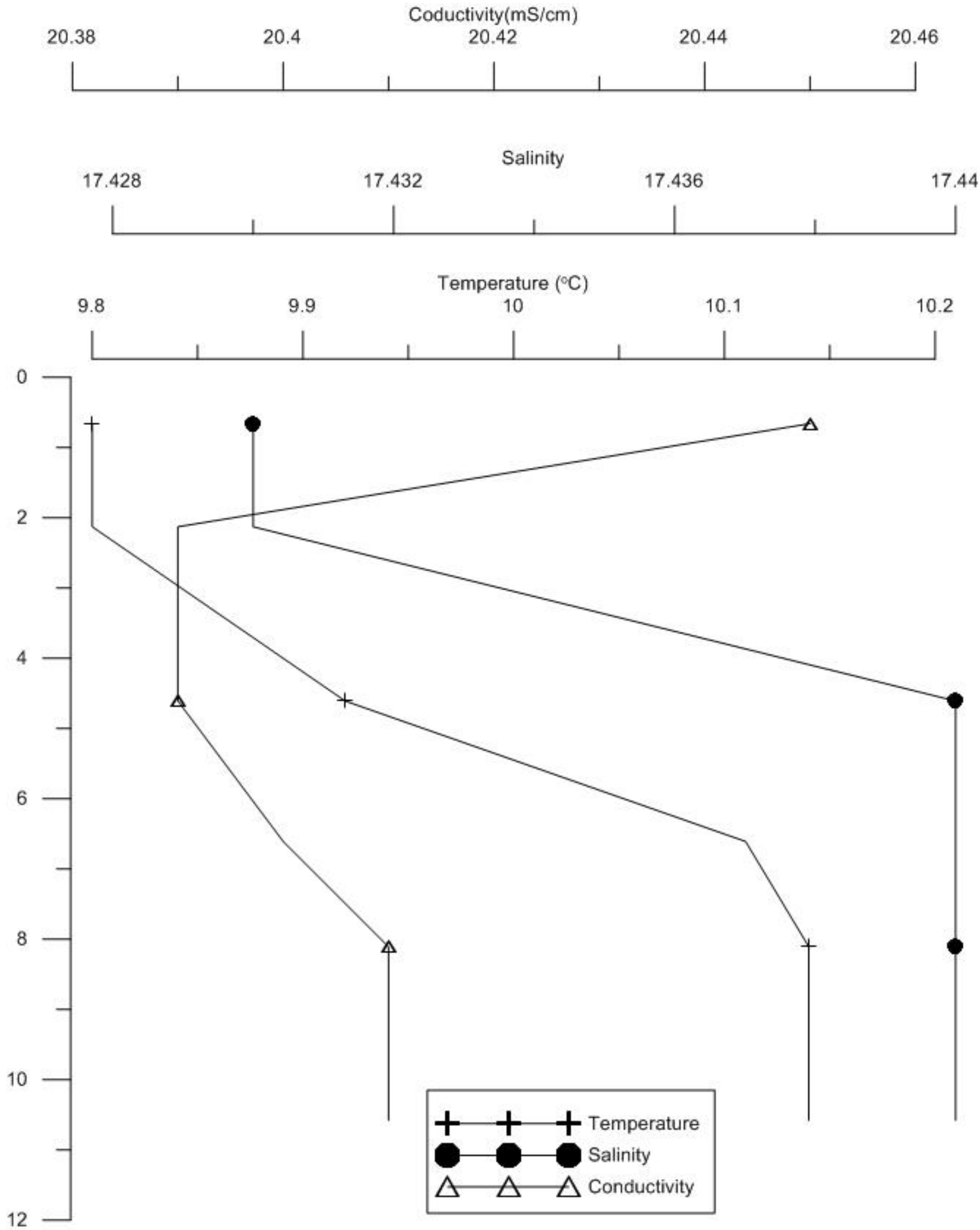

Figure 39.CTD from D7 Station for the second measurements in January2015

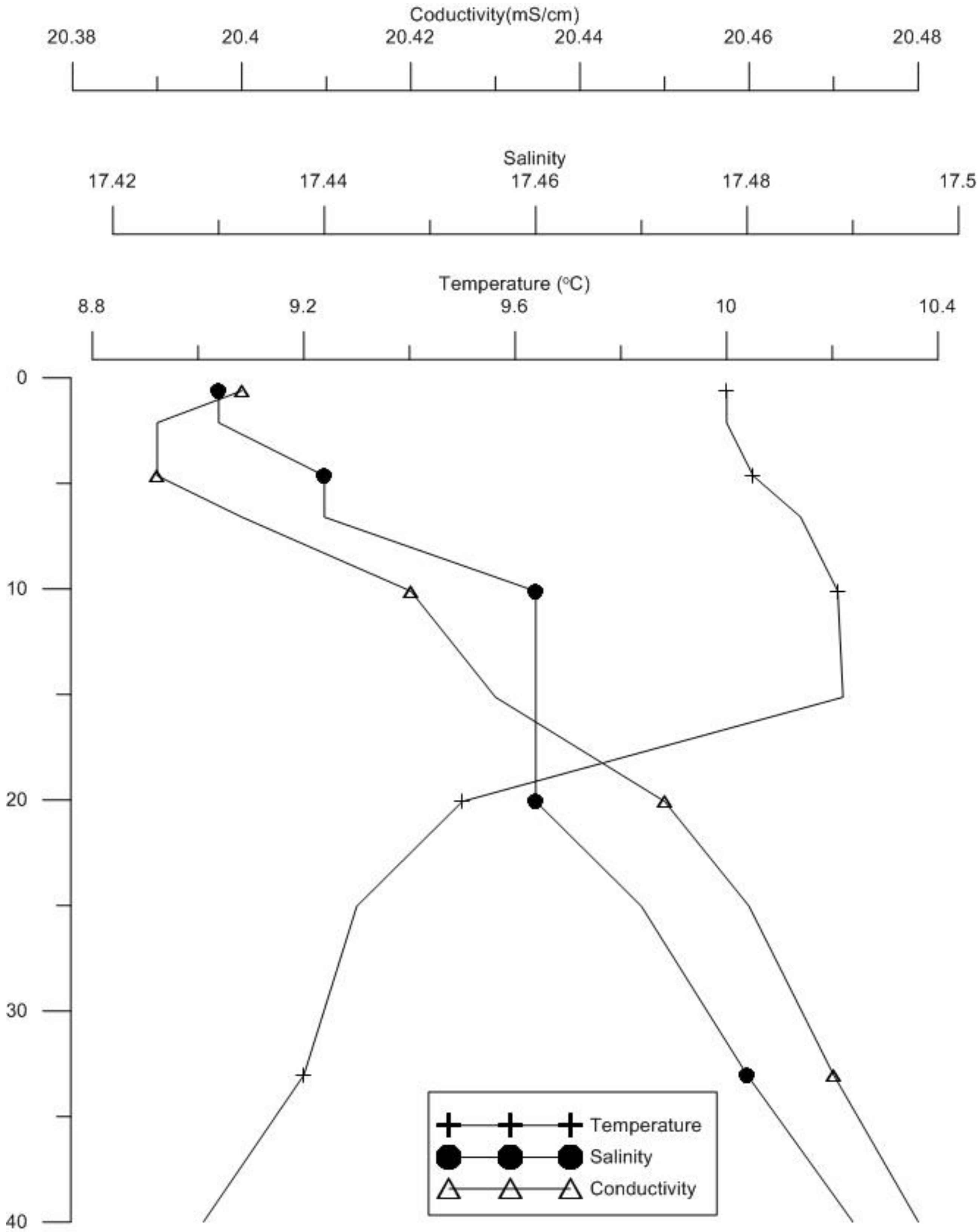

Figure 40.CTD from D8 Station for the second measurements in January2015

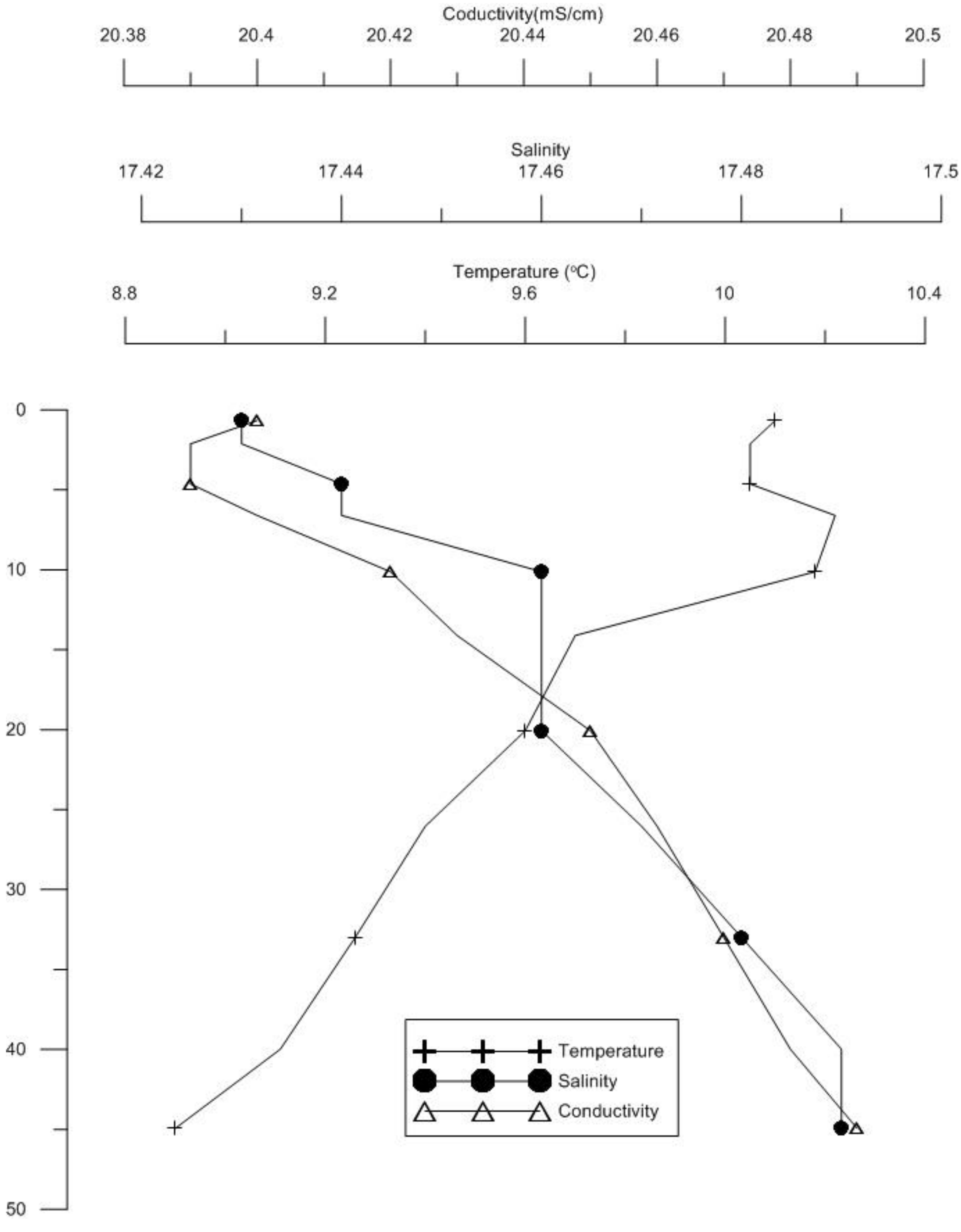

Figure 41.CTD from D9 Station for the second measurements in January2015

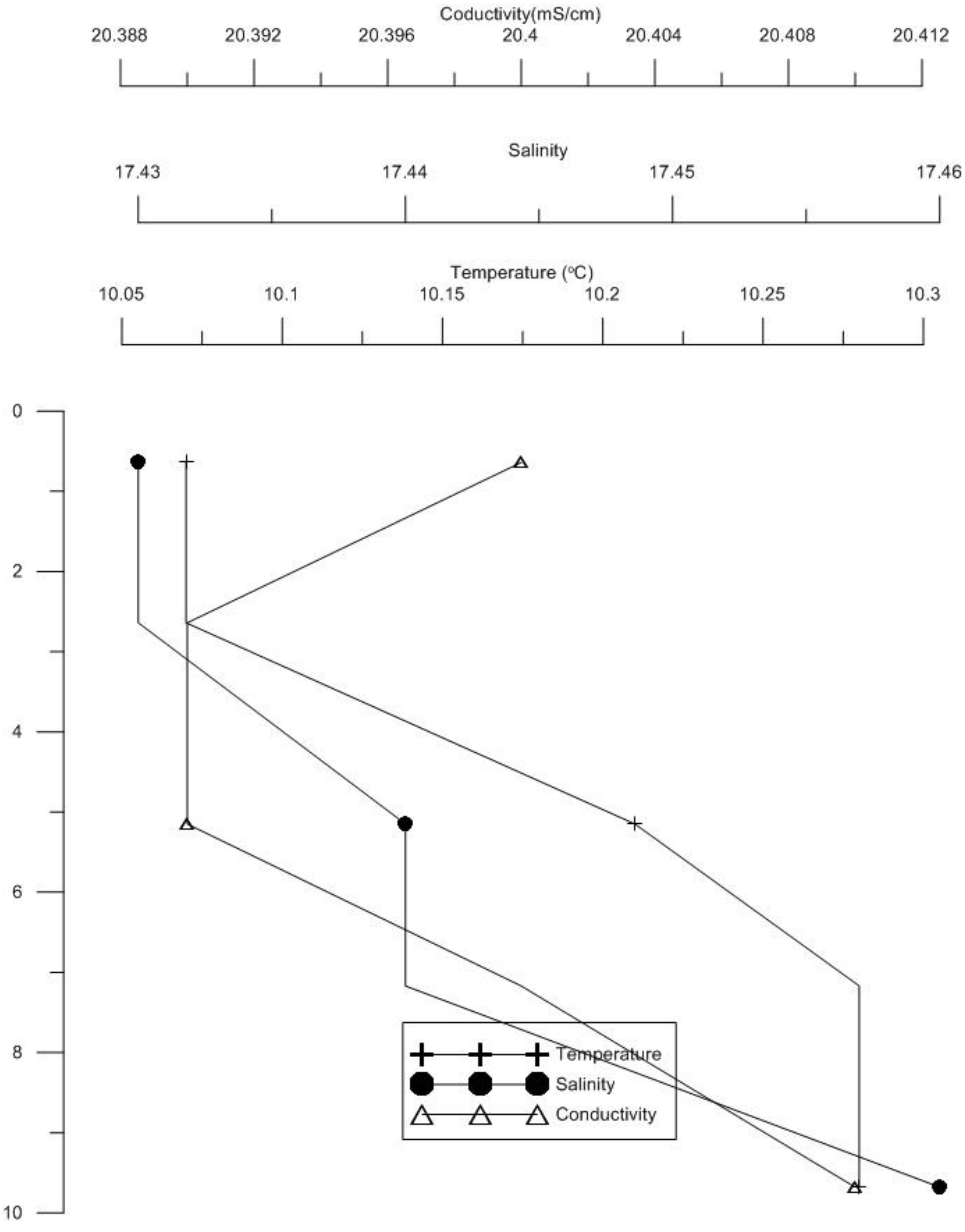

Figure 42.CTD from D10 Station for the second measurements in January2015

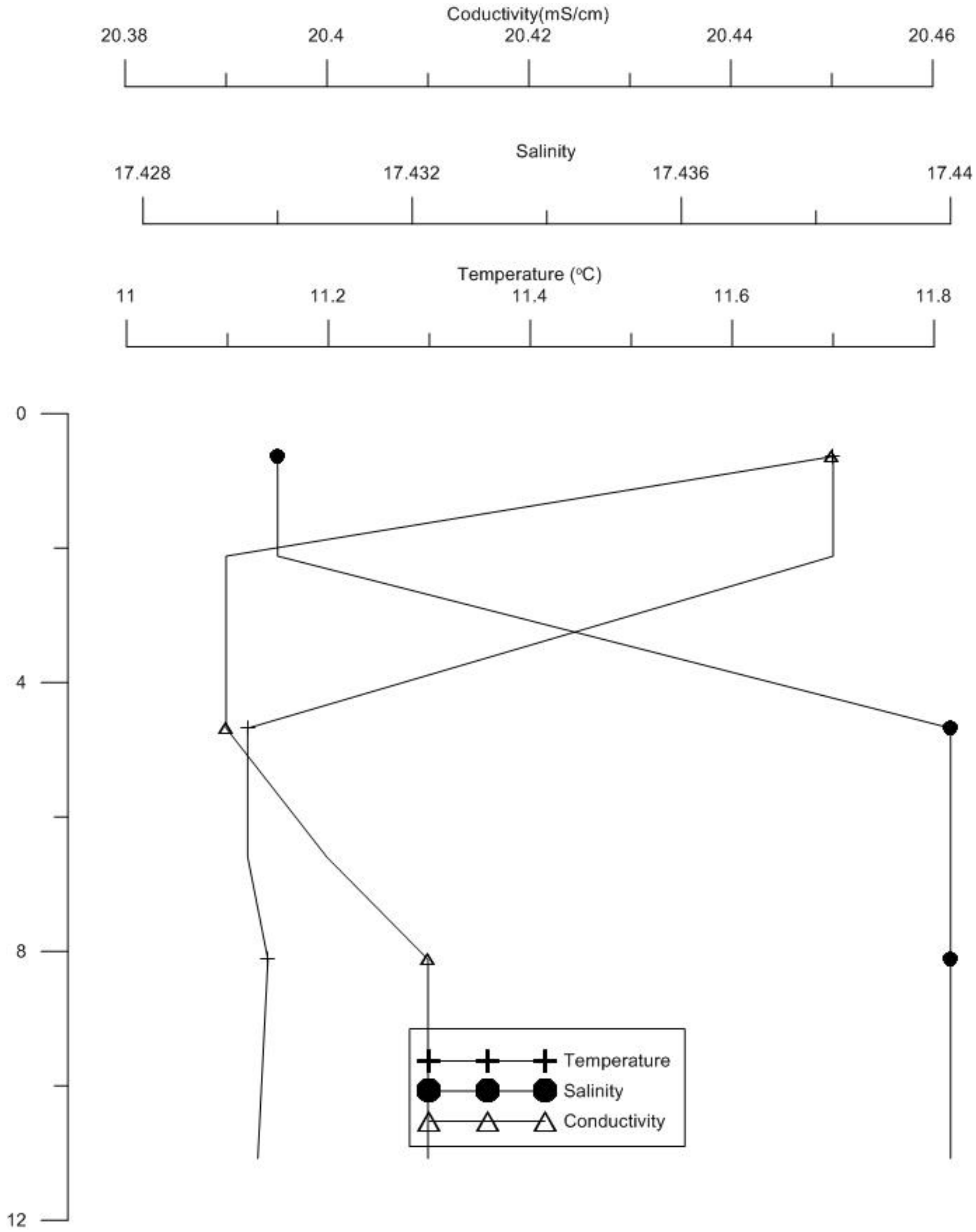

Figure 43.CTD from D11 Station for the second measurements in January2015

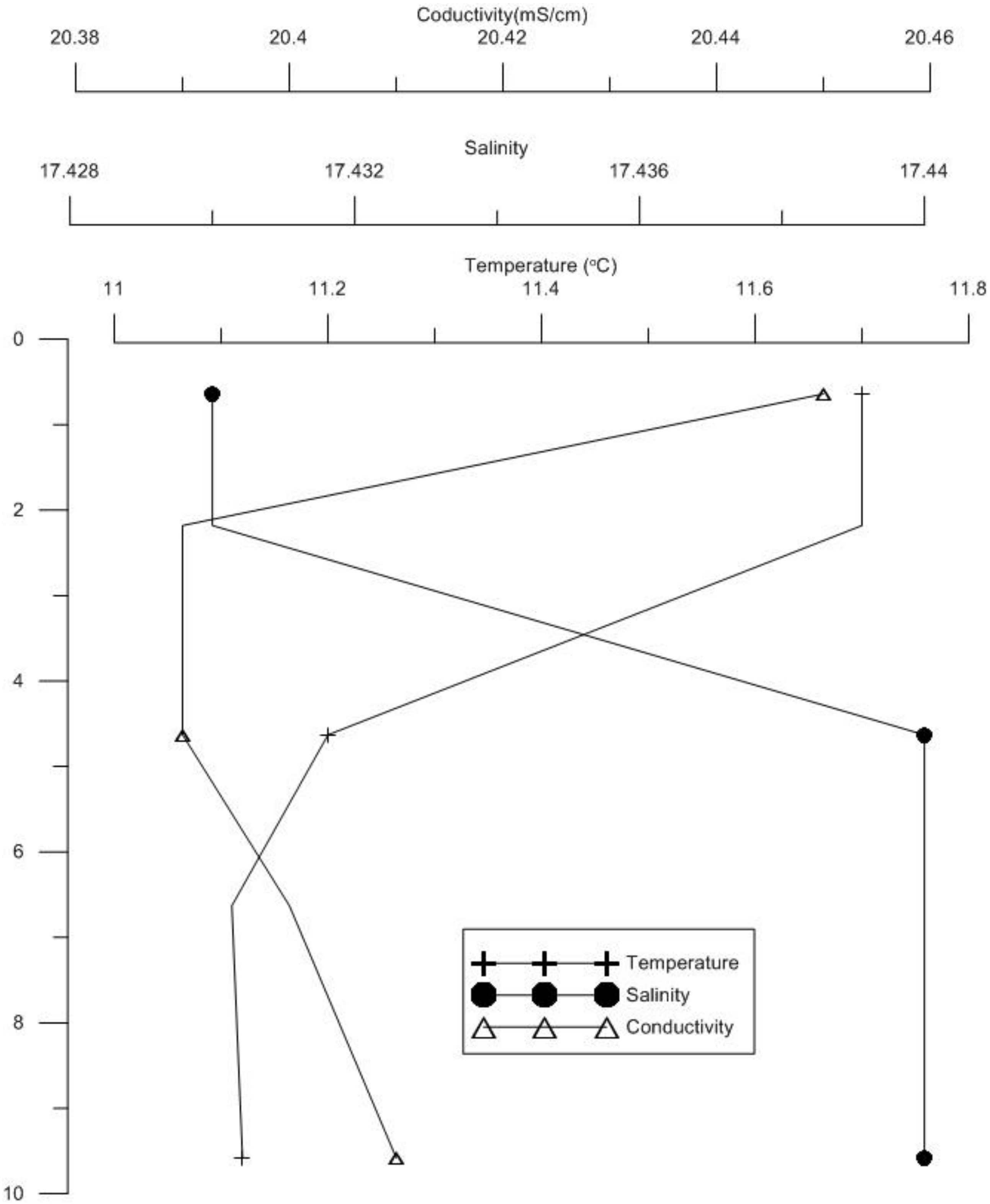

Figure 44.CTD from D12 Station for the second measurements in January2015

CTD graphs versus depth for each stations are given in the below. Conductivity, Salinity and Temperature results for the first period of February are given in Figures 45 -56.

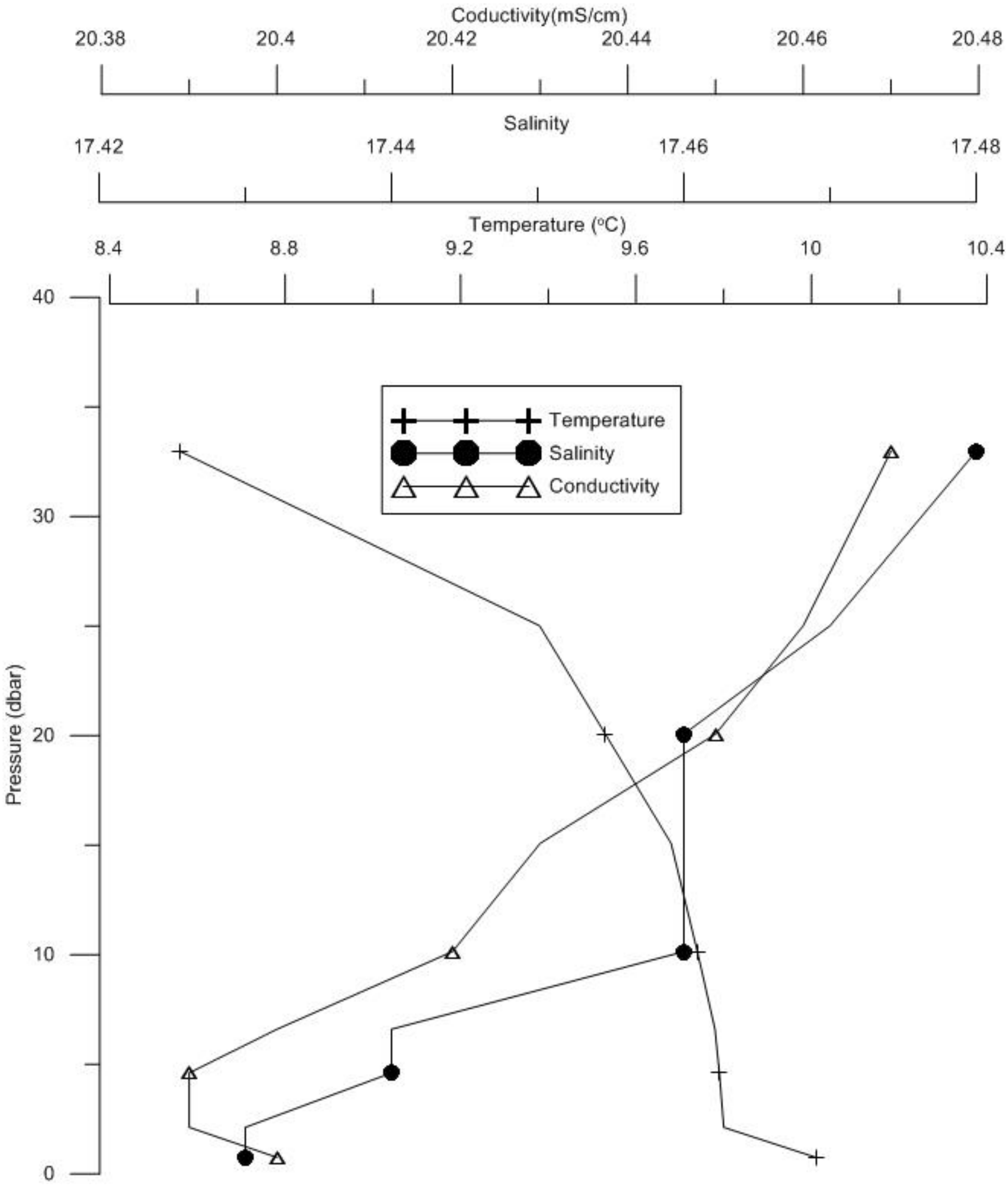

Figure 45. CTD from D1 Station for the first measurements in February2015

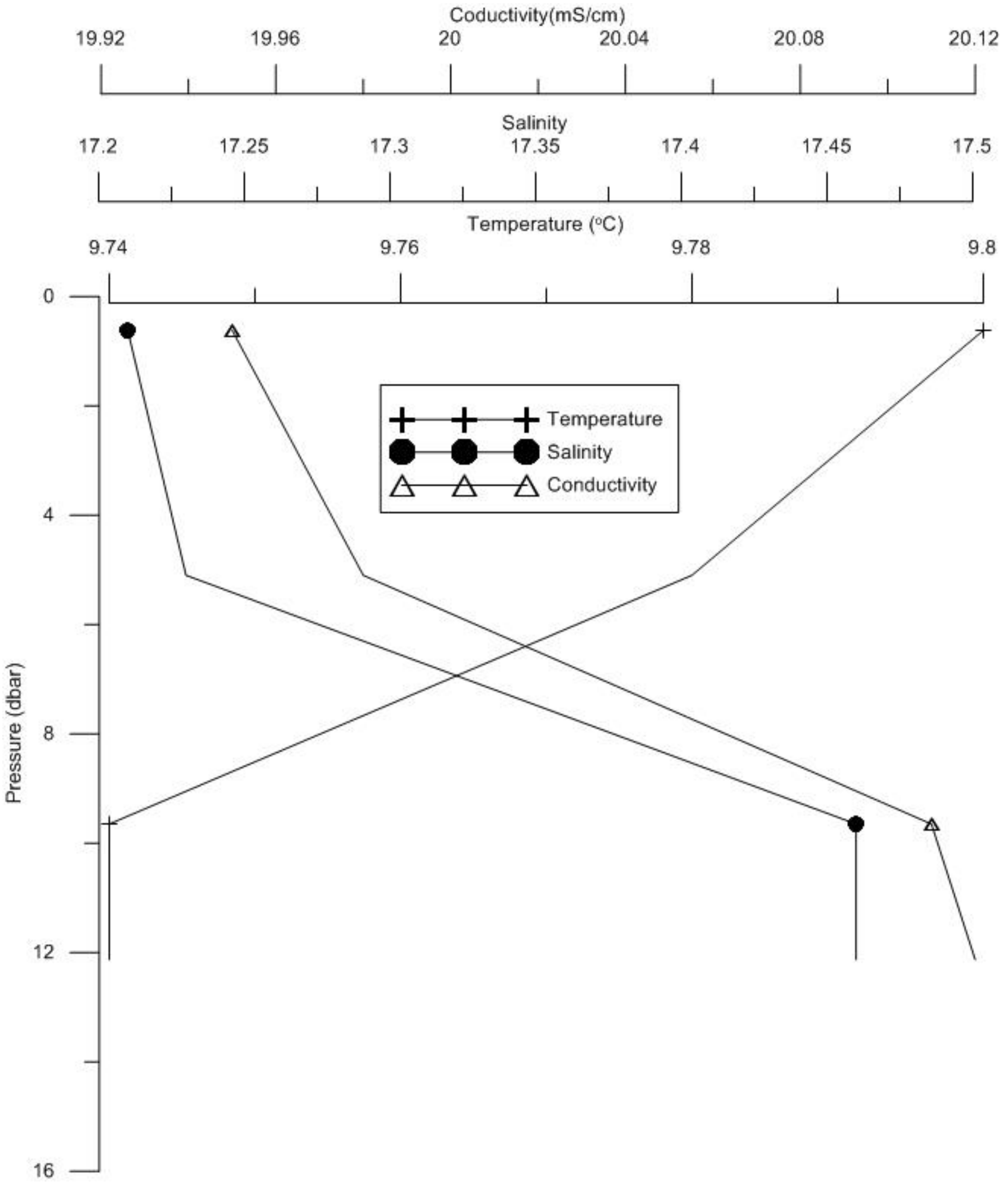

Figure 46.CTD from D2 Station for the first measurements in February2015

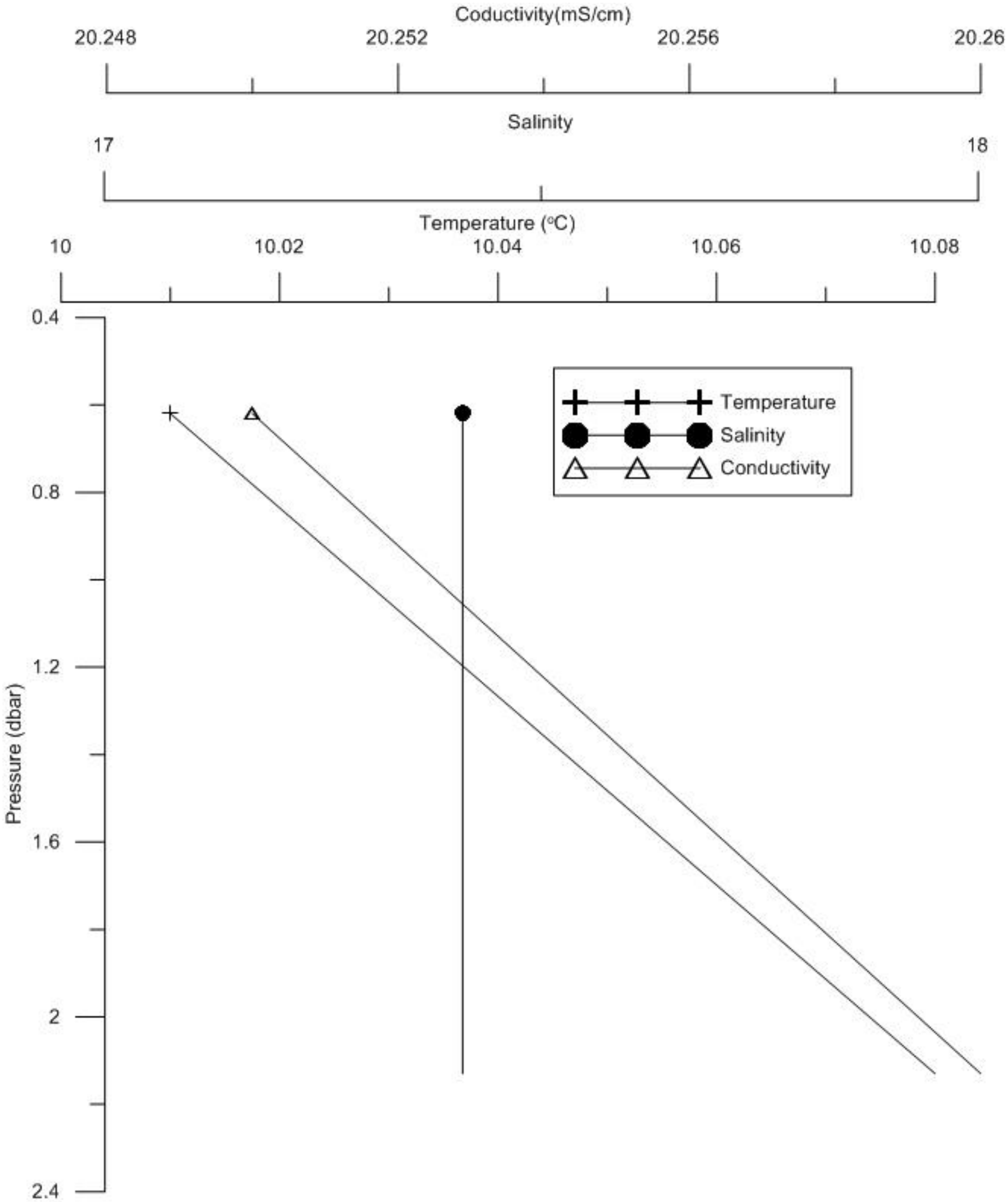

Figure 47.CTD from D3 Station for the first measurements in February2015

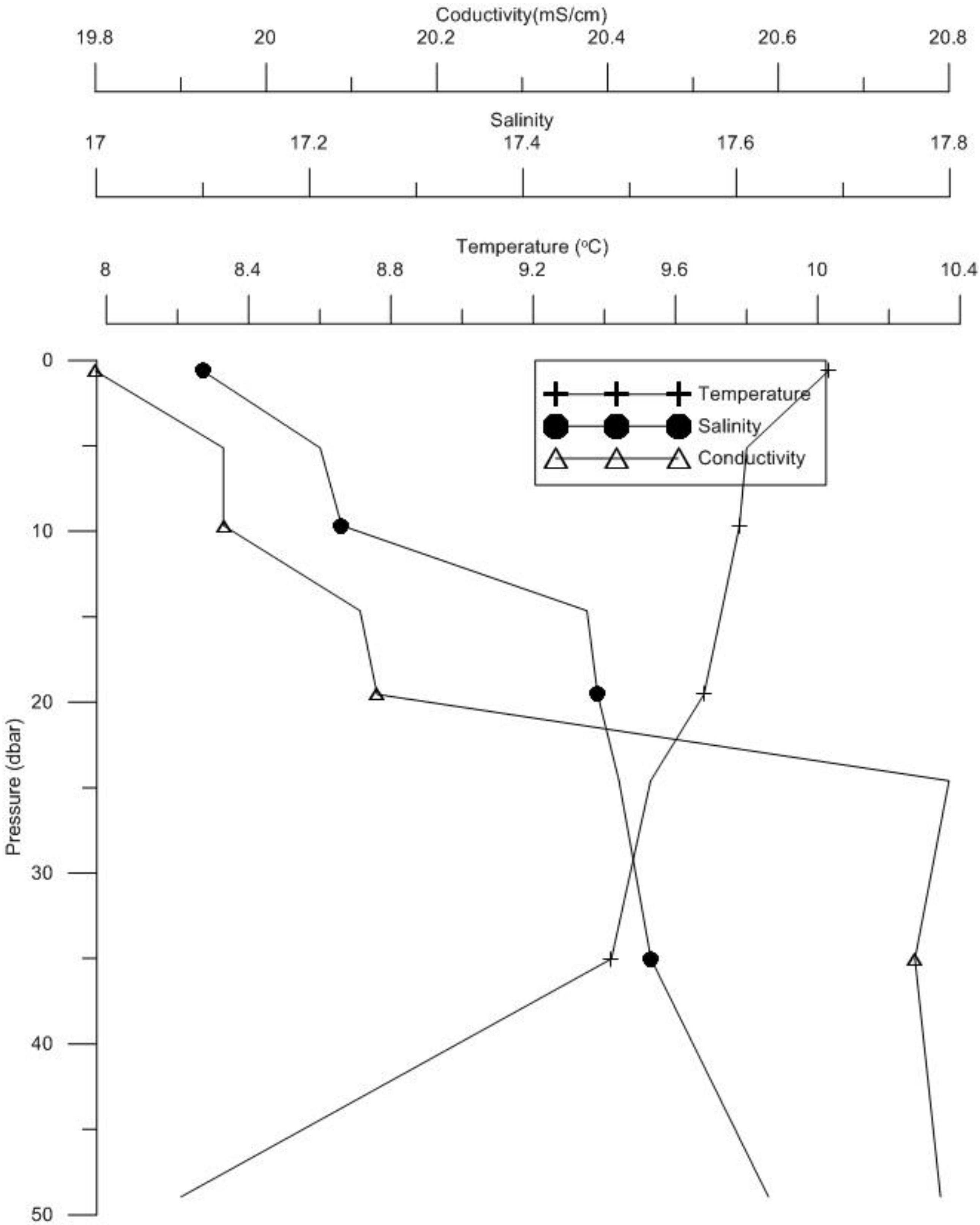

Figure 48.CTD from D4 Station for the first measurements in February2015

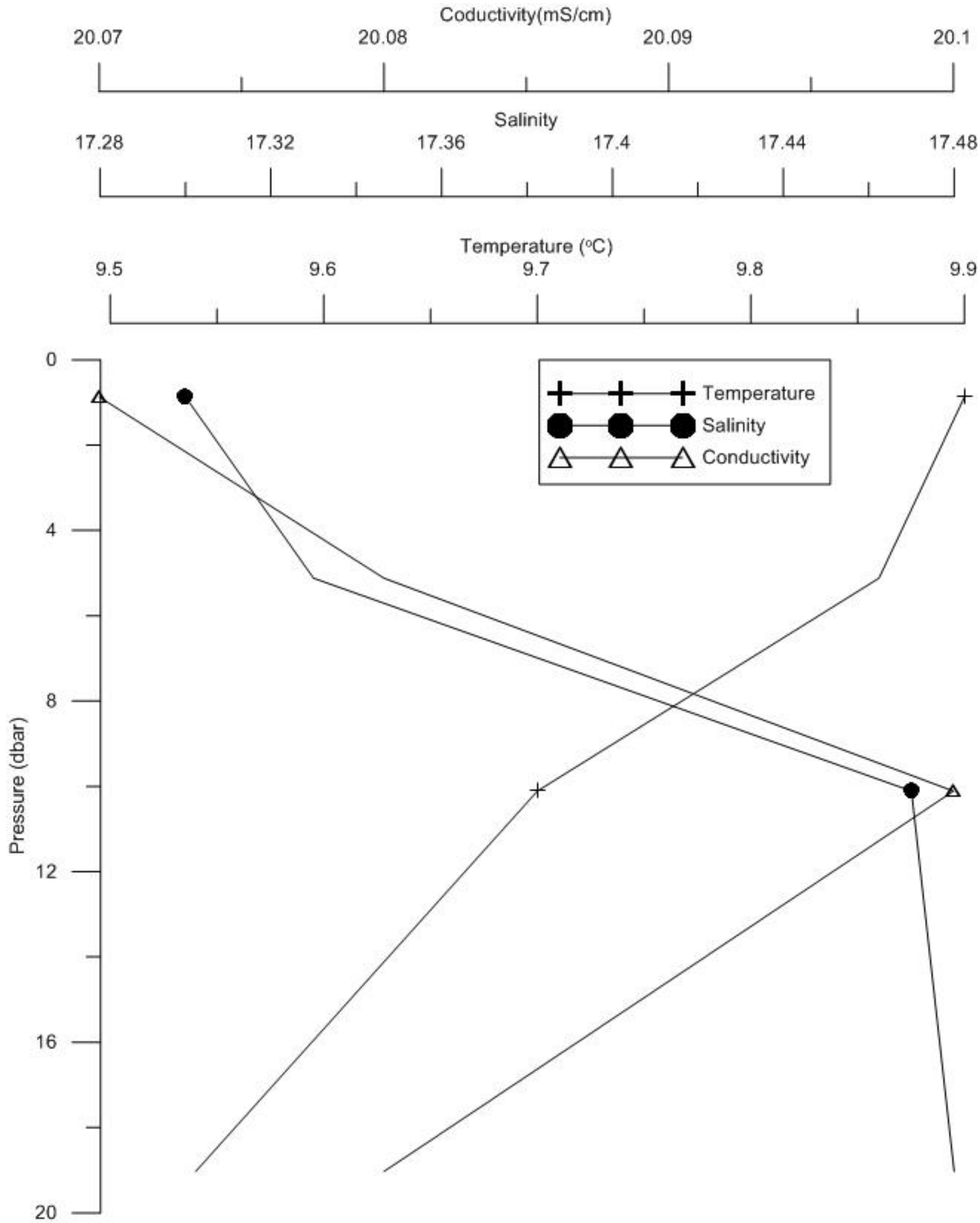

Figure 49.CTD from D5 Station for the first measurements in February2015

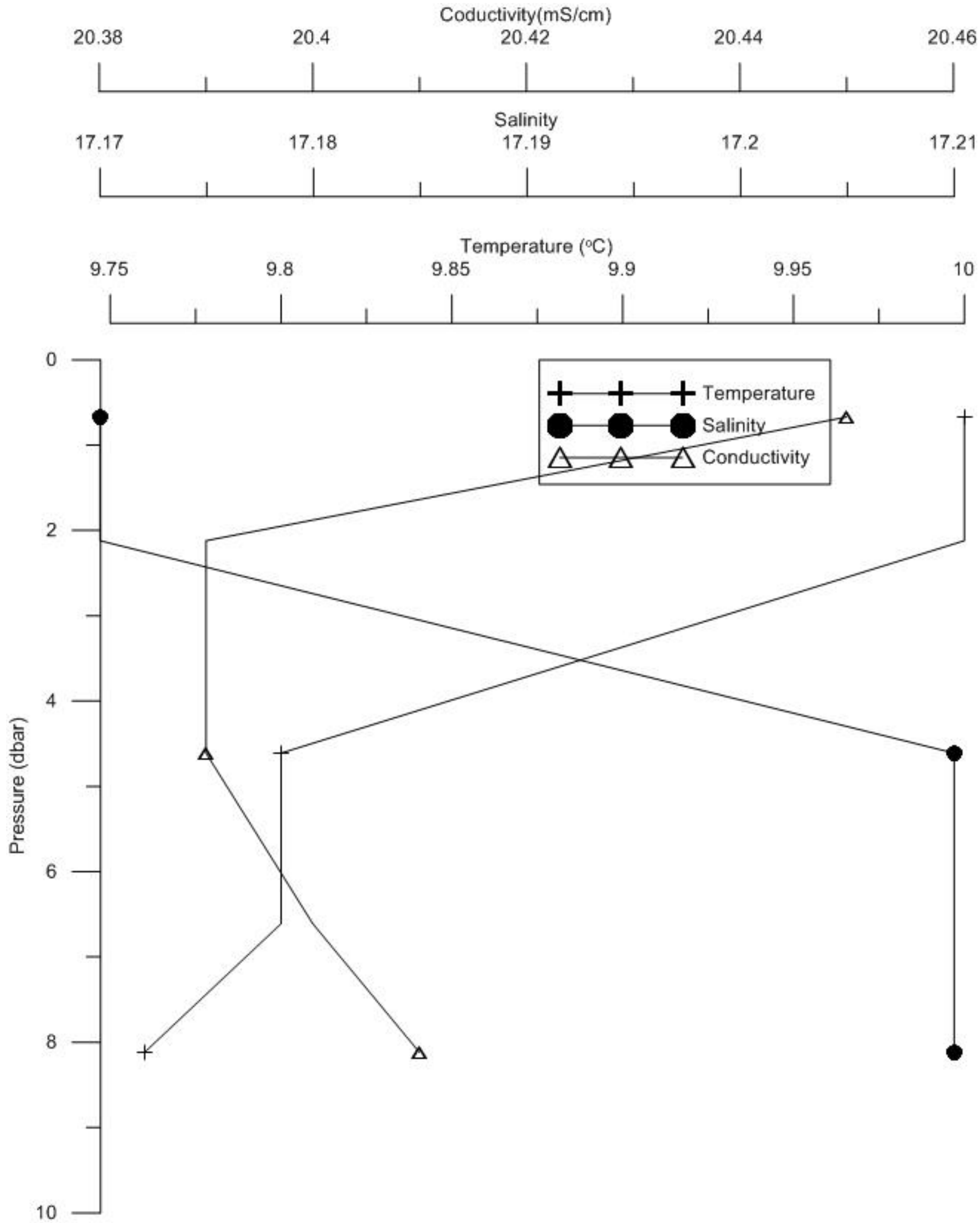

Figure 50.CTD from D6 Station for the first measurements in February2015

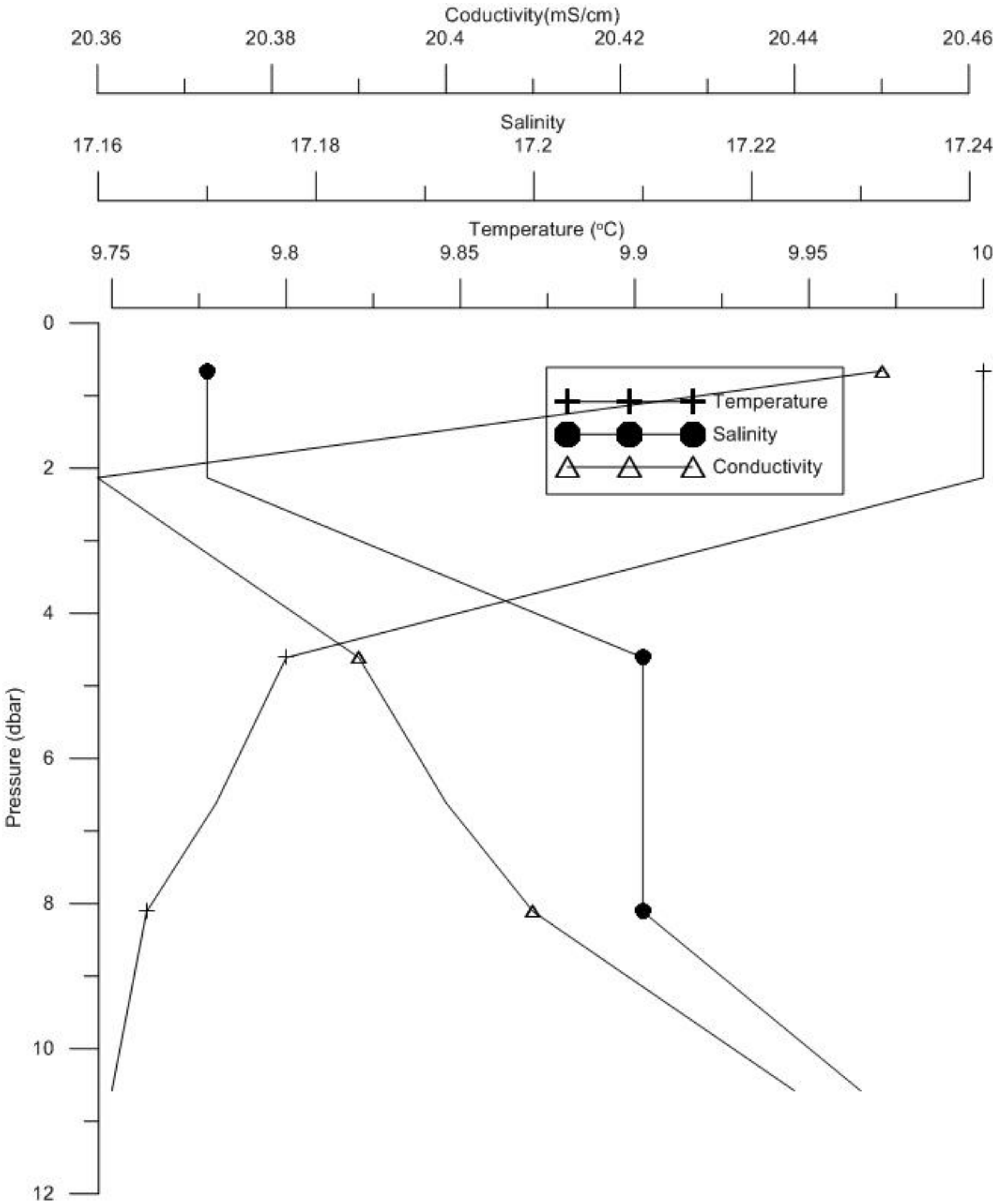

Figure 51.CTD from D7 Station for the first measurements in February2015

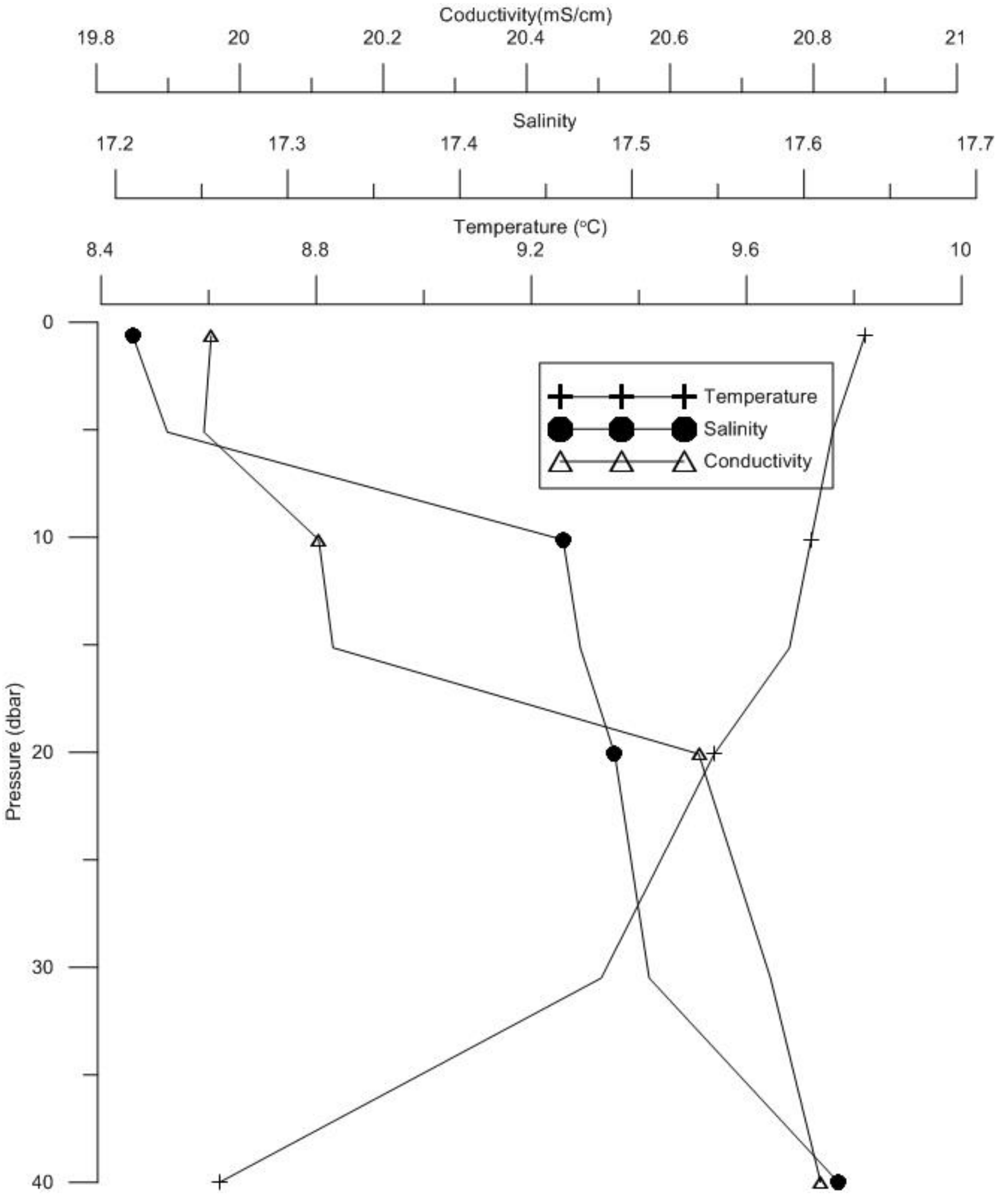

Figure 52.CTD from D8 Station for the first measurements in February2015

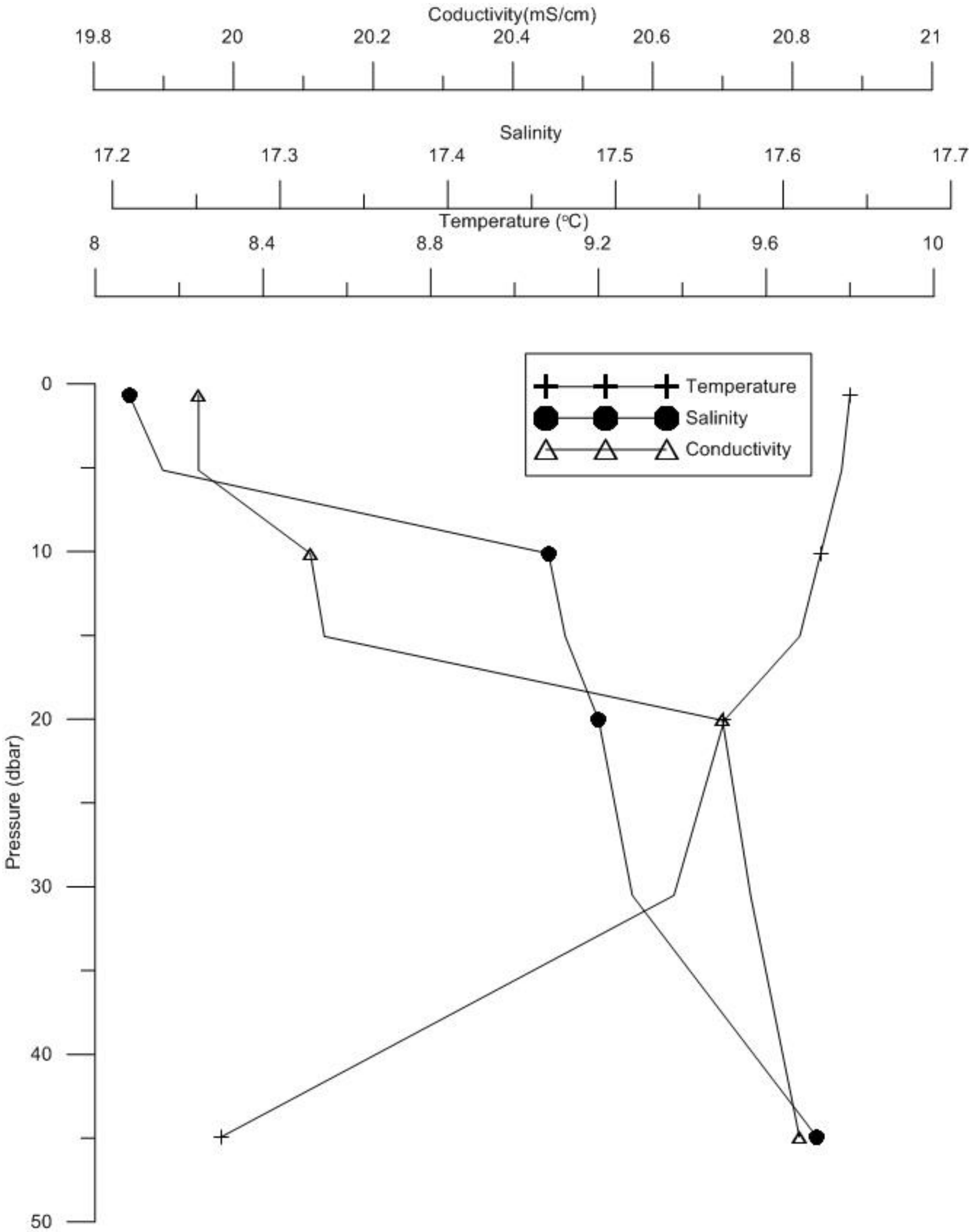

Figure 53.CTD from D9 Station for the first measurements in February2015

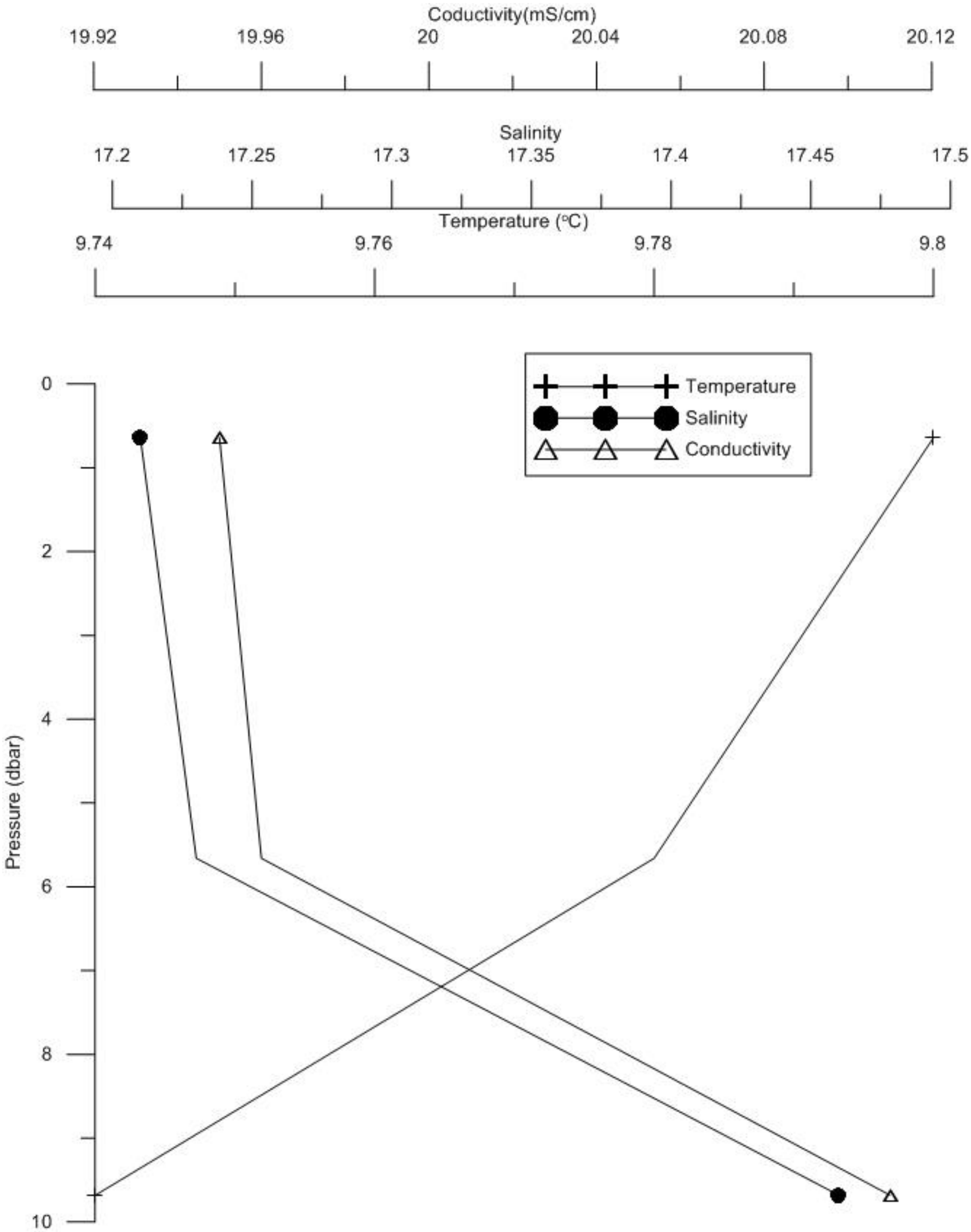

Figure 54.CTD from D10 Station for the first measurements in February2015

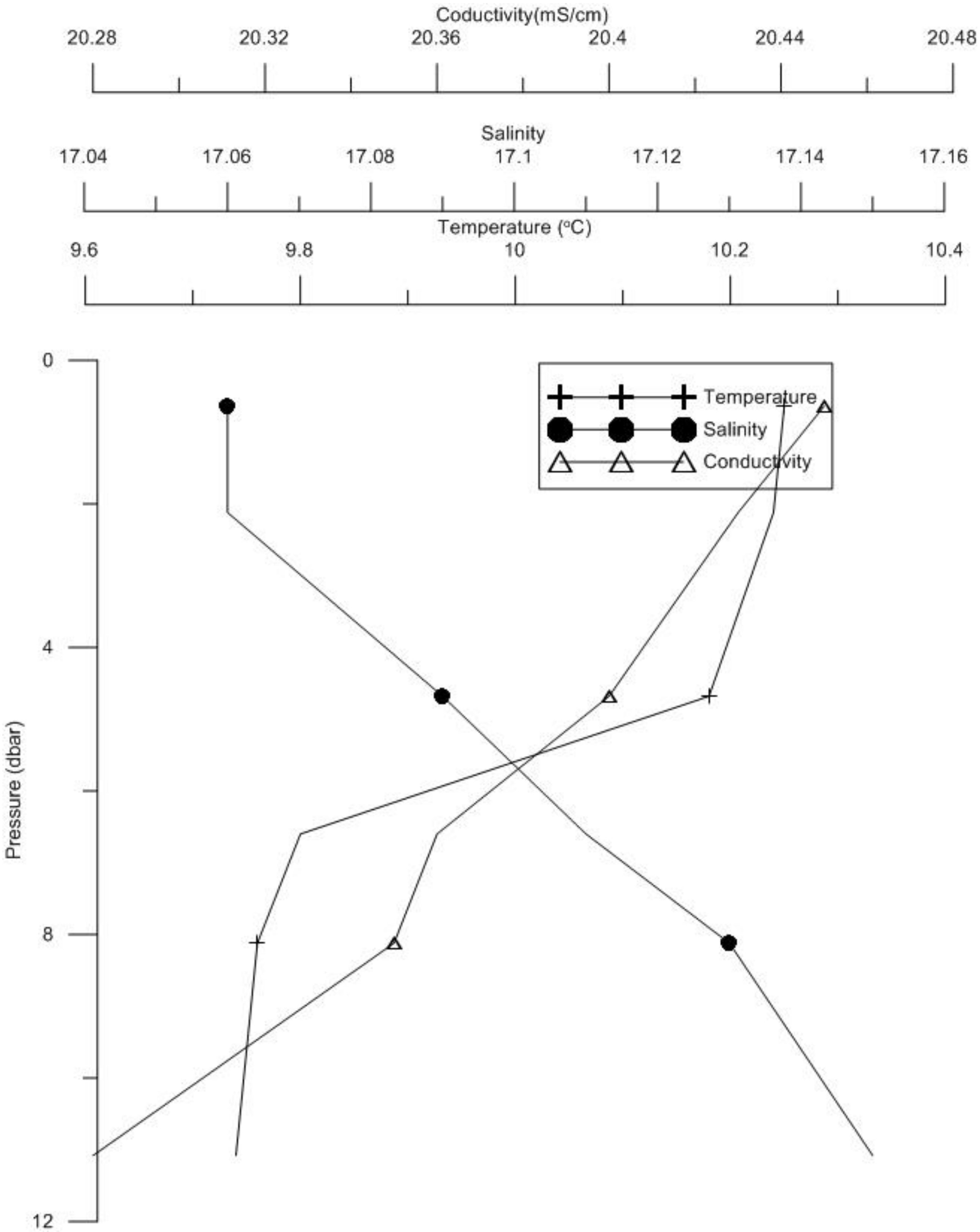

Figure 55.CTD from D11 Station for the first measurements in February2015

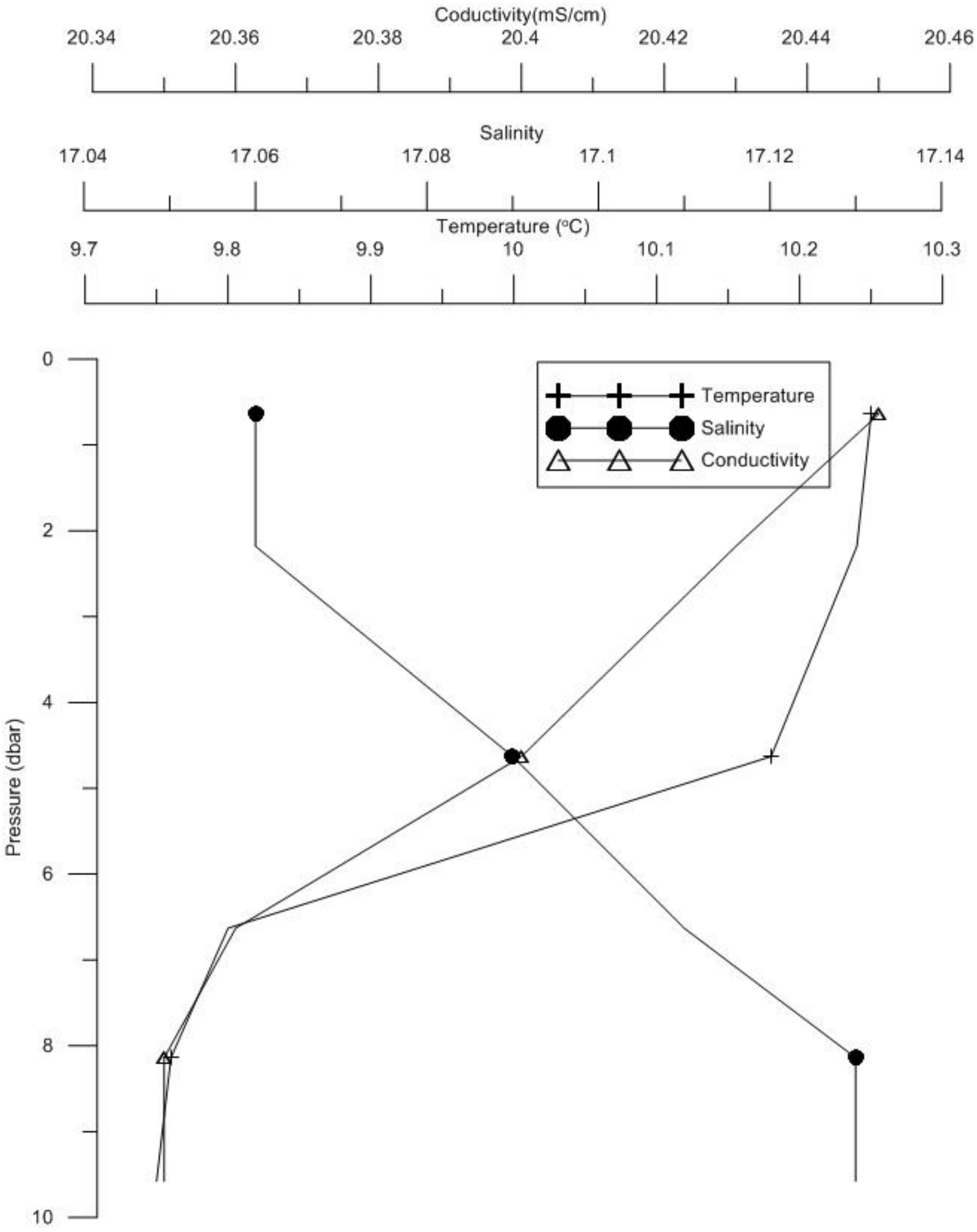

Figure 56.CTD from D12 Station for the first measurements in February2015

CTD graphs versus depth for each stations are given in the below. Conductivity, Salinity and Temperature results for the second period of February are given in Figures 57 -68.

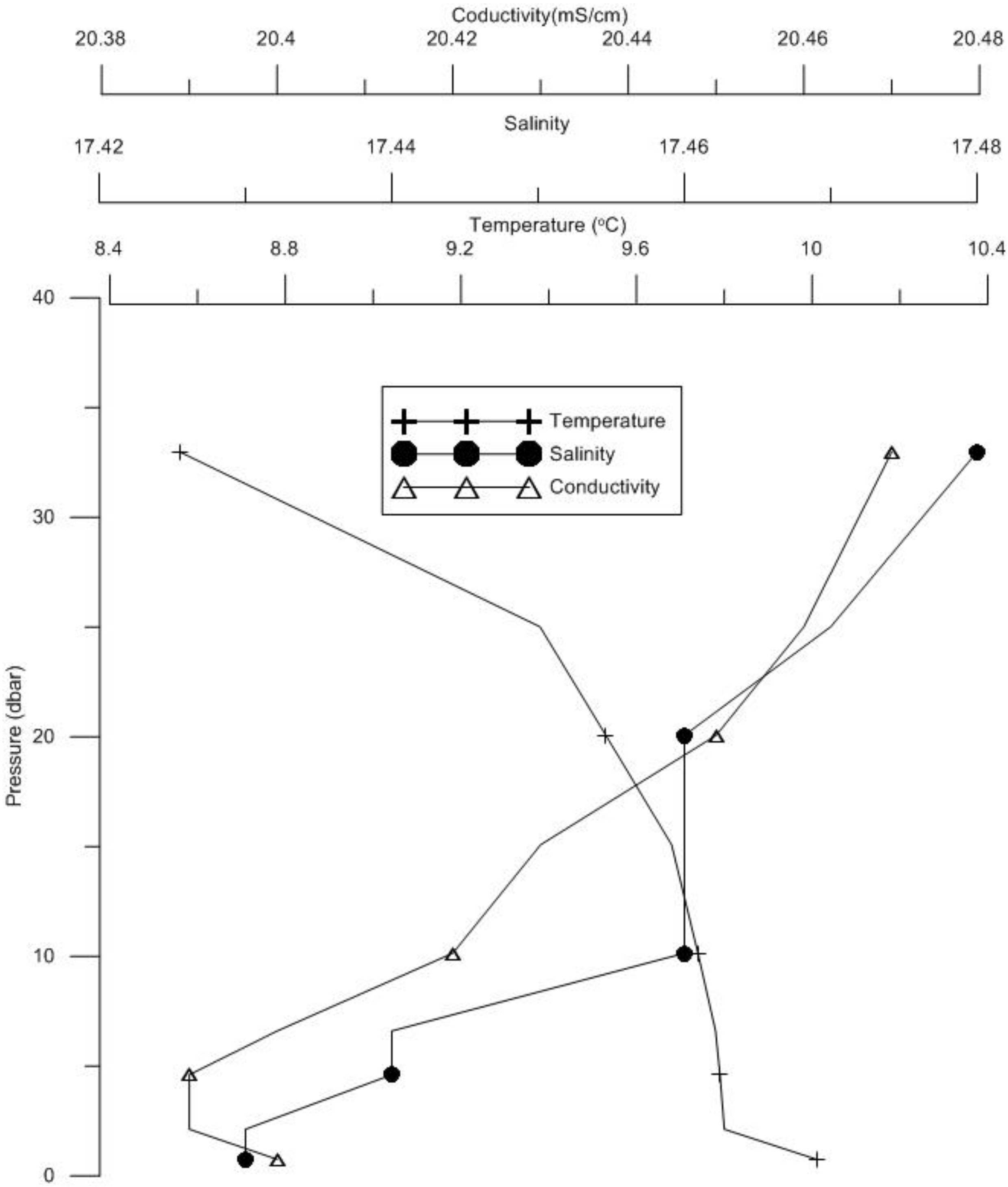

Figure 57. CTD from D1 Station for the second measurements in February2015

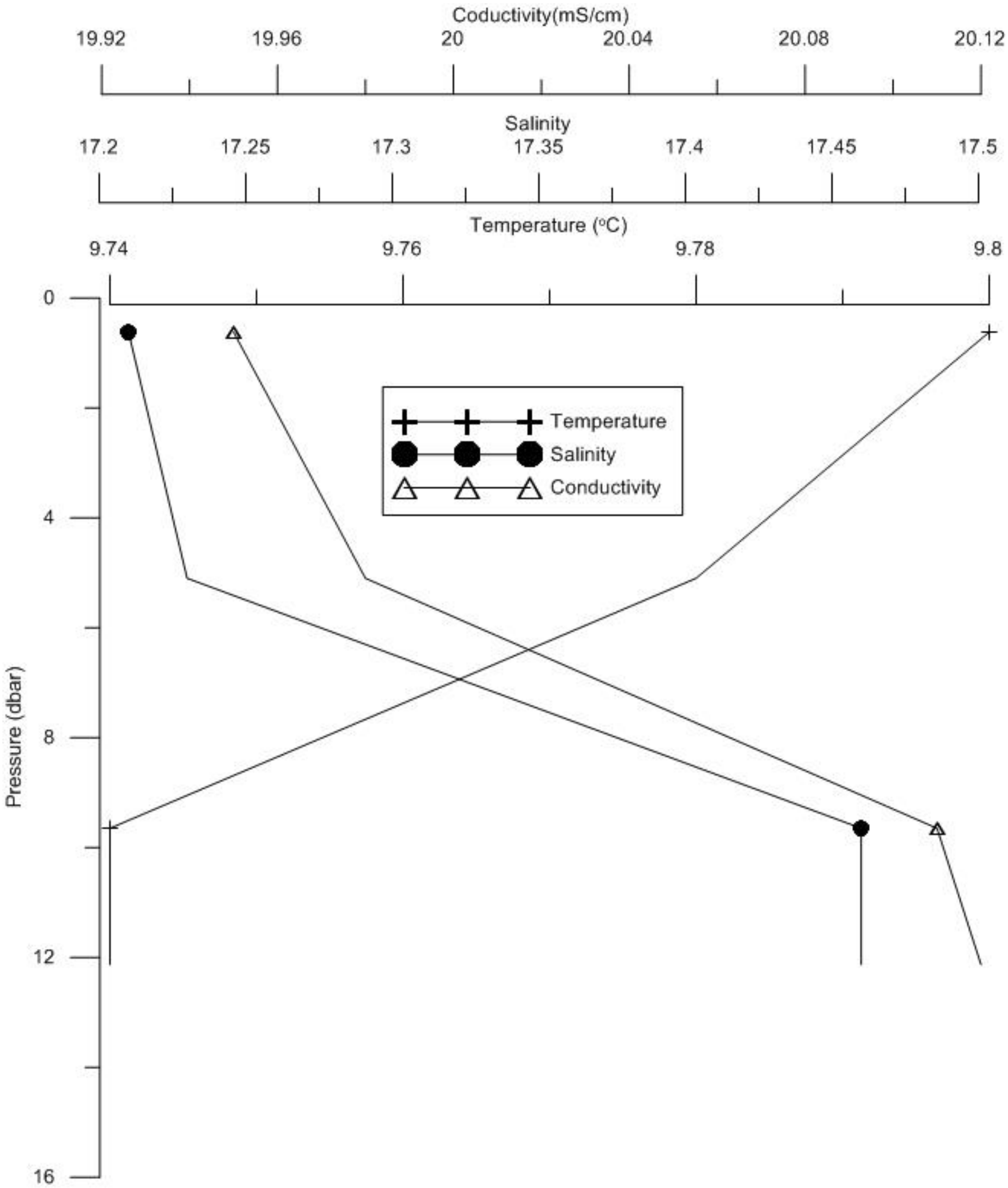

Figure 58.CTD from D2 Station for the second measurements in February2015

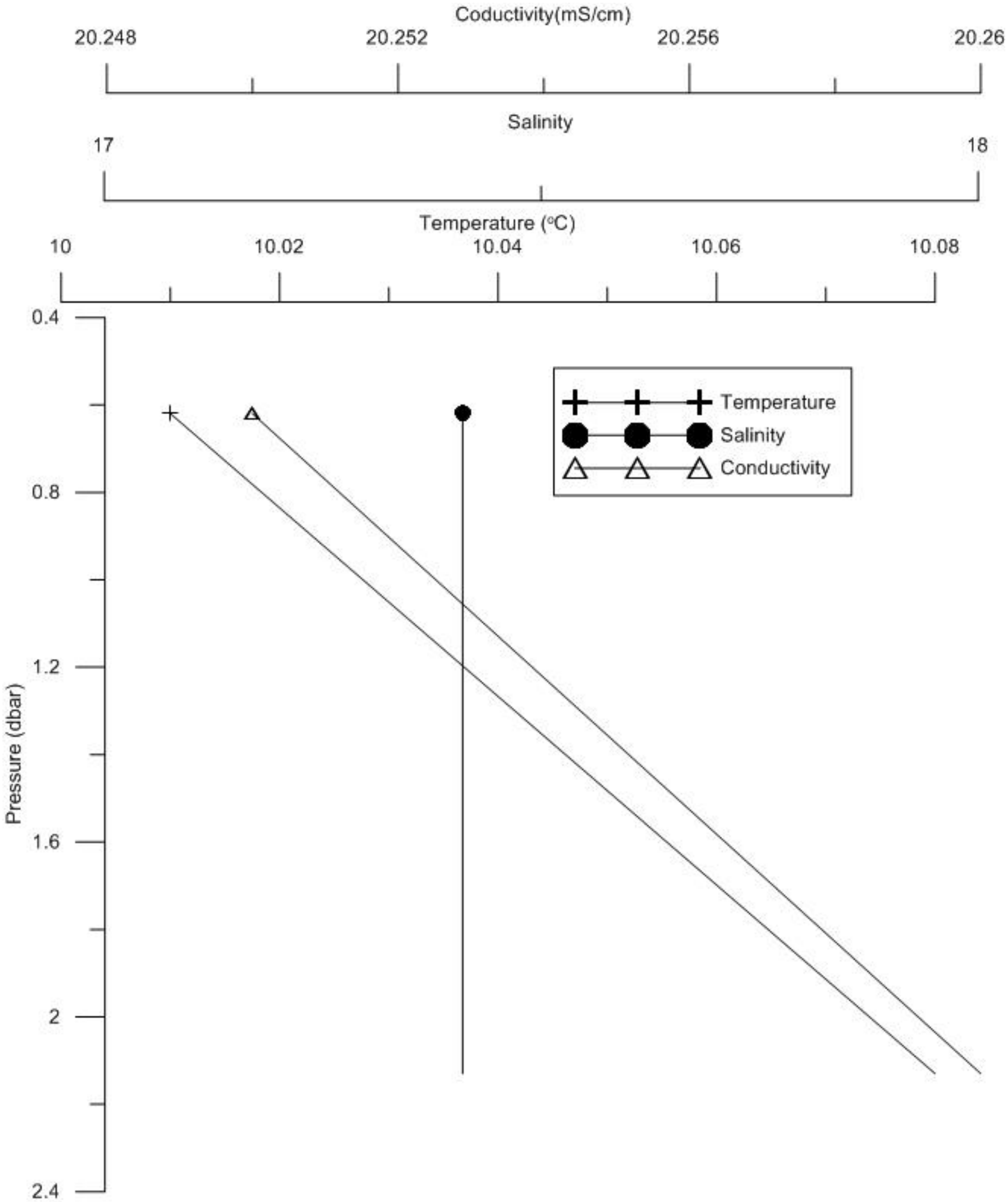

Figure 59.CTD from D3 Station for the second measurements in February2015

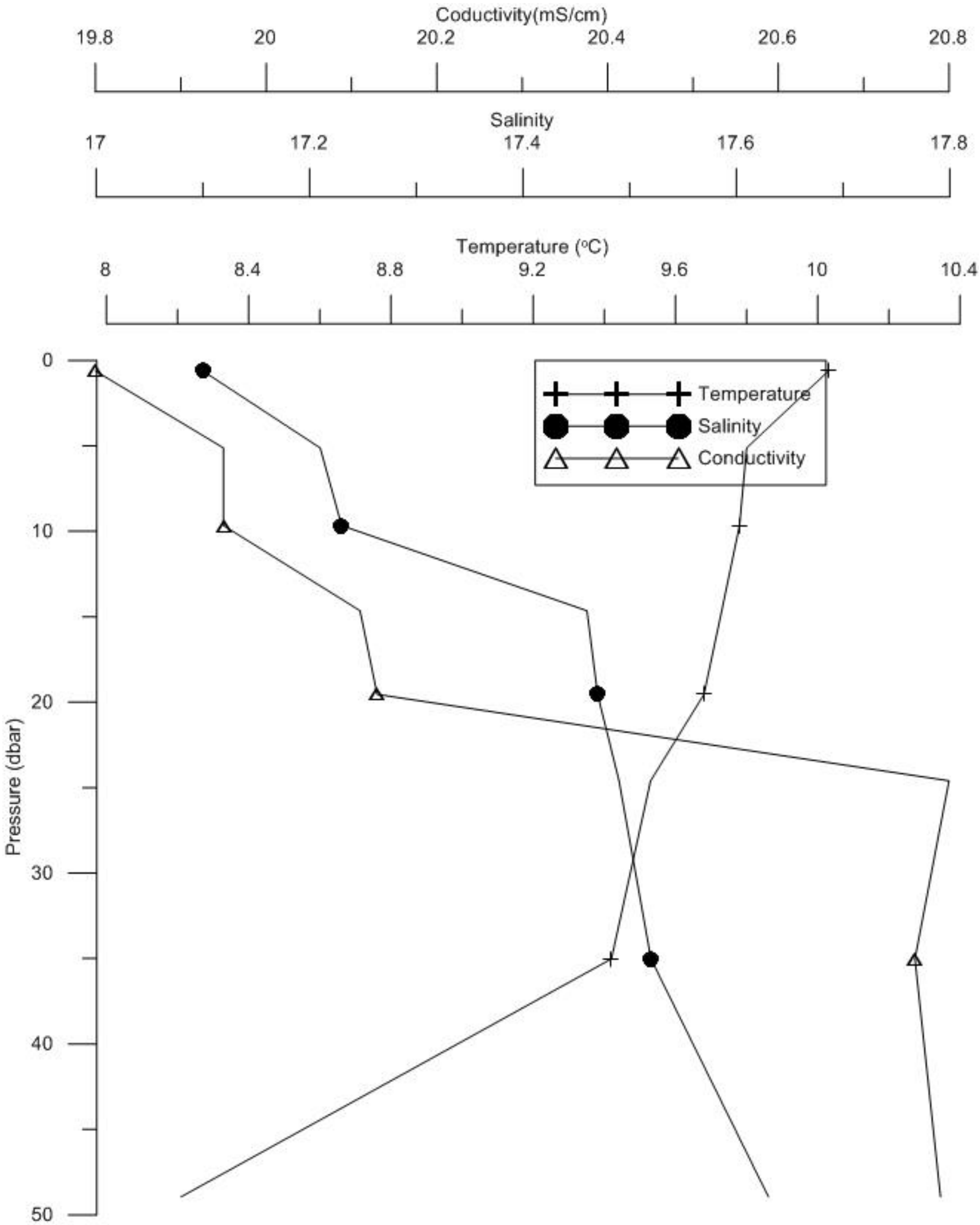

Figure 60.CTD from D4 Station for the second measurements in February2015

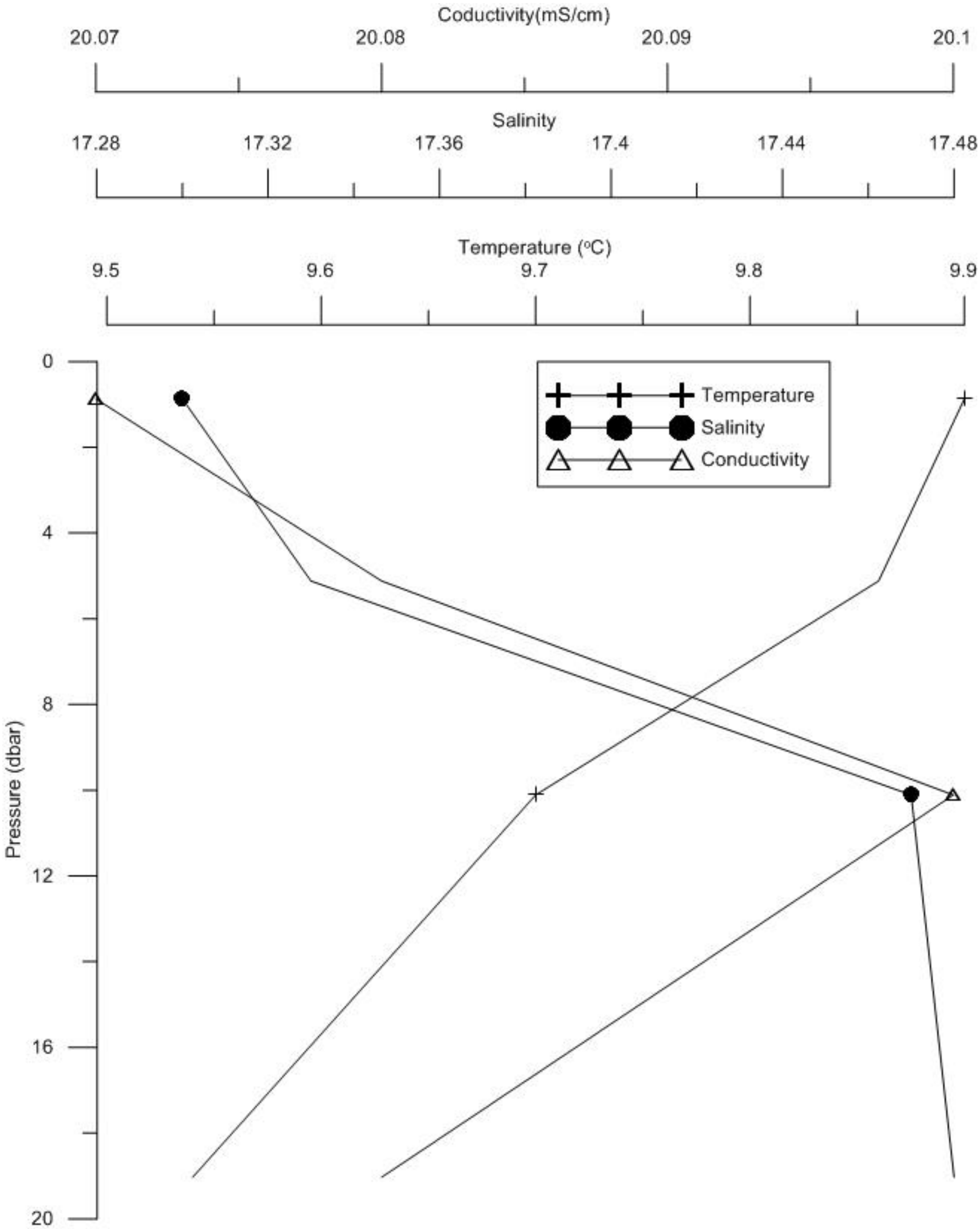

Figure 61.CTD from D5 Station for the second measurements in February2015

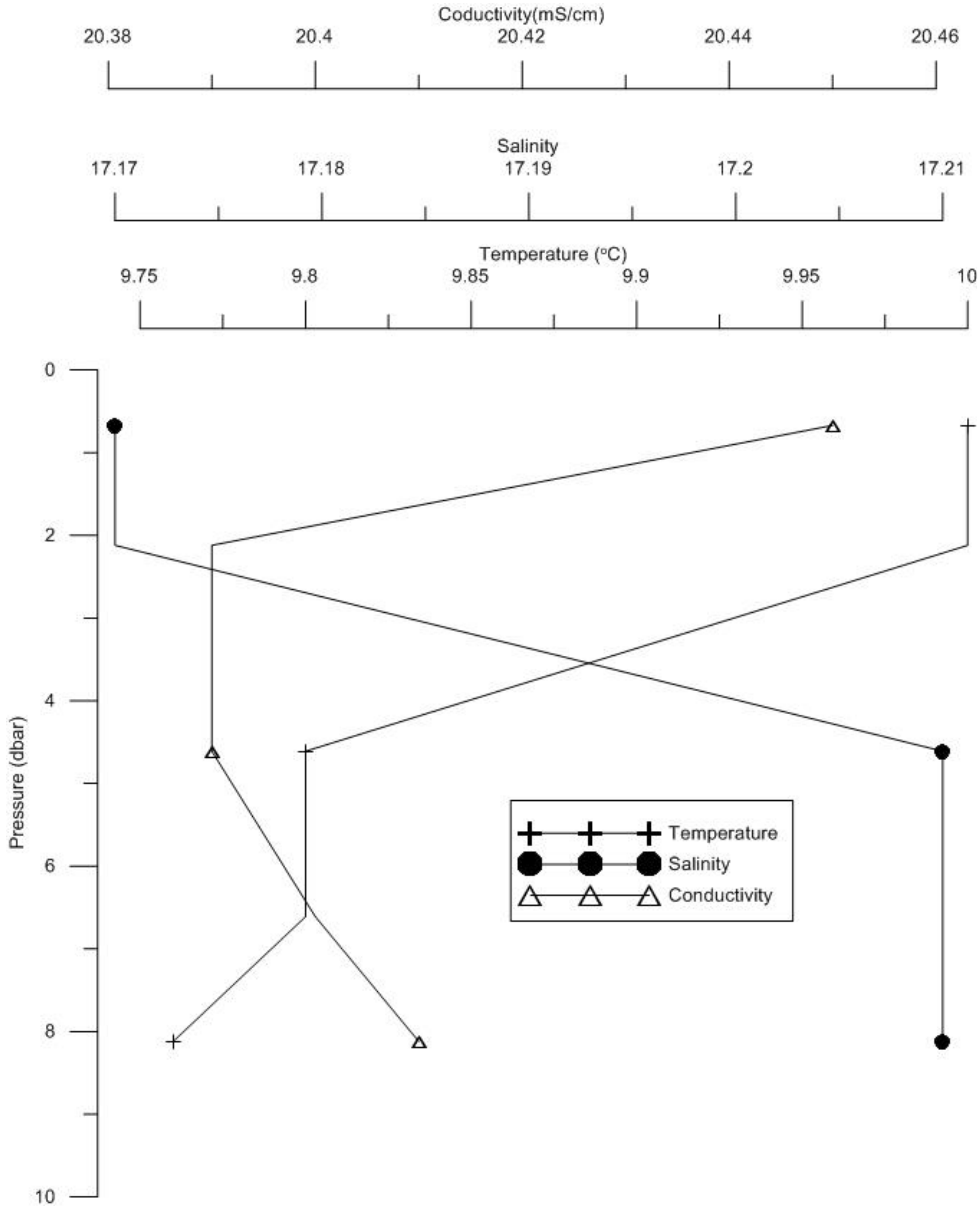

Figure 62.CTD from D6 Station for the second measurements in February2015

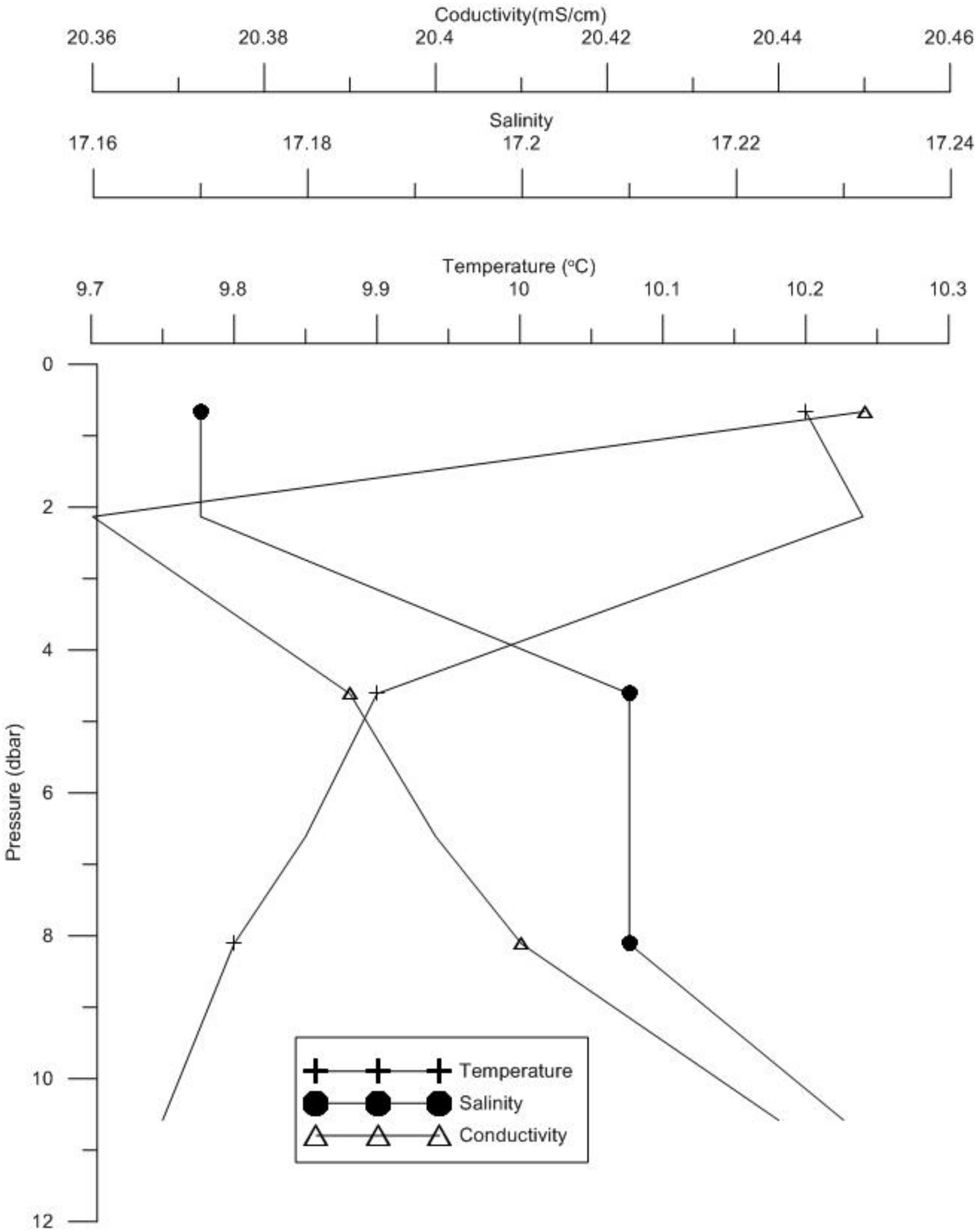

Figure 63.CTD from D7 Station for the seond measurements in February2015

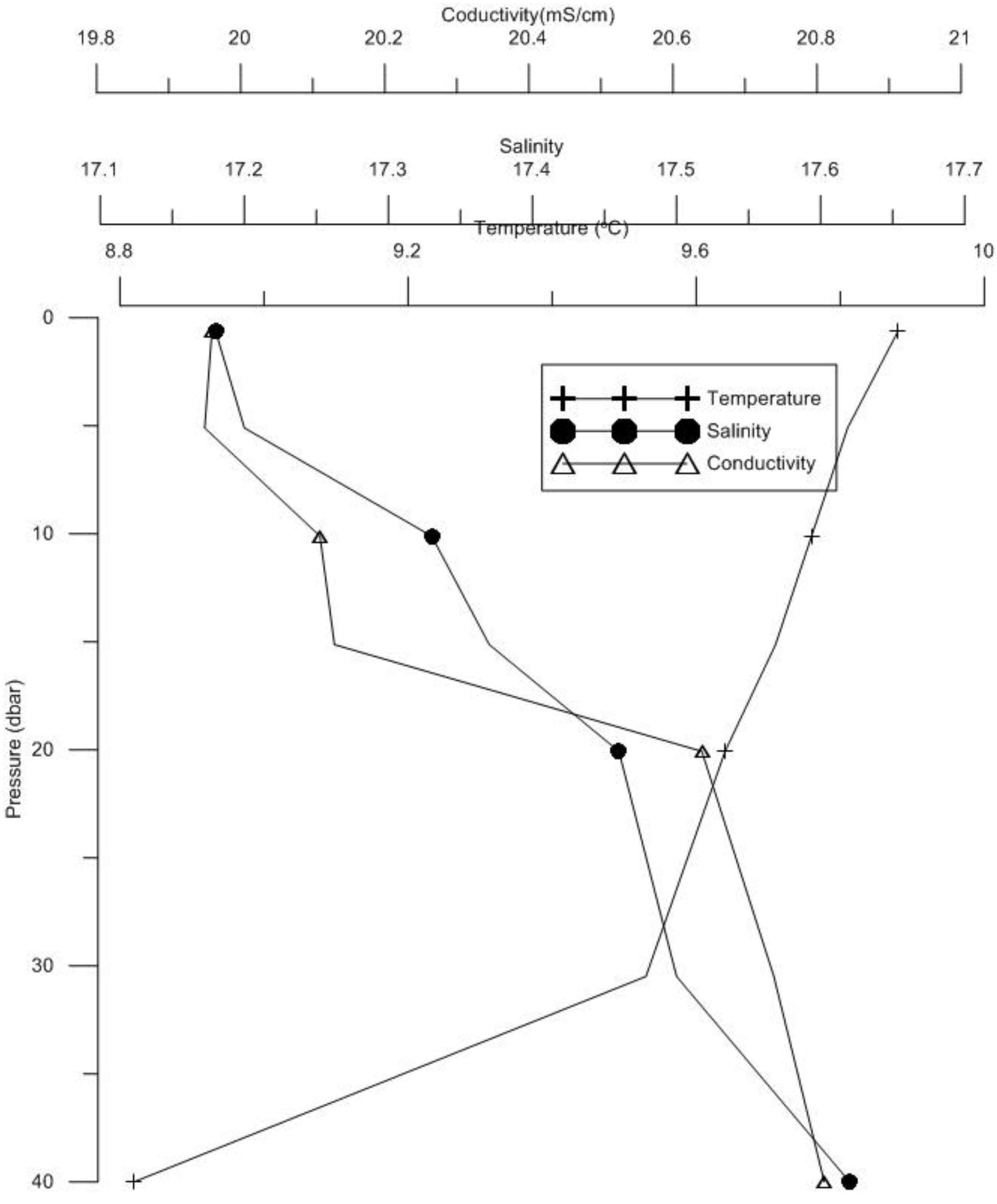

Figure 64.CTD from D8 Station for the second measurements in February2015

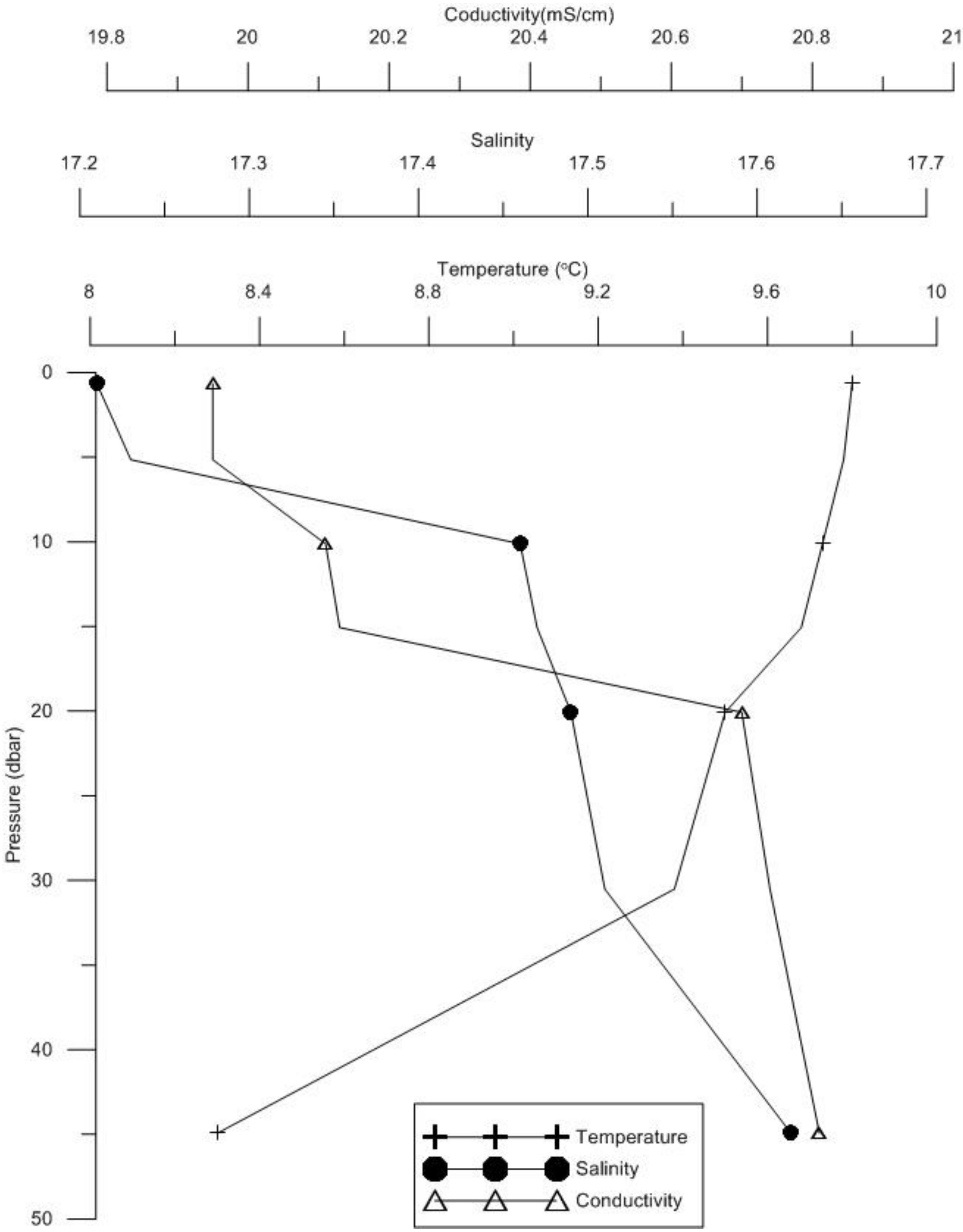

Figure 65.CTD from D9 Station for the second measurements in February2015

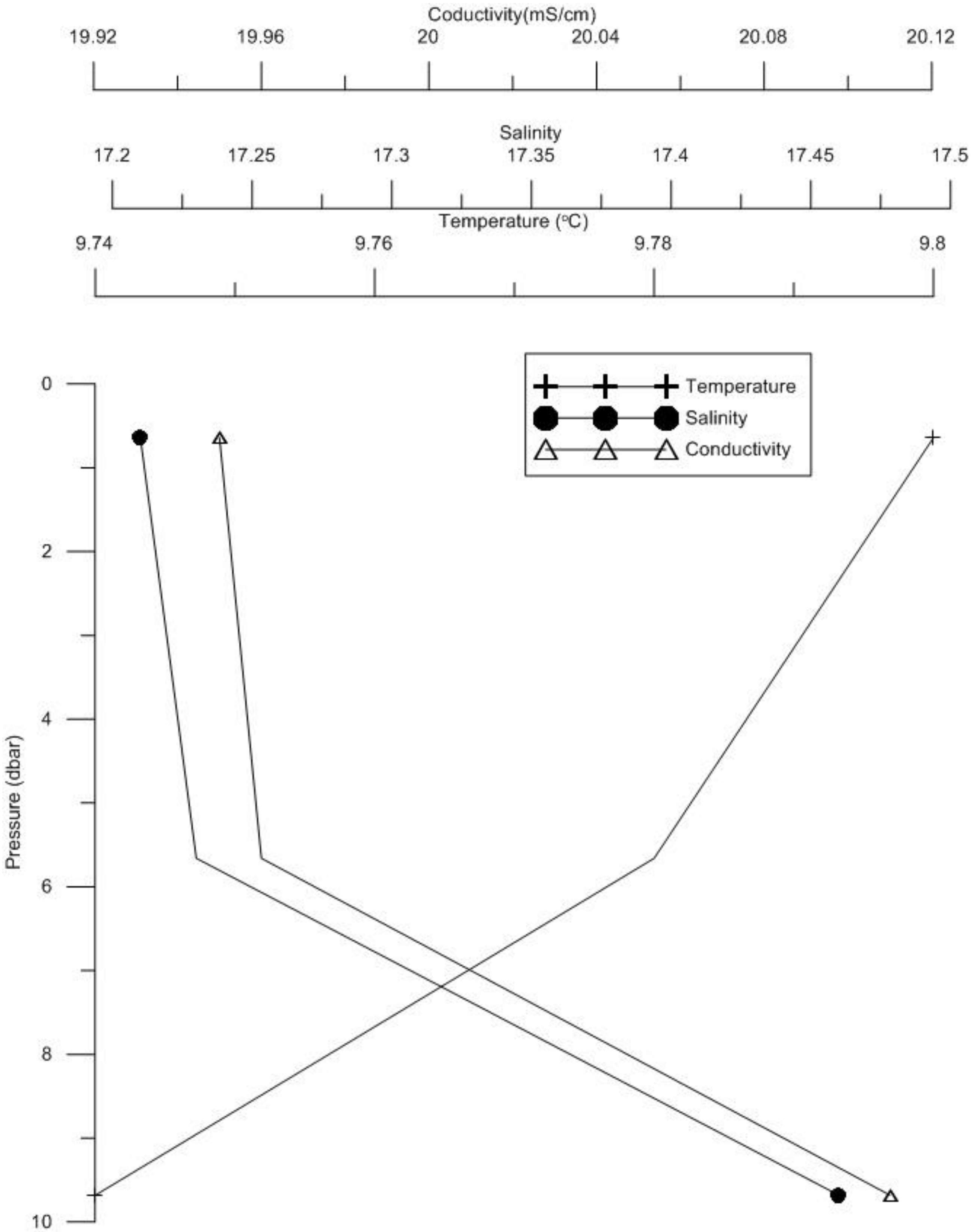

Figure 66.CTD from D10 Station for the second measurements in February2015

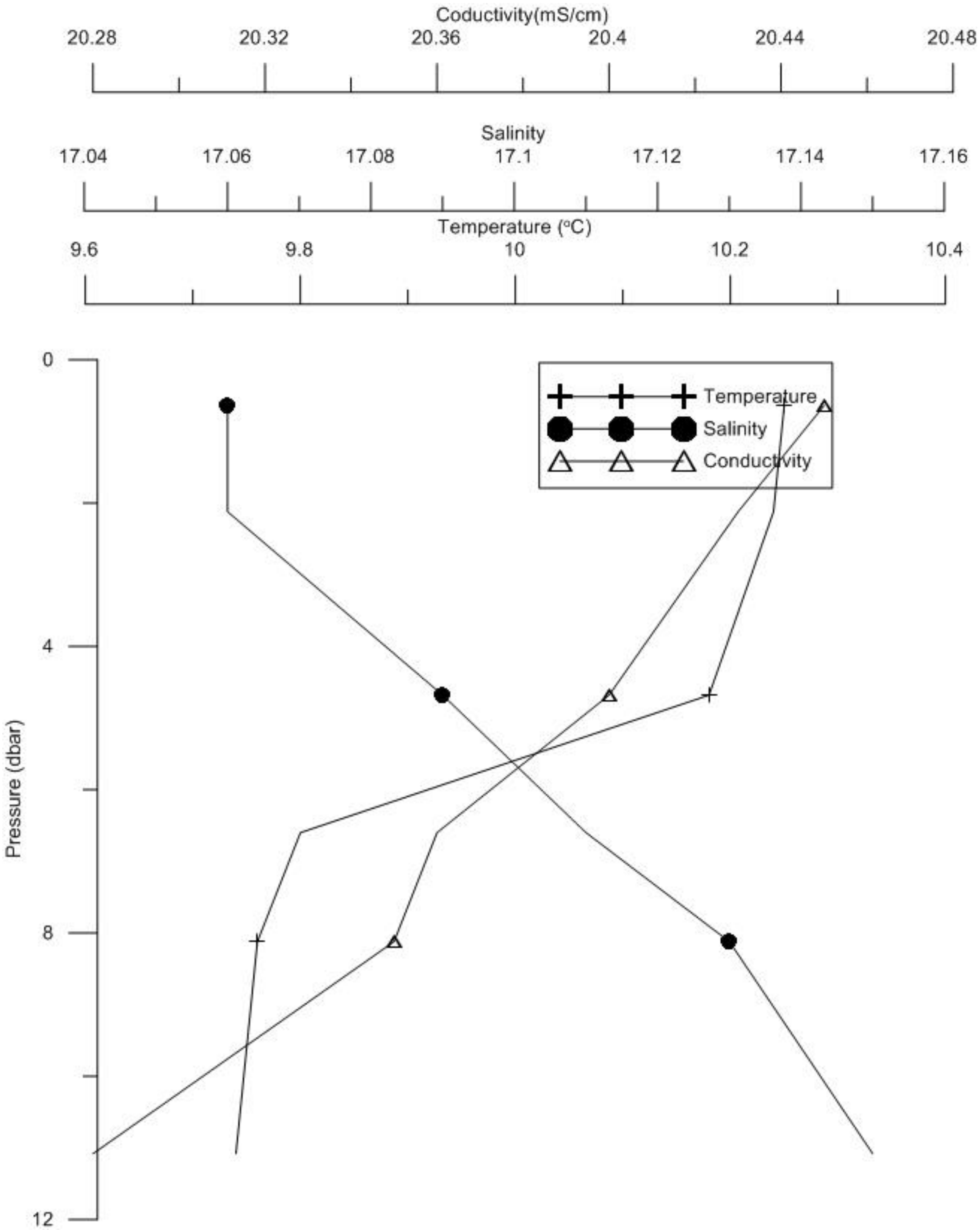

Figure 67.CTD from D11 Station for the second measurements in February2015

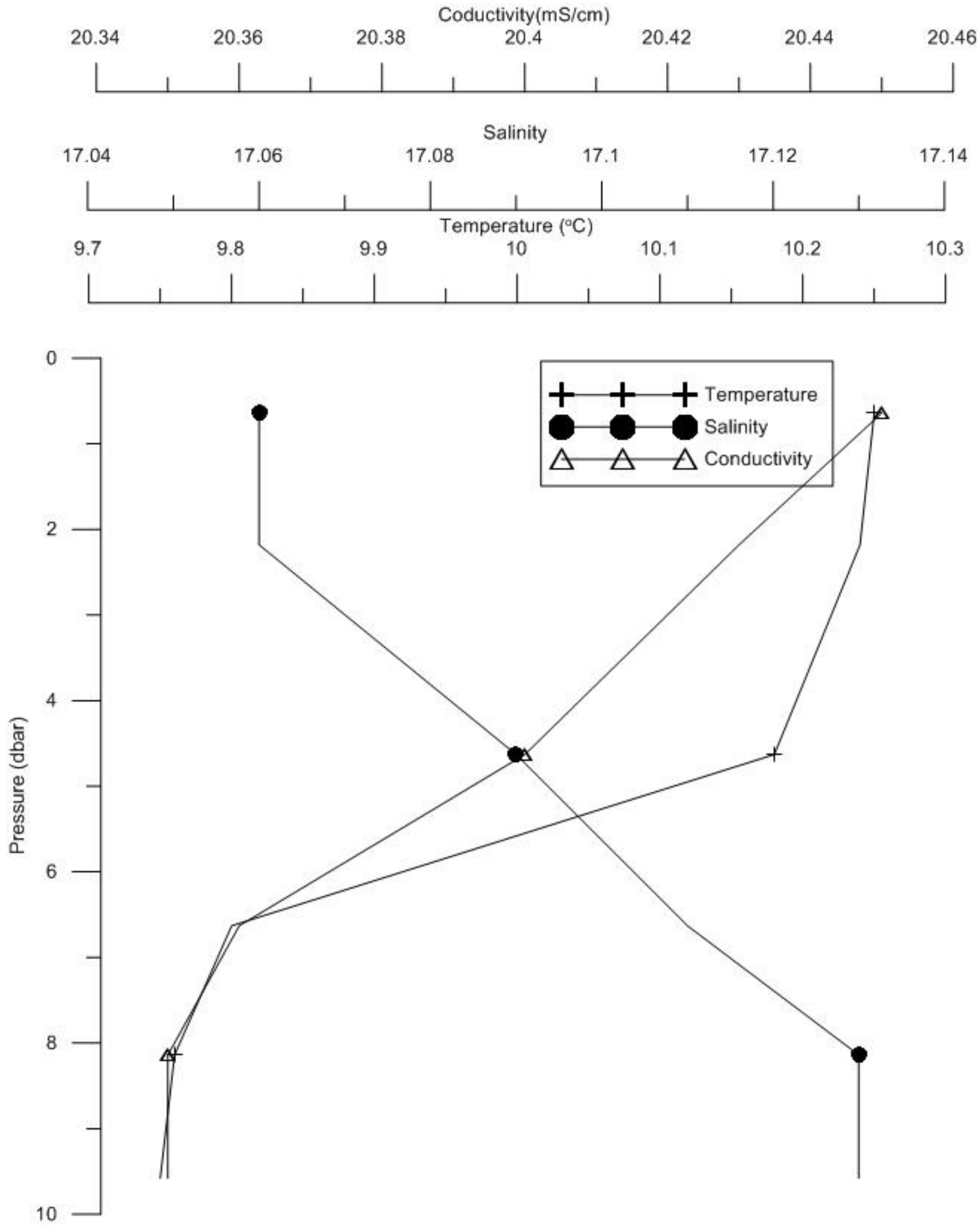

Figure 68.CTD from D12 Station for the second measurements in February2015

CTD graphs versus depth for each stations are given in the below. Conductivity, Salinity and Temperature results for the first period of March are given in Figures 69 -80.

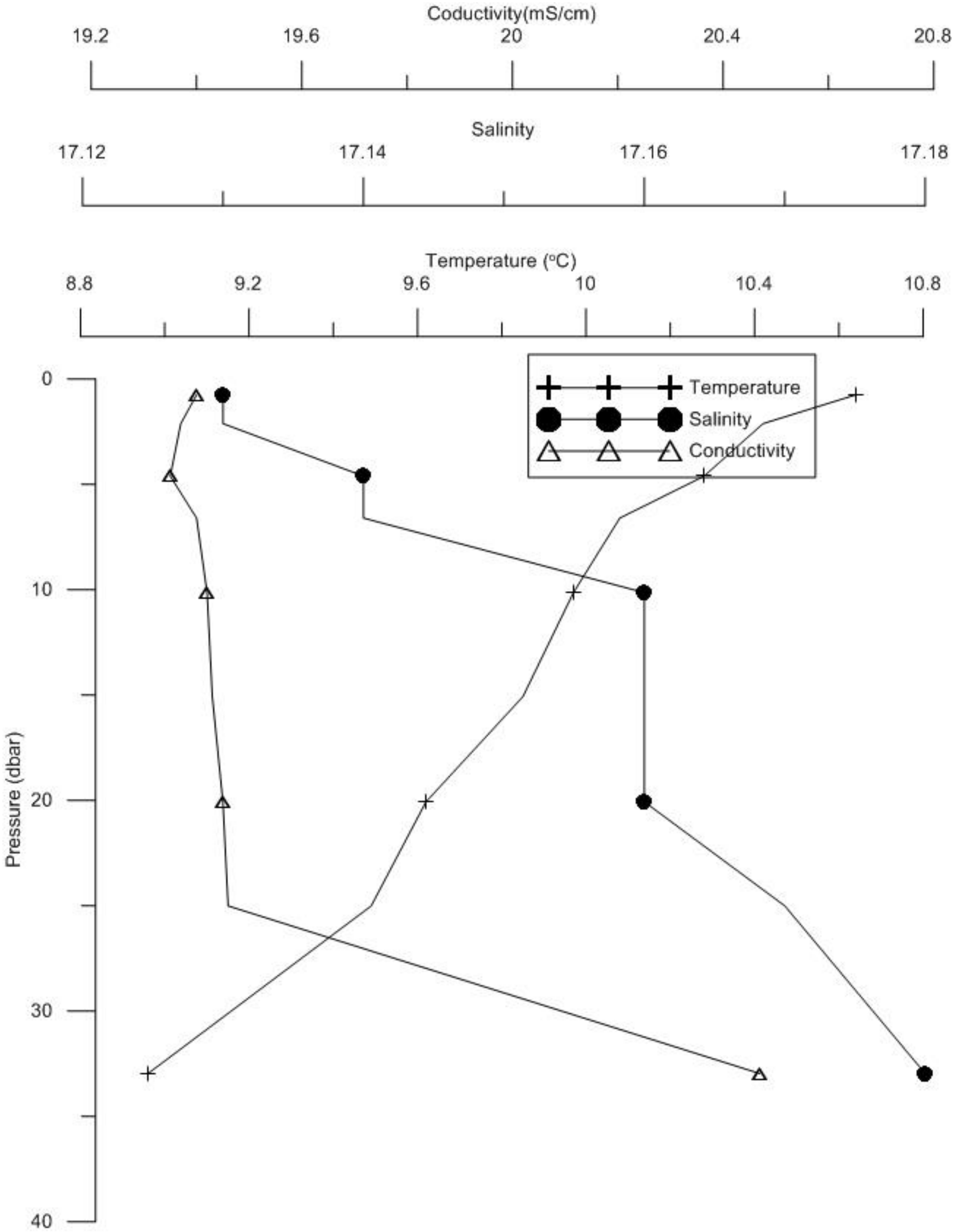

Figure 69. CTD from D1 Station for the first measurements in March2015

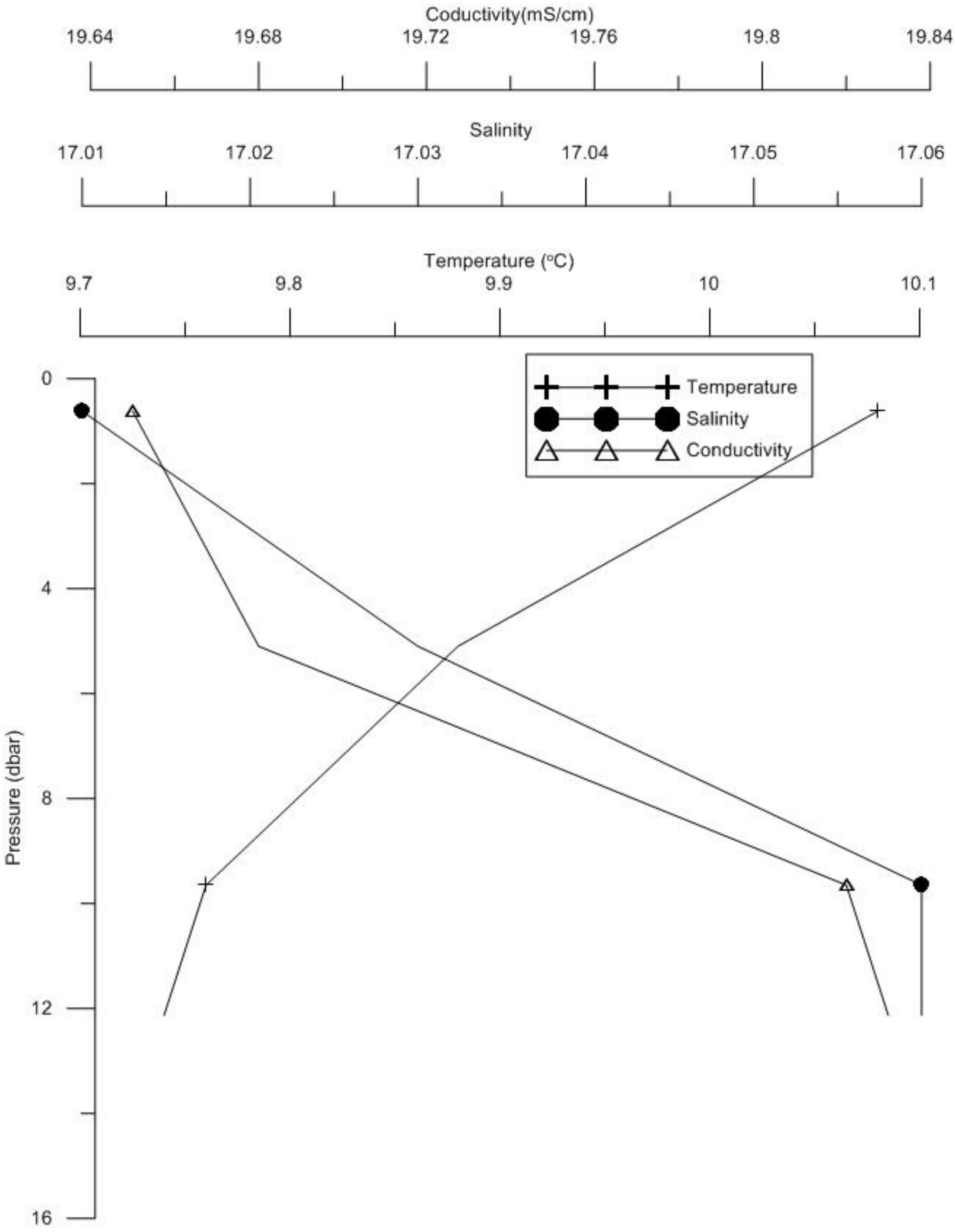

Figure 70.CTD from D2 Station for the first measurements in March2015

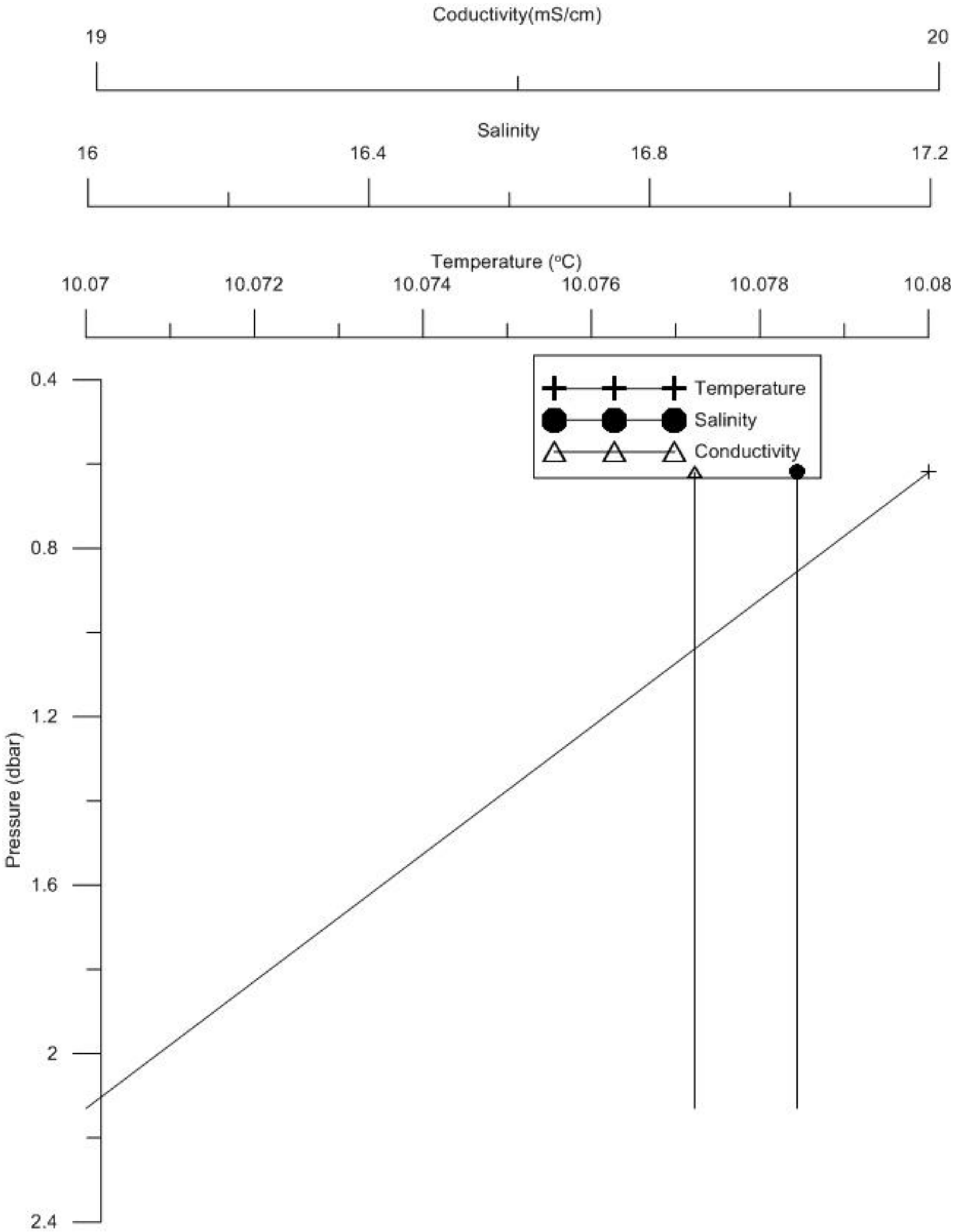

Figure 71.CTD from D3 Station for the first measurements in March2015

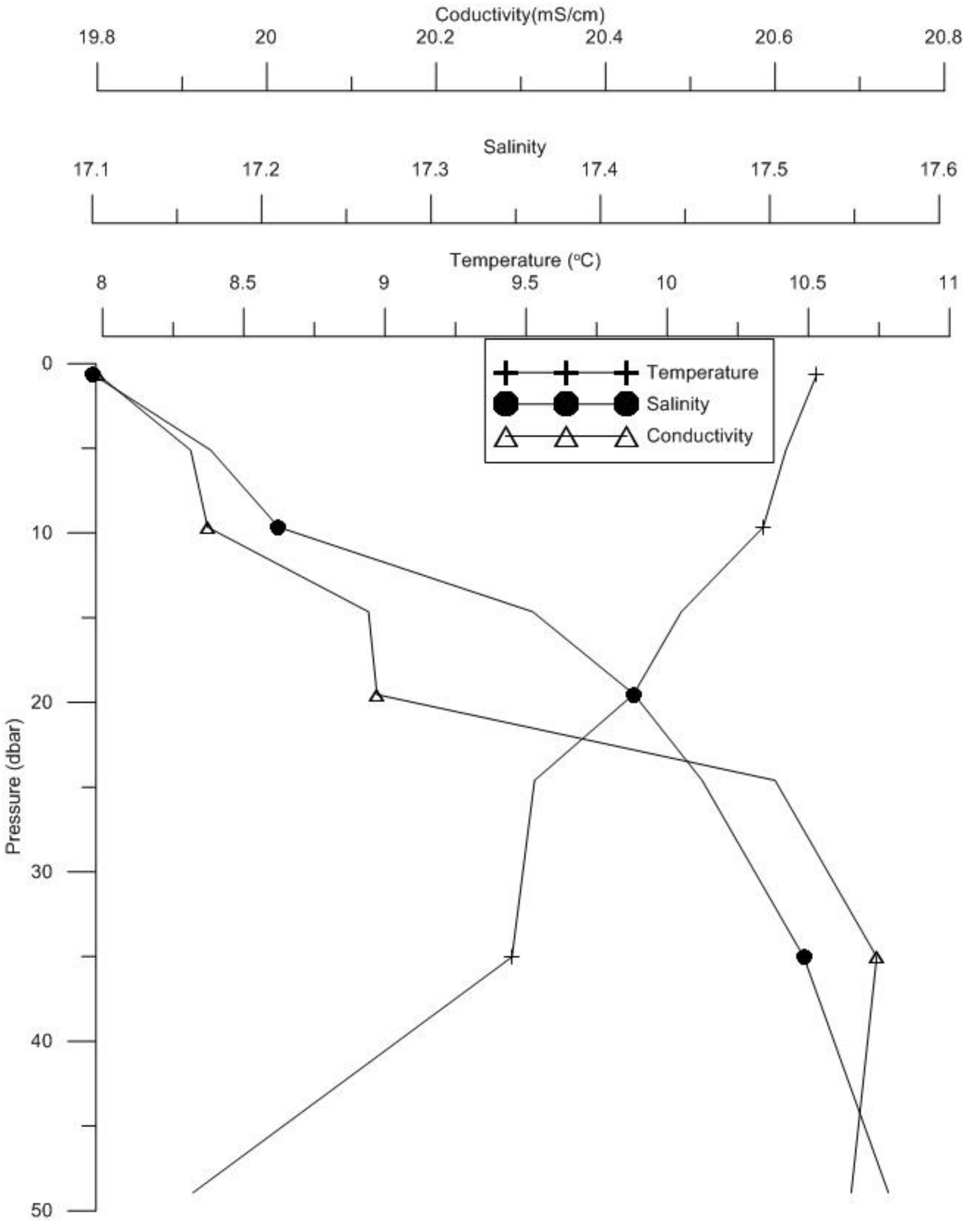

Figure 72.CTD from D4 Station for the first measurements in March2015

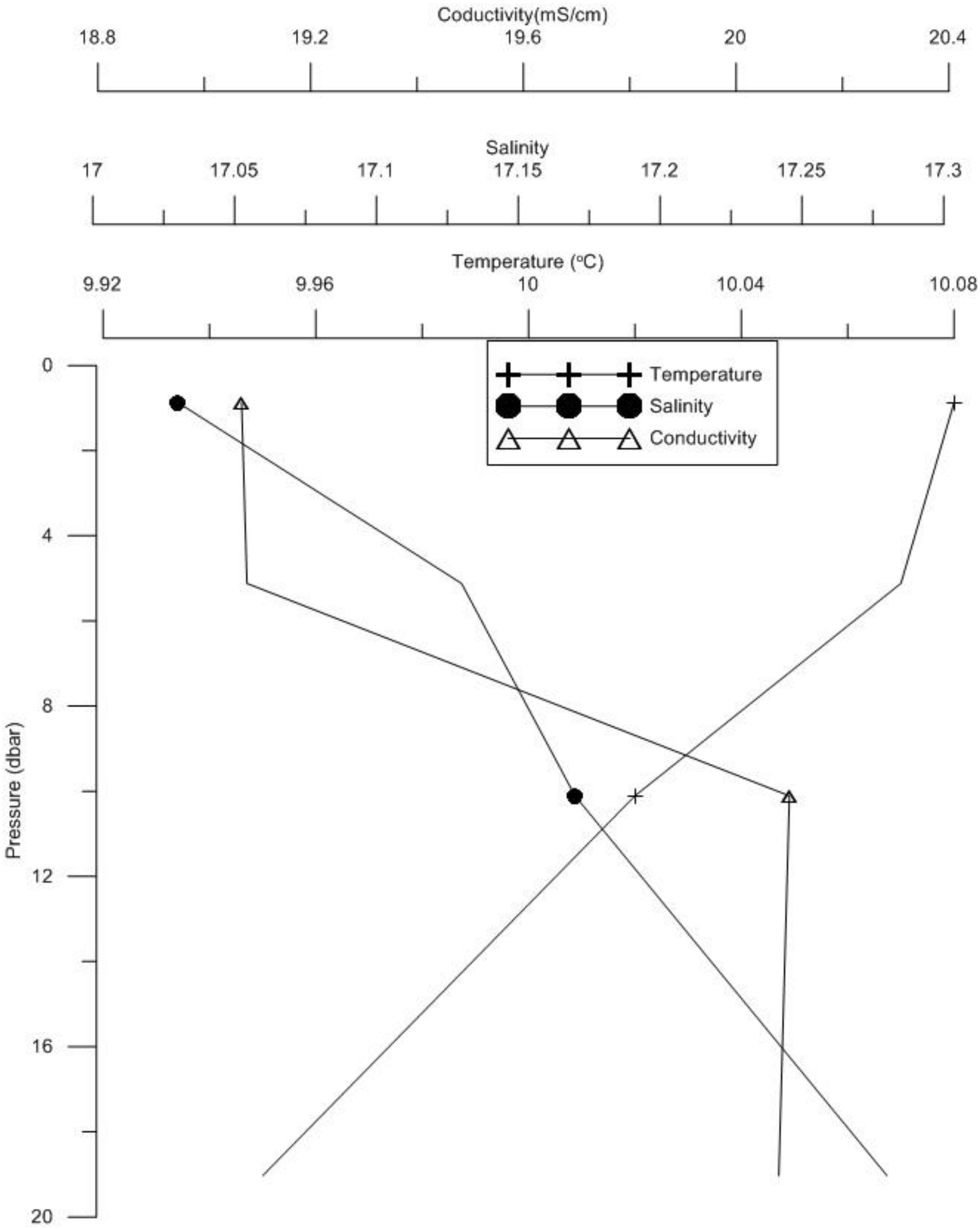

Figure 73.CTD from D5 Station for the first measurements in March2015

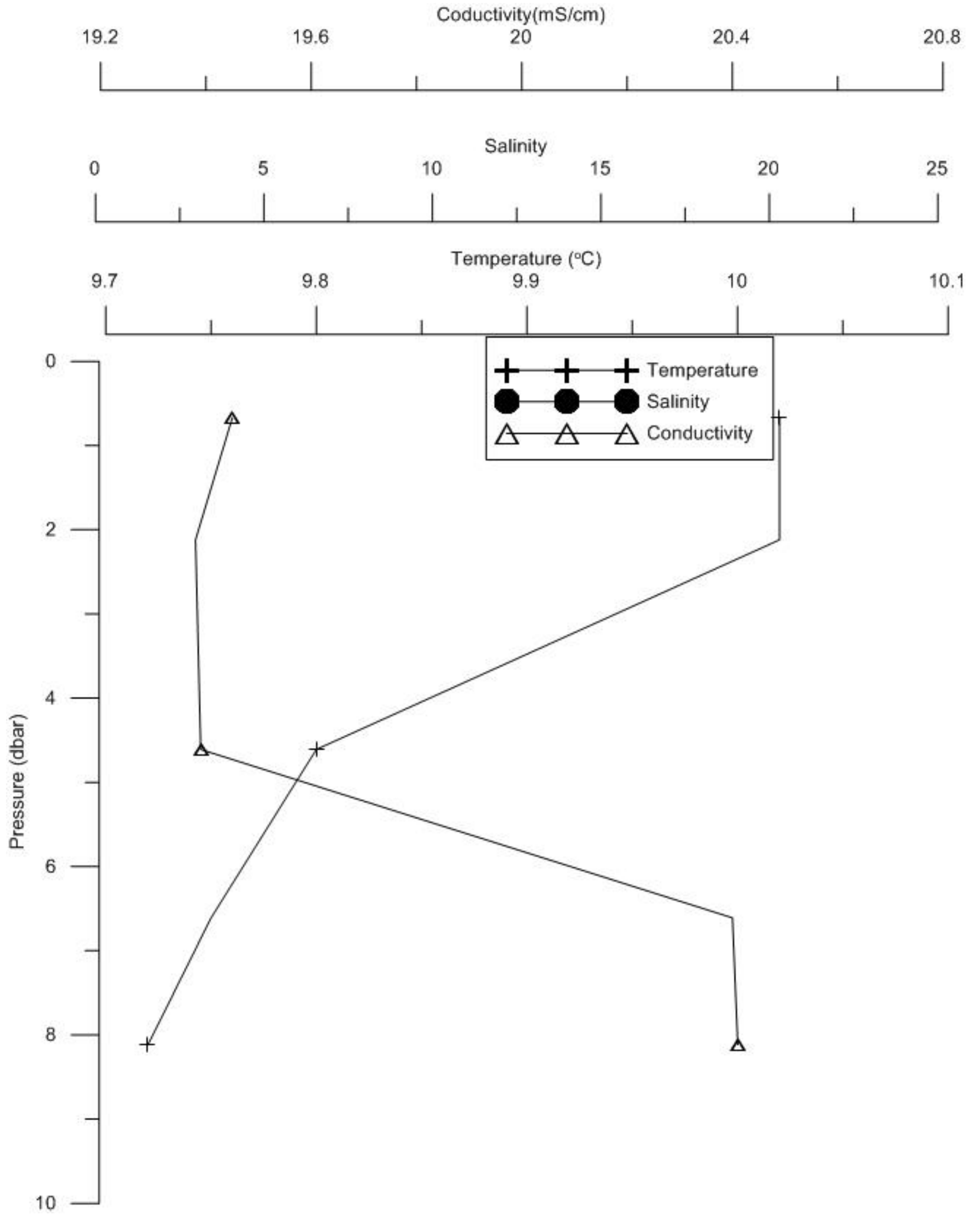

Figure 74.CTD from D6 Station for the first measurements in March2015

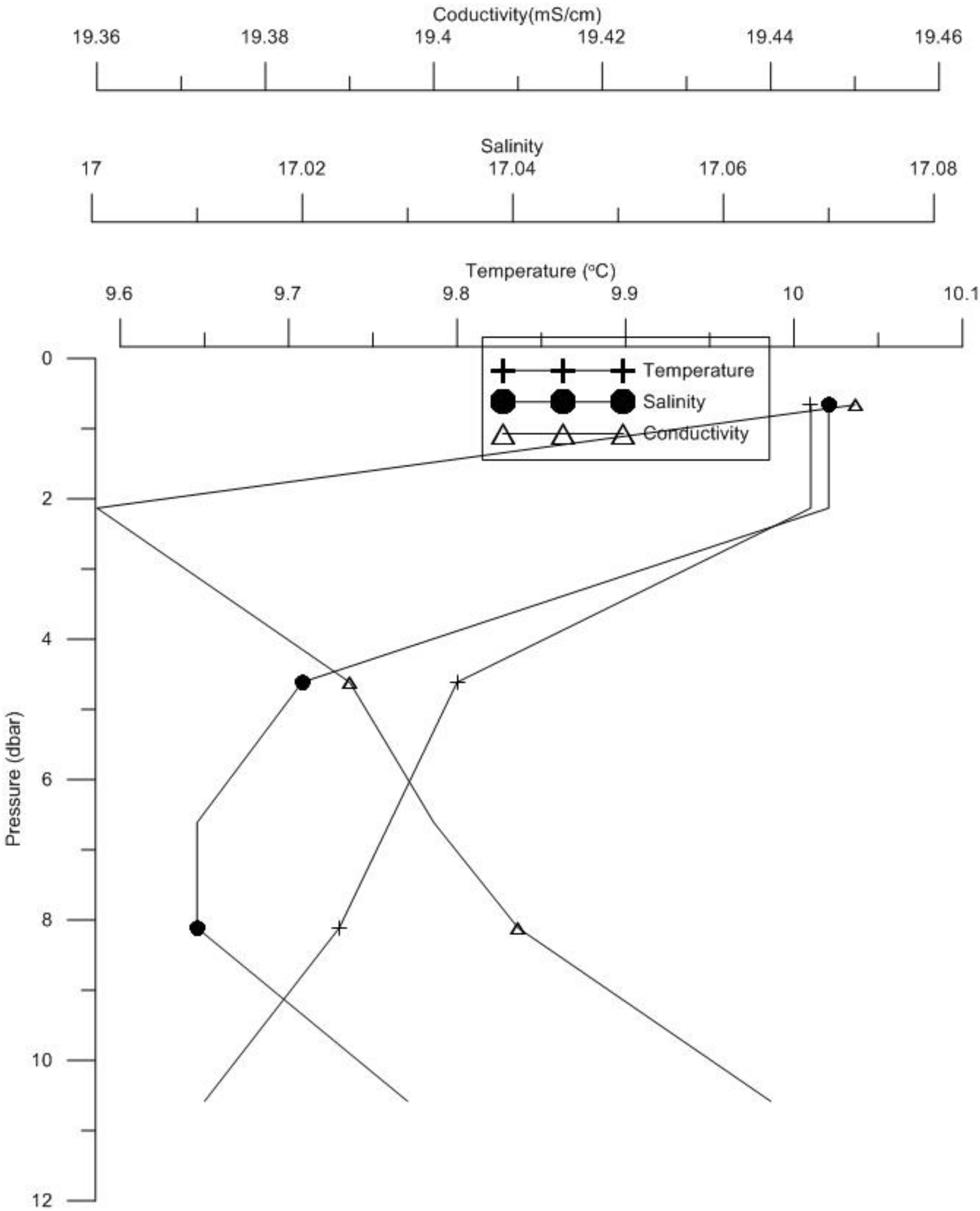

Figure 75.CTD from D7 Station for the first measurements in March2015

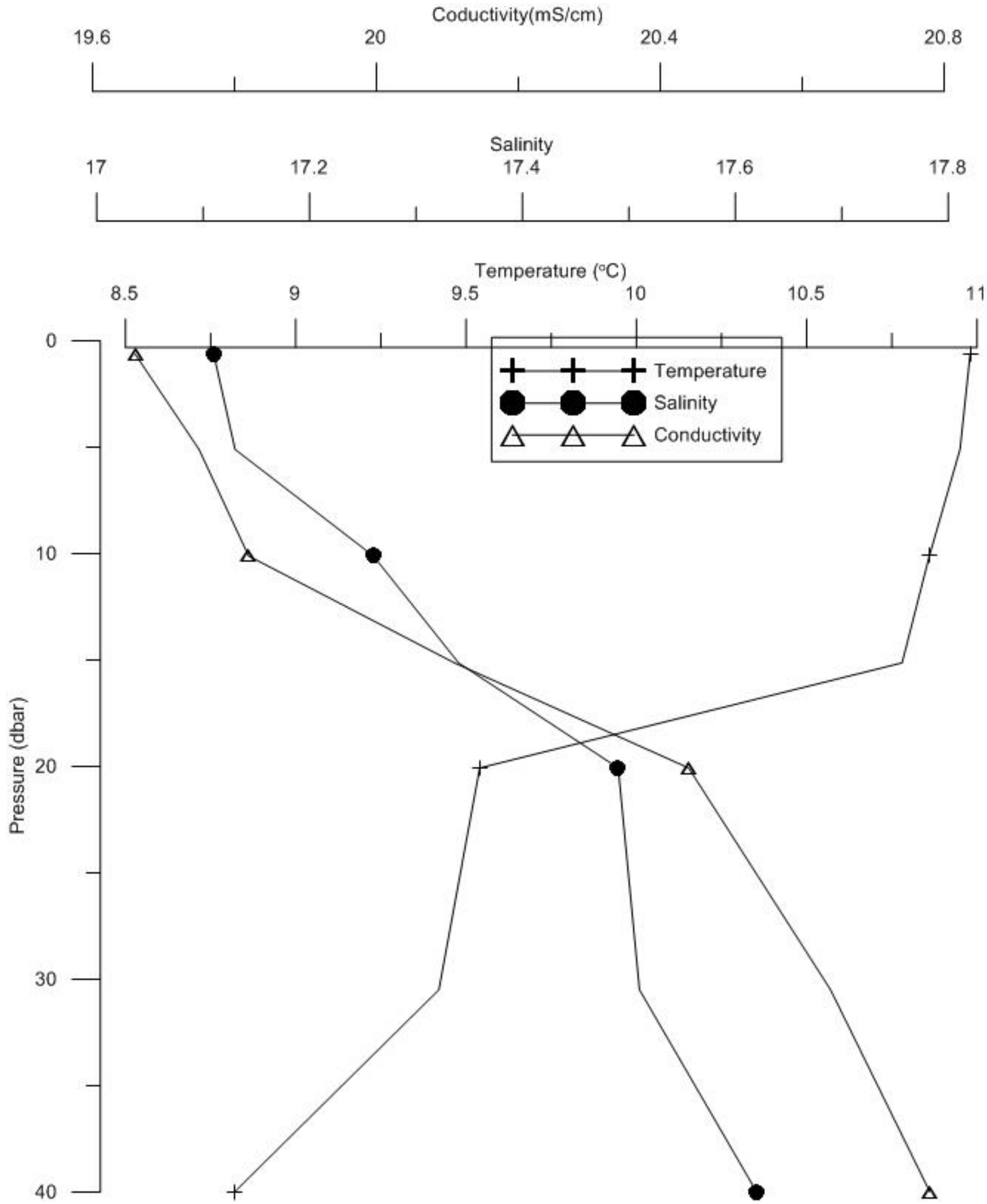

Figure 76.CTD from D8 Station for the first measurements in March2015

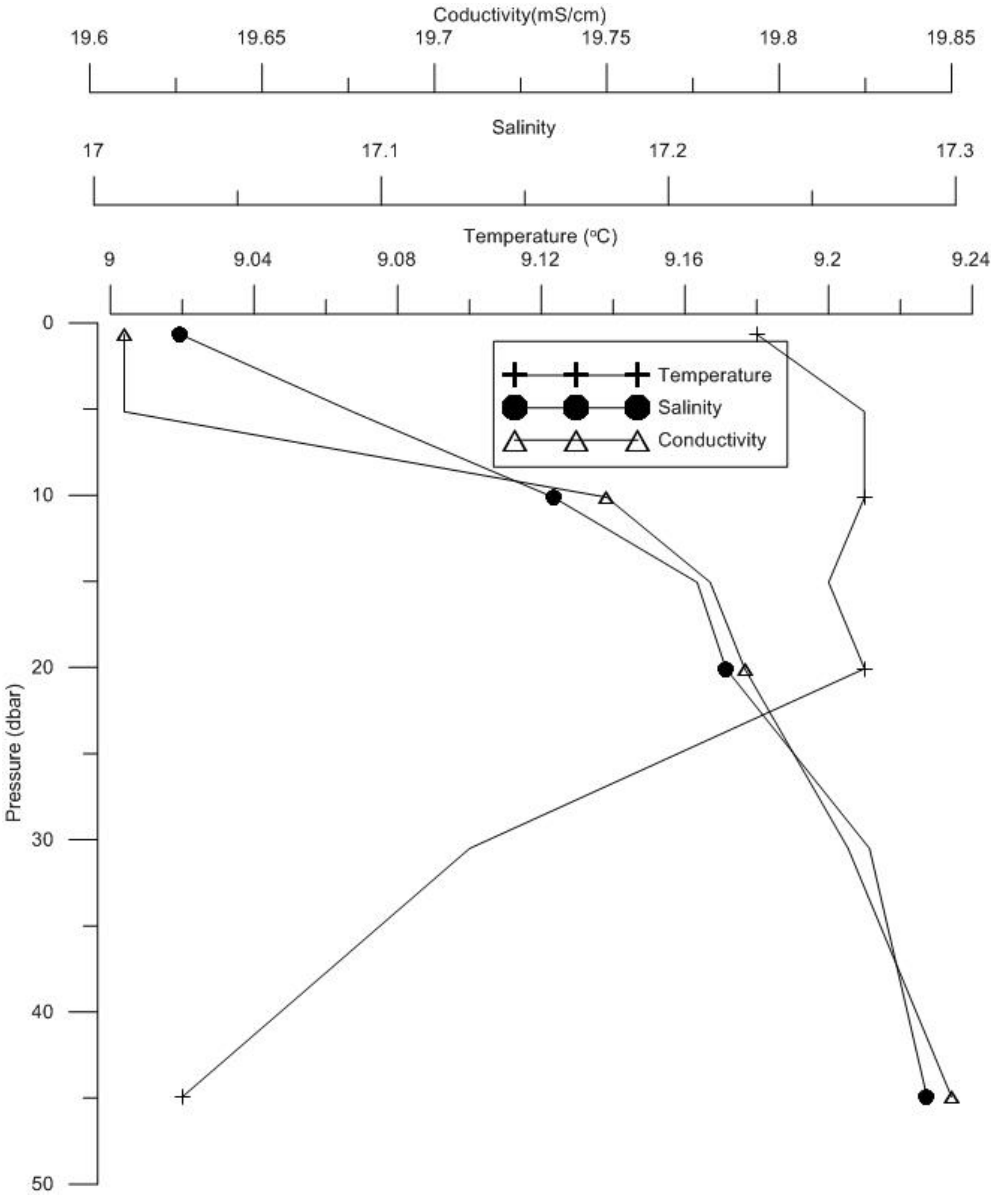

Figure 77.CTD from D9 Station for the first measurements in March2015

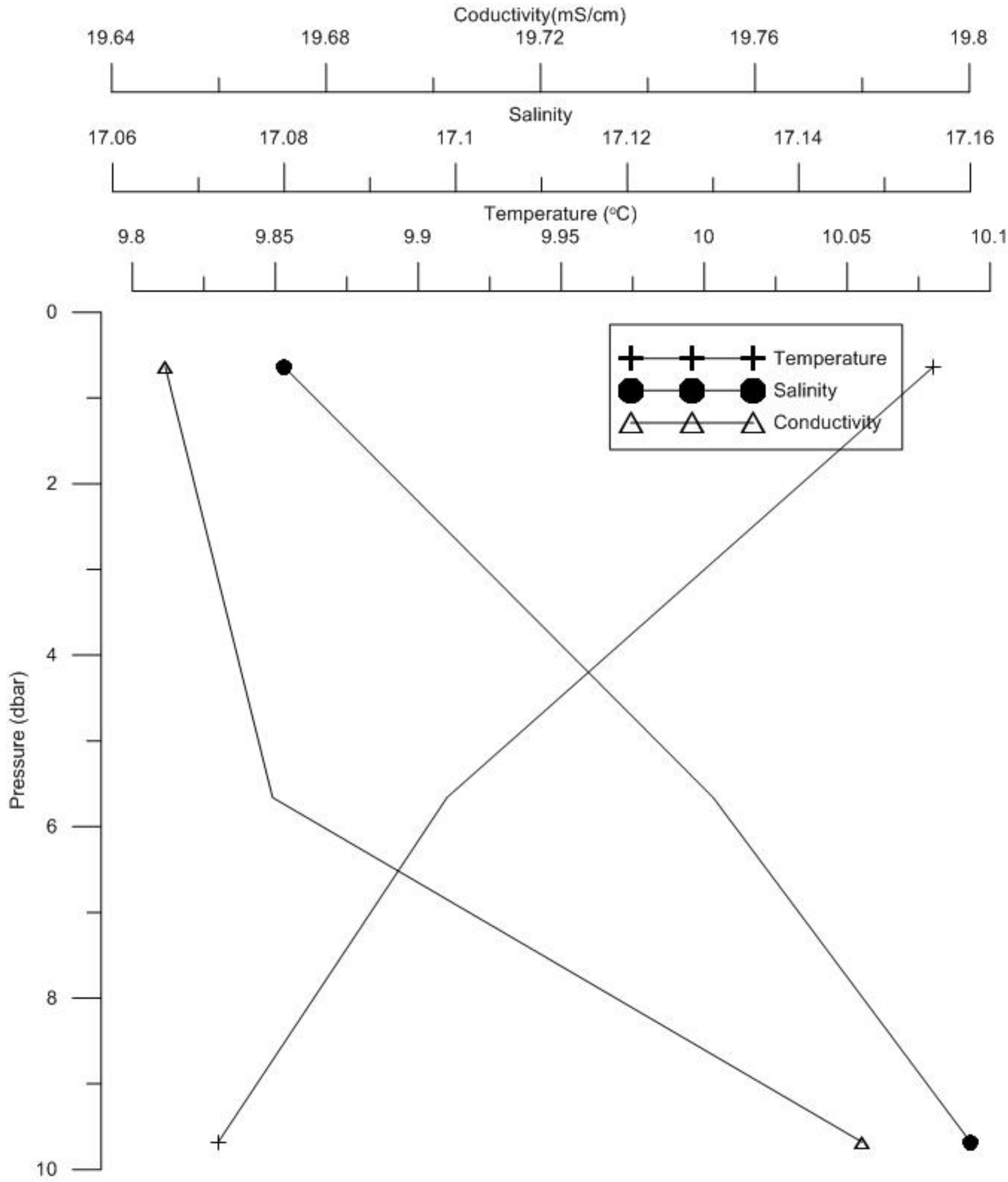

Figure 78.CTD from D10 Station for the first measurements in March2015

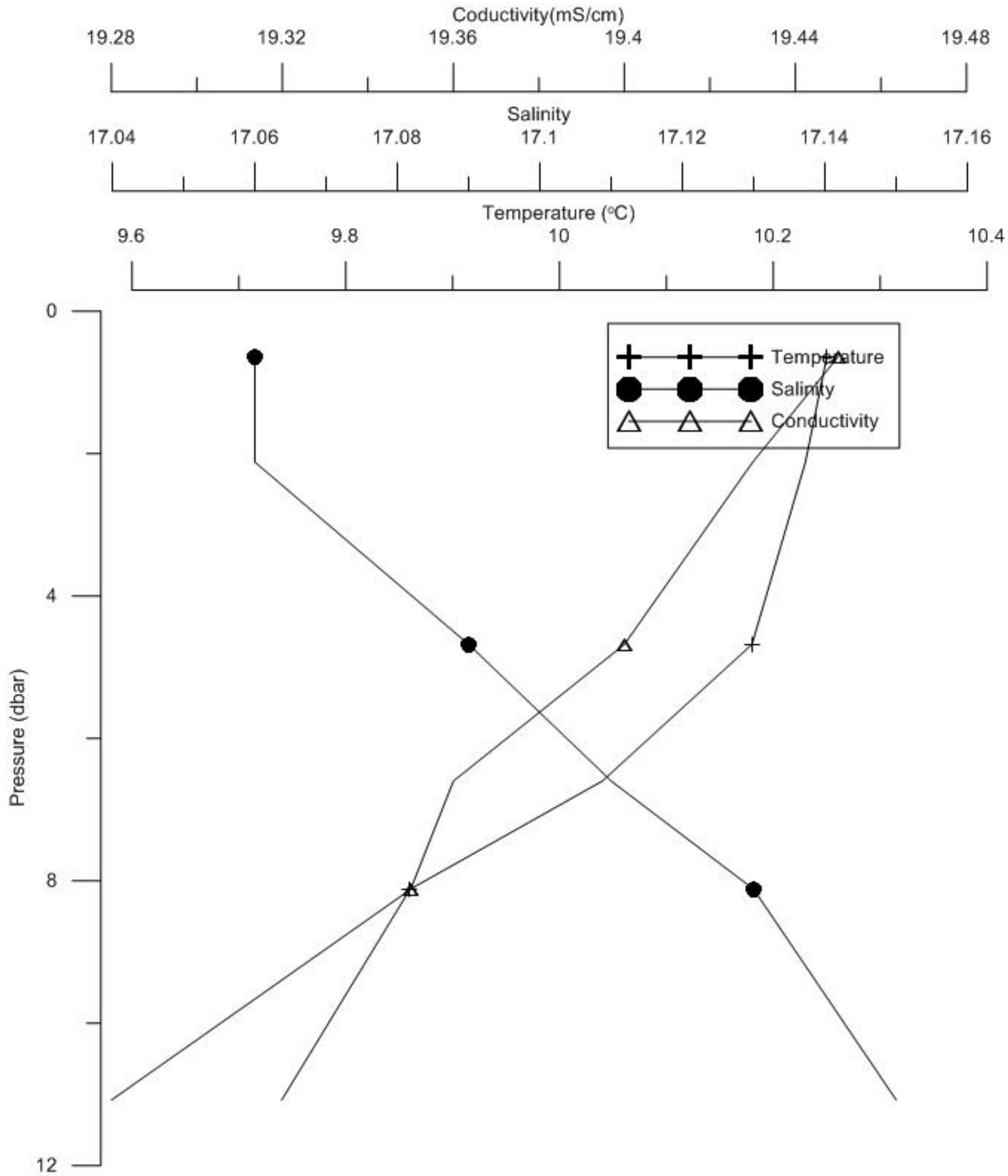

Figure 79.CTD from D11 Station for the first measurements in March2015

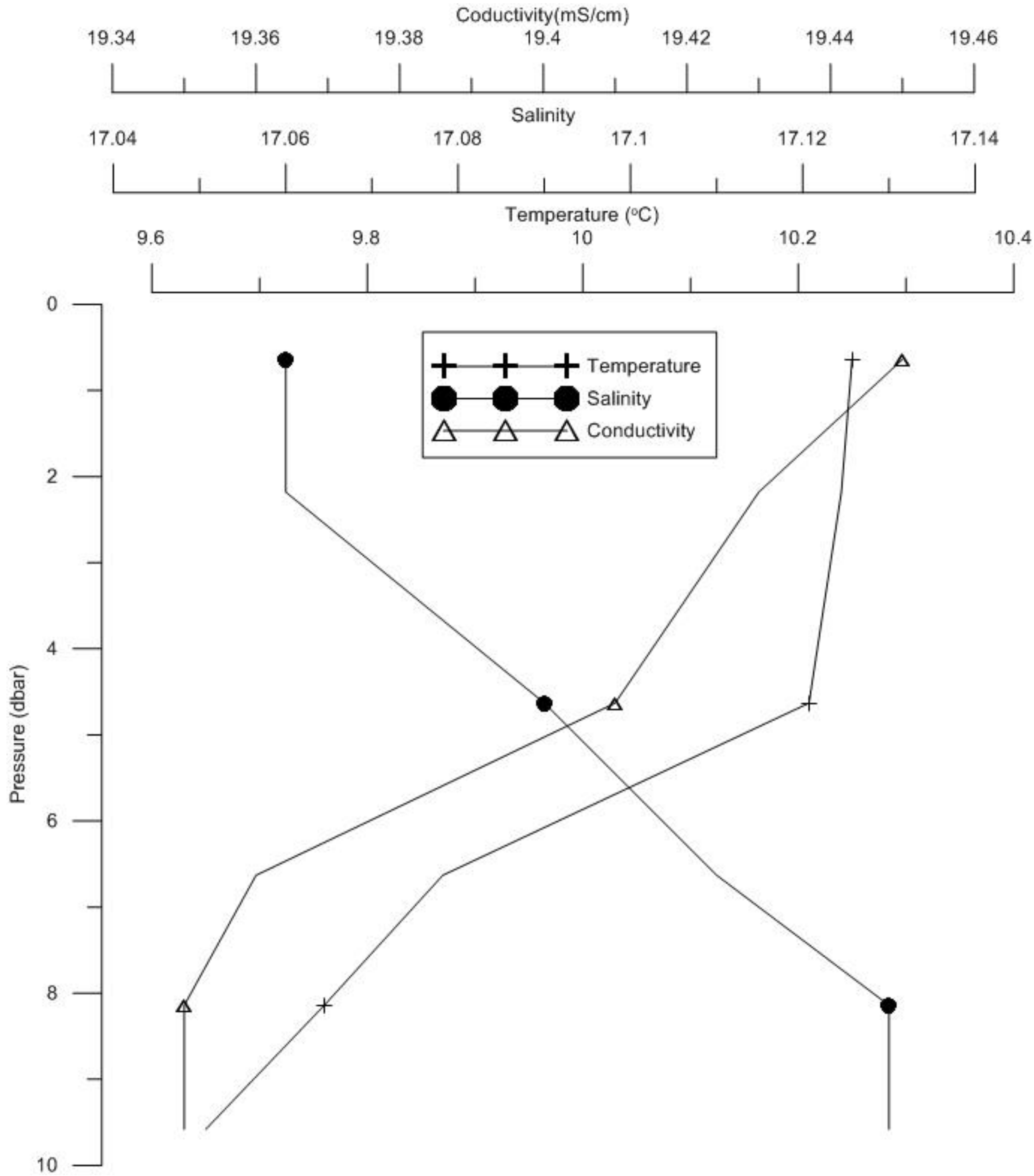

Figure 80.CTD from D12 Station for the first measurements in March2015

CTD graphs versus depth for each stations are given in the below. Conductivity, Salinity and Temperature results for the second period of March are given in Figures 81 -92.

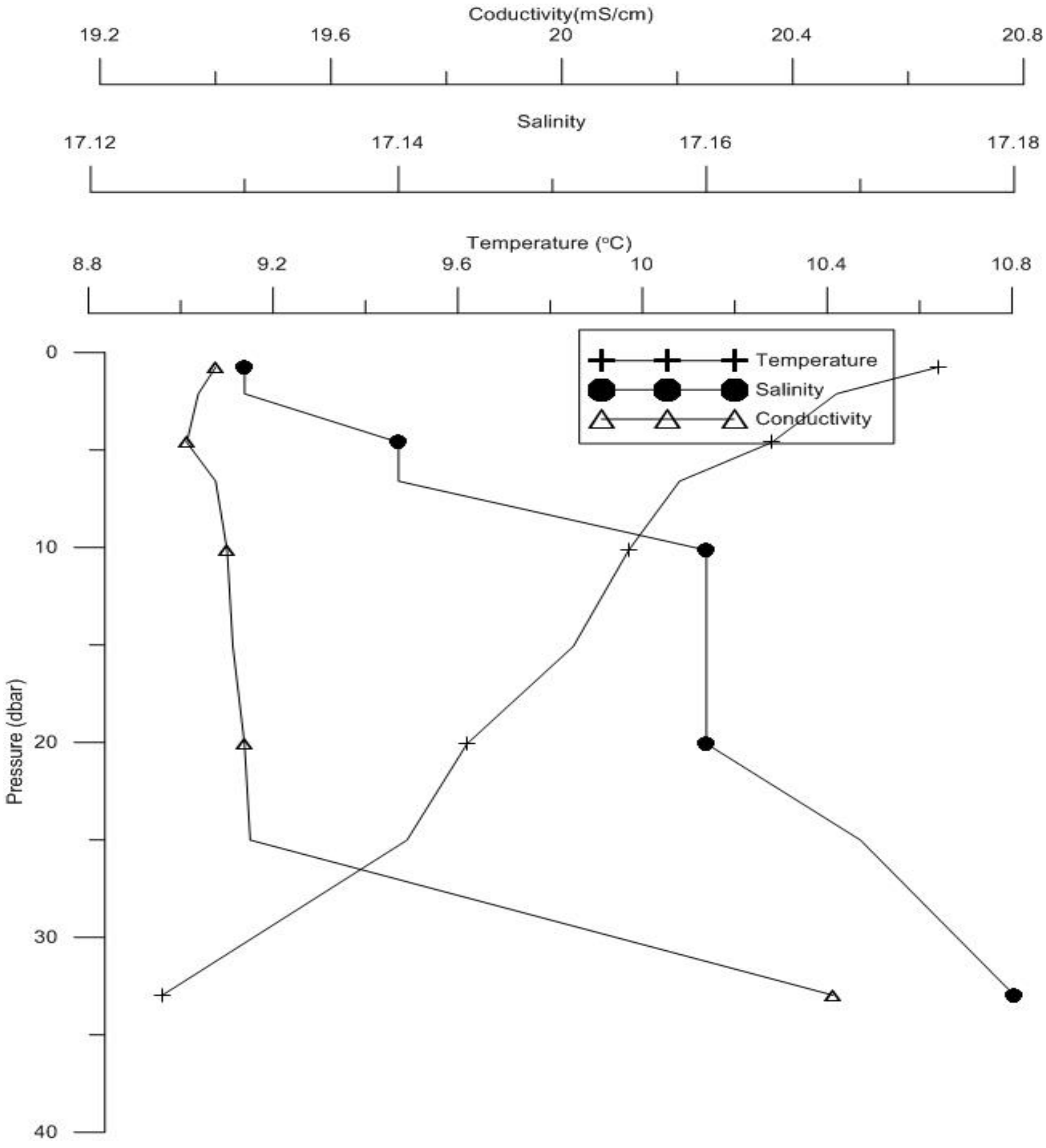

Figure 81. CTD from D1 Station for the second measurements in March 2015

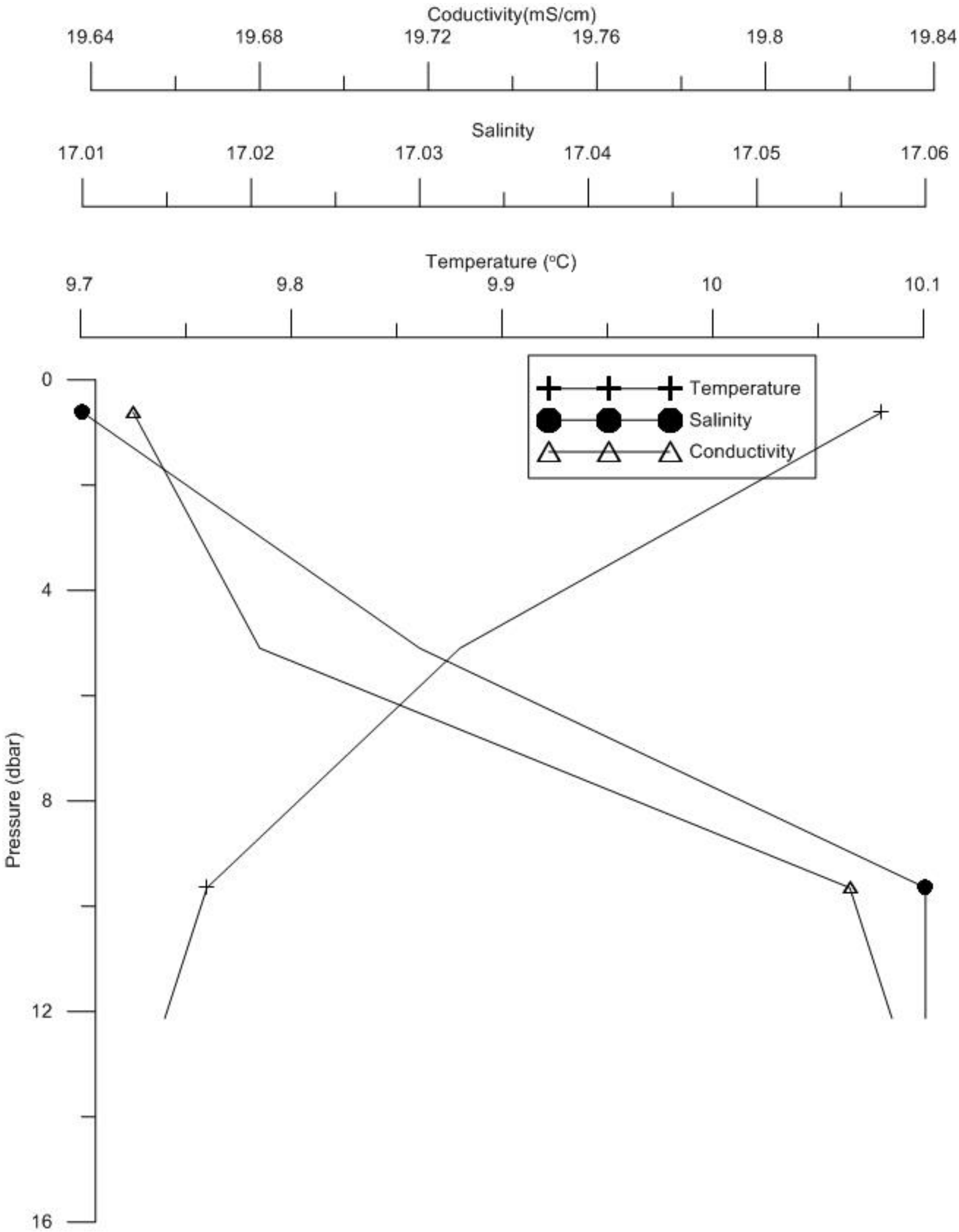

Figure 82.CTD from D2 Station for the second measurements in March2015

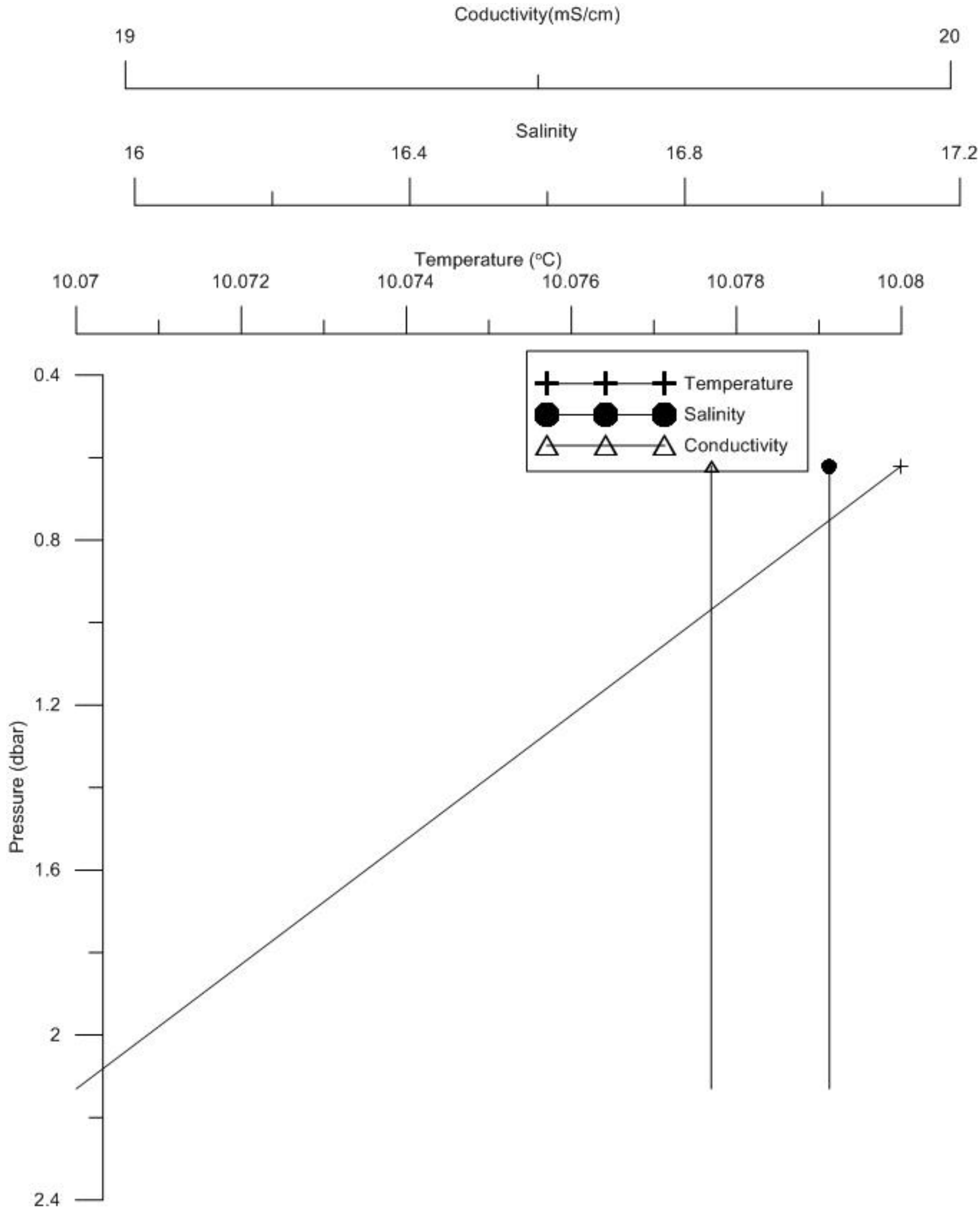

Figure 83.CTD from D3 Station for the second measurements in March2015

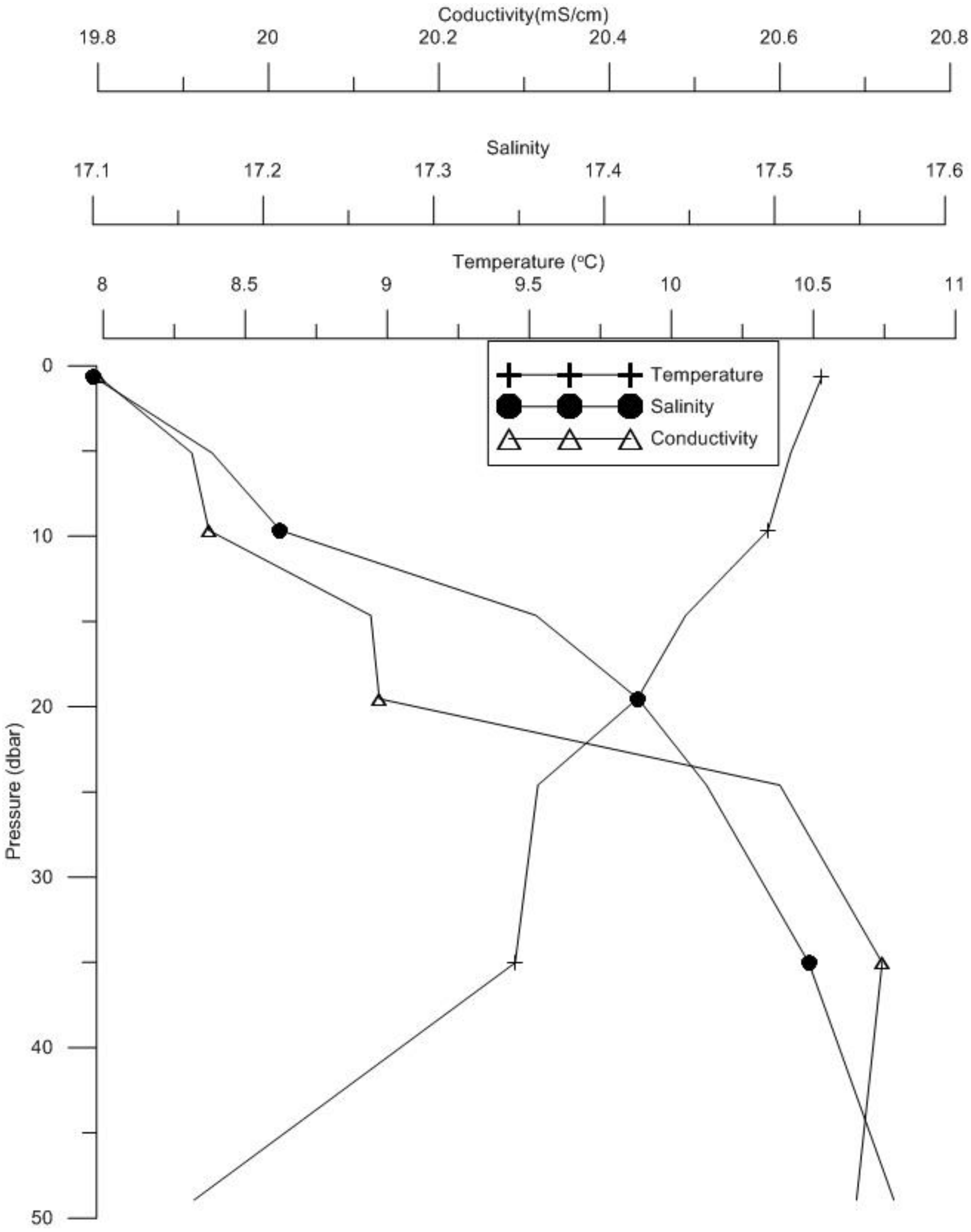

Figure 84.CTD from D4 Station for the second measurements in March2015

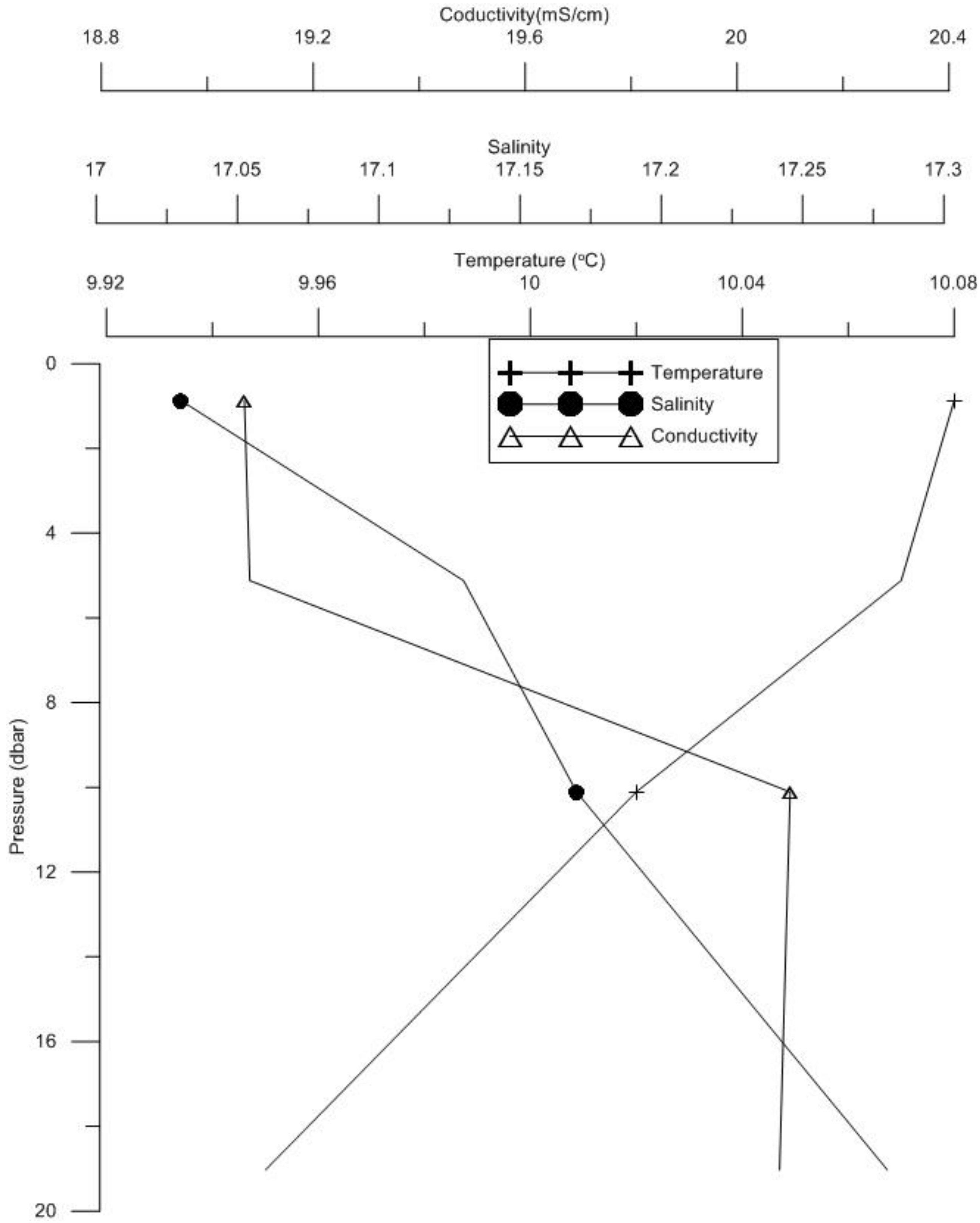

Figure 85.CTD from D5 Station for the second measurements in March2015

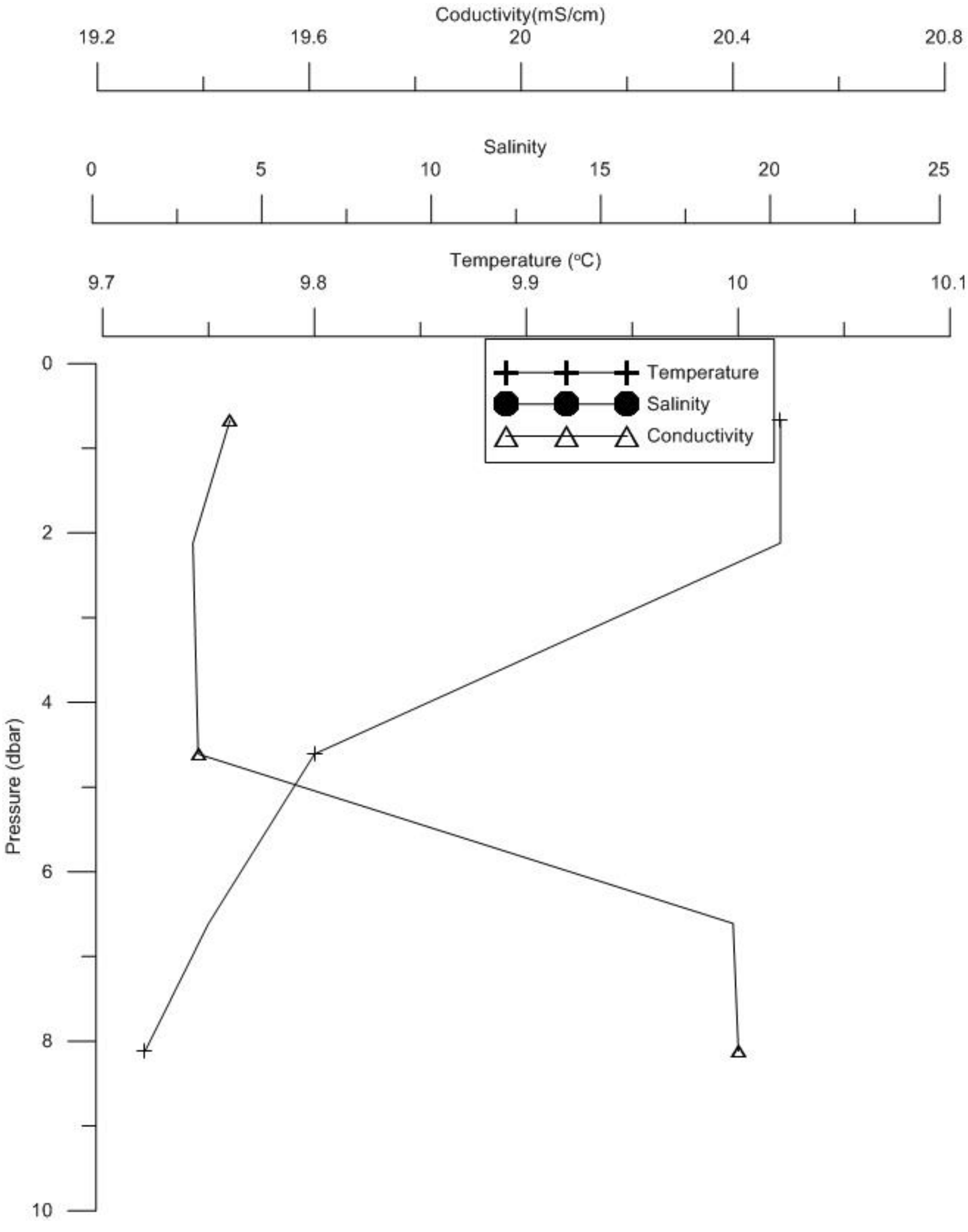

Figure 86.CTD from D6 Station for the second measurements in March2015

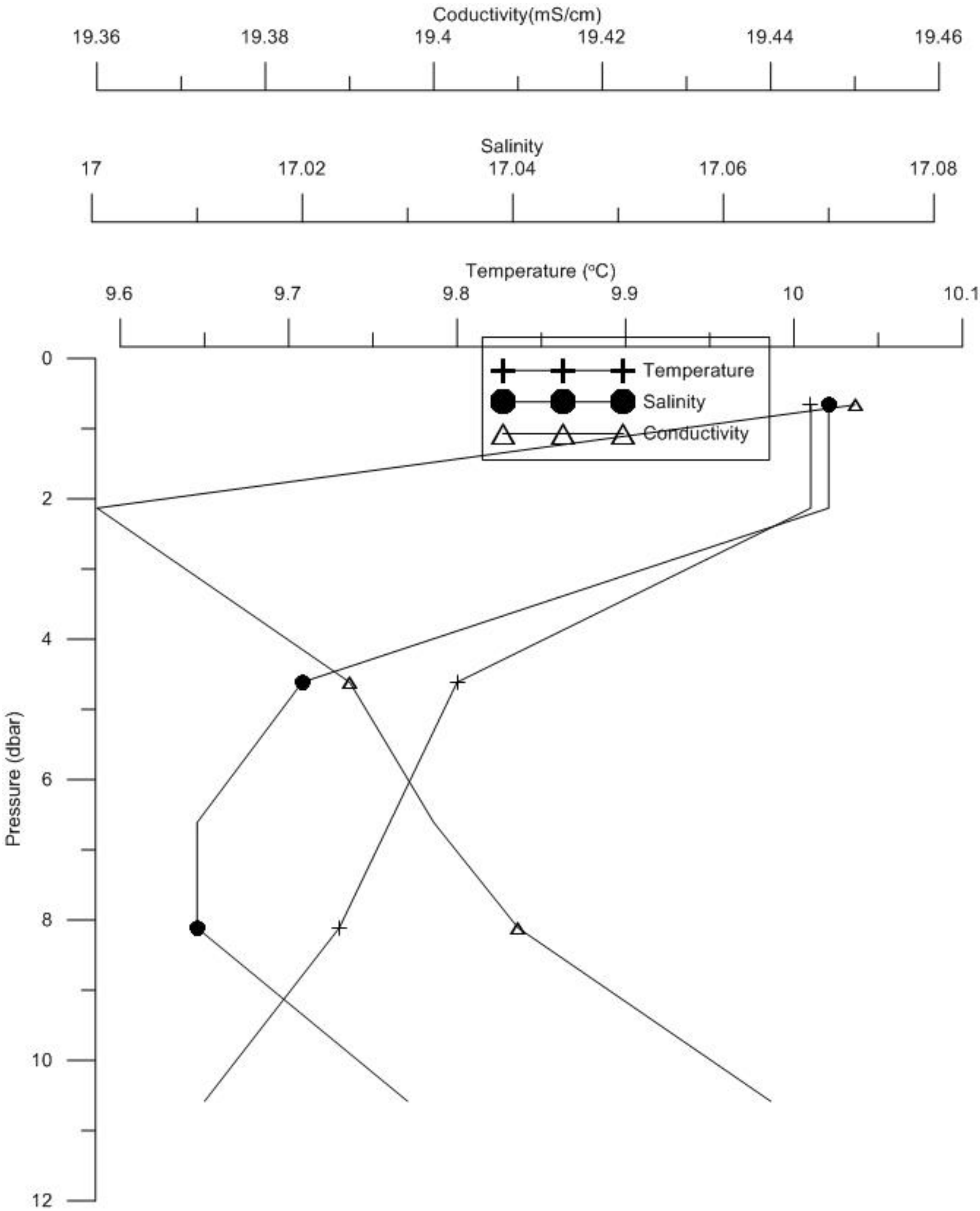

Figure 87.CTD from D7 Station for the second measurements in March2015

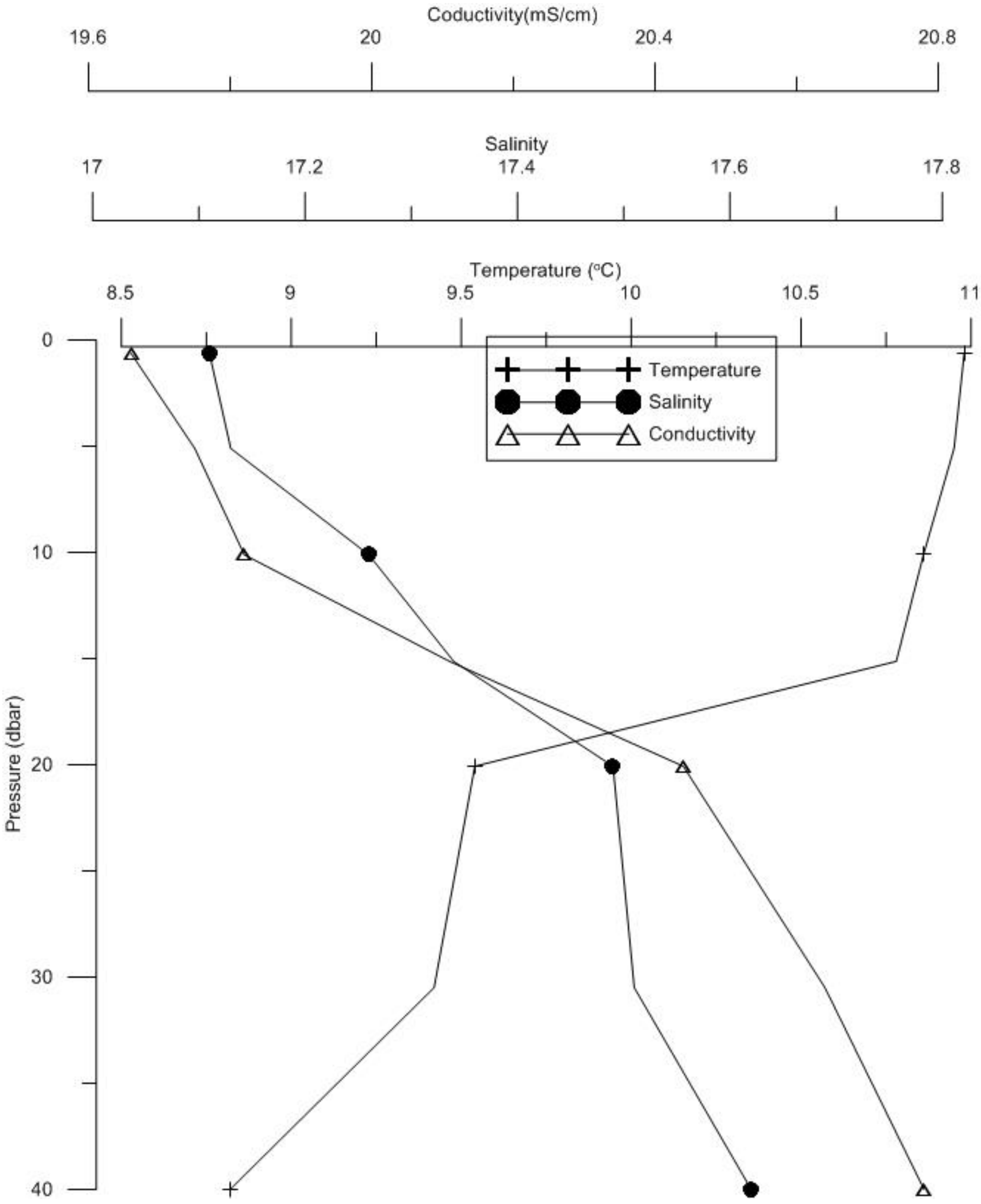

Figure 88.CTD from D8 Station for the second measurements in March2015

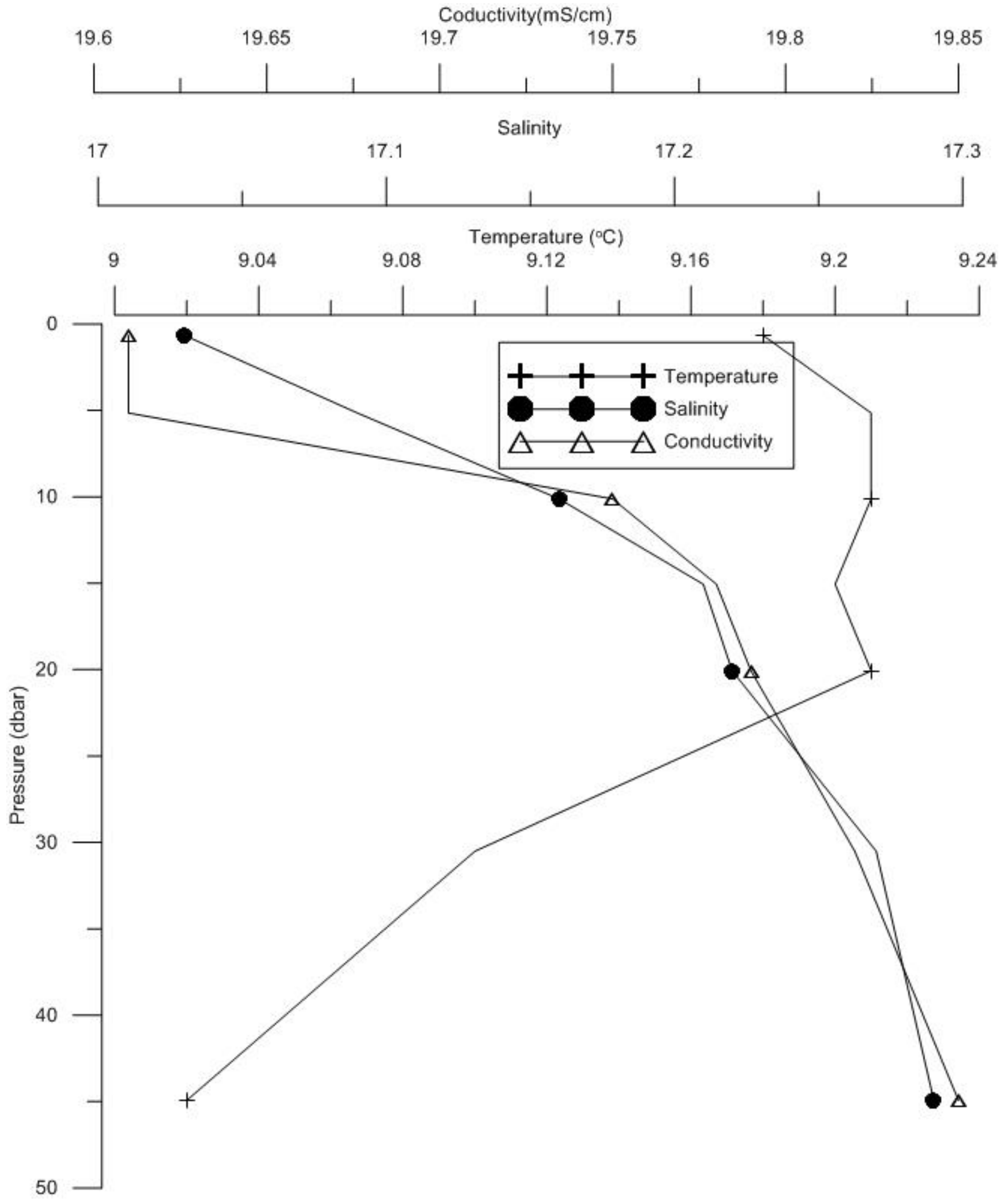

Figure 89.CTD from D9 Station for the secondmeasurements in March2015

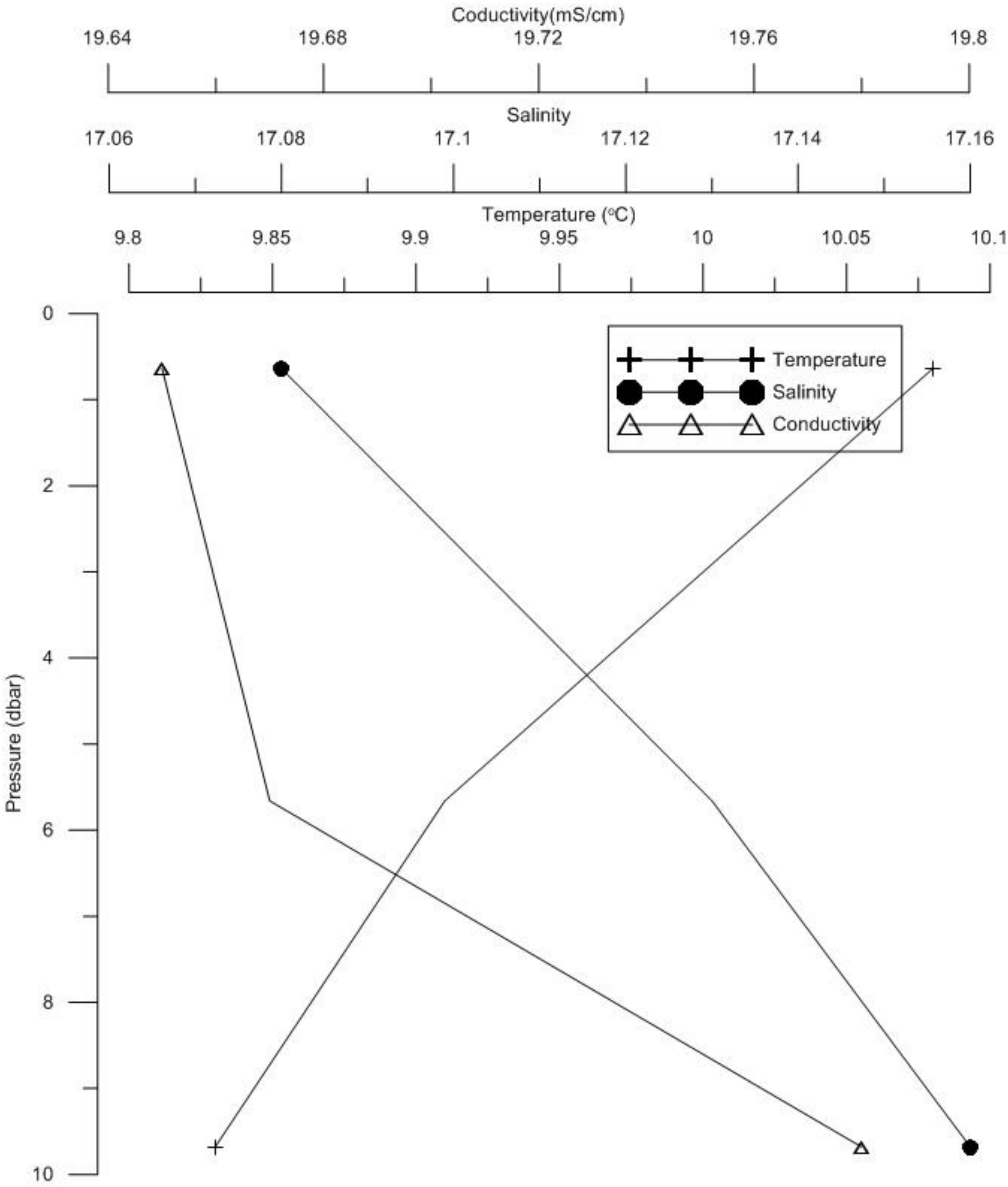

Figure 90.CTD from D10 Station for the second measurements in March2015

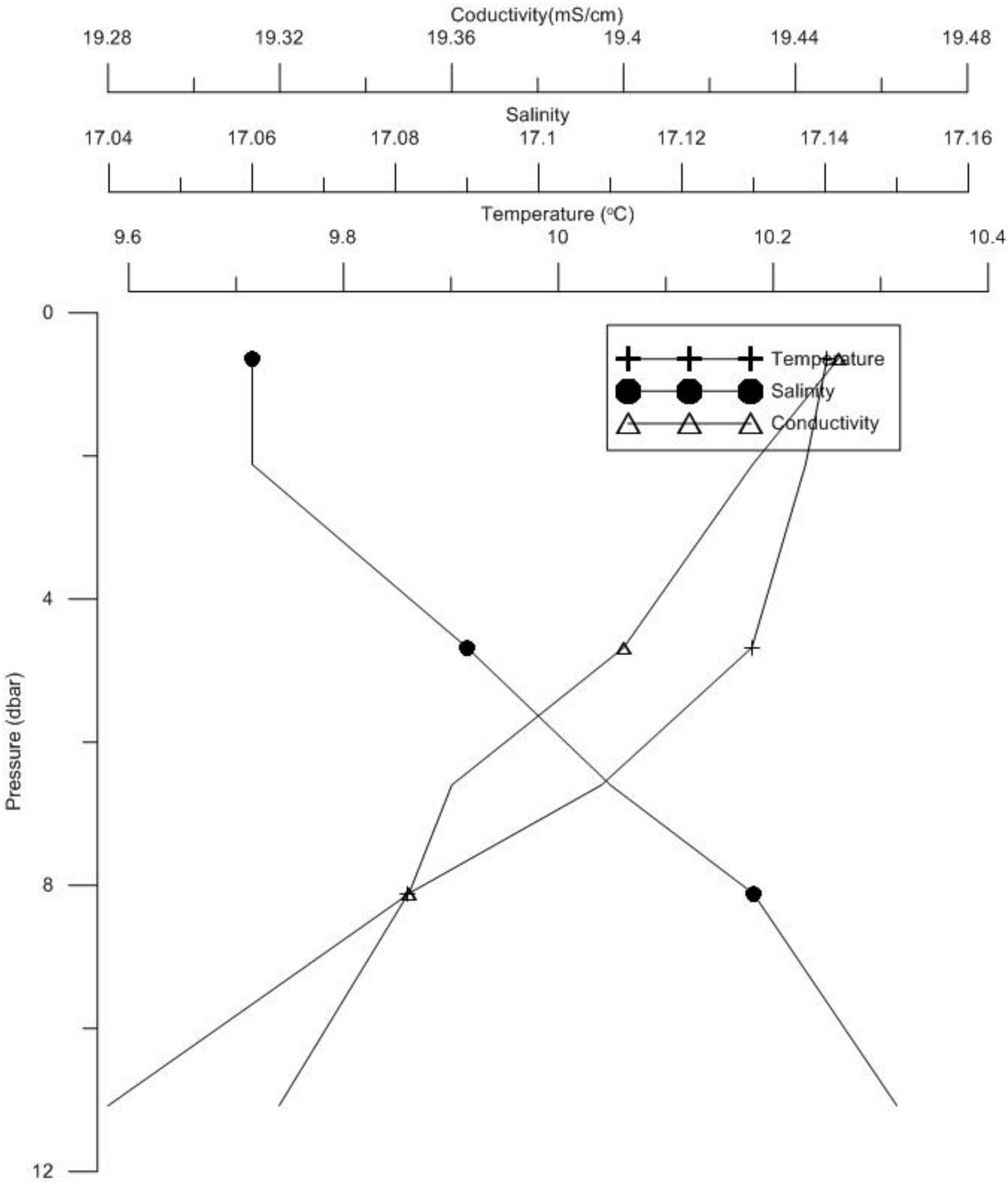

Figure 91.CTD from D11 Station for the secondmeasurements in March2015

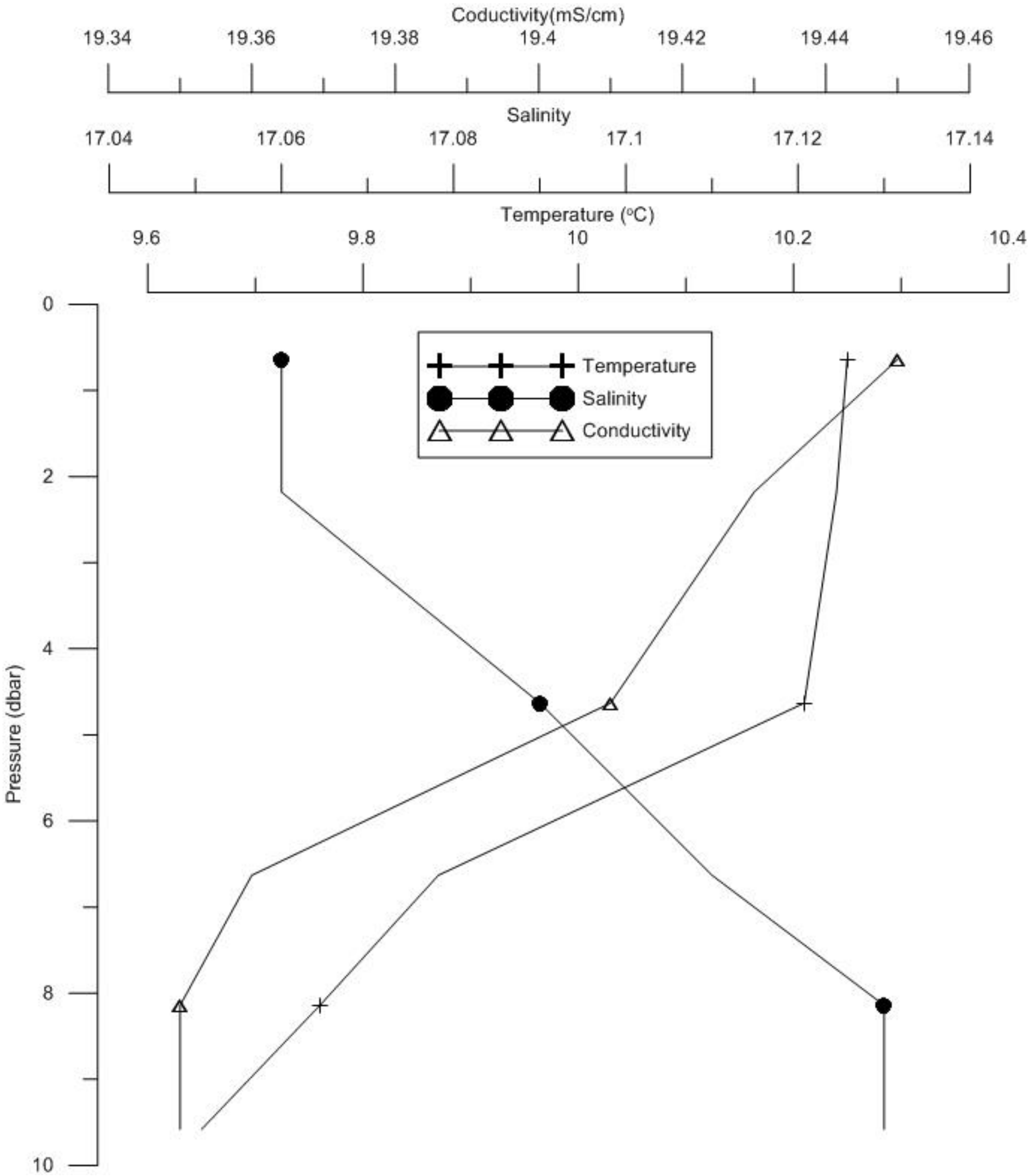

Figure 92.CTD from D12 Station for the second measurements in March2015

CTD graphs versus depth for each stations are given in the below. Conductivity, Salinity and Temperature results for the first period of April are given in Figures 93 -104.

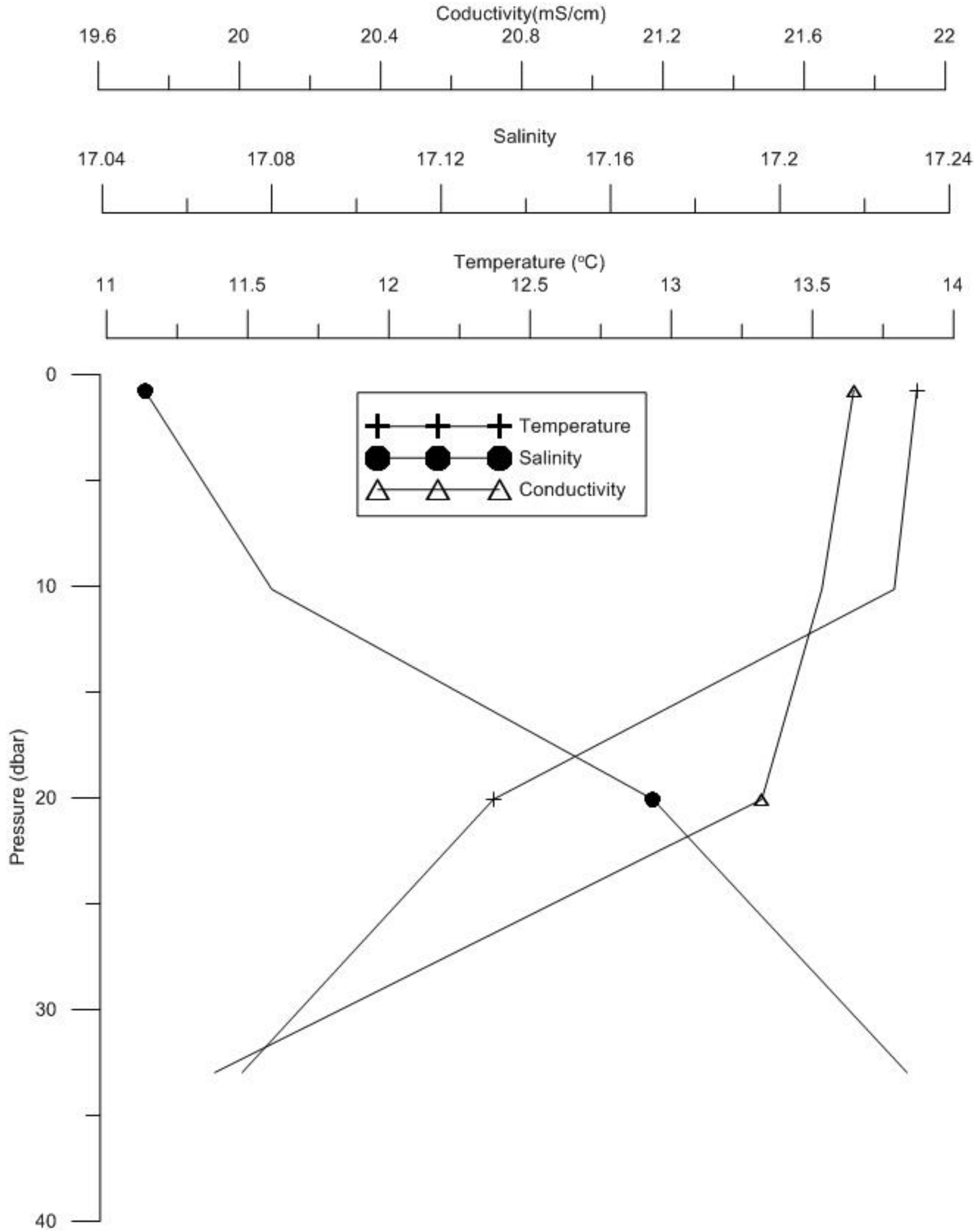

Figure 93. CTD from D1 Station for the first measurements in April2015

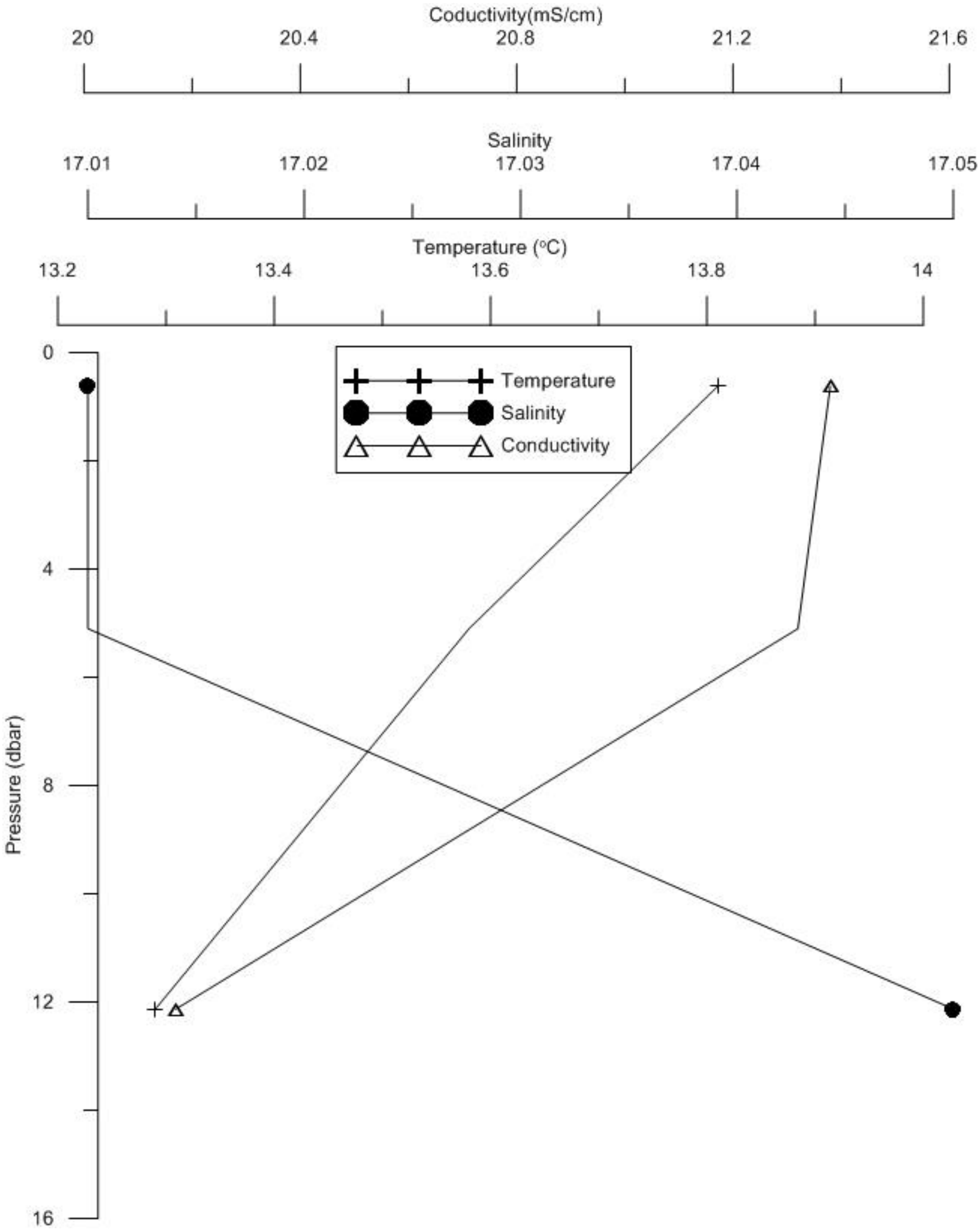

Figure 94.CTD from D2 Station for the first measurements in April2015

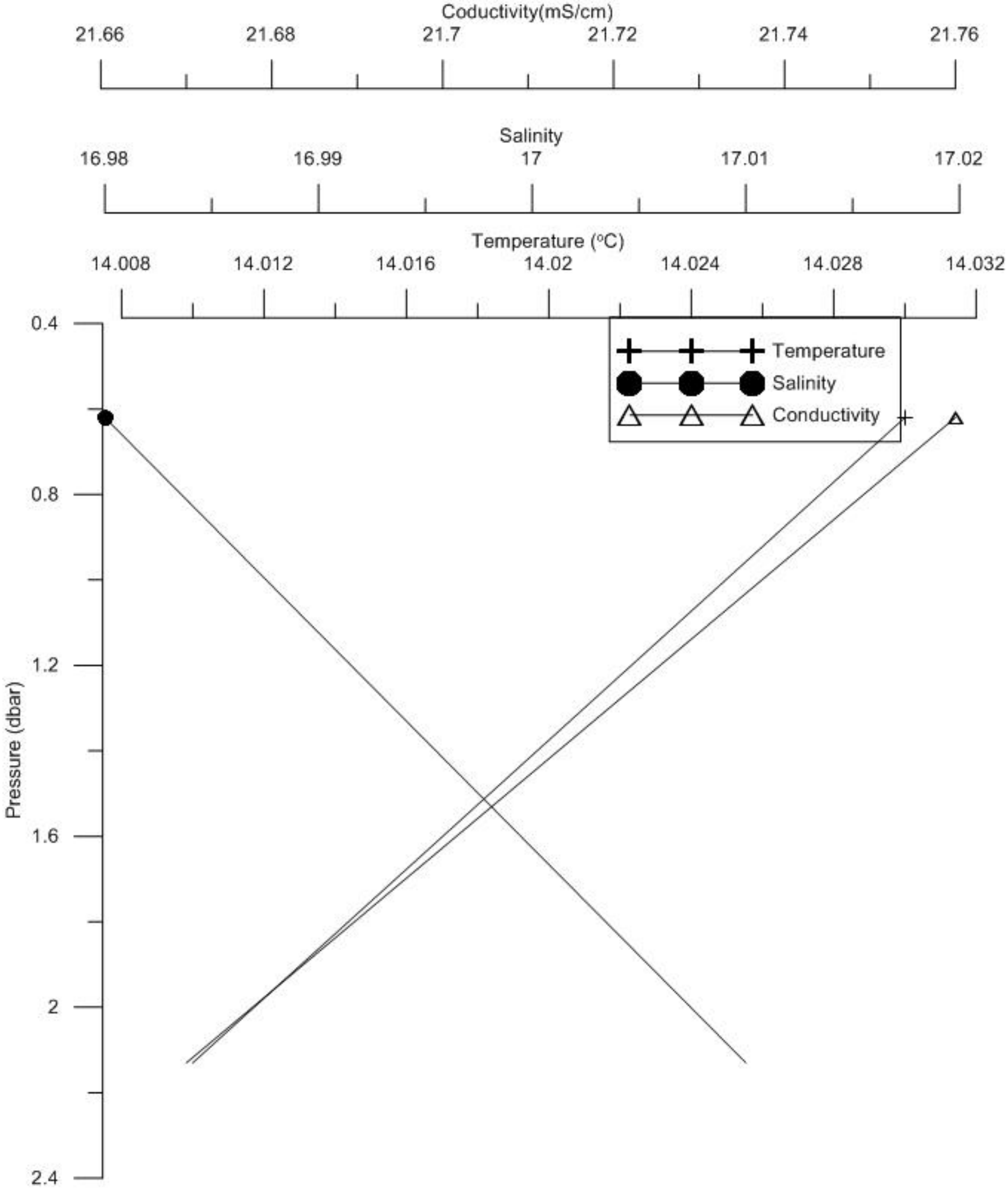

Figure 95.CTD from D3 Station for the first measurements in April2015

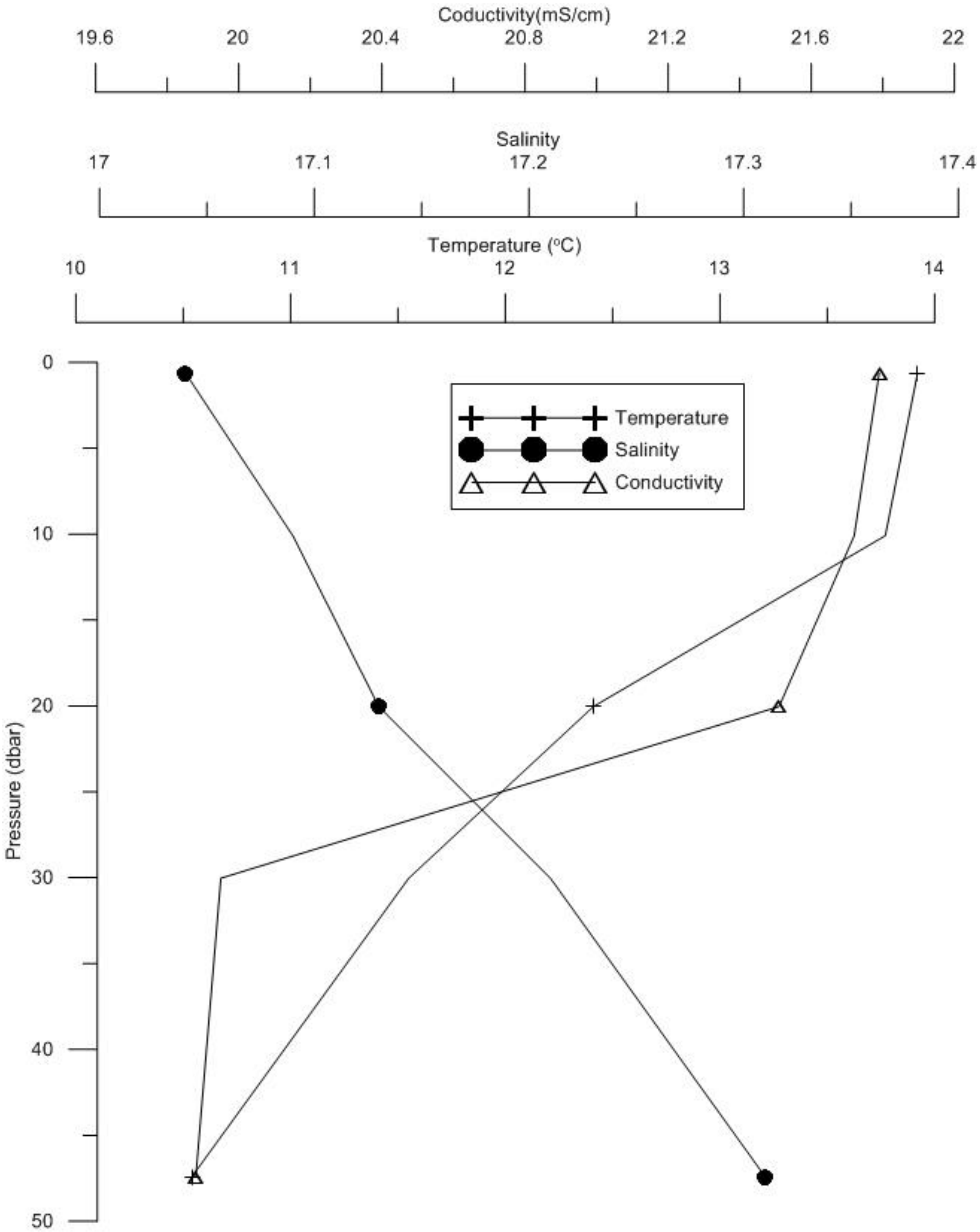

Figure 96.CTD from D4 Station for the first measurements in April2015

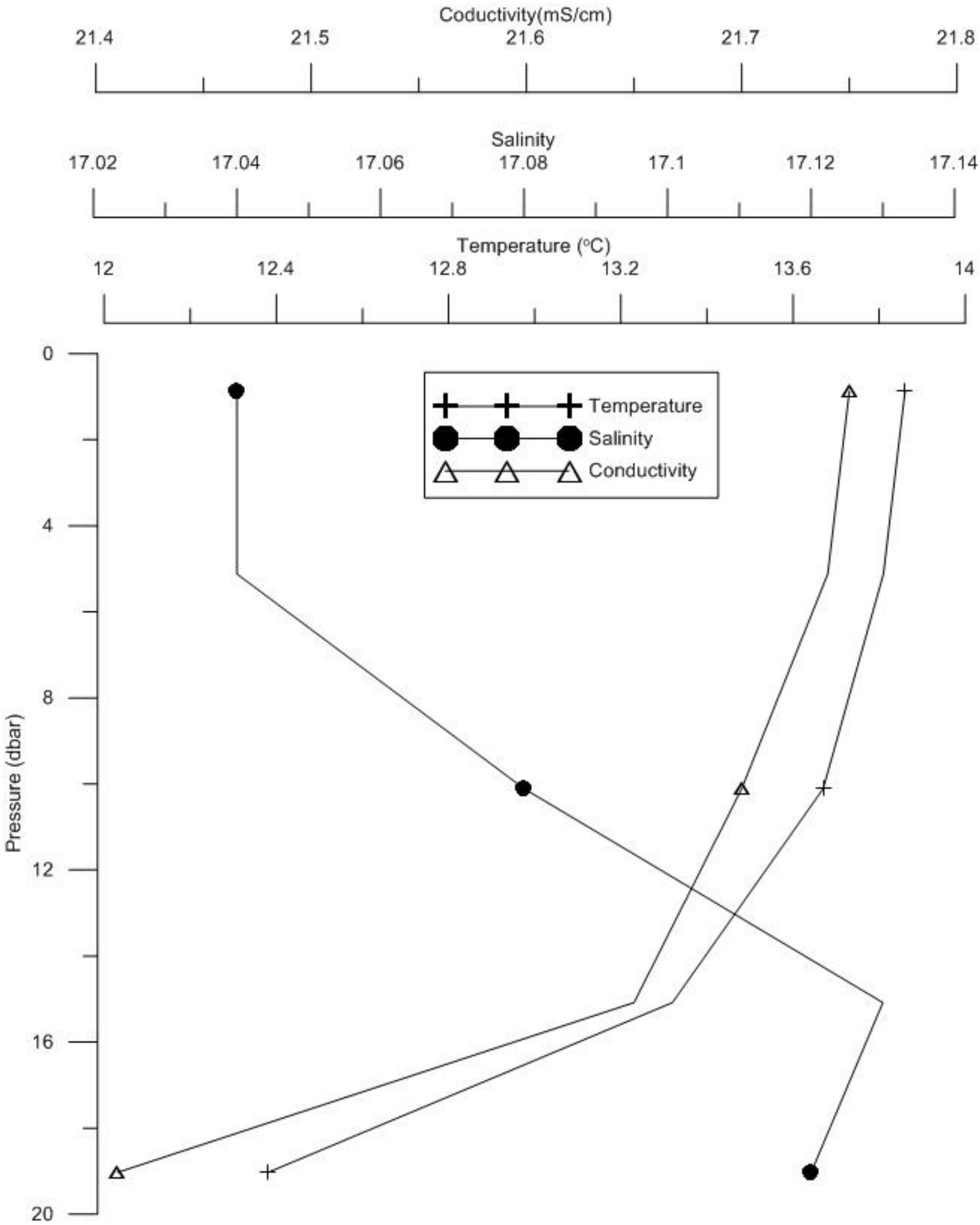

Figure 97.CTD from D5 Station for the first measurements in April2015

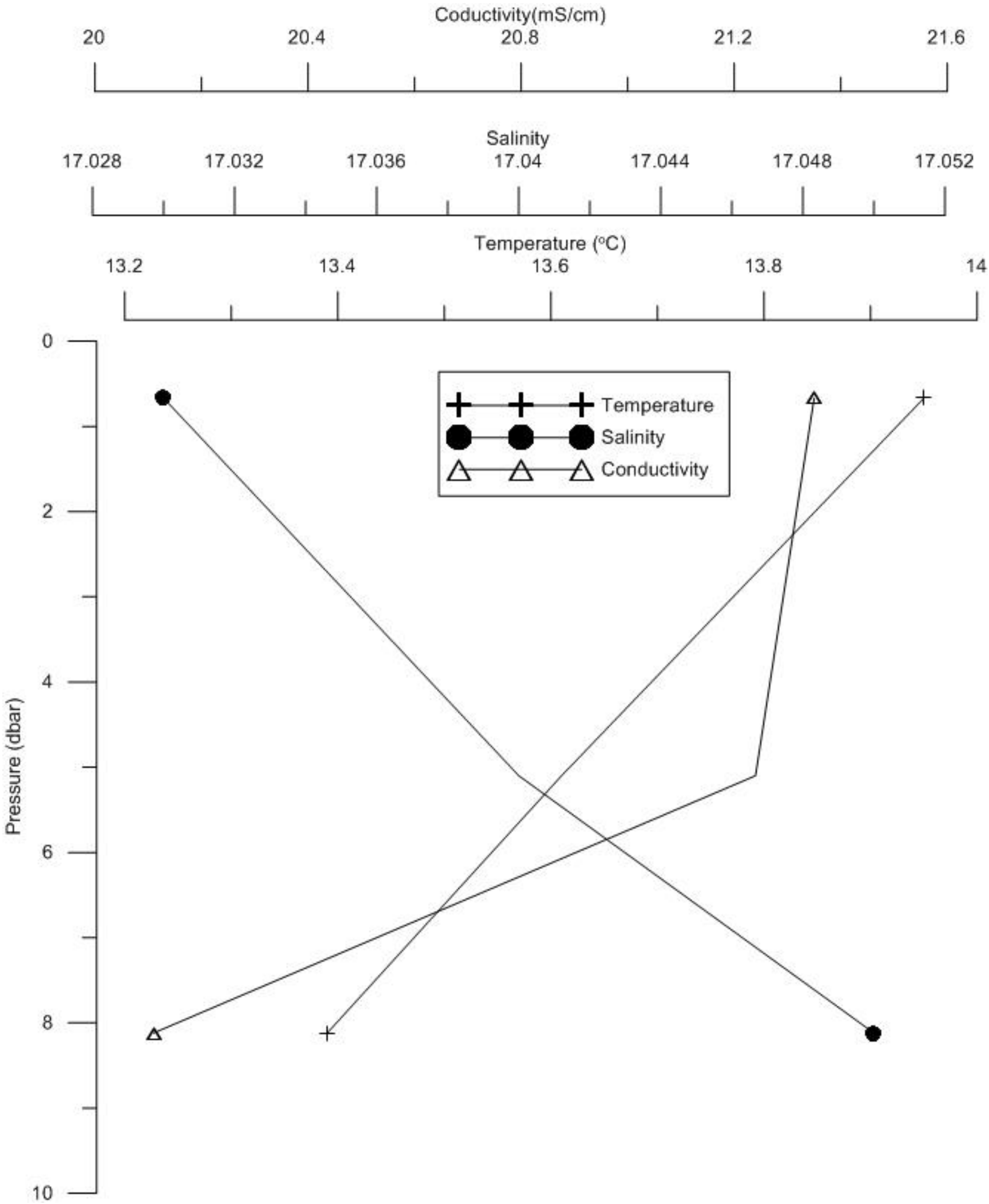

Figure 98.CTD from D6 Station for the first measurements in April2015

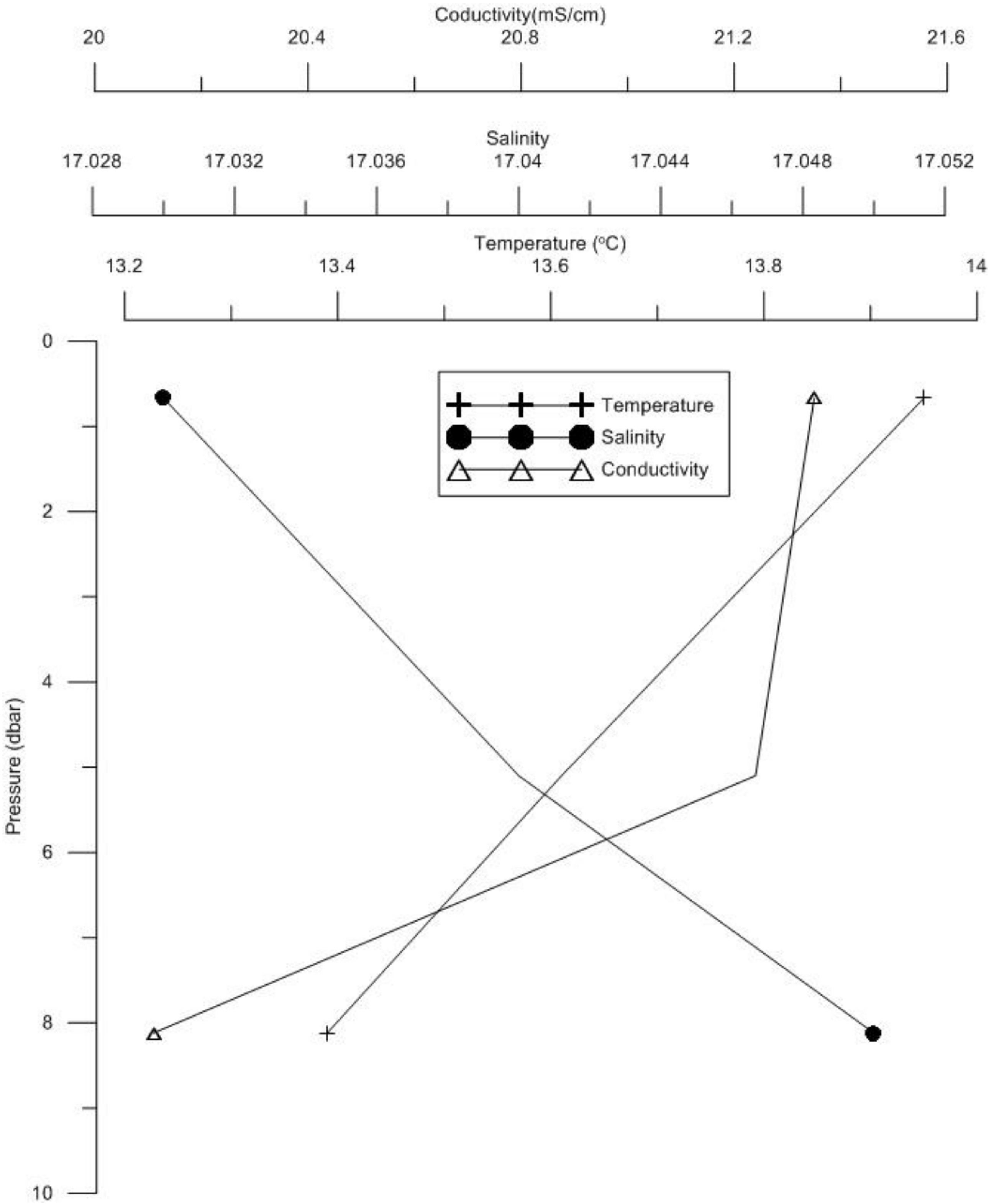

Figure 99.CTD from D7 Station for the first measurements in April2015

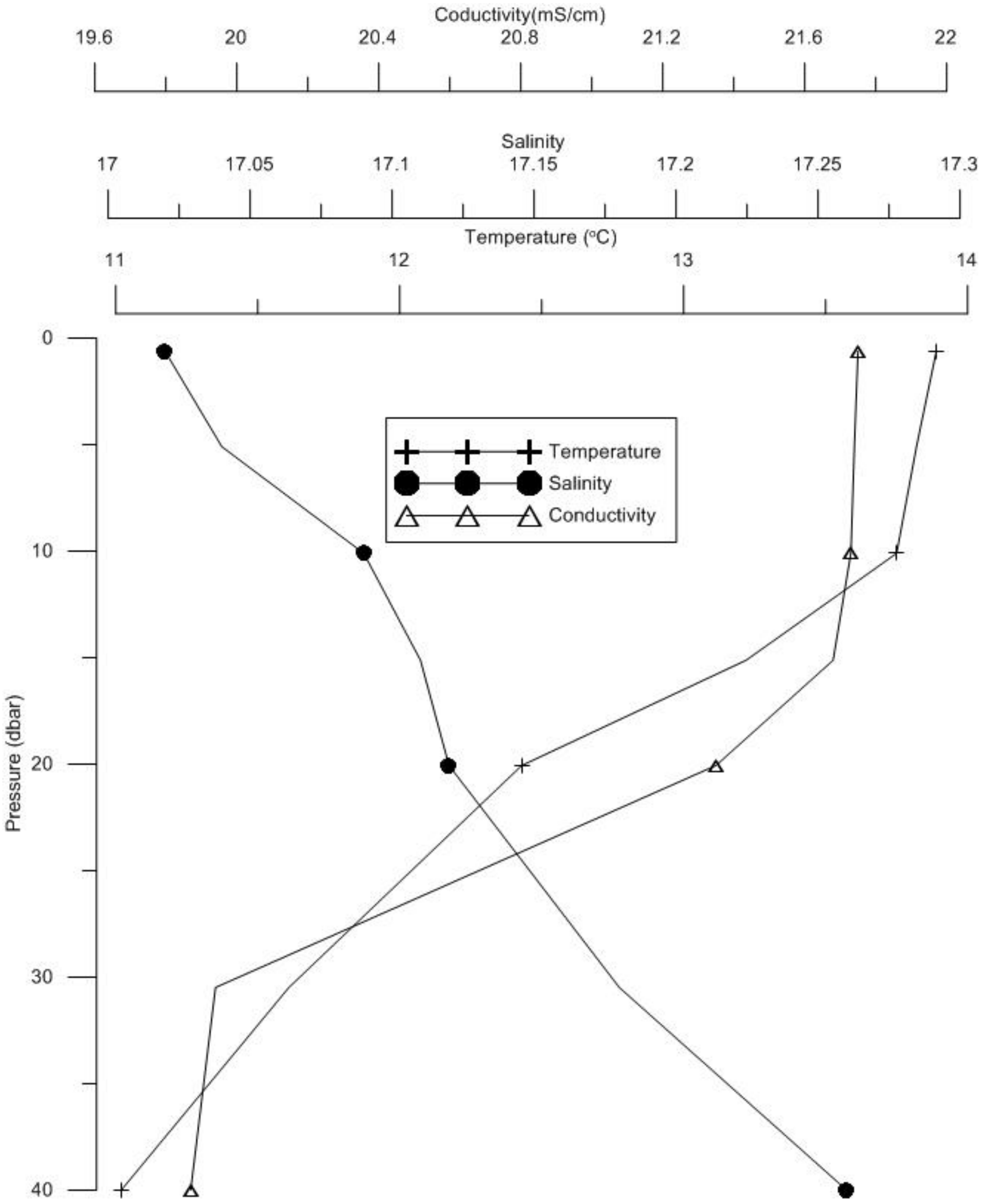

Figure 100.CTD from D8 Station for the first measurements in April2015

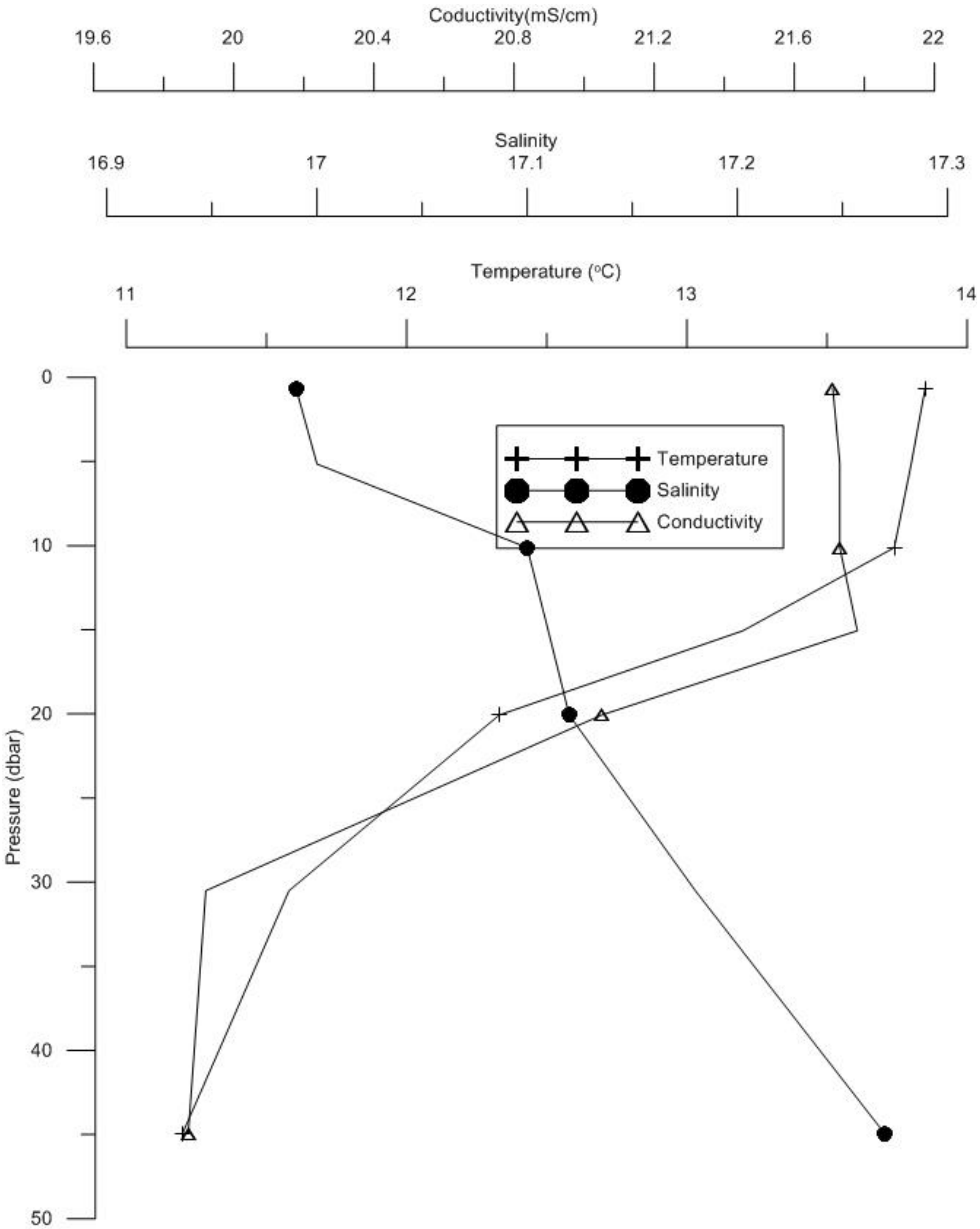

Figure 101.CTD from D9 Station for the first measurements in April2015

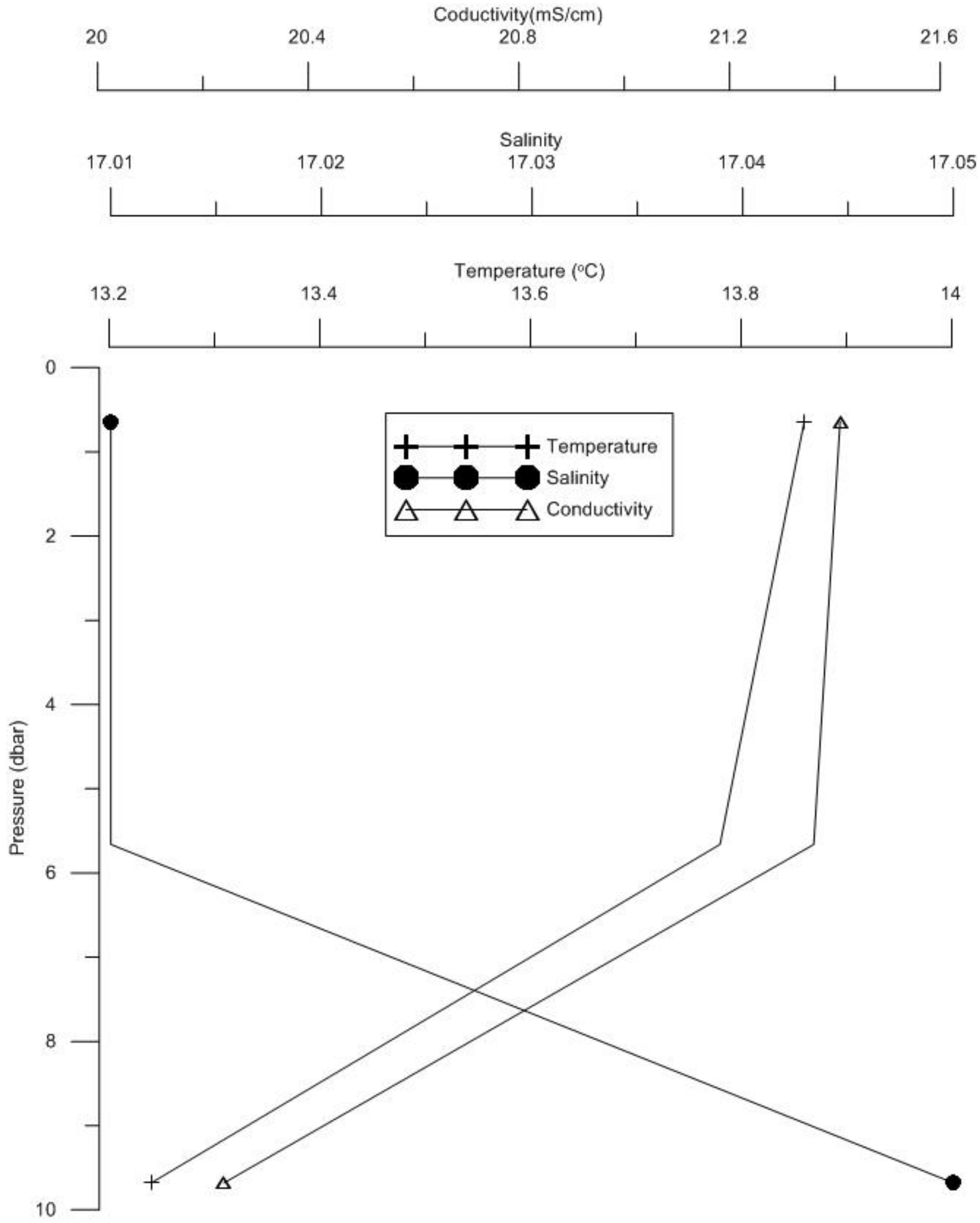

Figure 102.CTD from D10 Station for the first measurements in April2015

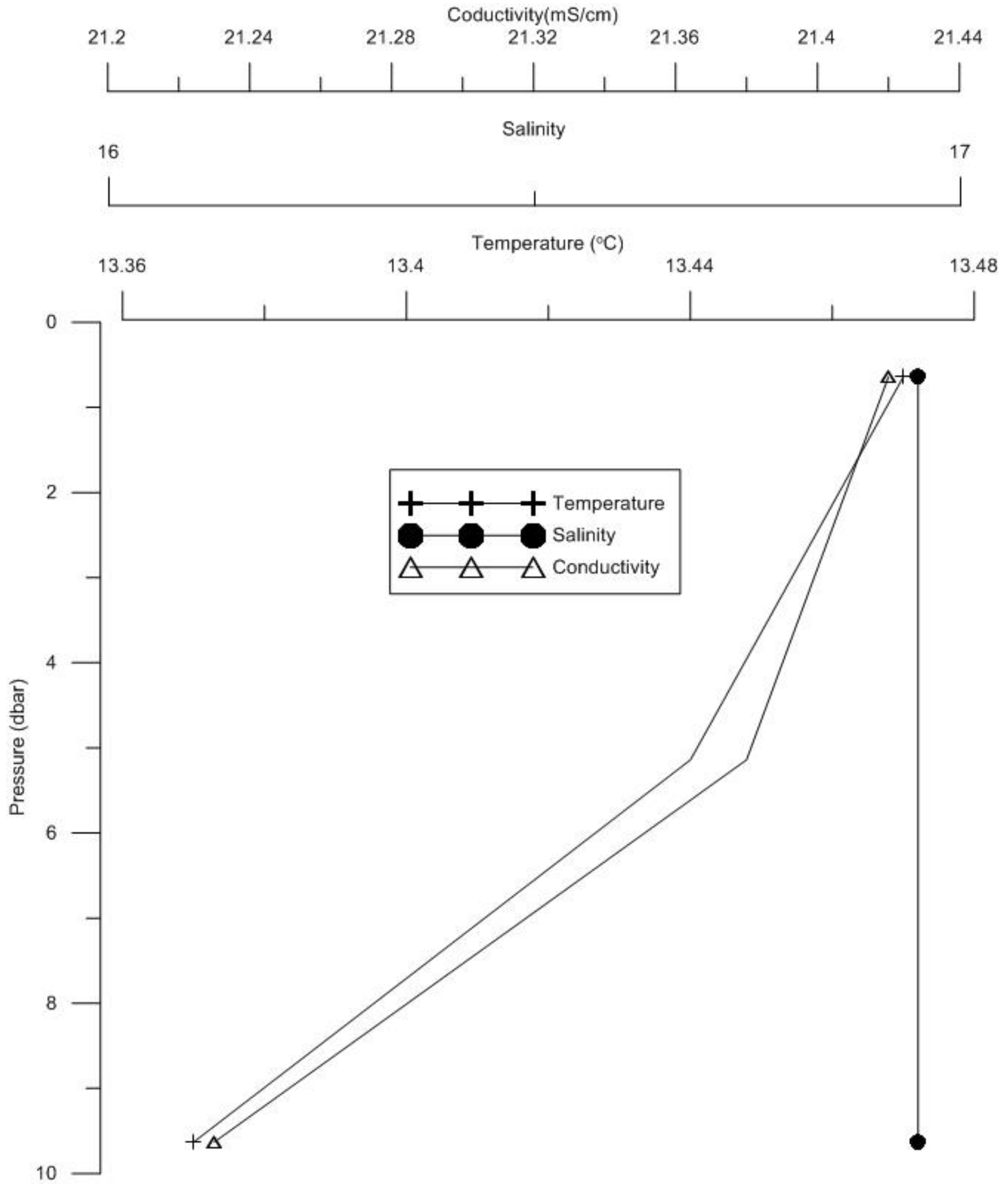

Figure 103.CTD from D11 Station for the first measurements in April2015

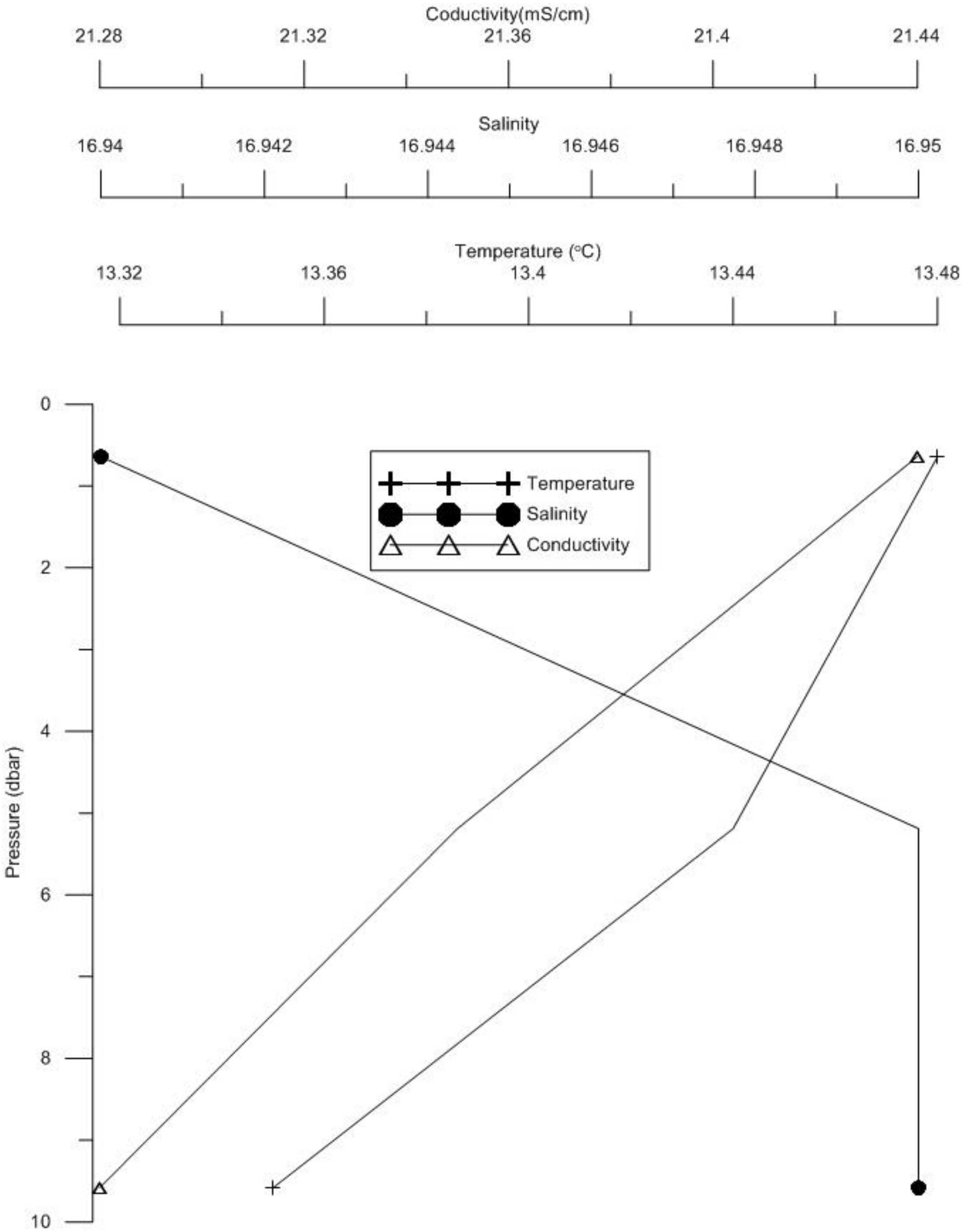

Figure 104.CTD from D12 Station for the first measurements in April2015

CTD graphs versus depth for each stations are given in the below. Conductivity, Salinity and Temperature results for the second period of April are given in Figures 105 -116.

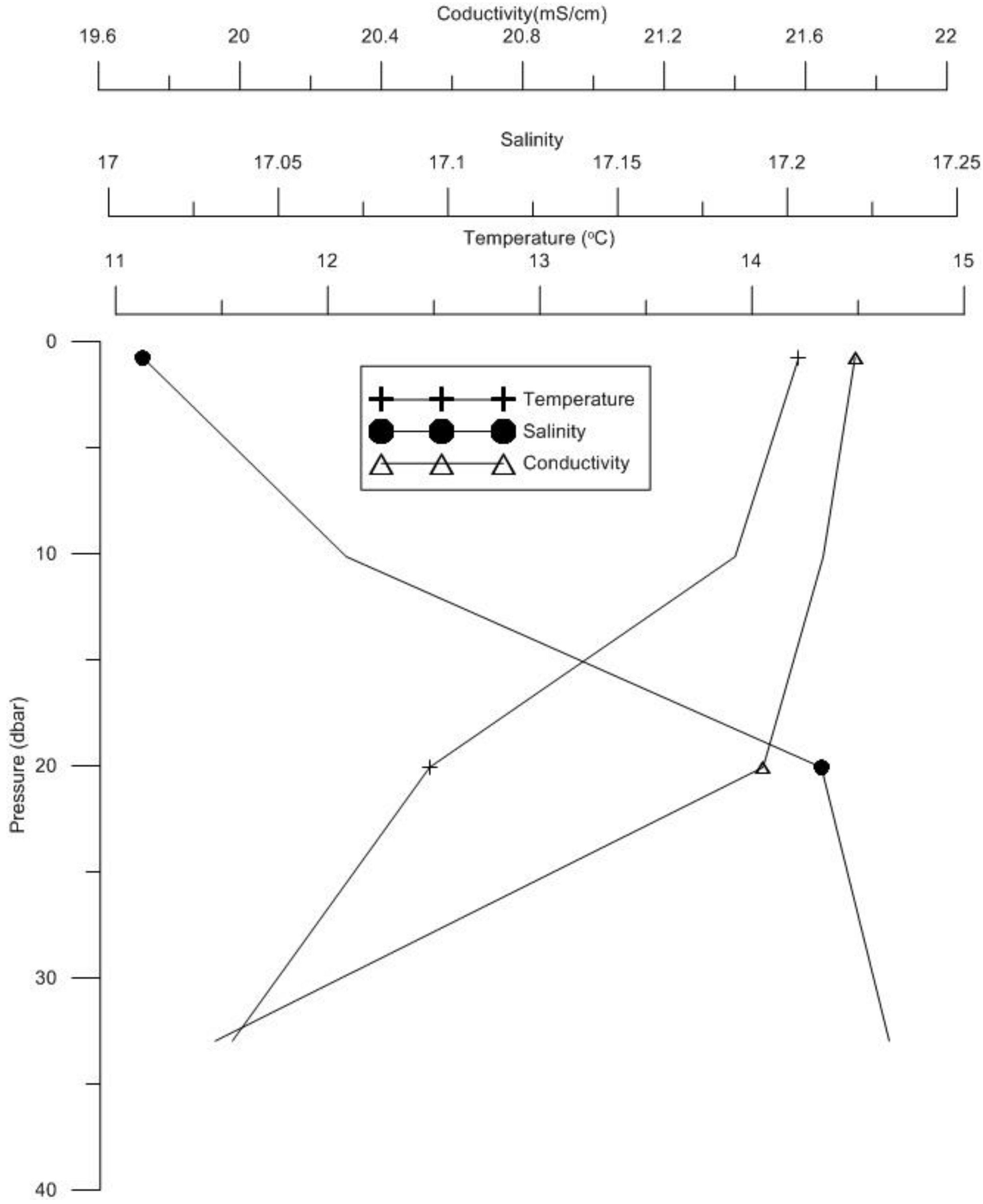

Figure 105. CTD from D1 Station for the second measurements in April2015

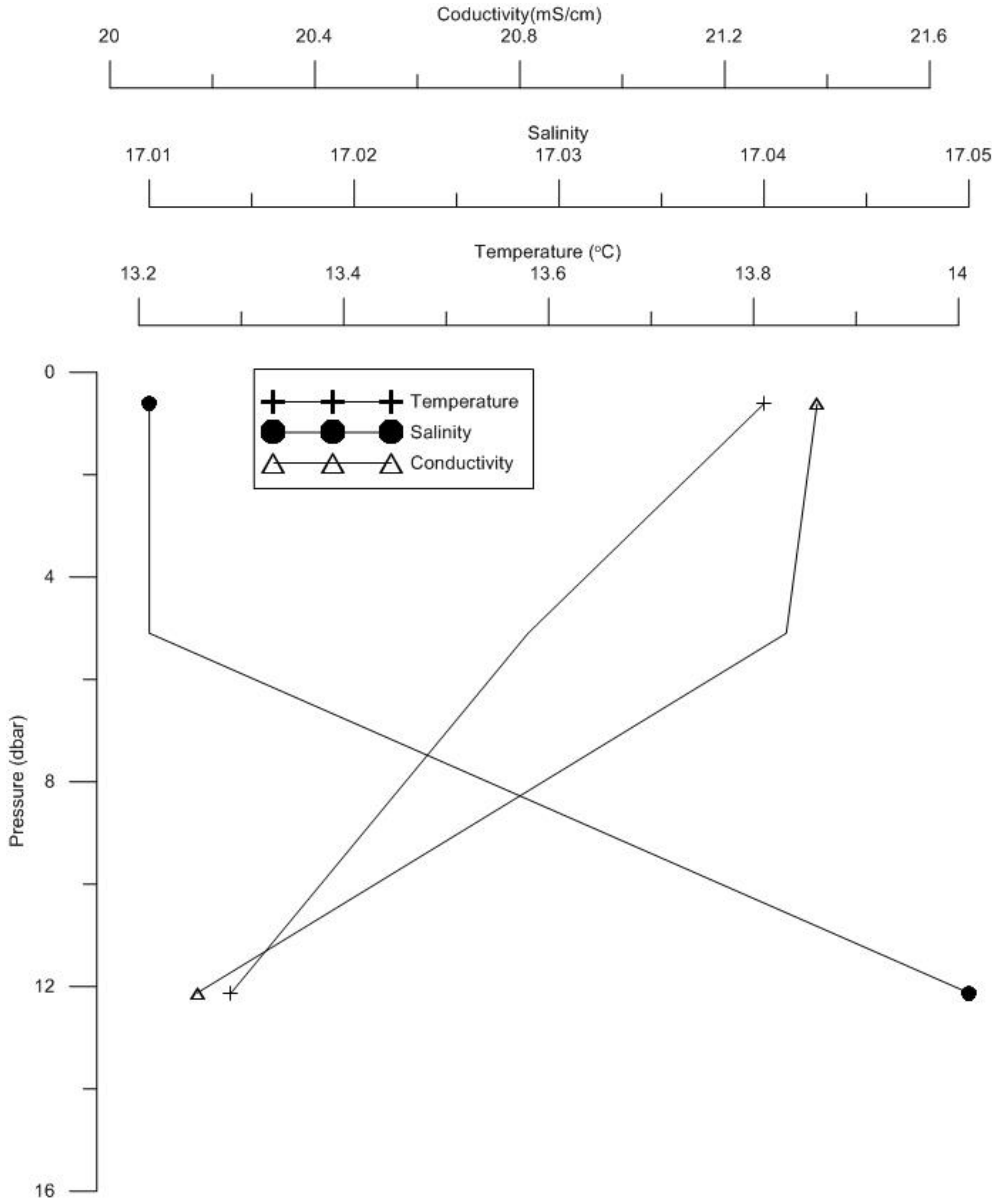

Figure 106.CTD from D2 Station for the second measurements in April2015

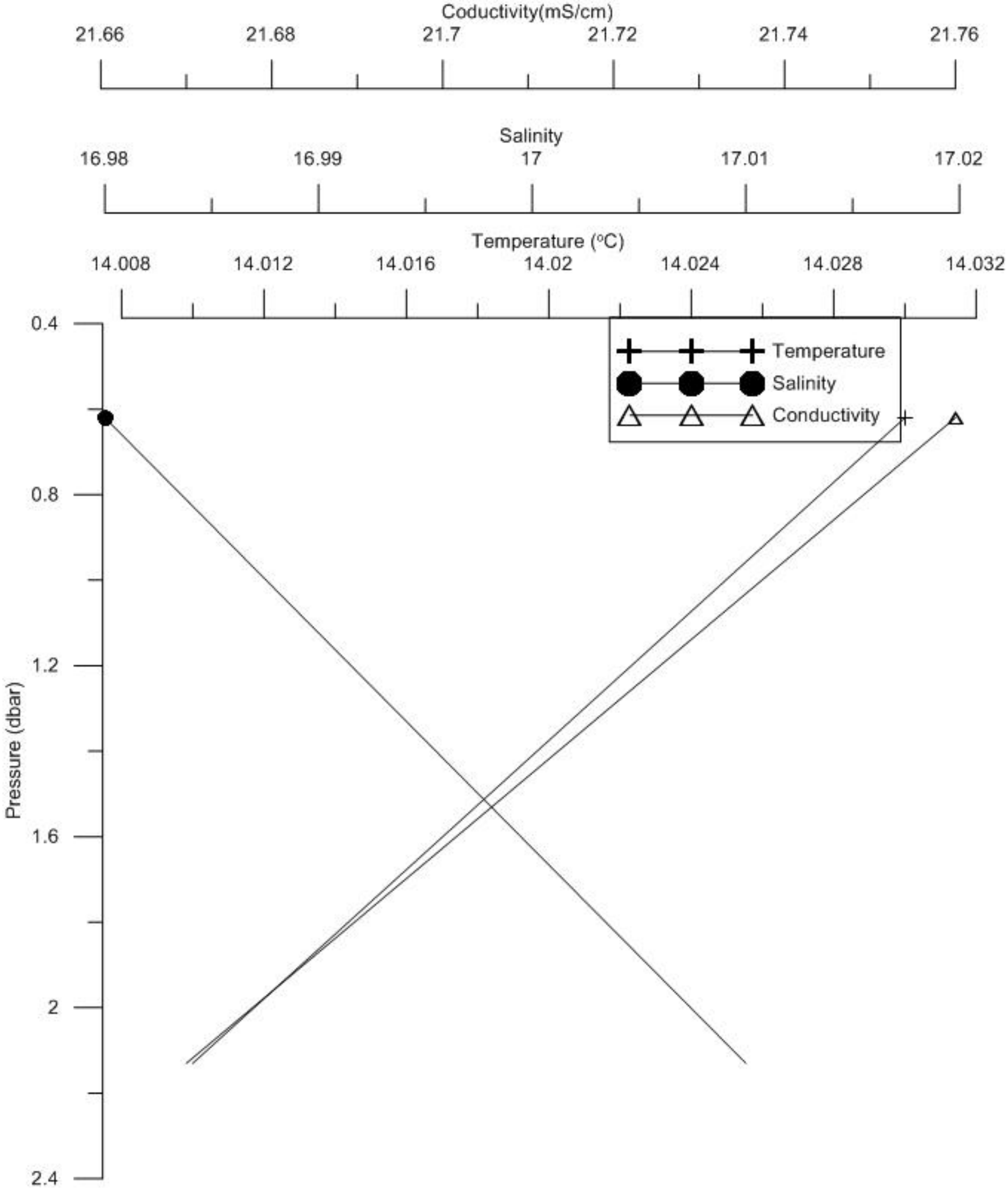

Figure 107.CTD from D3 Station for the second measurements in April2015

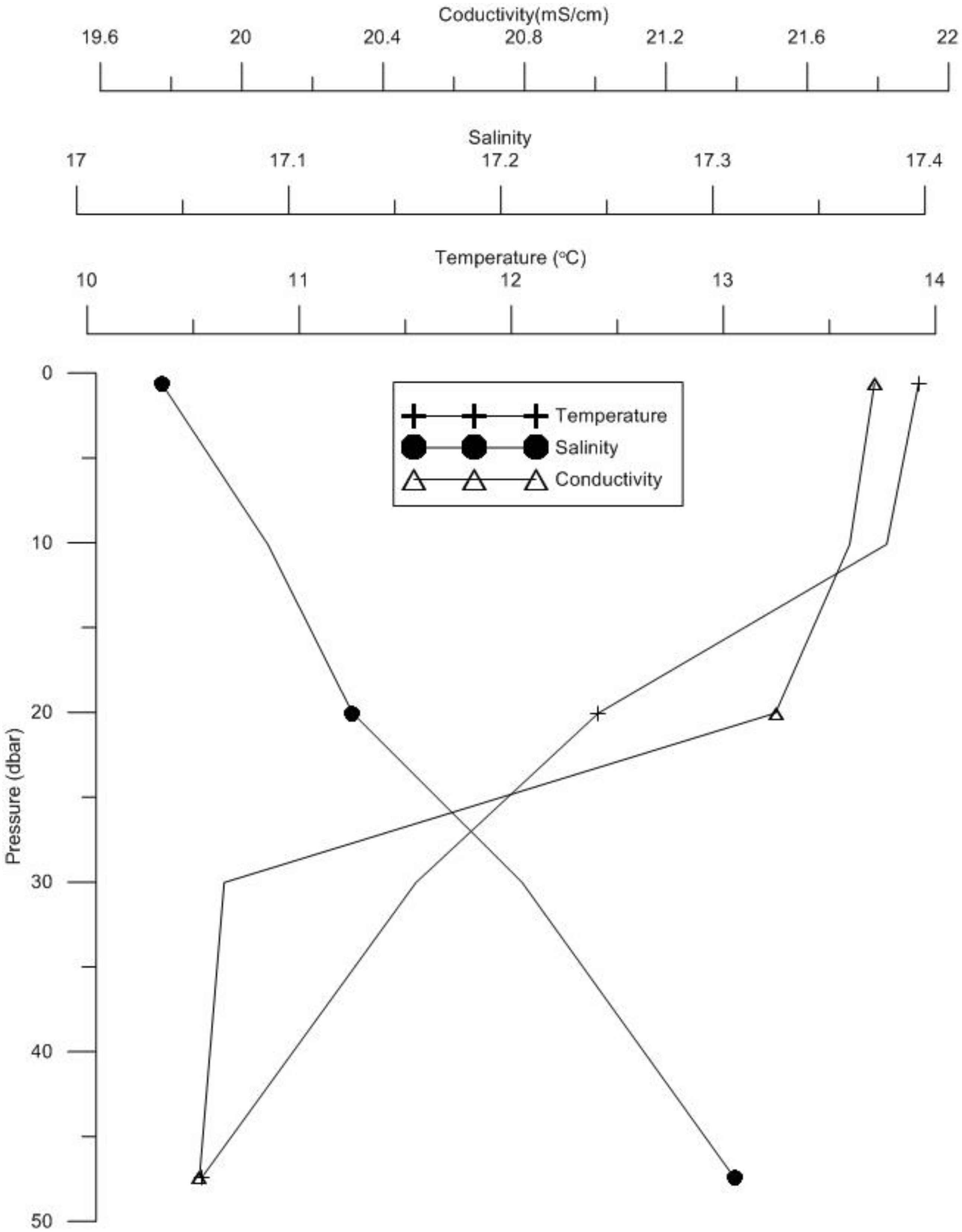

Figure 108.CTD from D4 Station for the second measurements in April2015

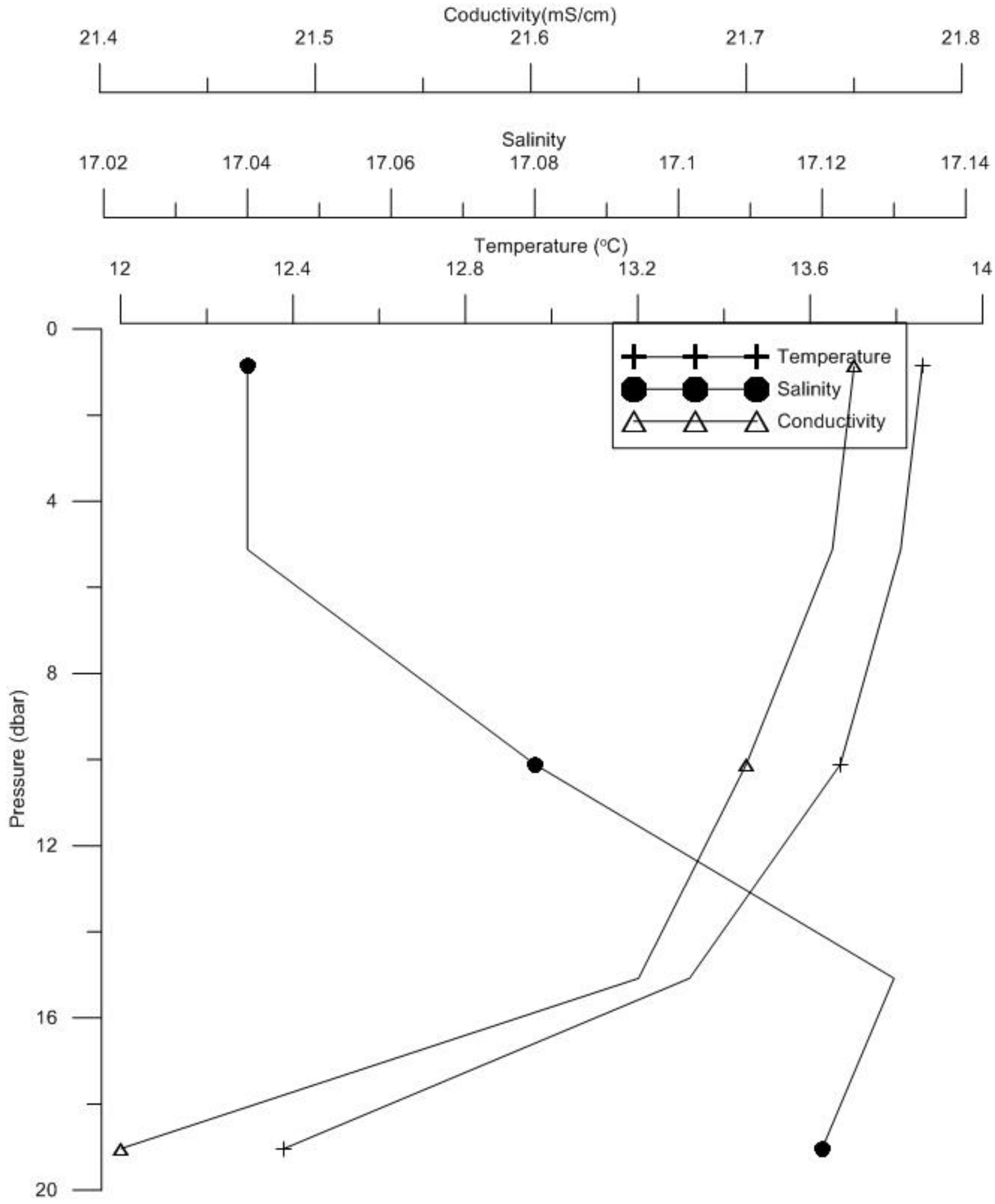

Figure 109.CTD from D5 Station for the second measurements in April2015

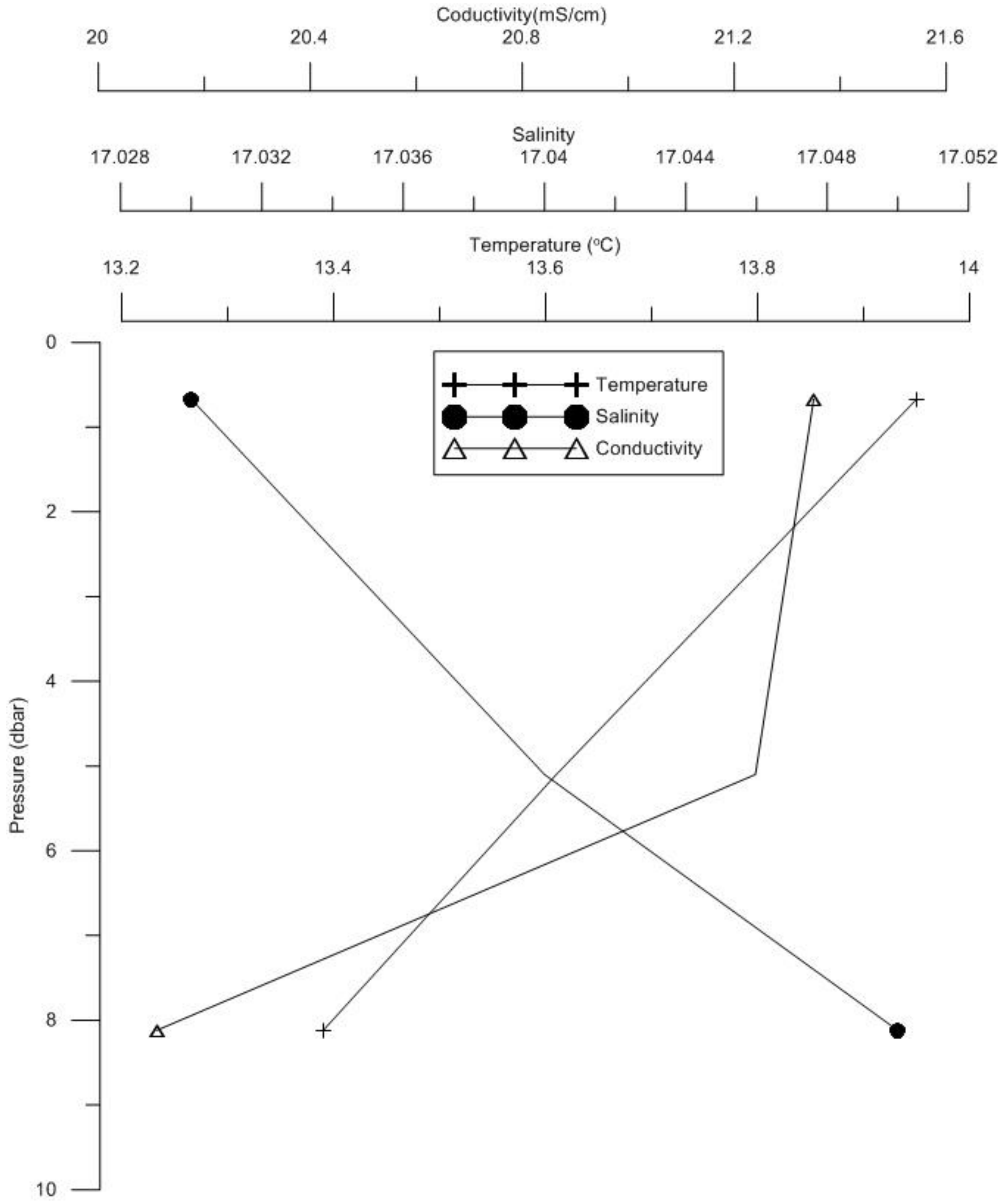

Figure 110.CTD from D6 Station for the second measurements in April2015

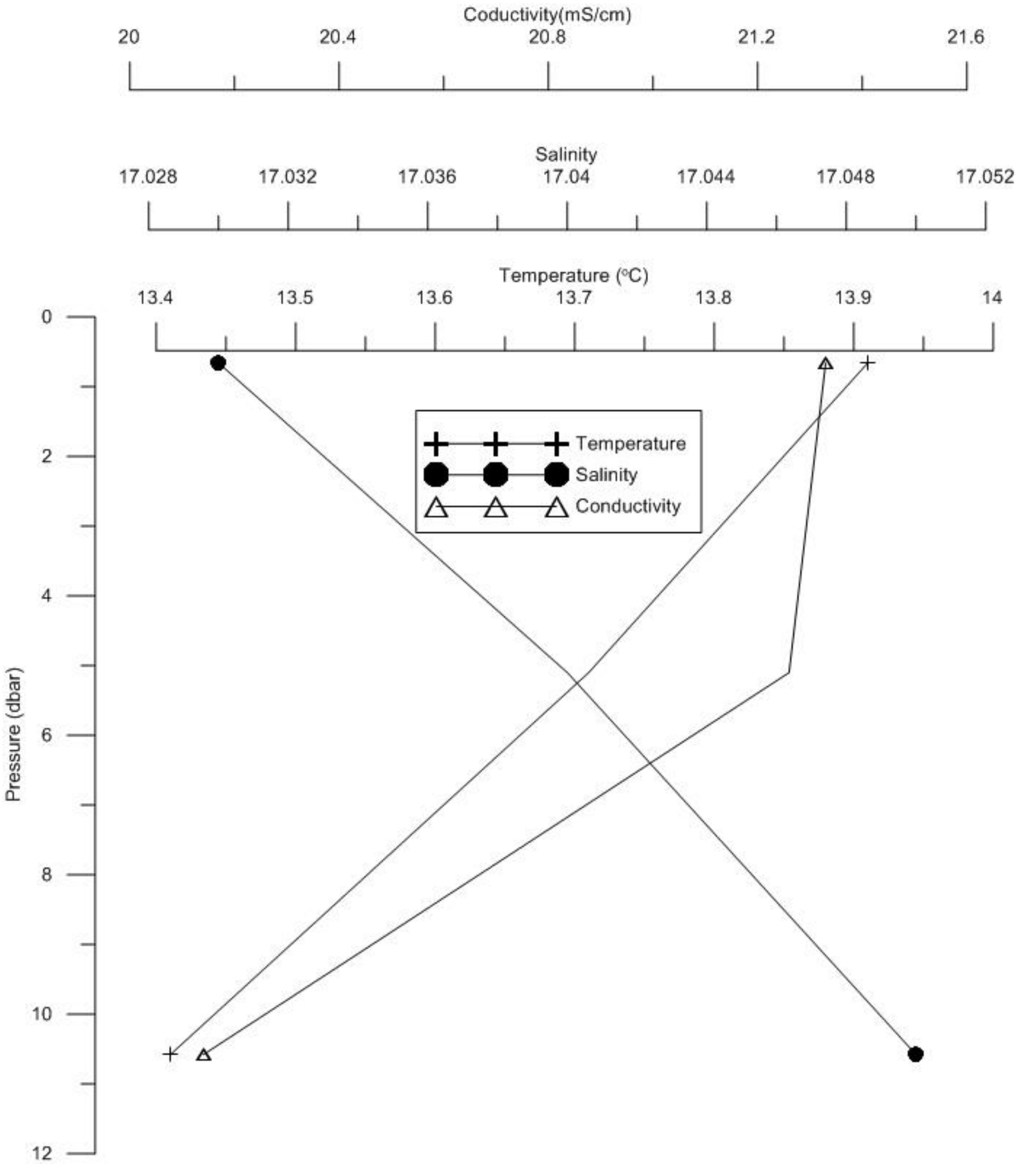

Figure 111.CTD from D7 Station for the second measurements in April2015

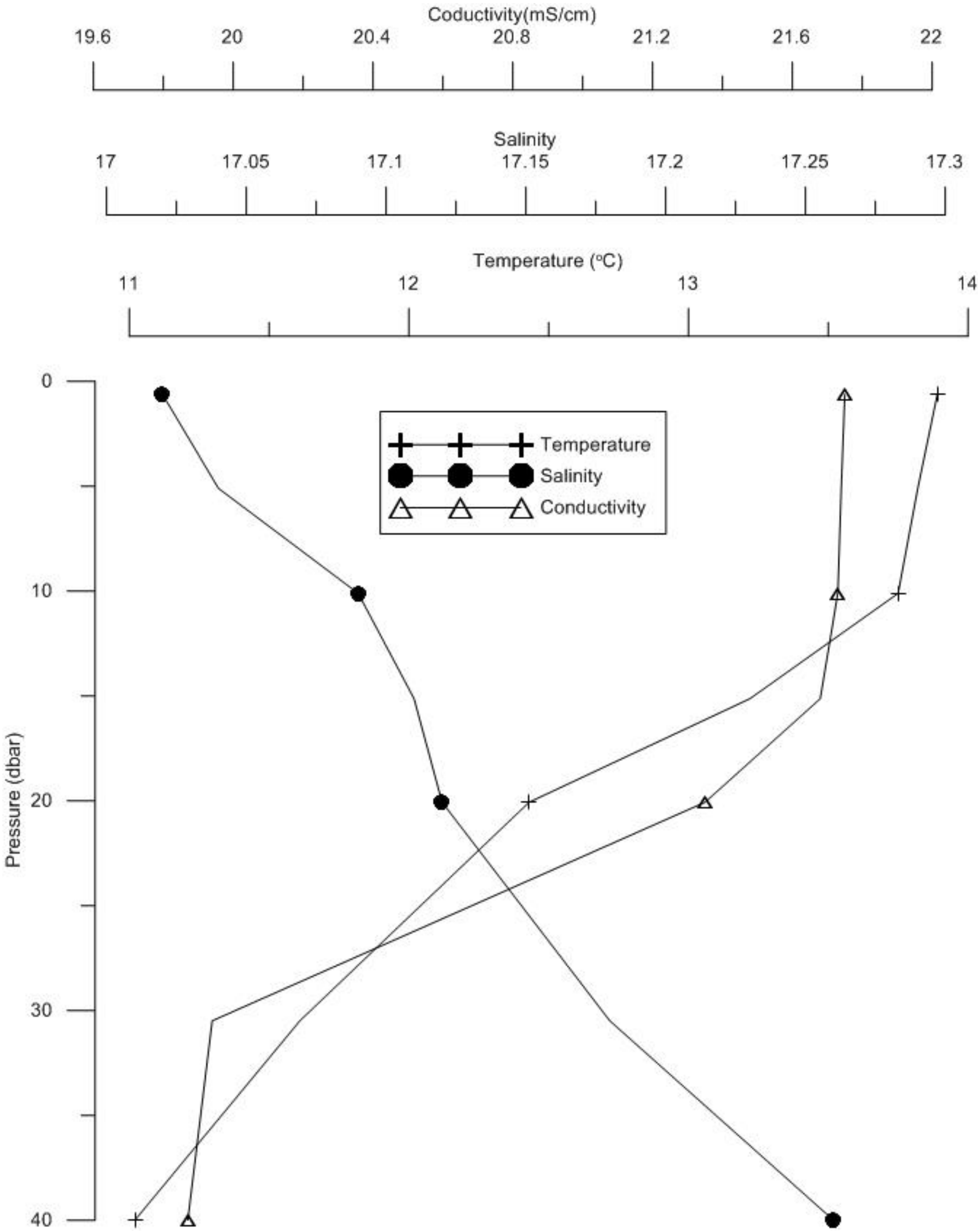

Figure 112.CTD from D8 Station for the second measurements in April2015

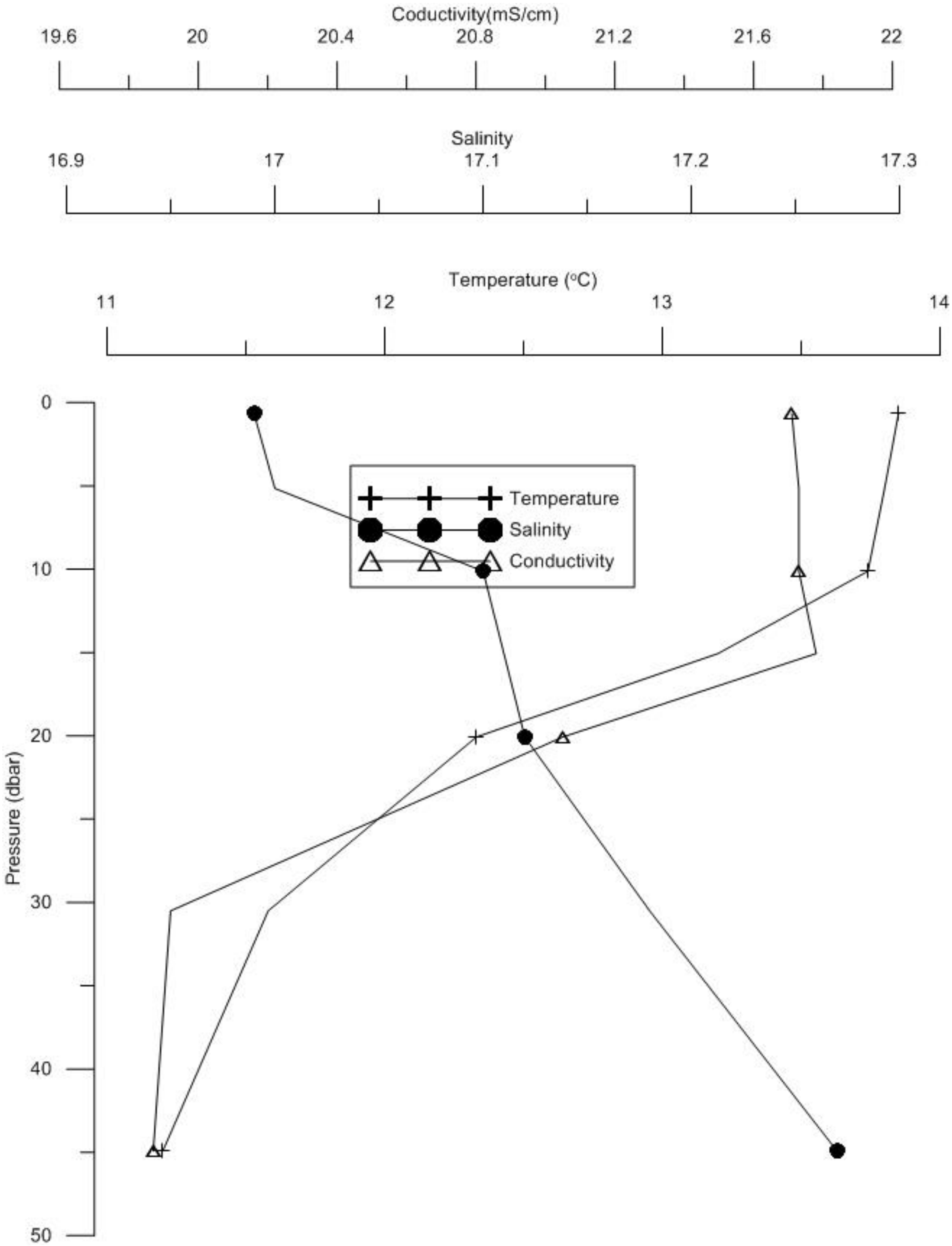

Figure 113.CTD from D9 Station for the second measurements in April2015

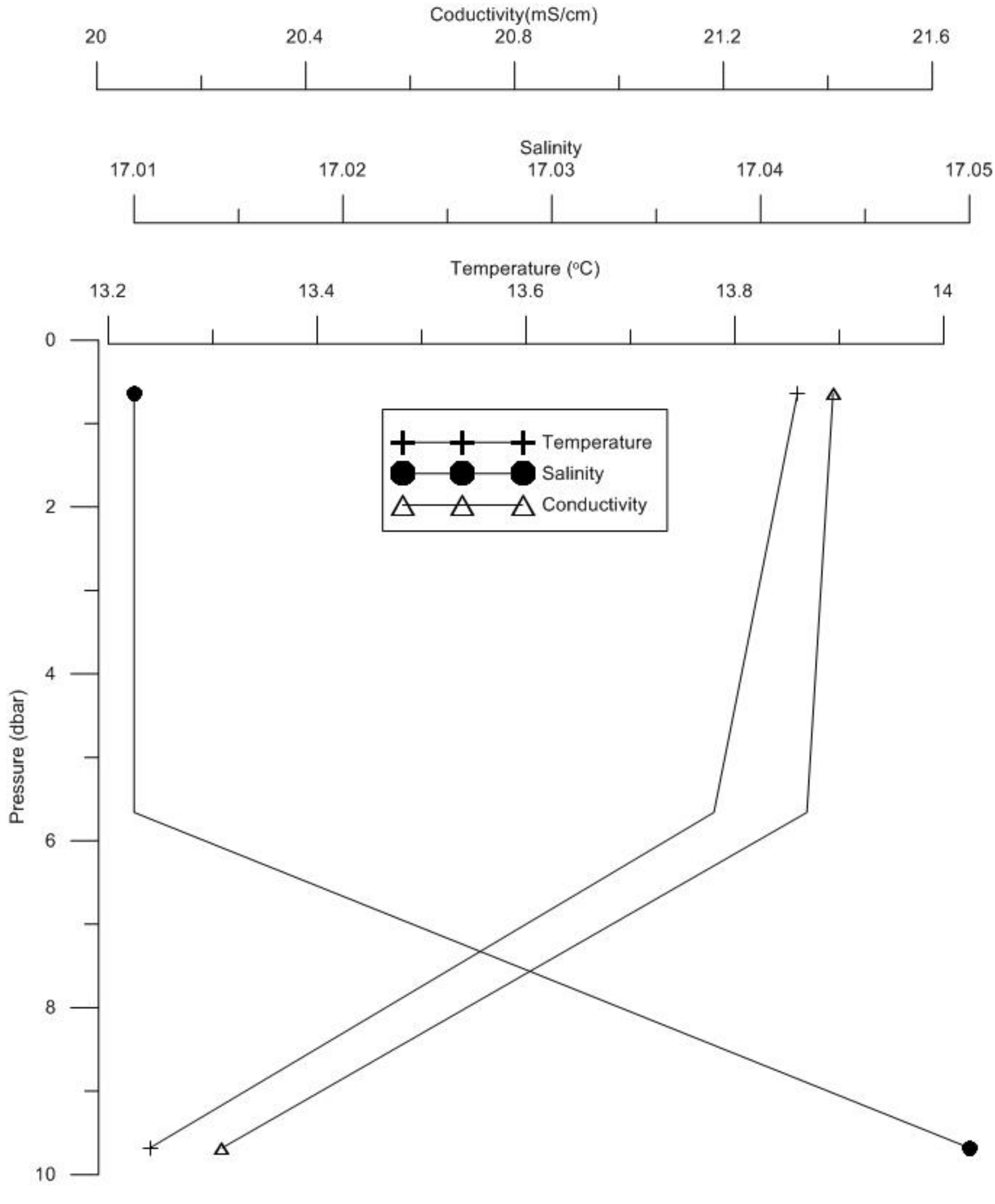

Figure 114.CTD from D10 Station for the second measurements in April2015

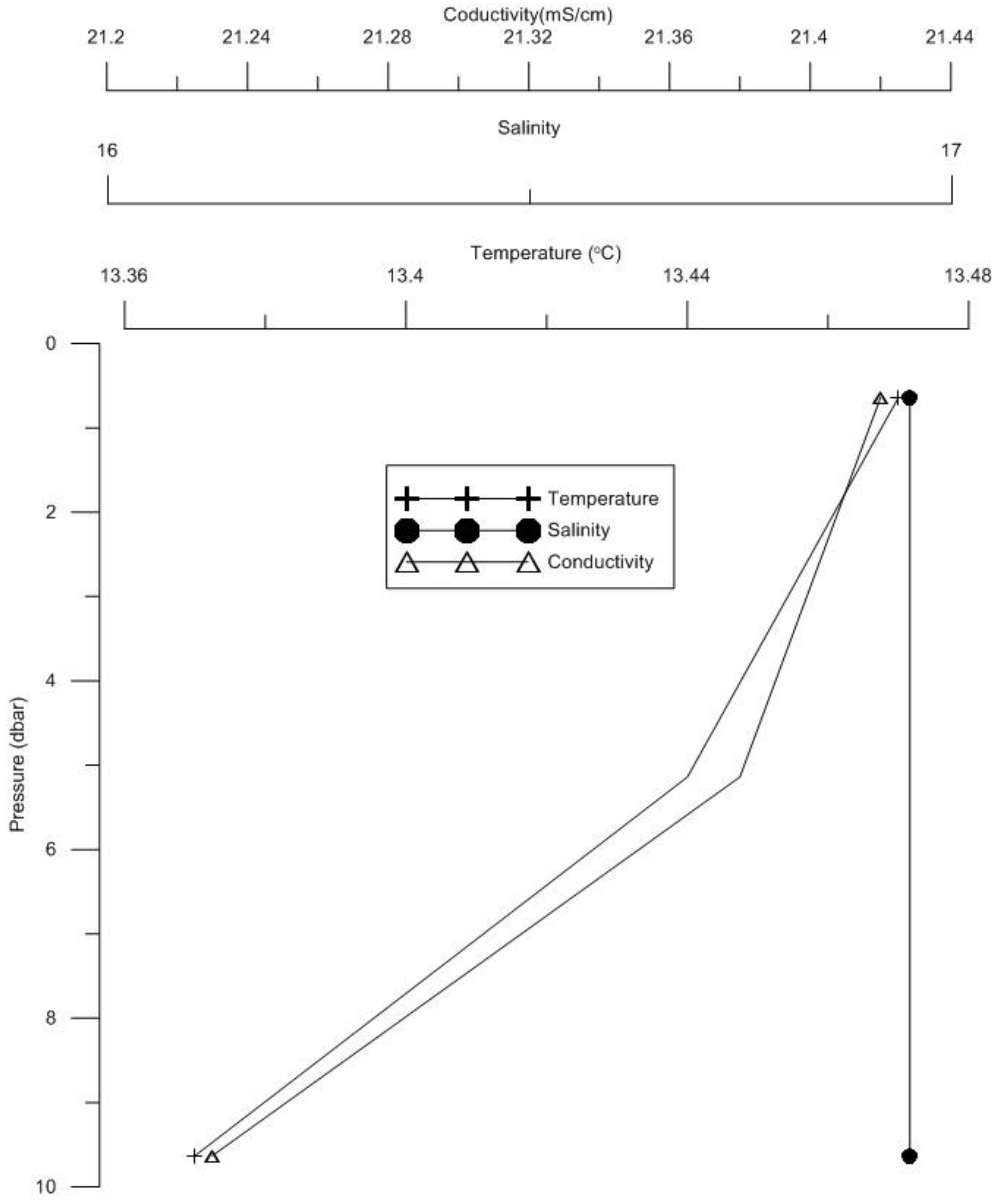

Figure 115.CTD from D11 Station for the second measurements in April2015

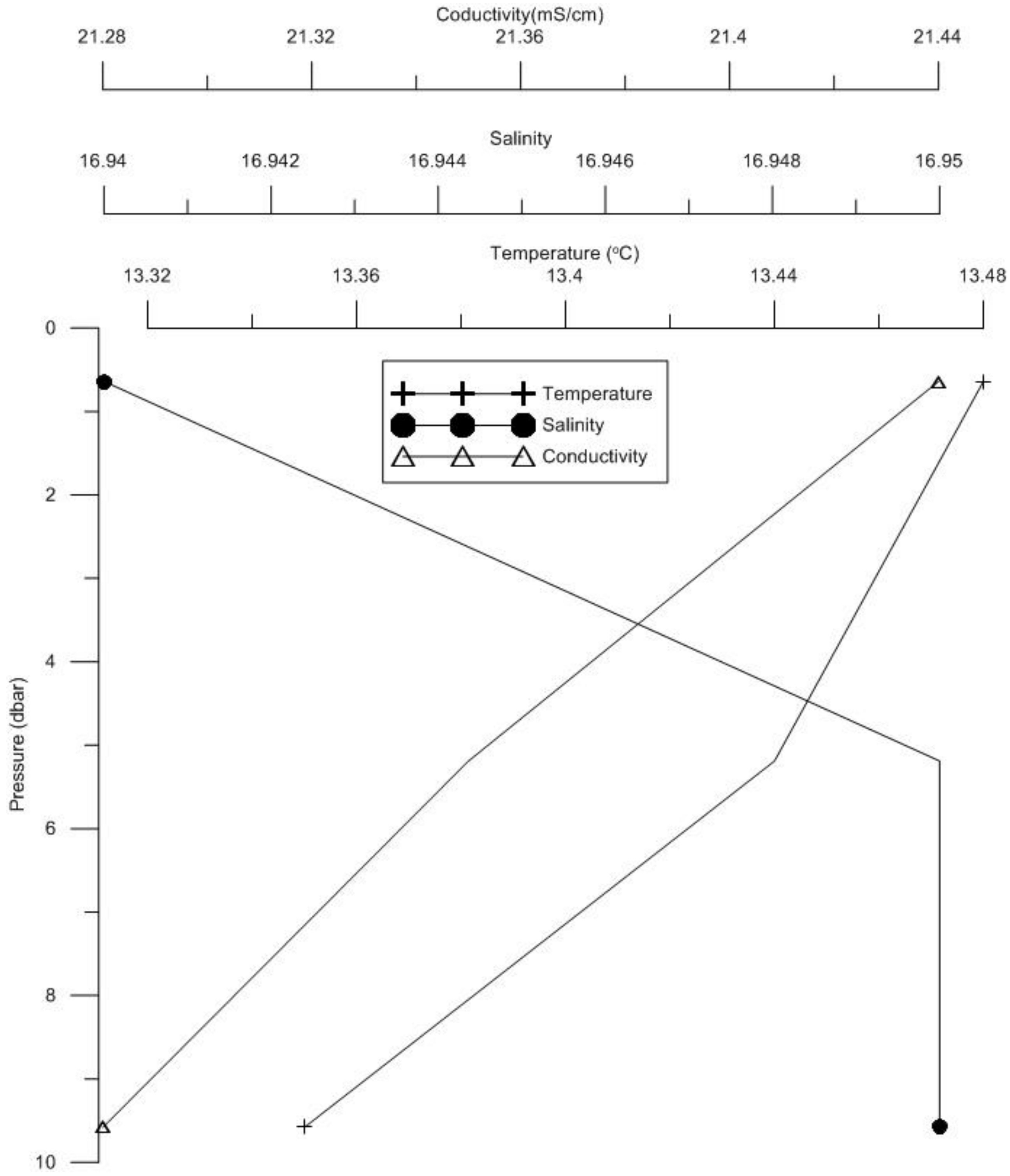

Figure 116.CTD from D12 Station for the second measurements in April2015

CTD graphs versus depth for each stations are given in the below. Conductivity, Salinity and Temperature results for the first period of May are given in Figures 117 -128.

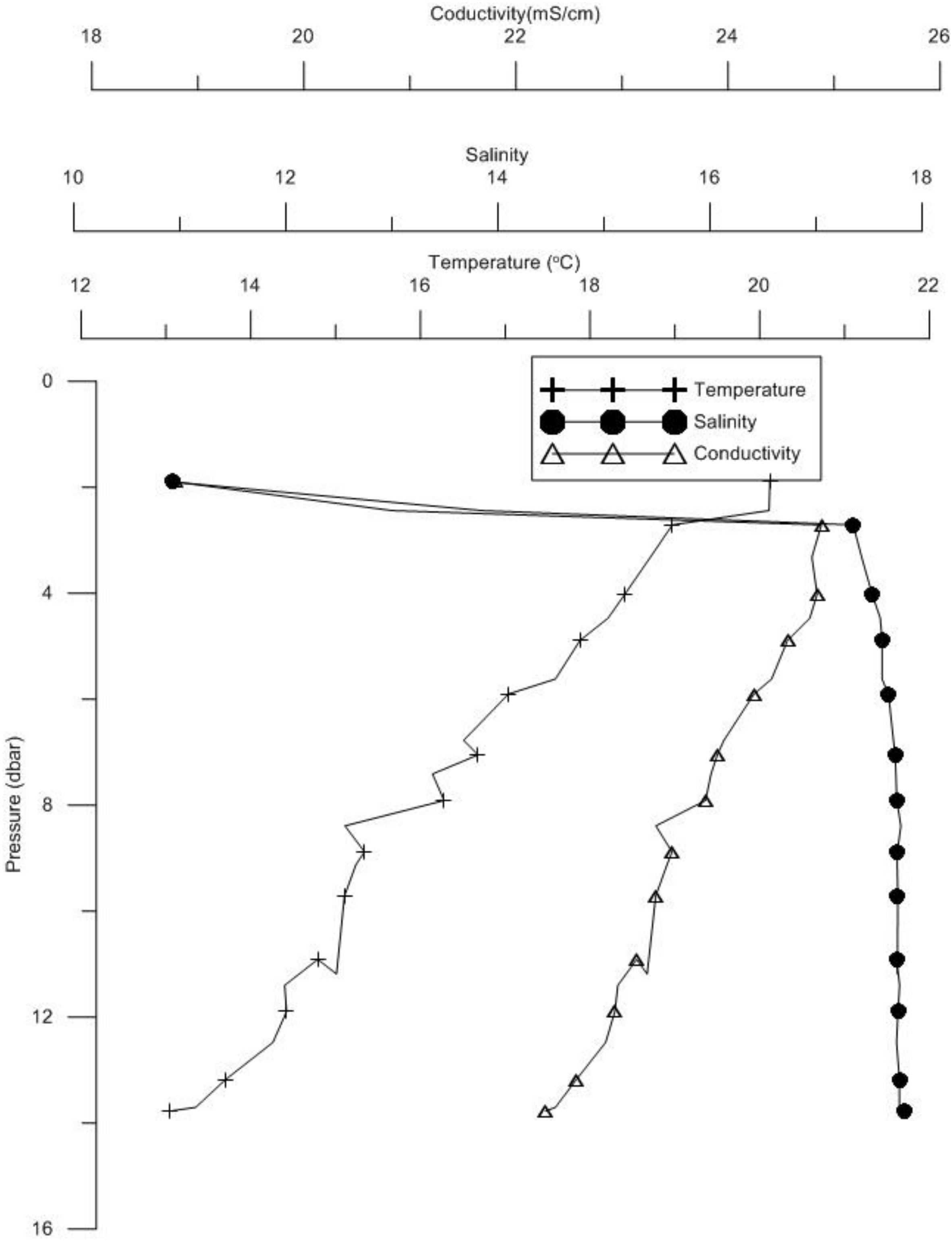

Figure 117. CTD from D1 Station for the first measurements in May2015

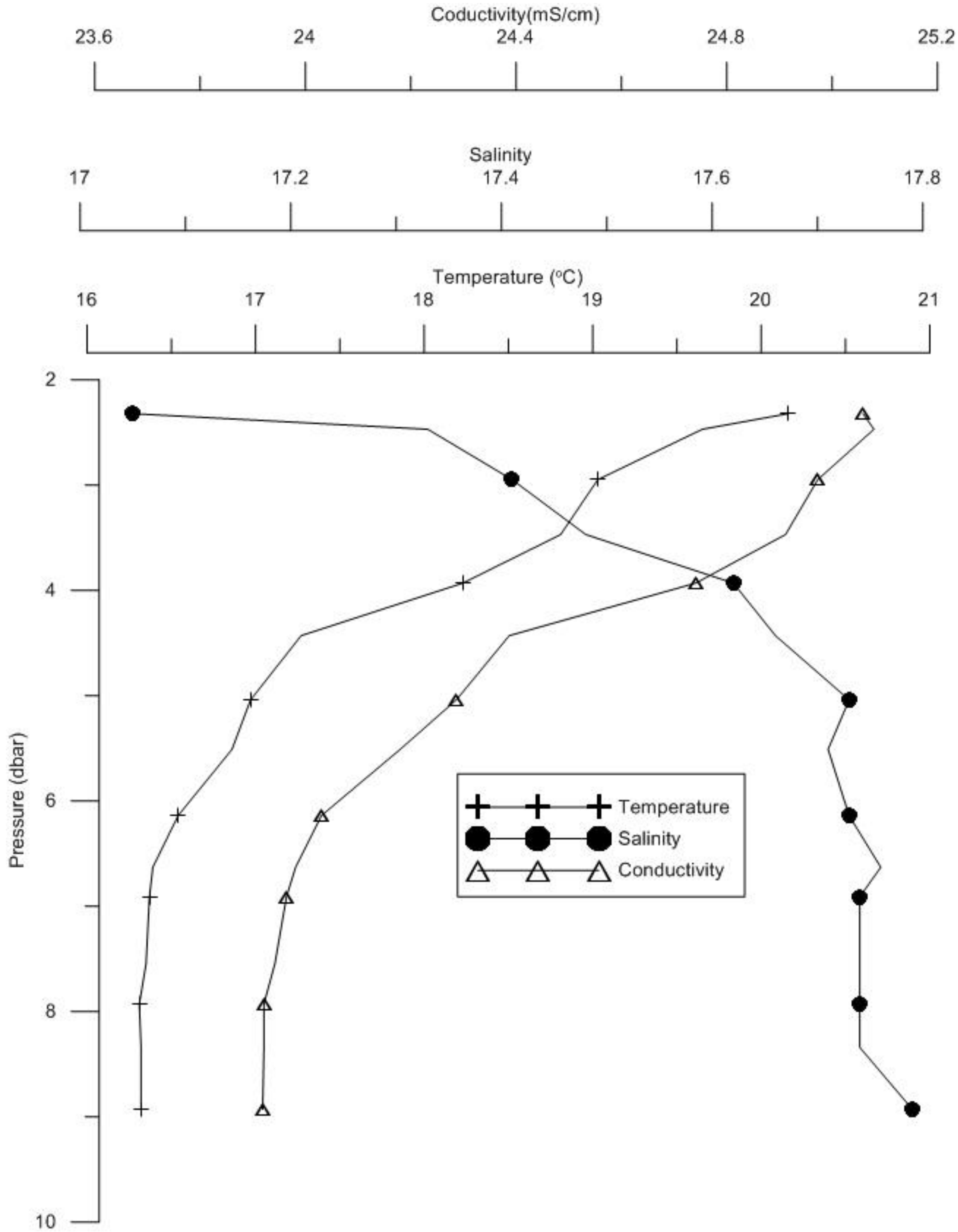

Figure 118.CTD from D2 Station for the first measurements in May2015

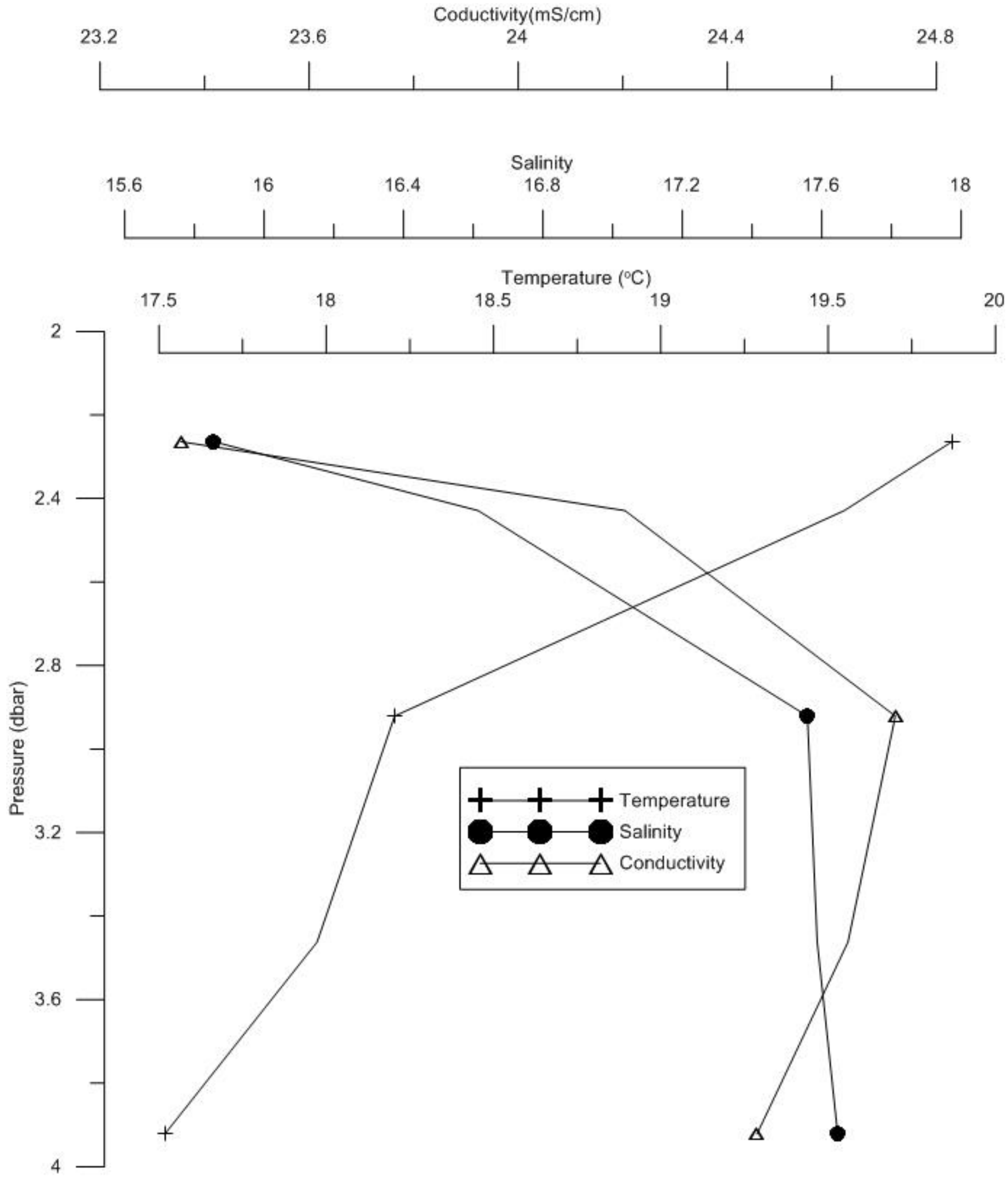

Figure 119.CTD from D3 Station for the first measurements in May2015

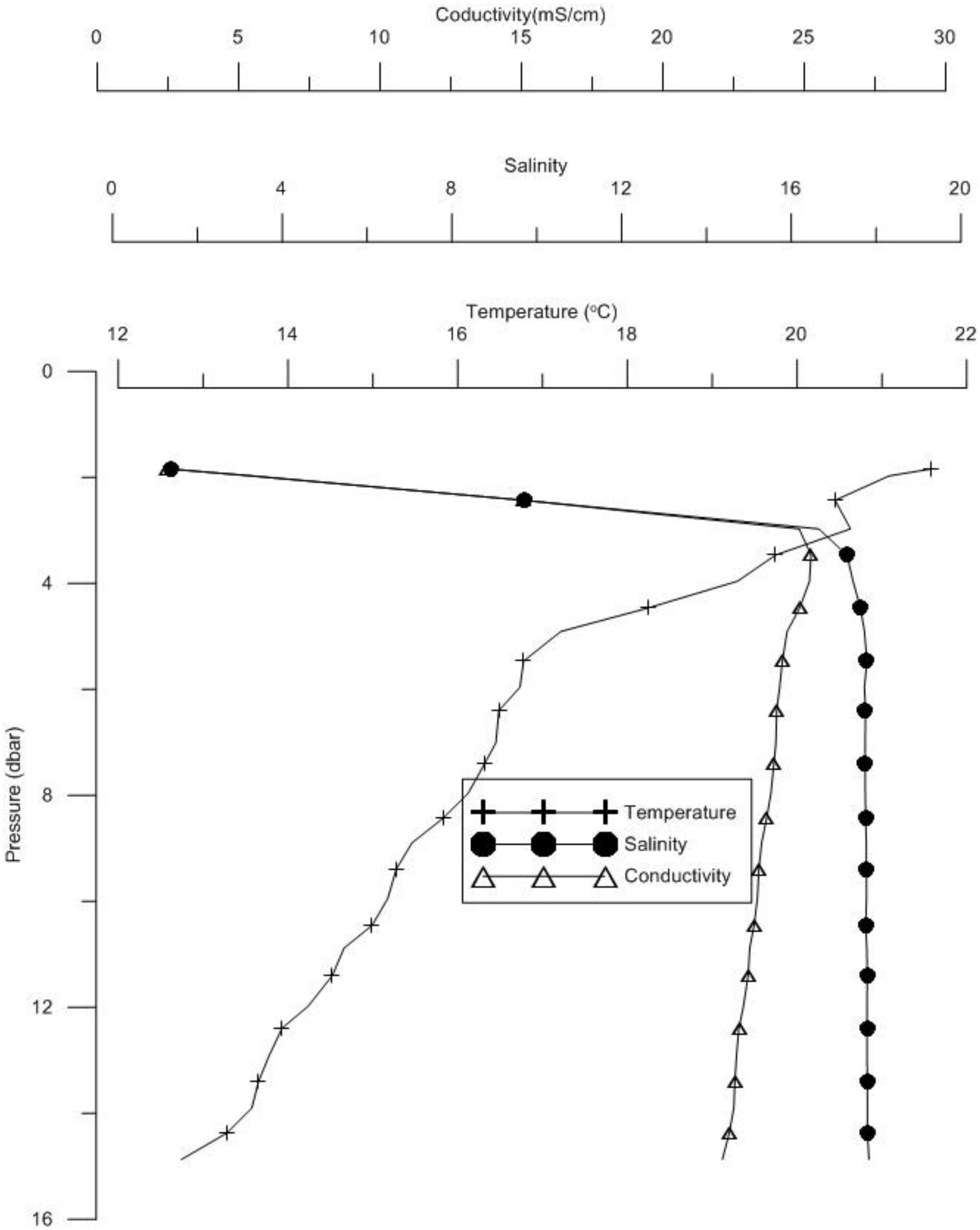

Figure 120.CTD from D4 Station for the first measurements in May2015

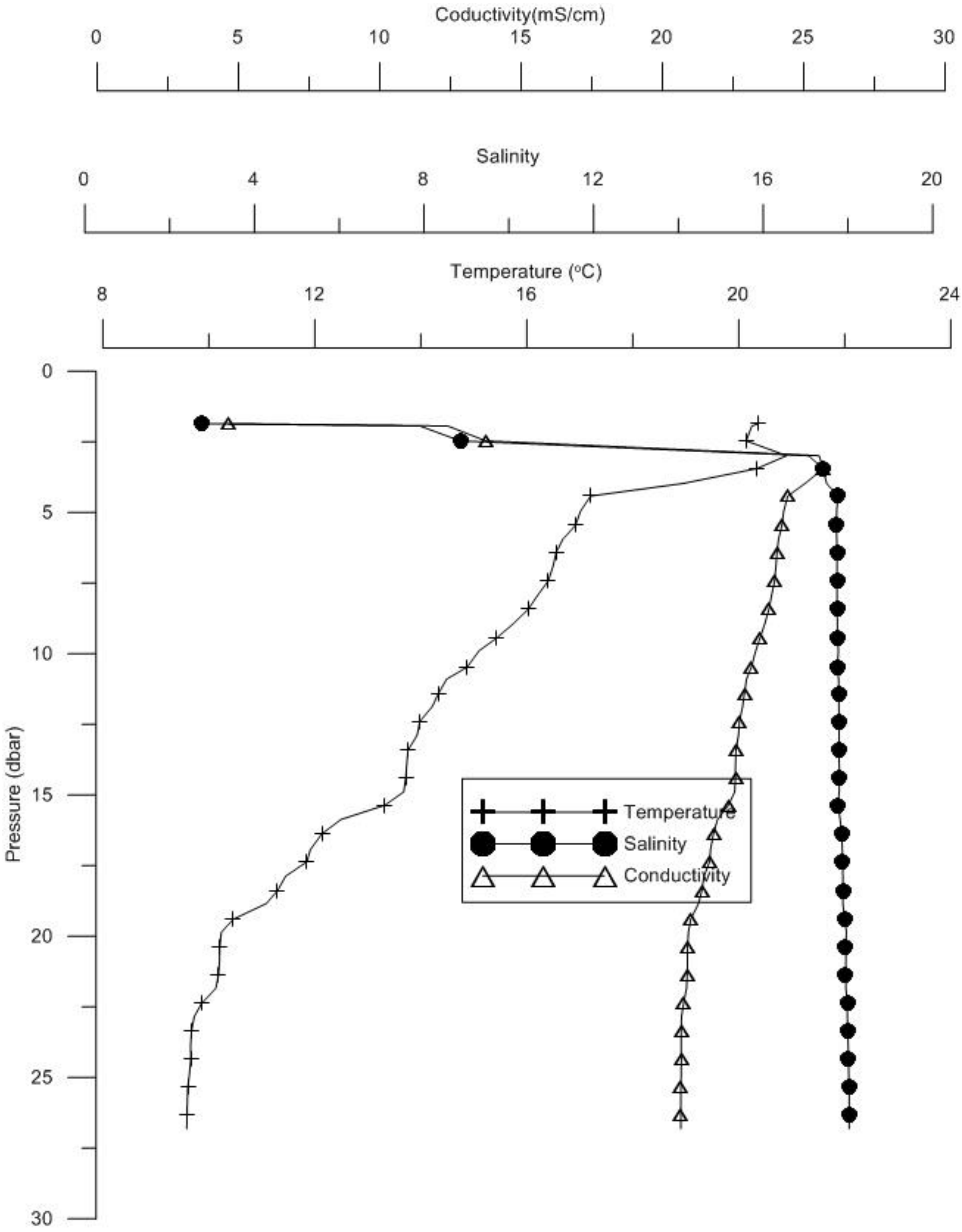

Figure 121.CTD from D5 Station for the first measurements in May2015

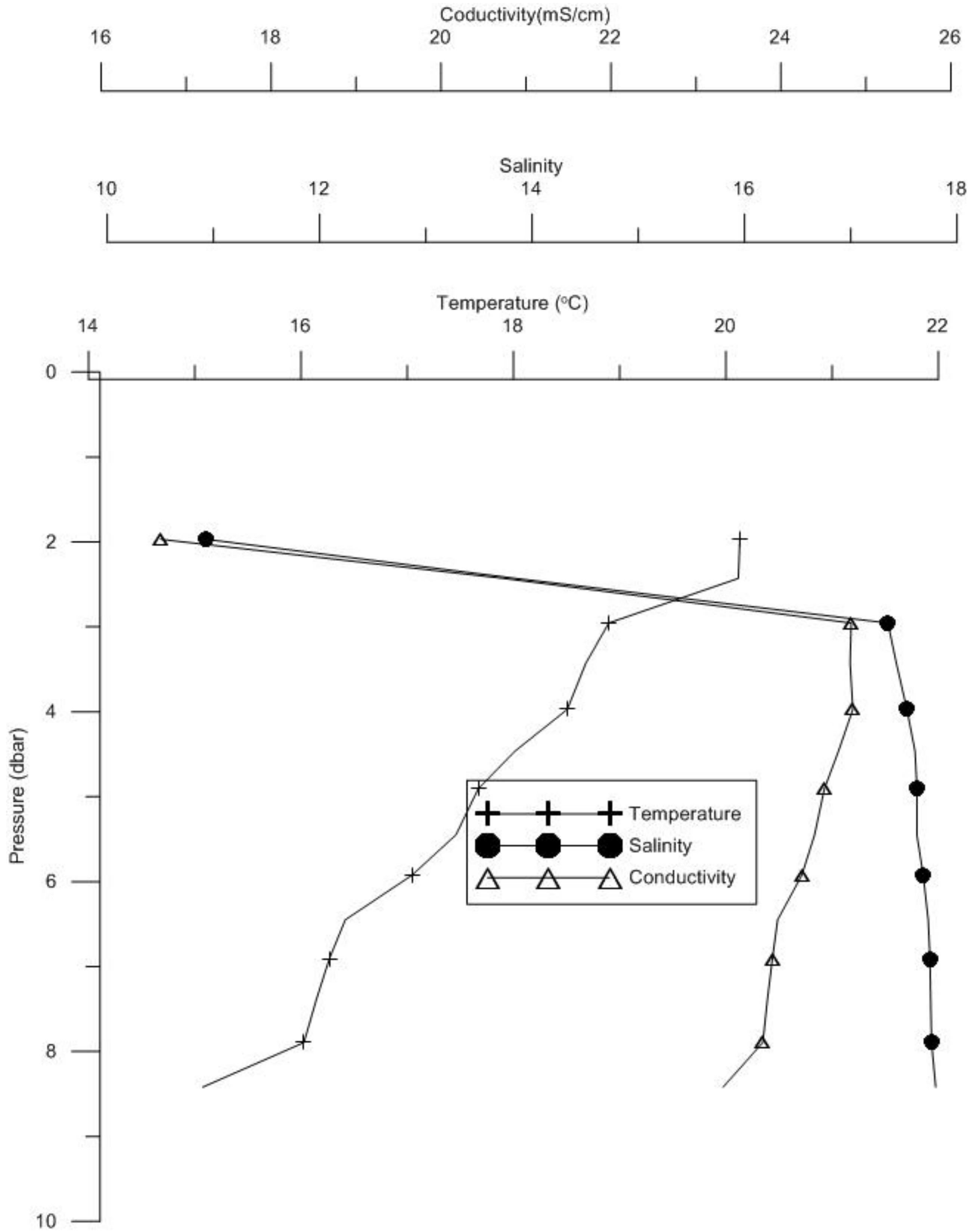

Figure 122.CTD from D6 Station for the first measurements in May2015

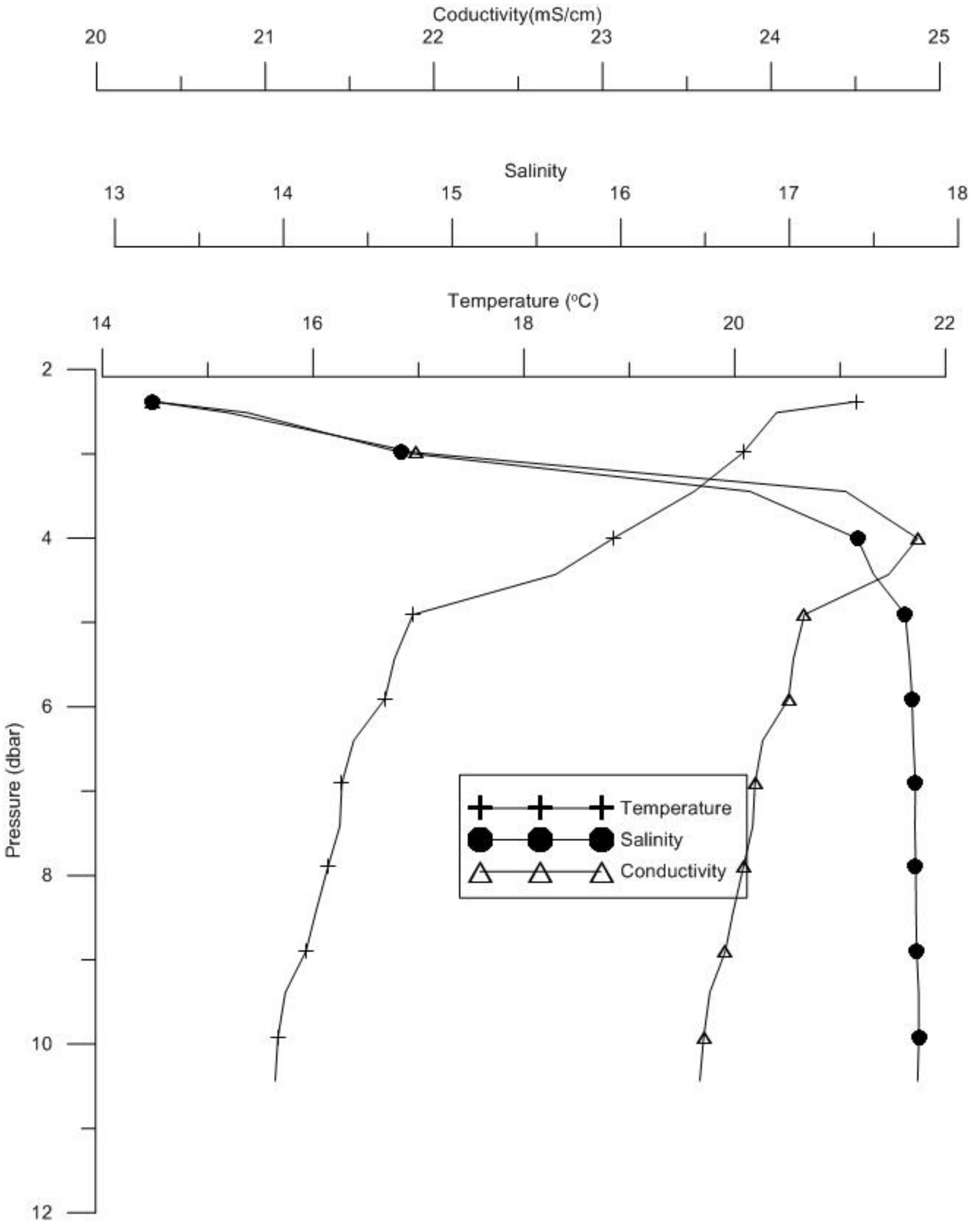

Figure 123.CTD from D7 Station for the first measurements in May2015

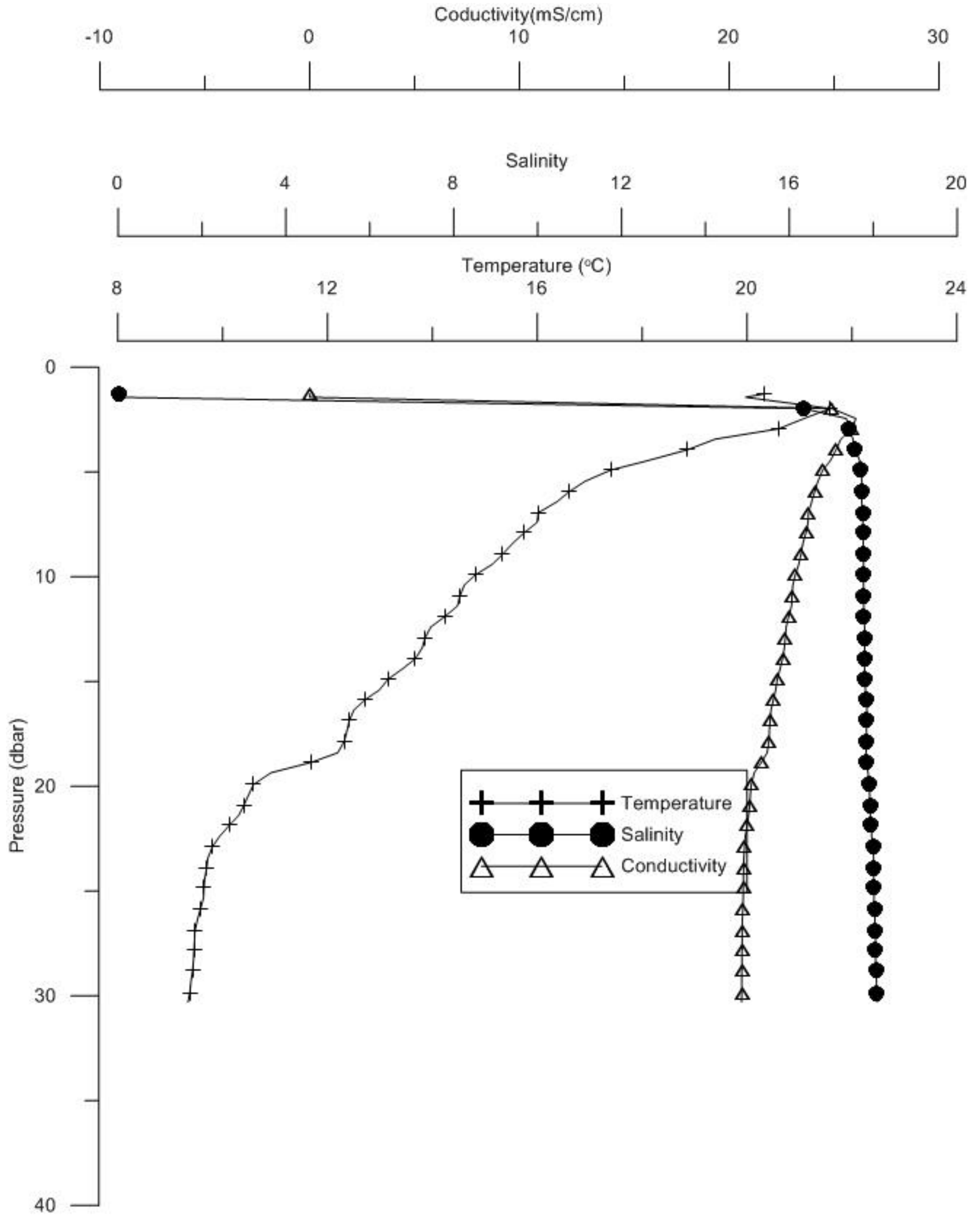

Figure 124.CTD from D8 Station for the first measurements in May2015

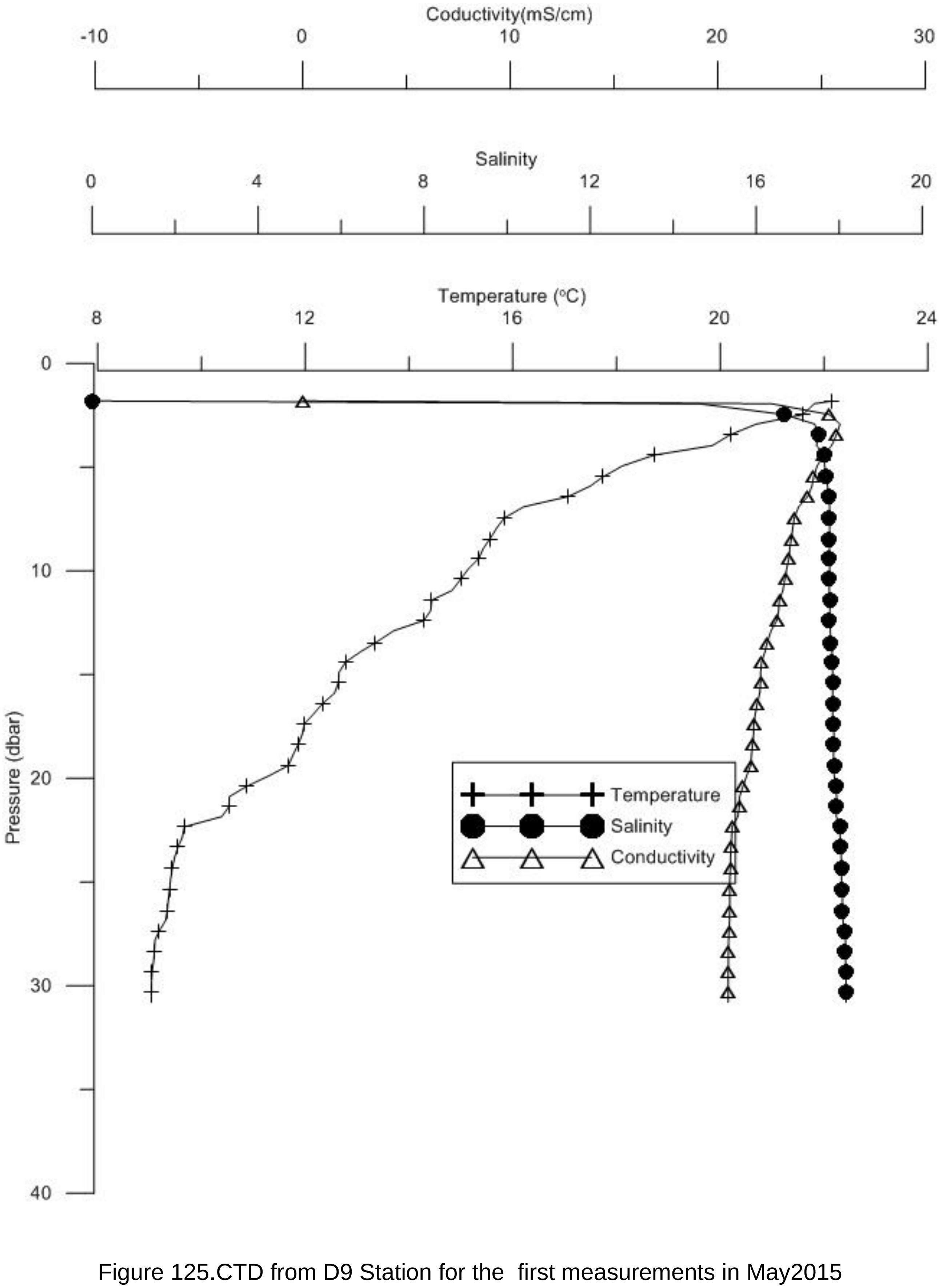

Figure 125.CTD from D9 Station for the first measurements in May2015

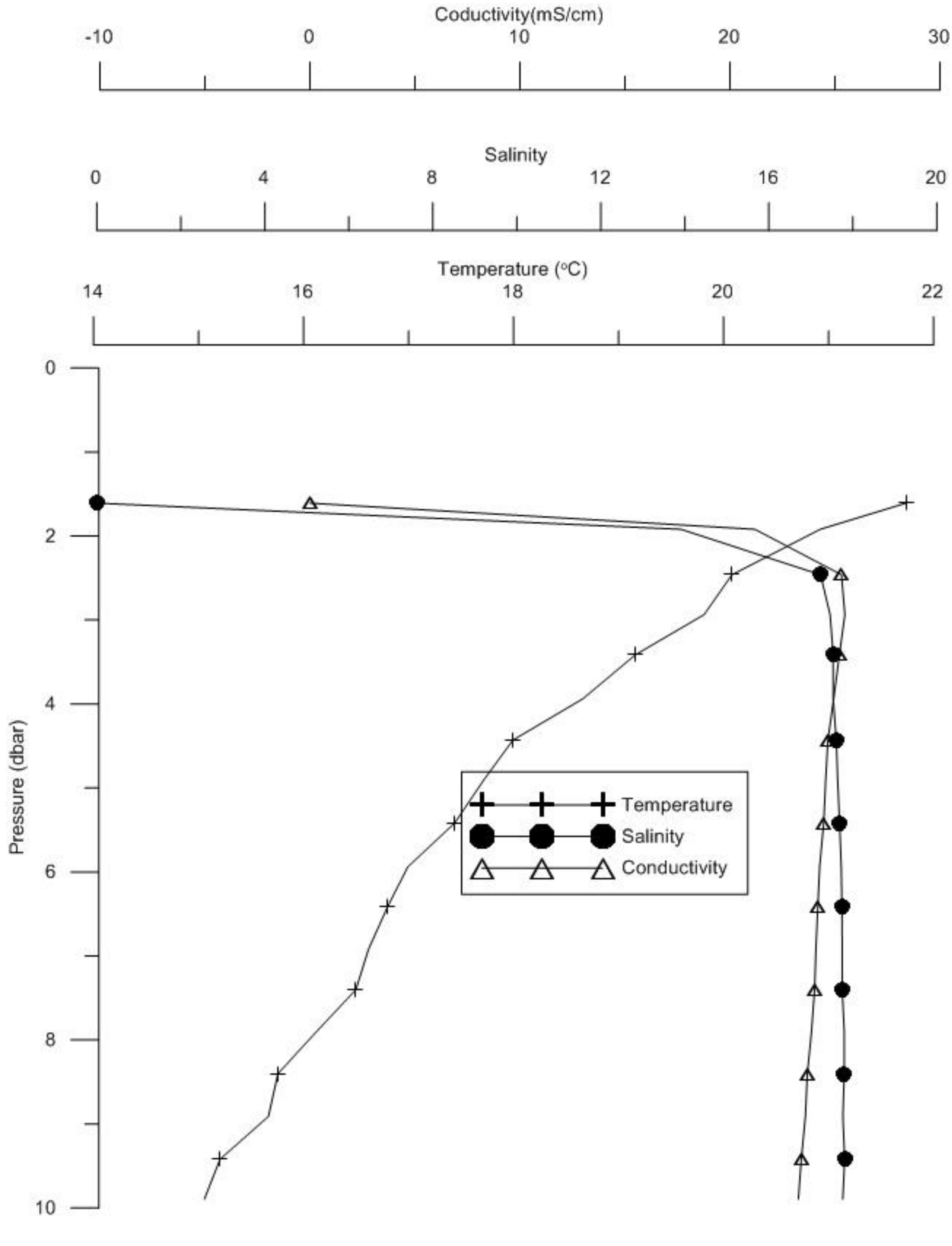

Figure 126.CTD from D10 Station for the first measurements in May2015

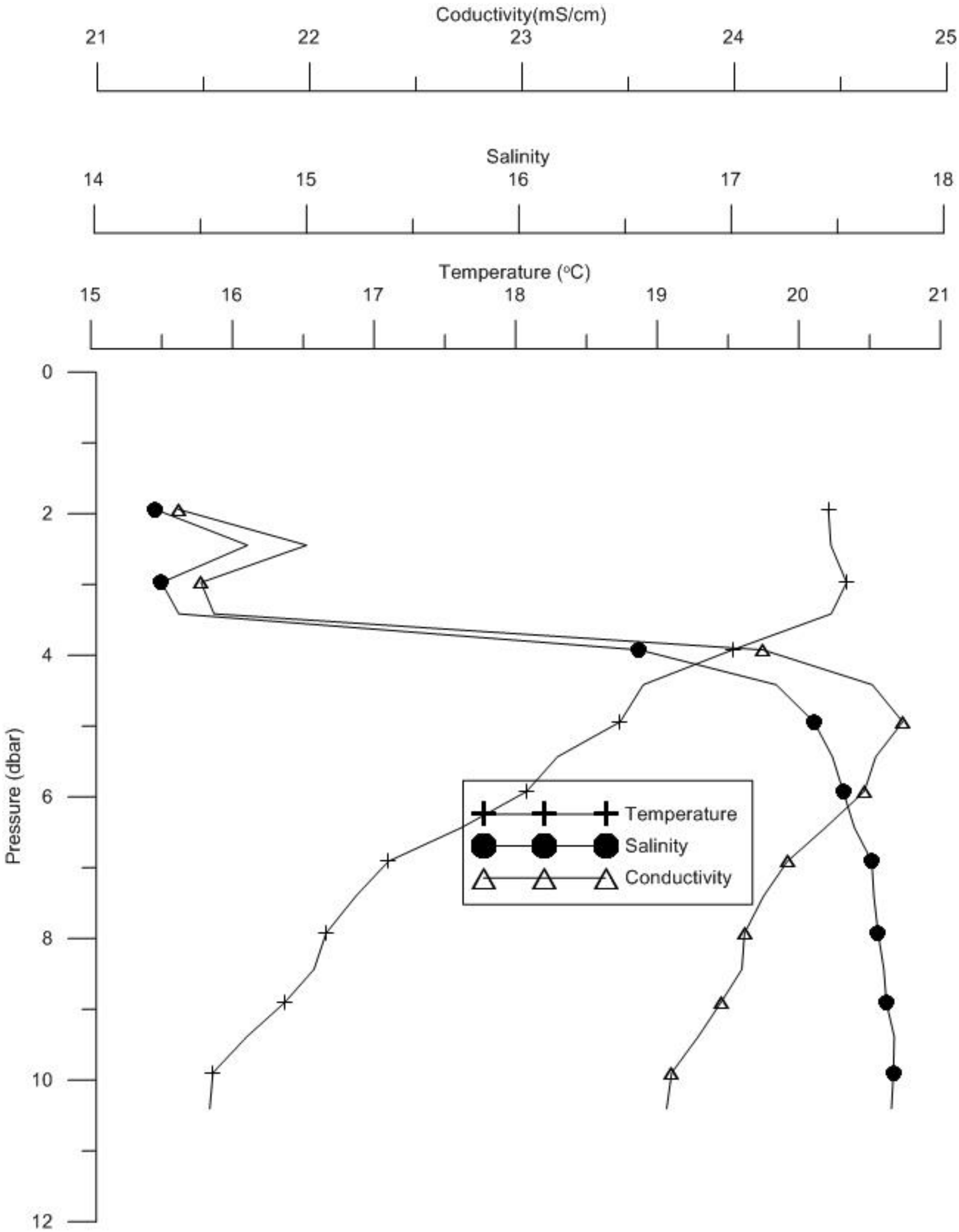

Figure 127.CTD from D11 Station for the first measurements in May2015

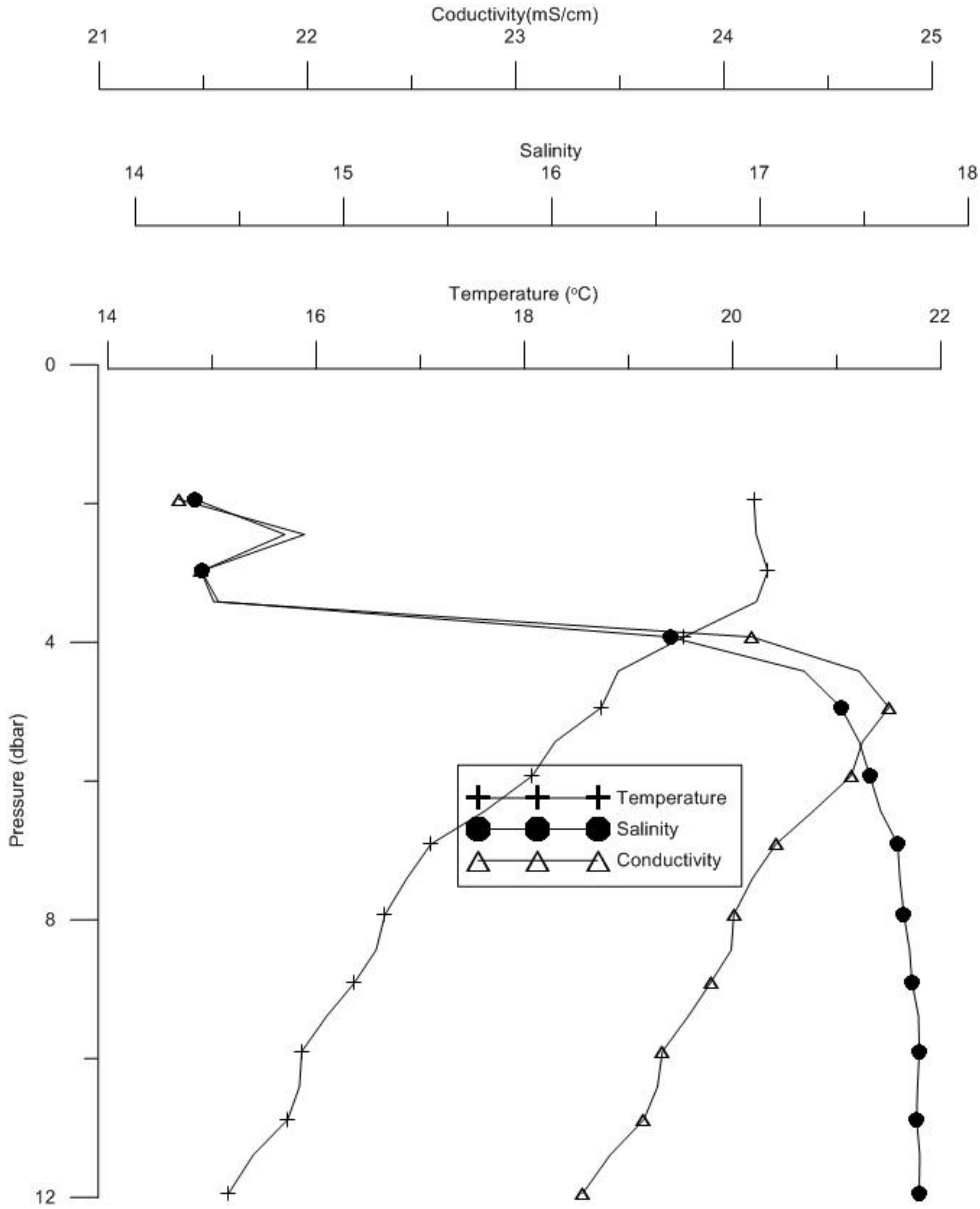

Figure 128.CTD from D12 Station for the first measurements in May2015

CTD graphs versus depth for each stations are given in the below. Conductivity, Salinity and Temperature results for the second period of May are given in Figures 129 -140.

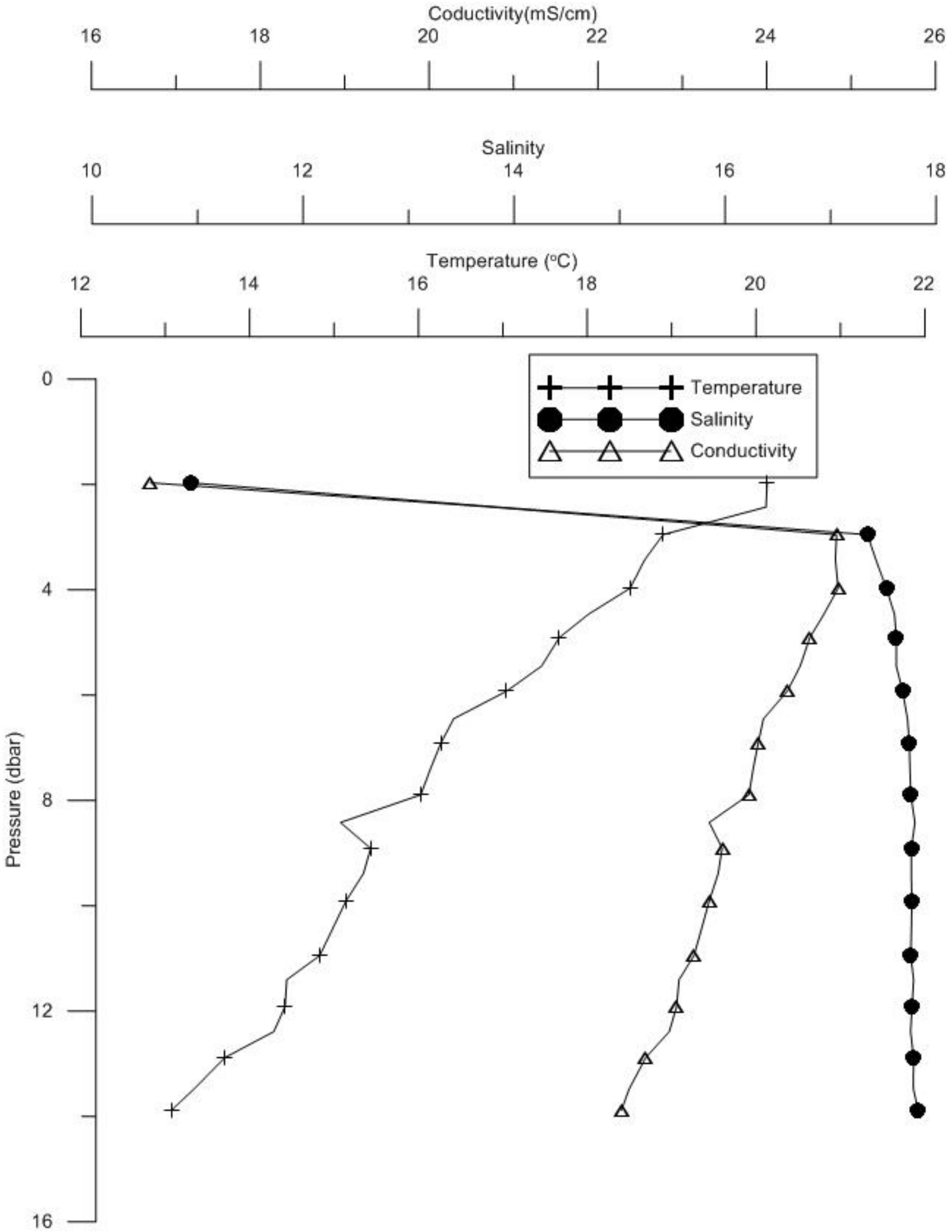

Figure 129. CTD from D1 Station for the second measurements in May2015

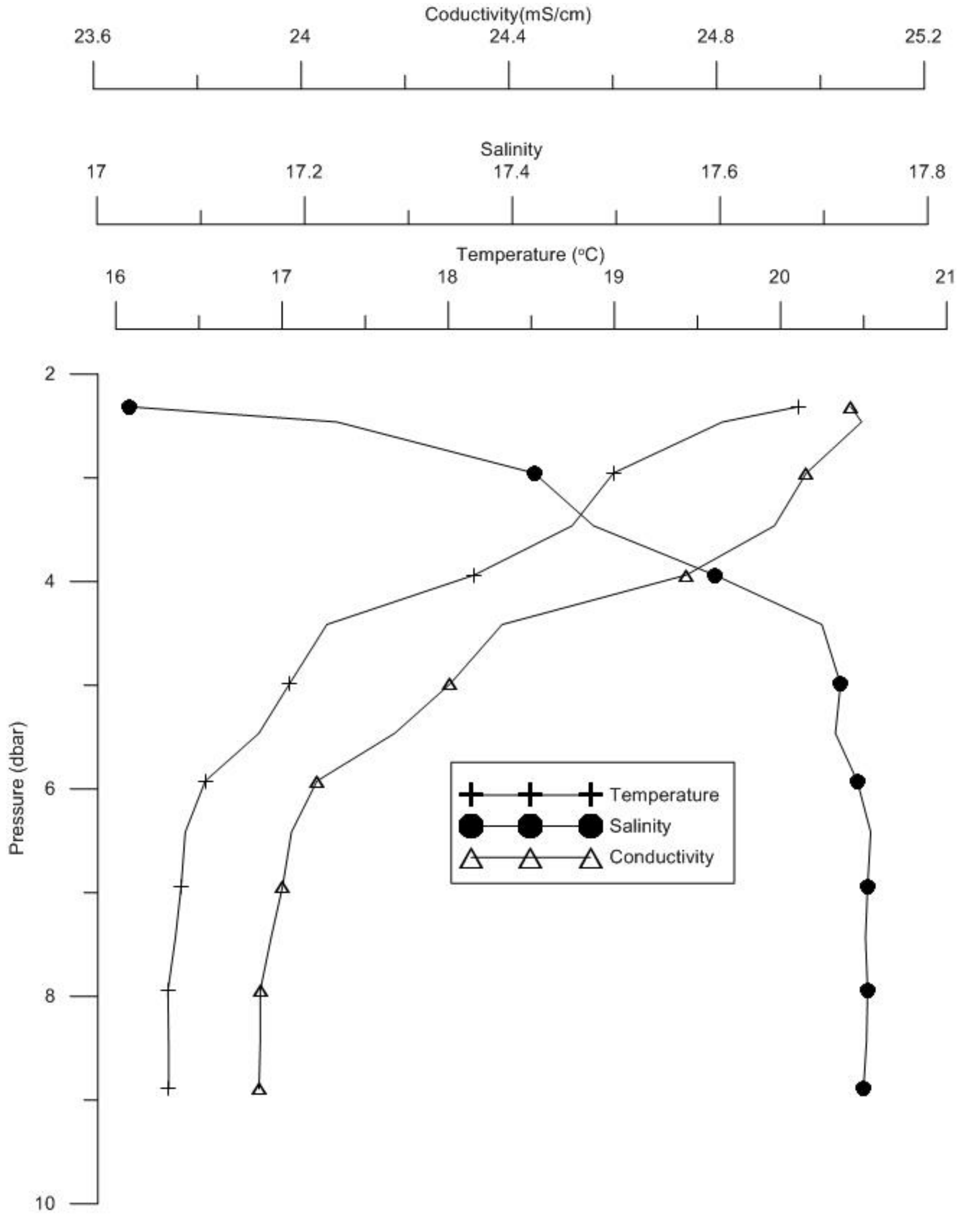

Figure 130.CTD from D2 Station for the second measurements in May2015

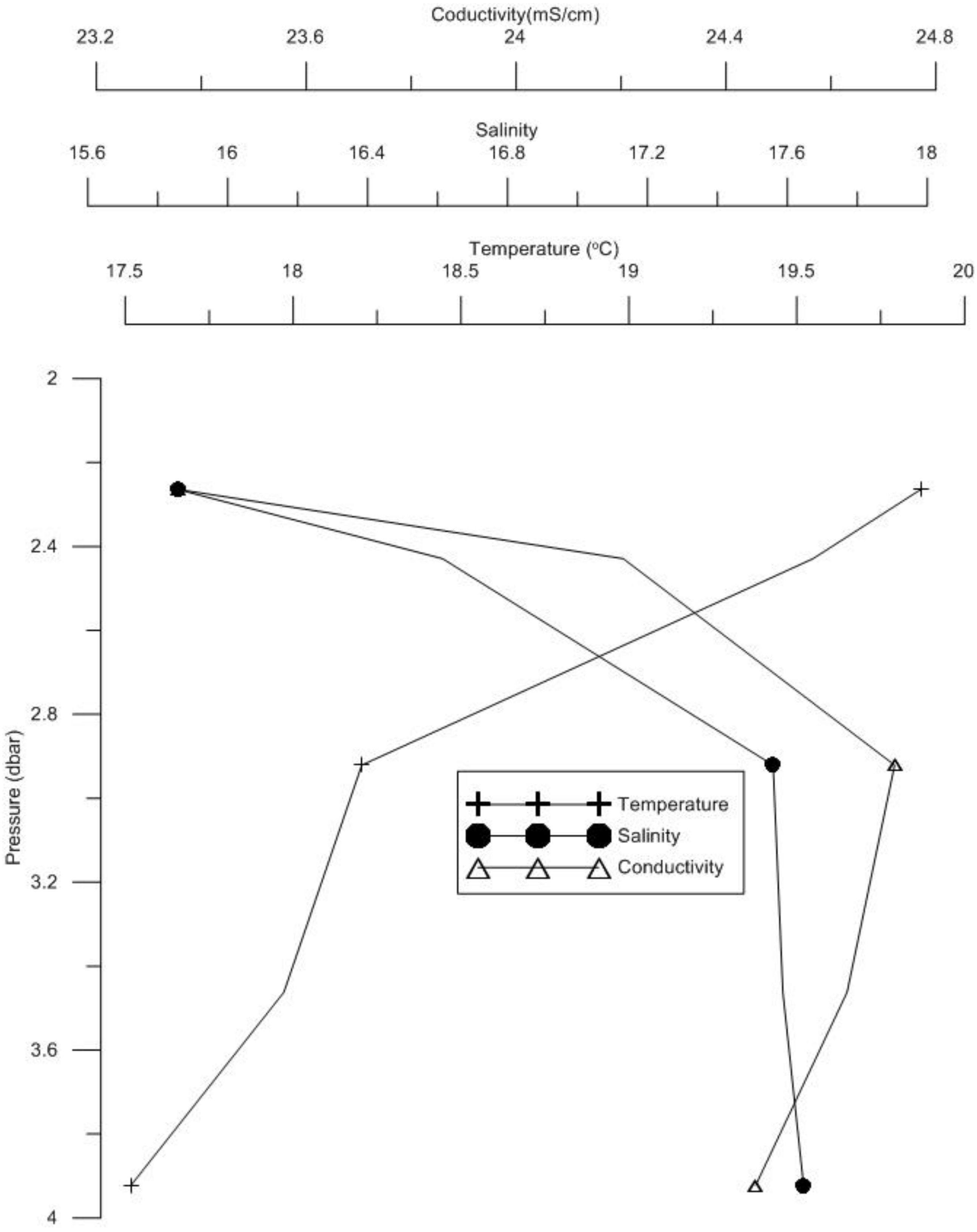

Figure 131.CTD from D3 Station for the second measurements in May2015

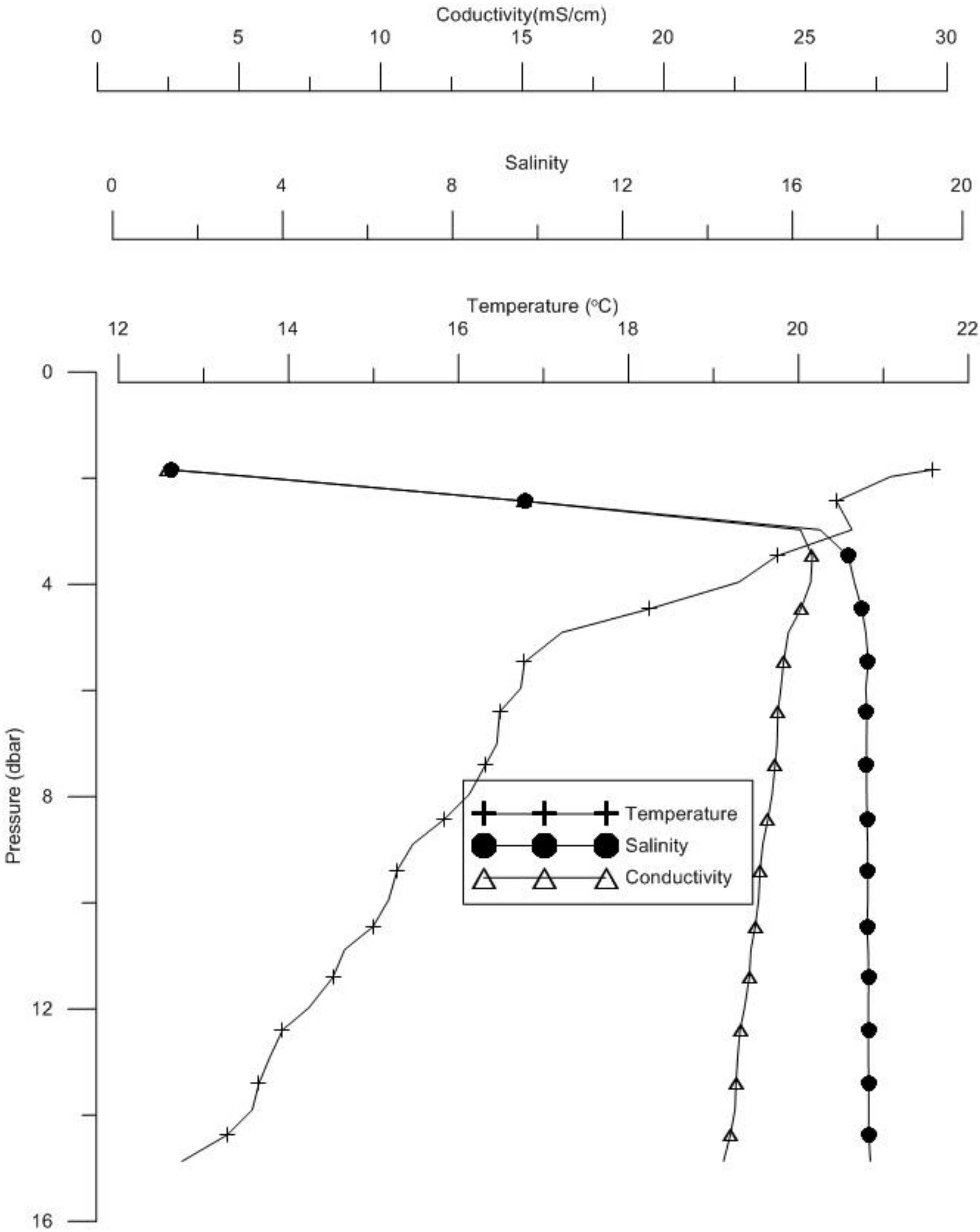

Figure 132.CTD from D4 Station for the second measurements in May2015

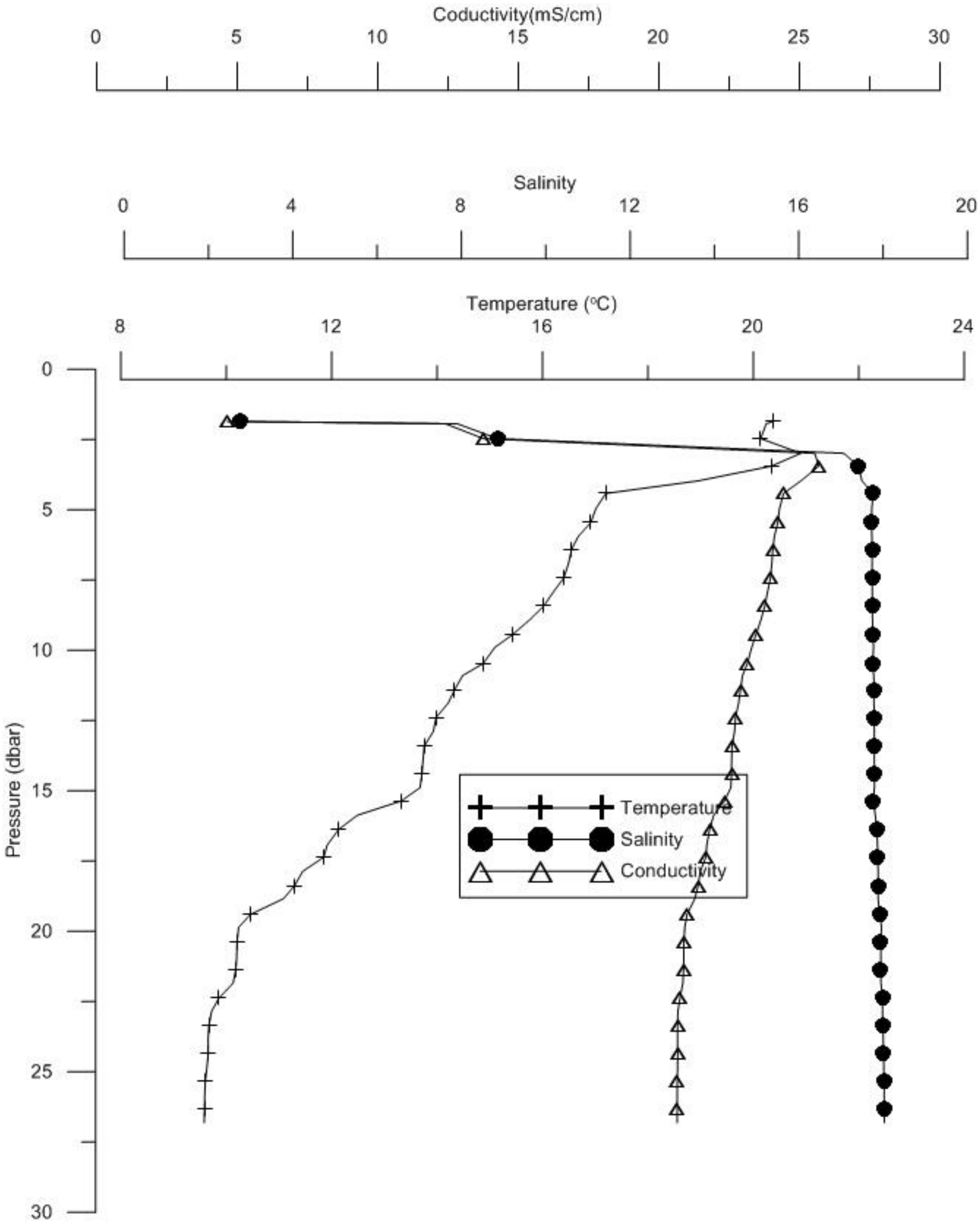

Figure 133.CTD from D5 Station for the second measurements in May2015

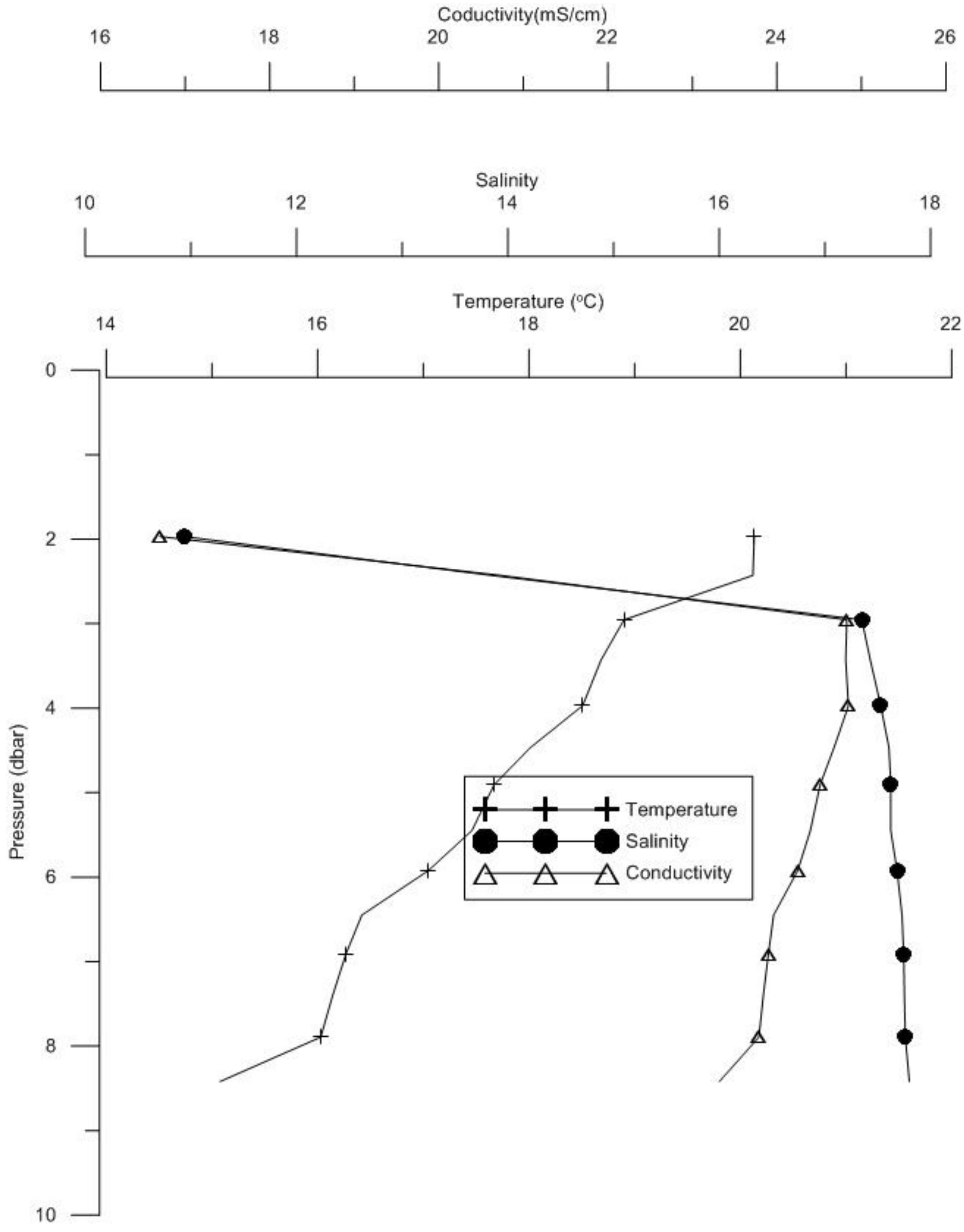

Figure 134.CTD from D6 Station for the second measurements in May2015

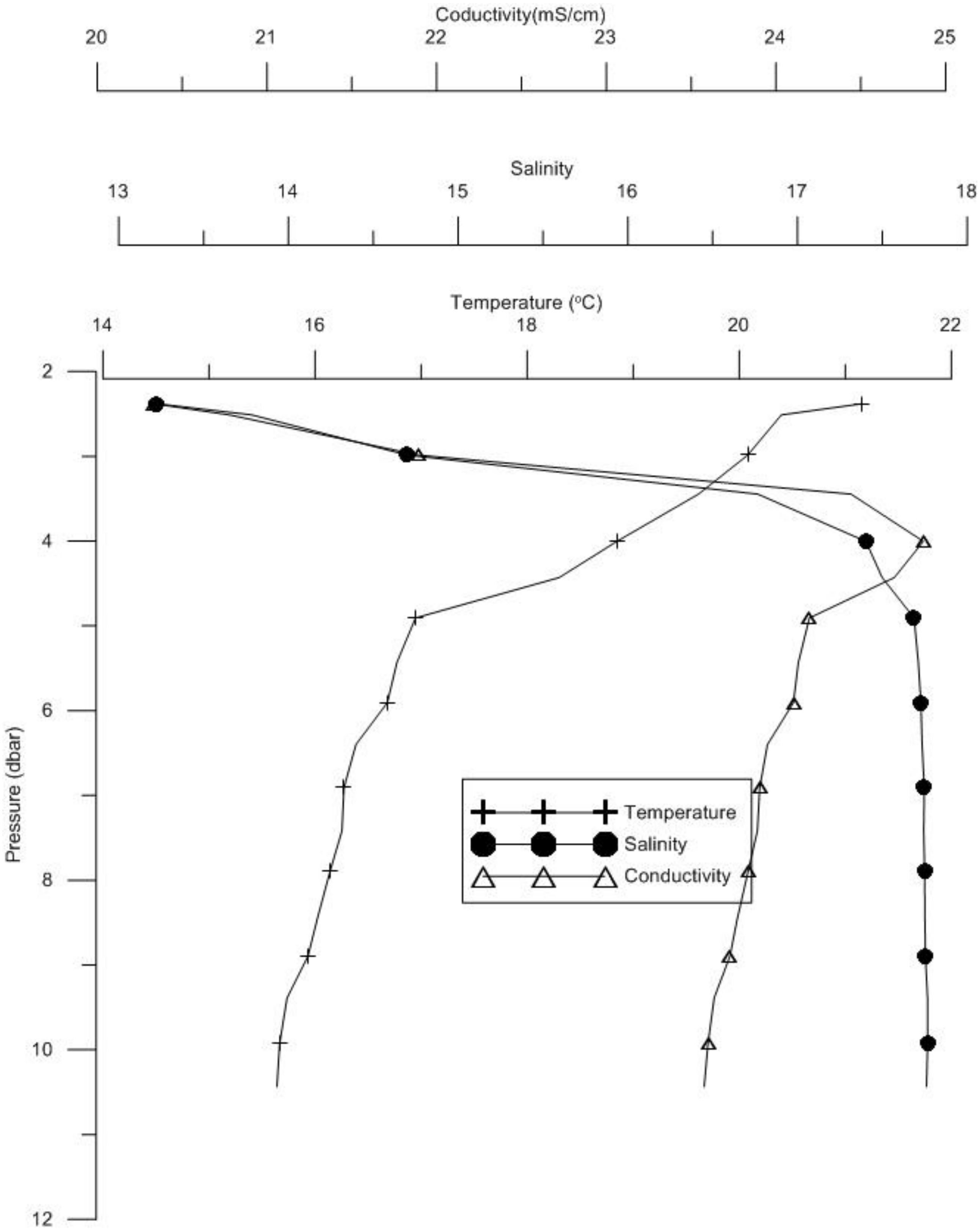

Figure 135.CTD from D7 Station for the second measurements in May2015

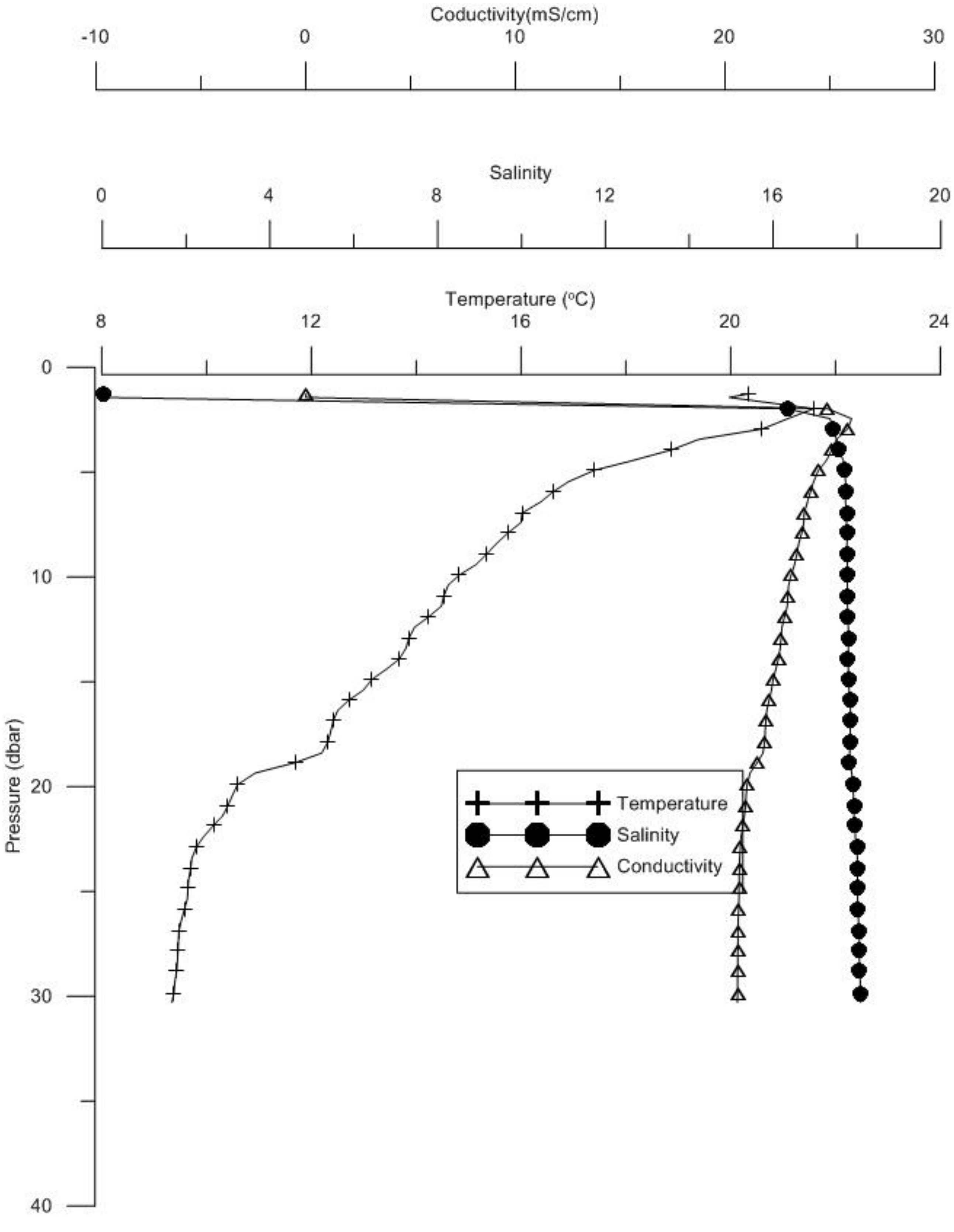

Figure 136.CTD from D8 Station for the second measurements in May2015

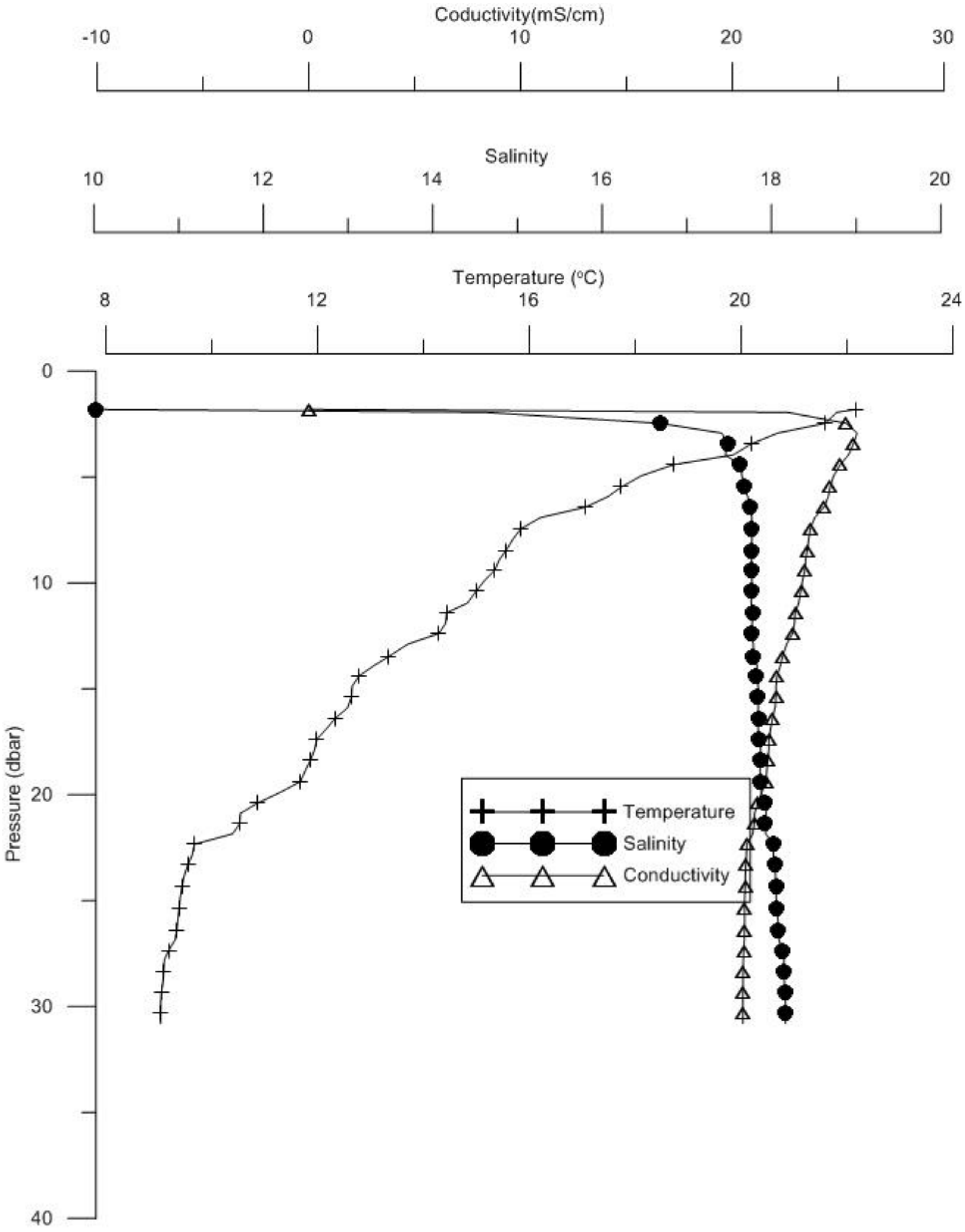

Figure 137.CTD from D9 Station for the second measurements in May2015

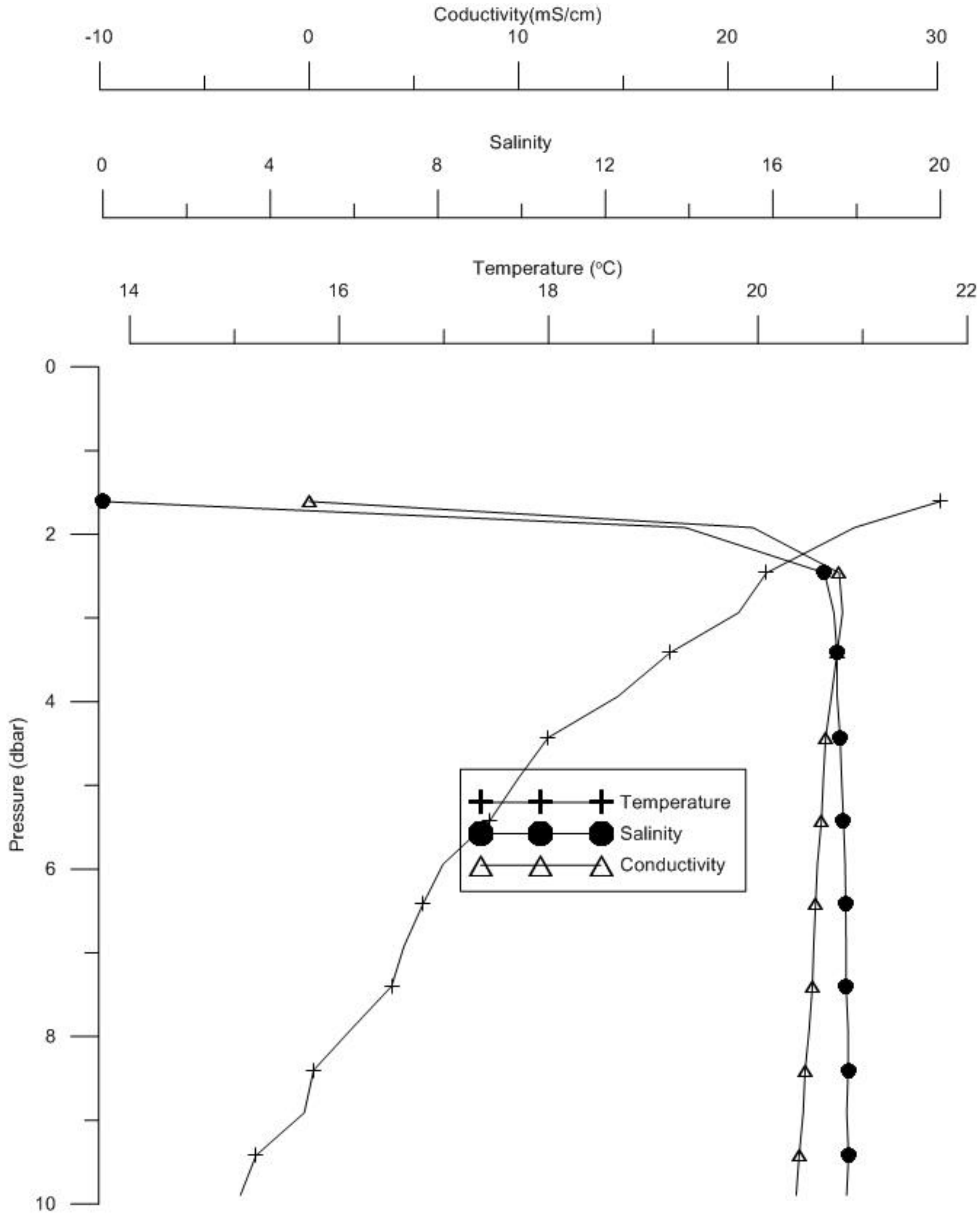

Figure 138.CTD from D10 Station for the second measurements in May2015

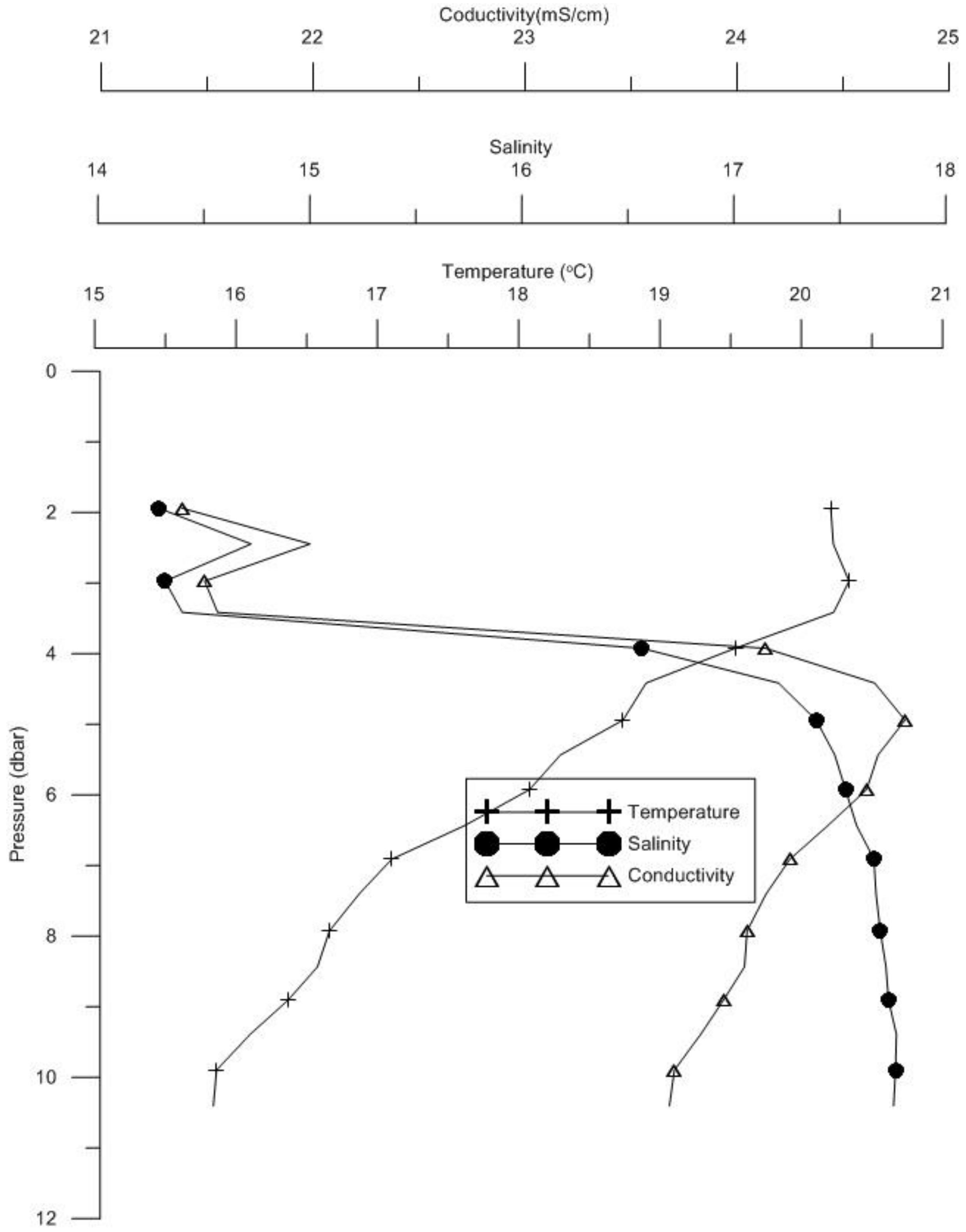

Figure 139.CTD from D11 Station for the second measurements in May2015

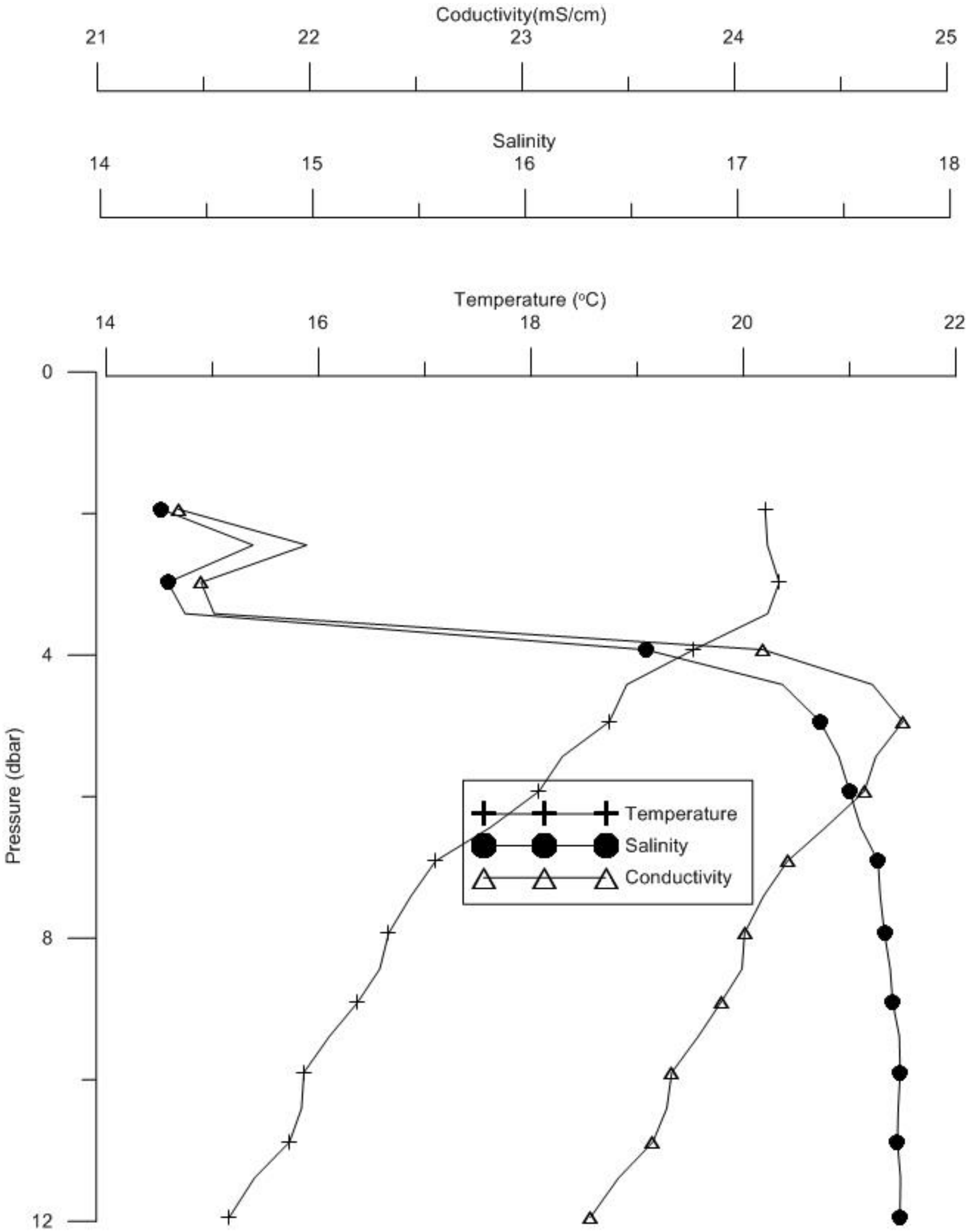

Figure 140.CTD from D12 Station for the second measurements in May2015

CTD graphs versus depth for each stations are given in the below. Conductivity, Salinity and Temperature results for June are given in Figures 141 -152.

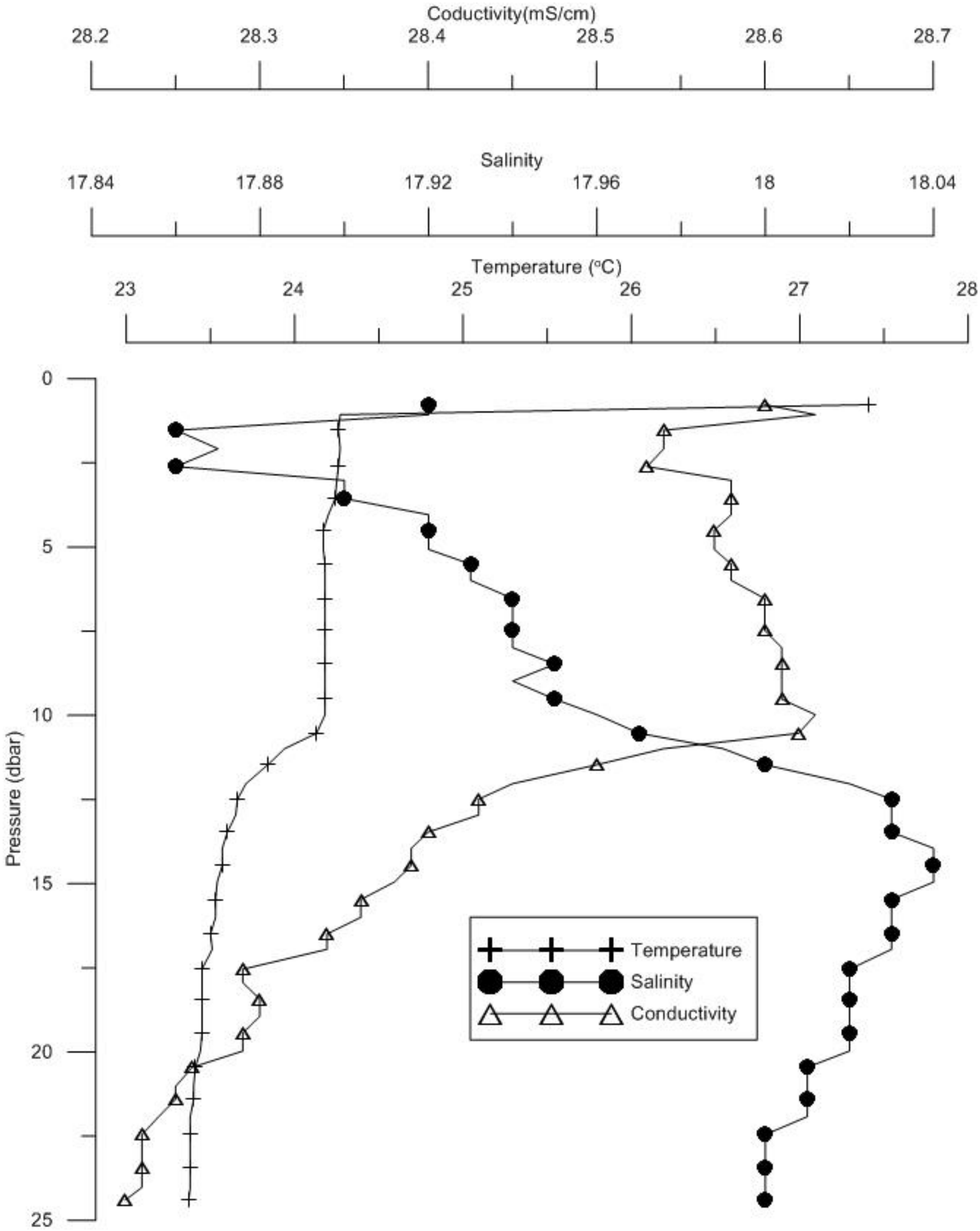

Figure 141. CTD from D1 Station for measurements in June2015

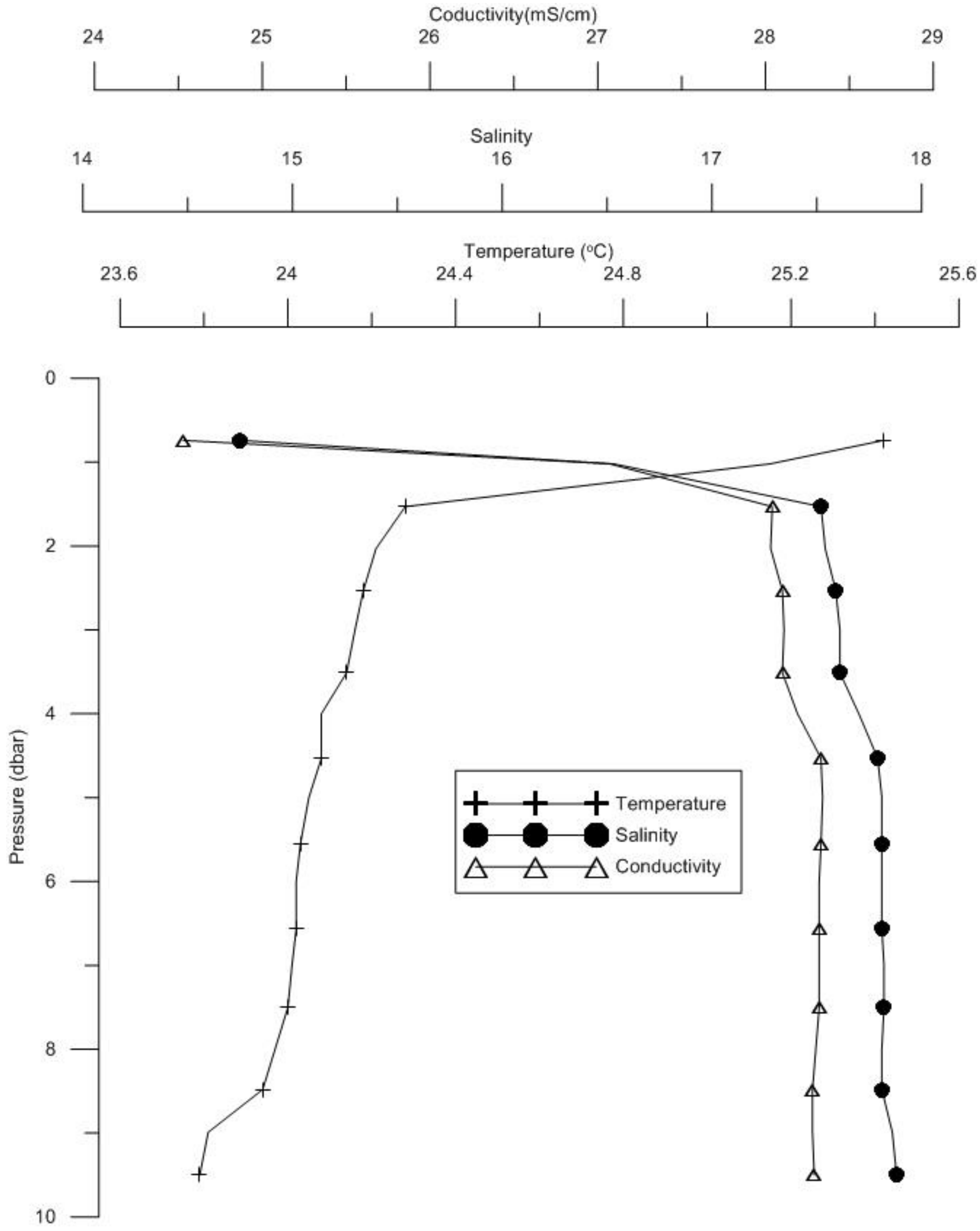

Figure 142.CTD from D2 Station for measurements in June2015

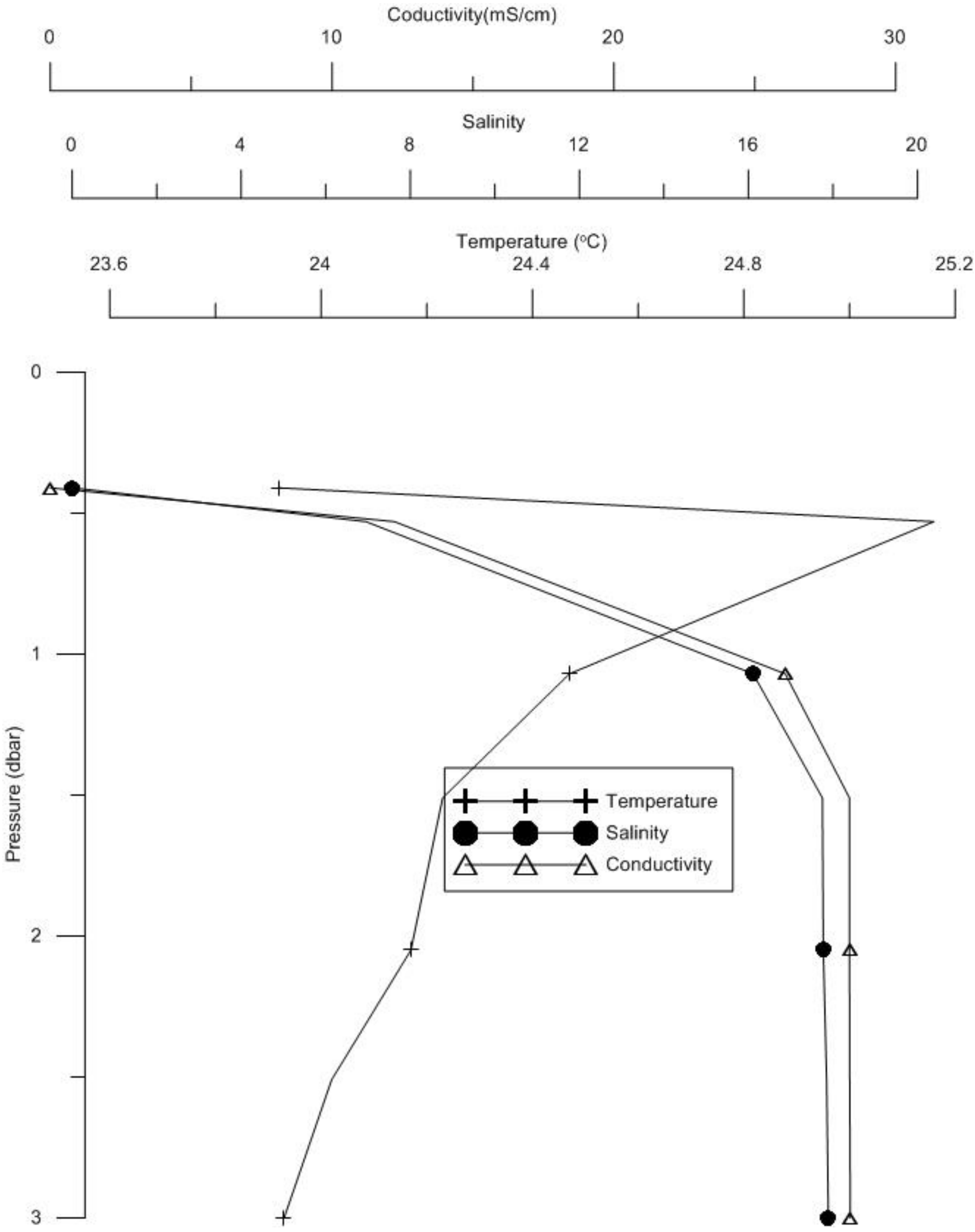

Figure 143.CTD from D3 Station for measurements in June2015

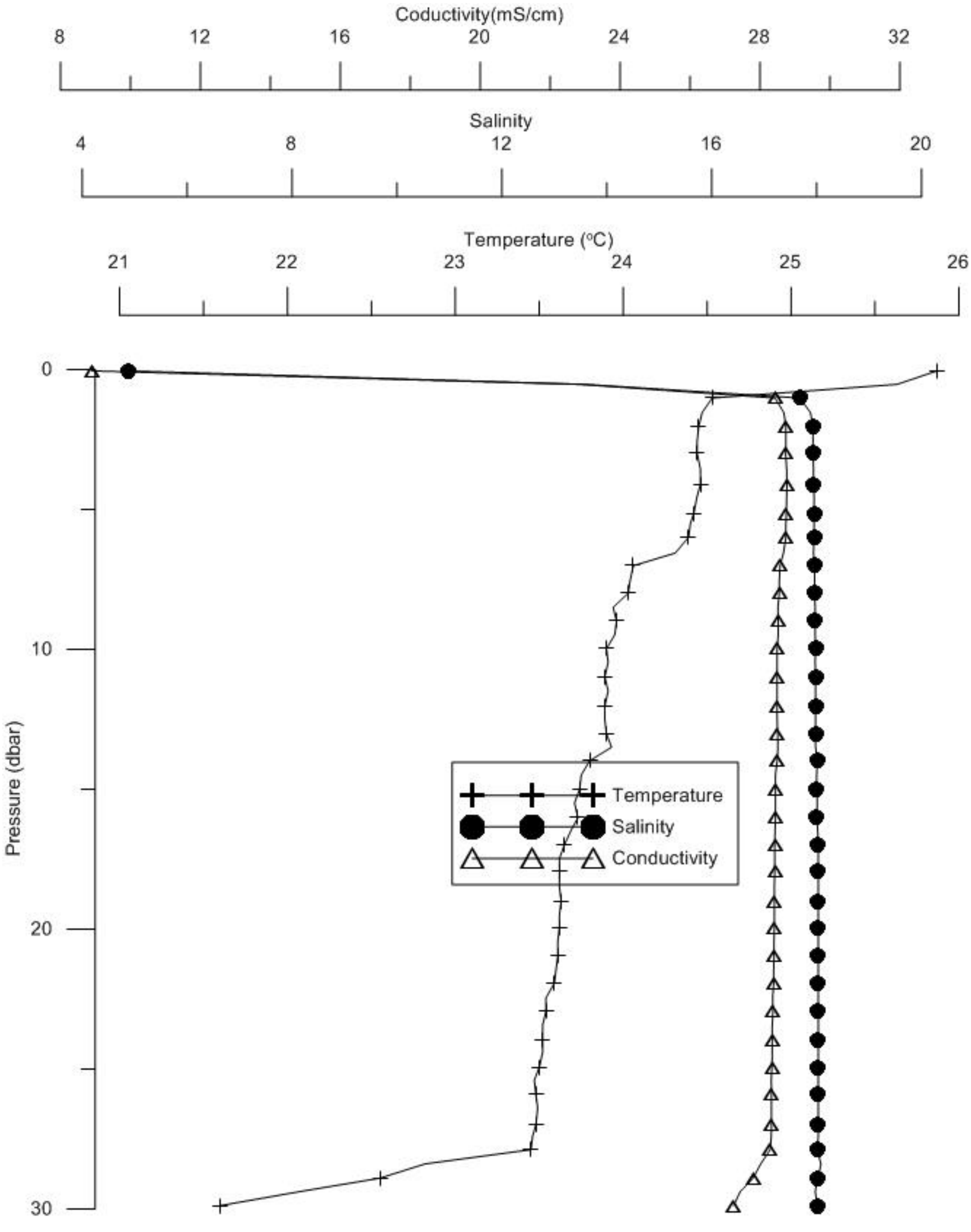

Figure 144.CTD from D4 Station for measurements in June2015

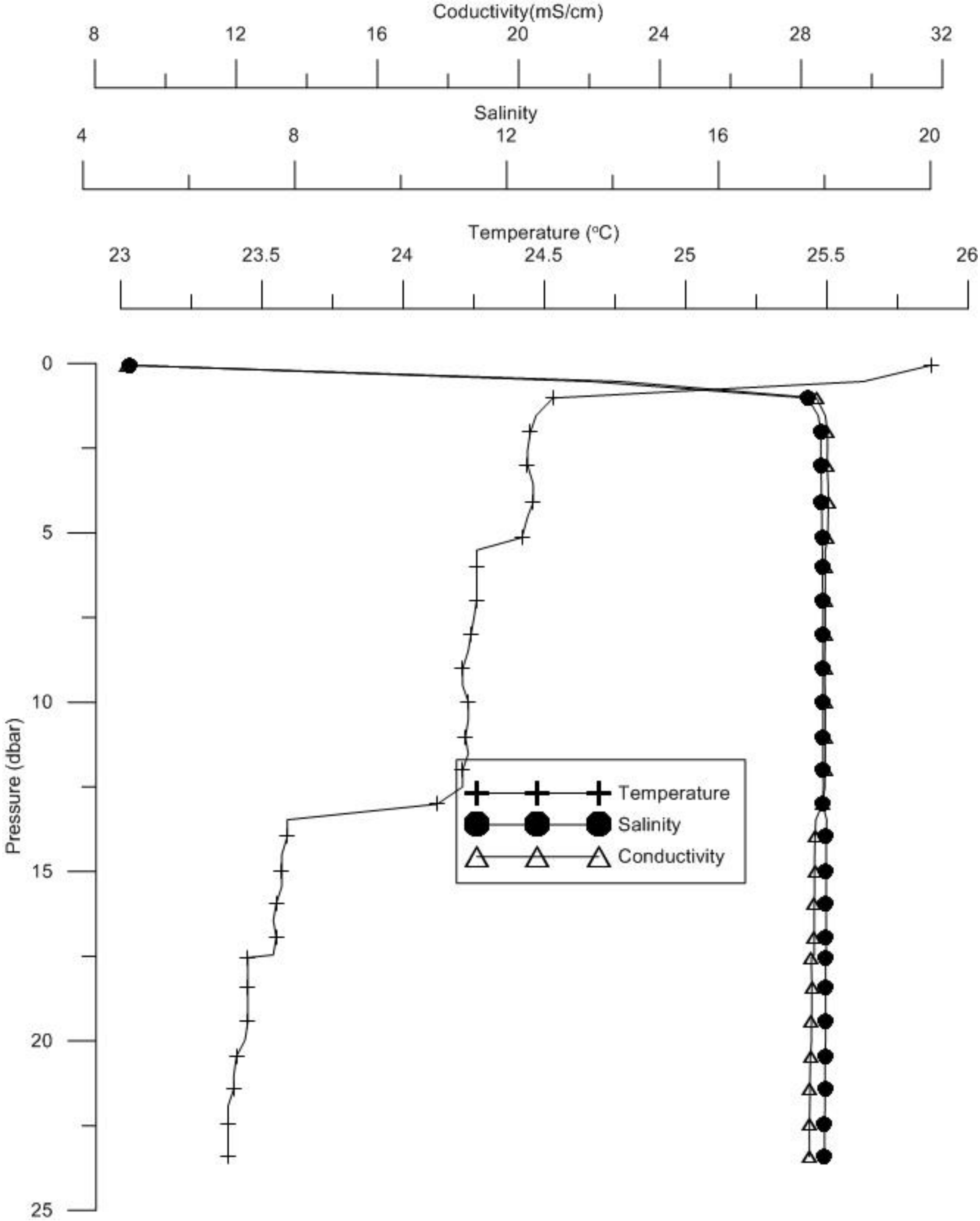

Figure 145.CTD from D5 Station for measurements in June2015

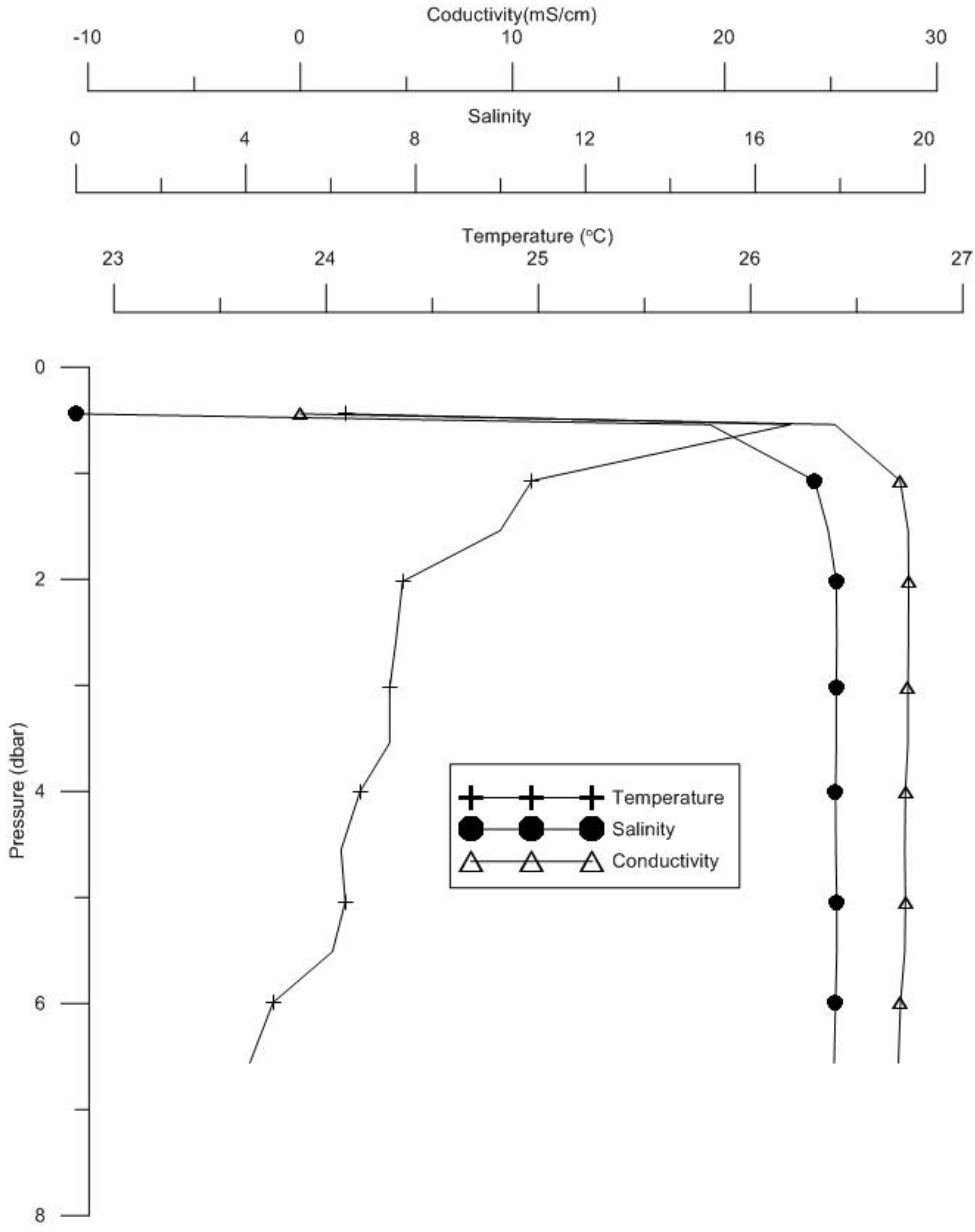

Figure 146.CTD from D6 Station for measurements in June2015

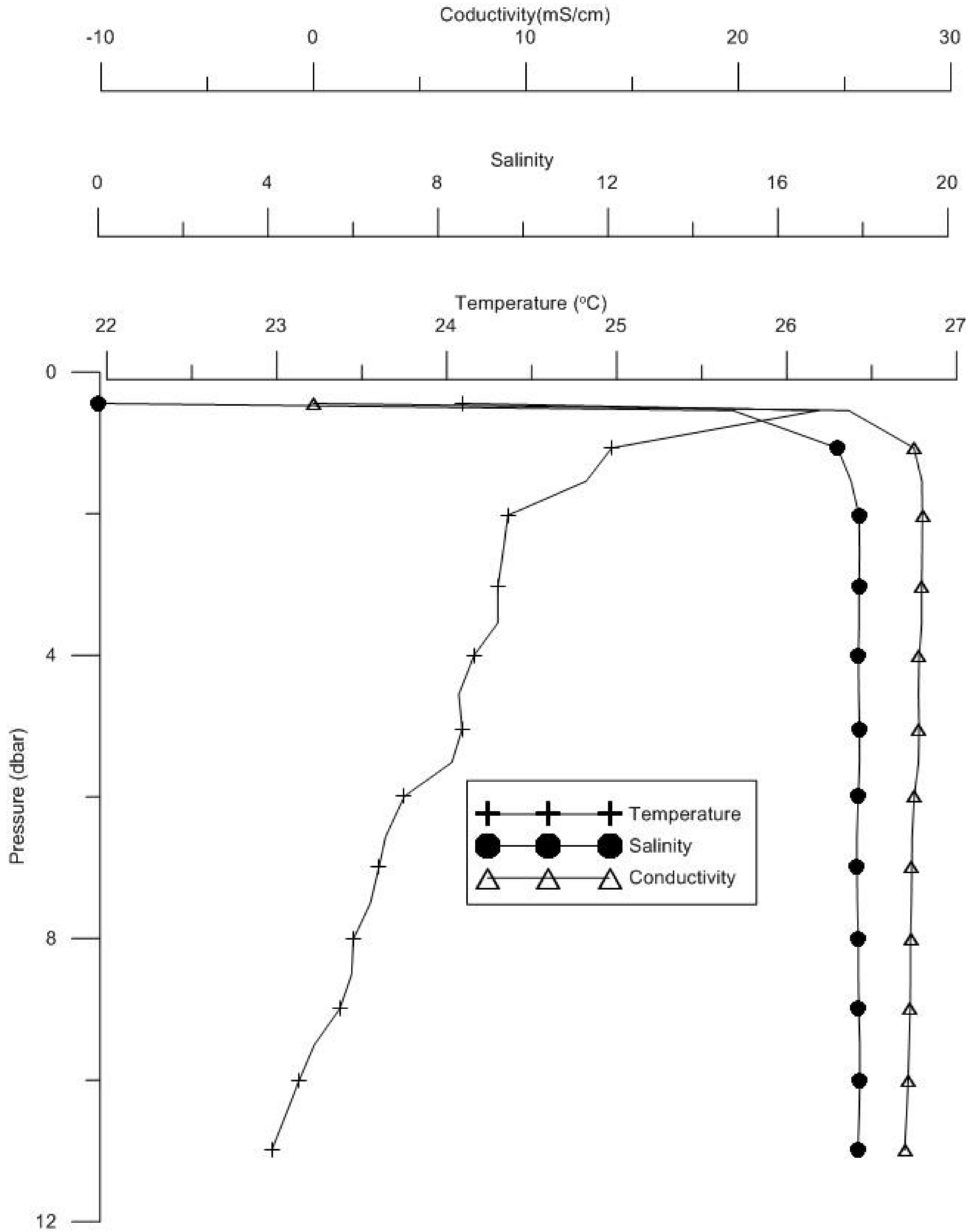

Figure 147.CTD from D7 Station for measurements in June2015

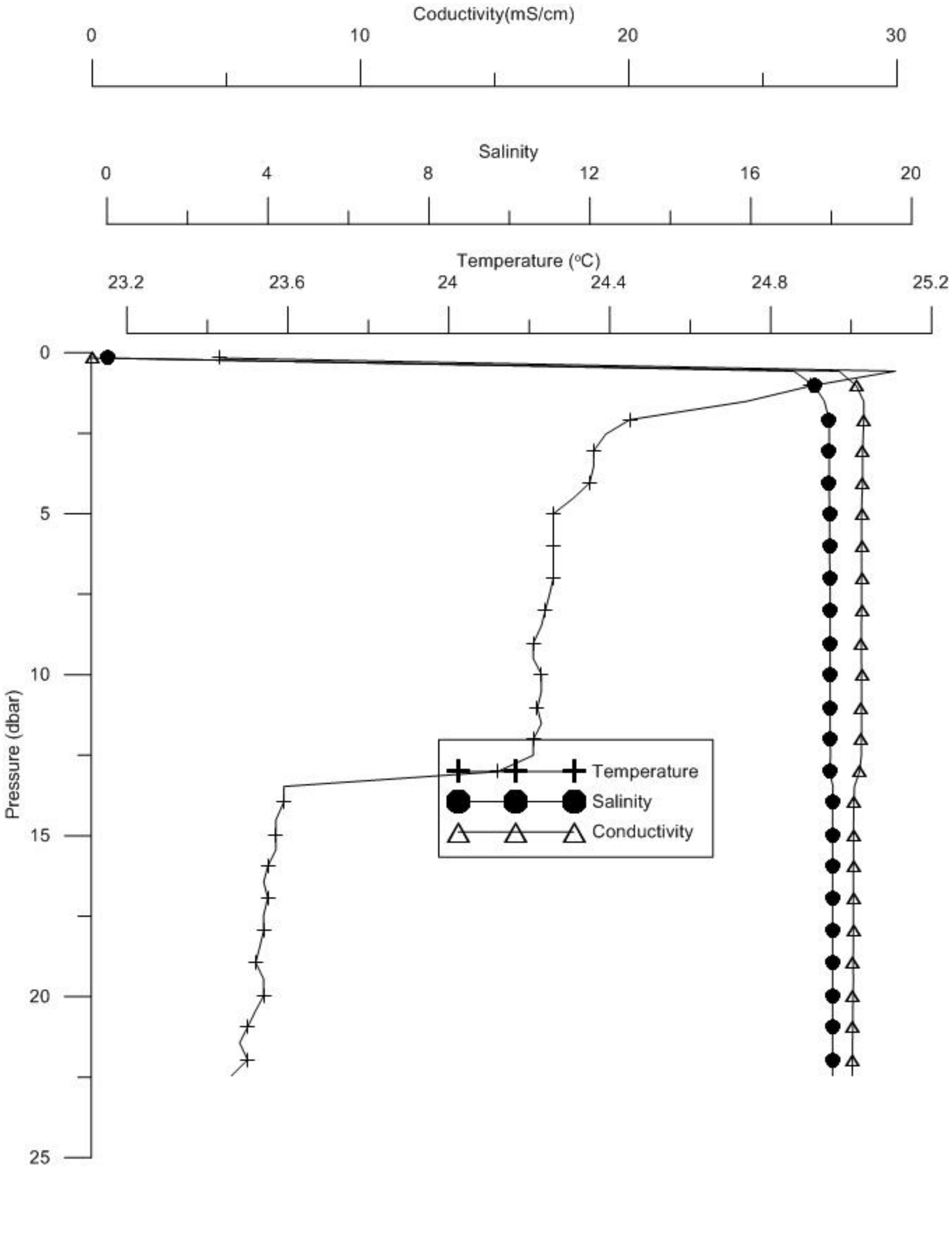

Figure 148.CTD from D8 Station for measurements in June2015

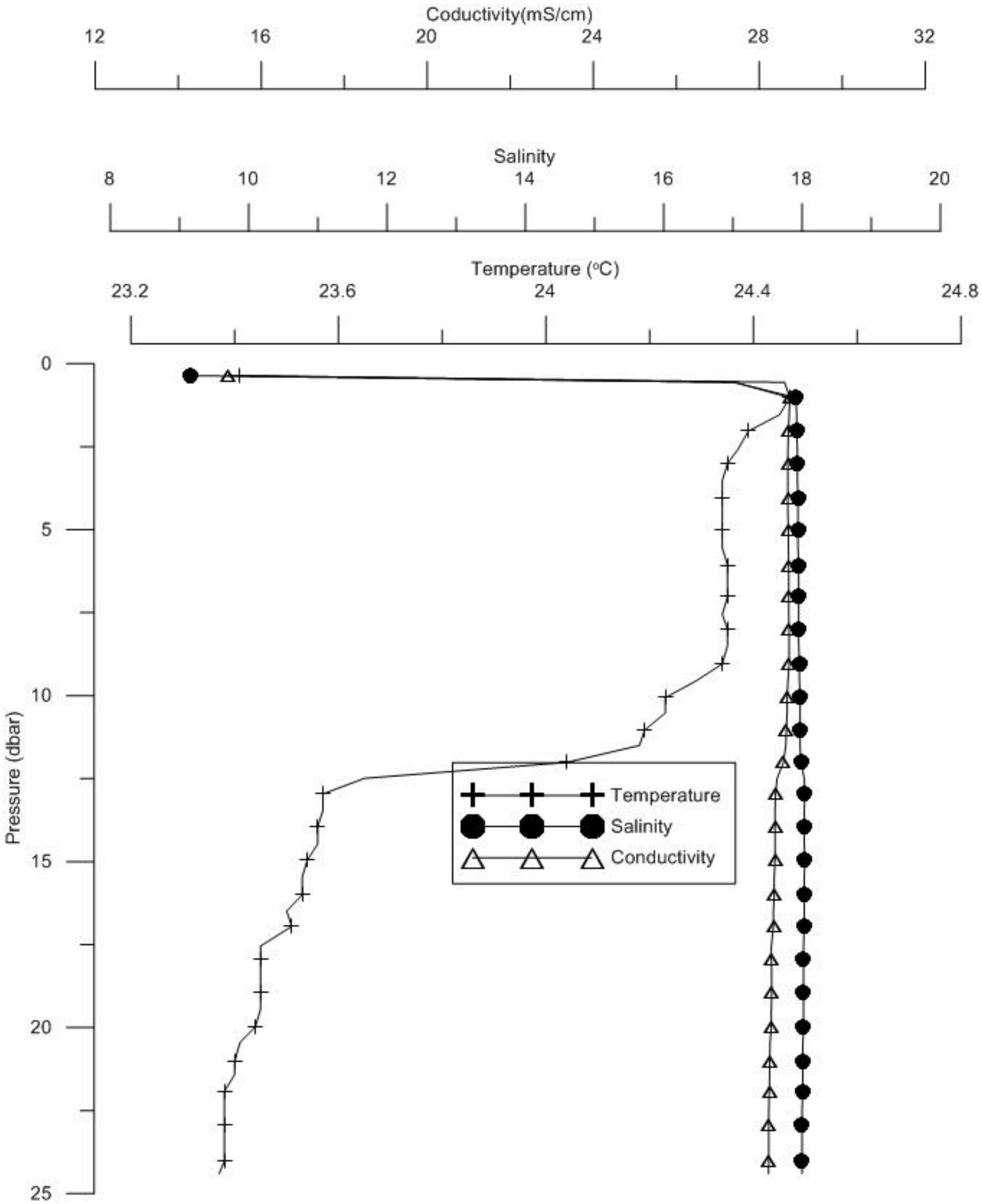

Figure 149.CTD from D9 Station for measurements in June2015

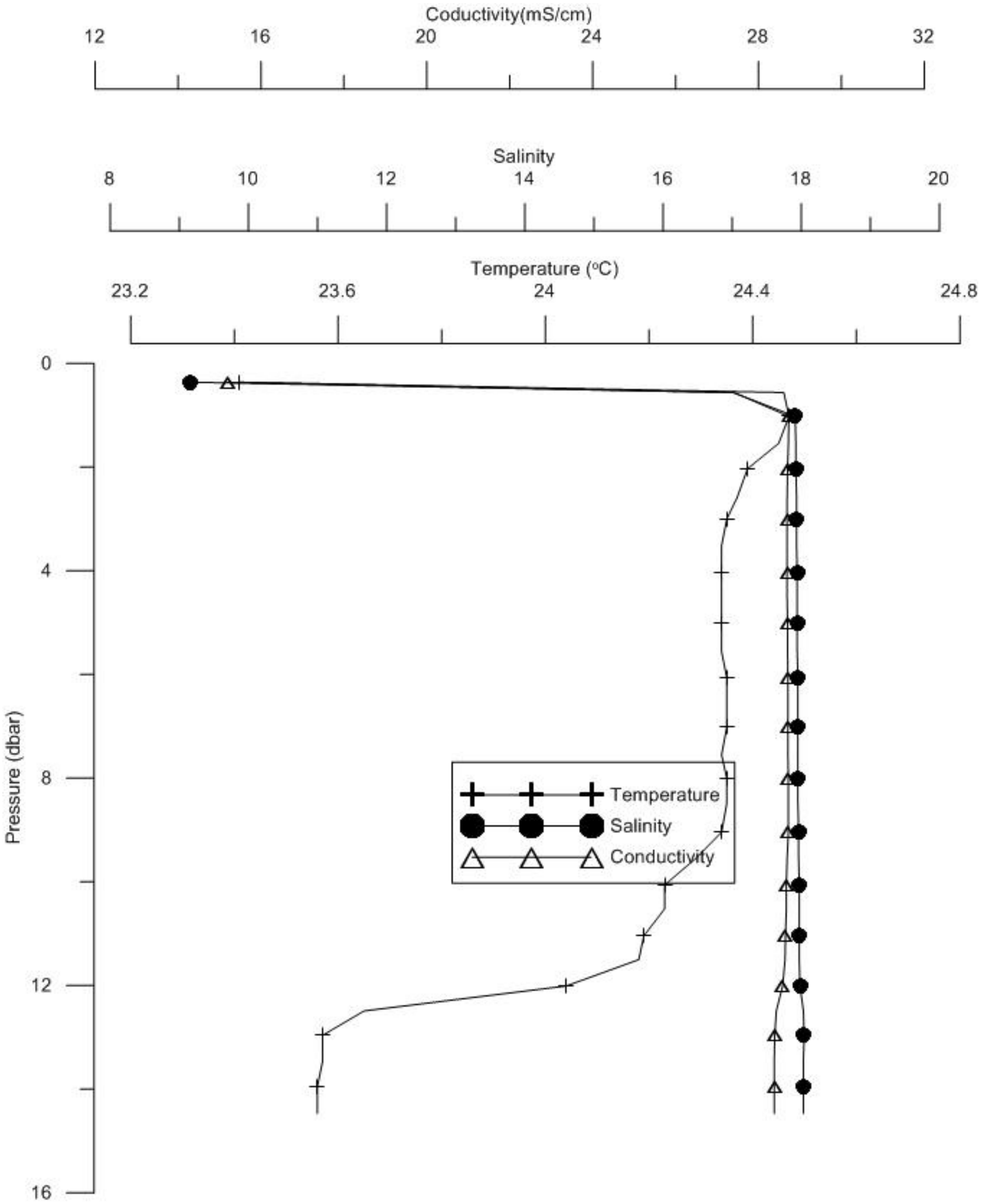

Figure 150.CTD from D10 Station for measurements in June2015

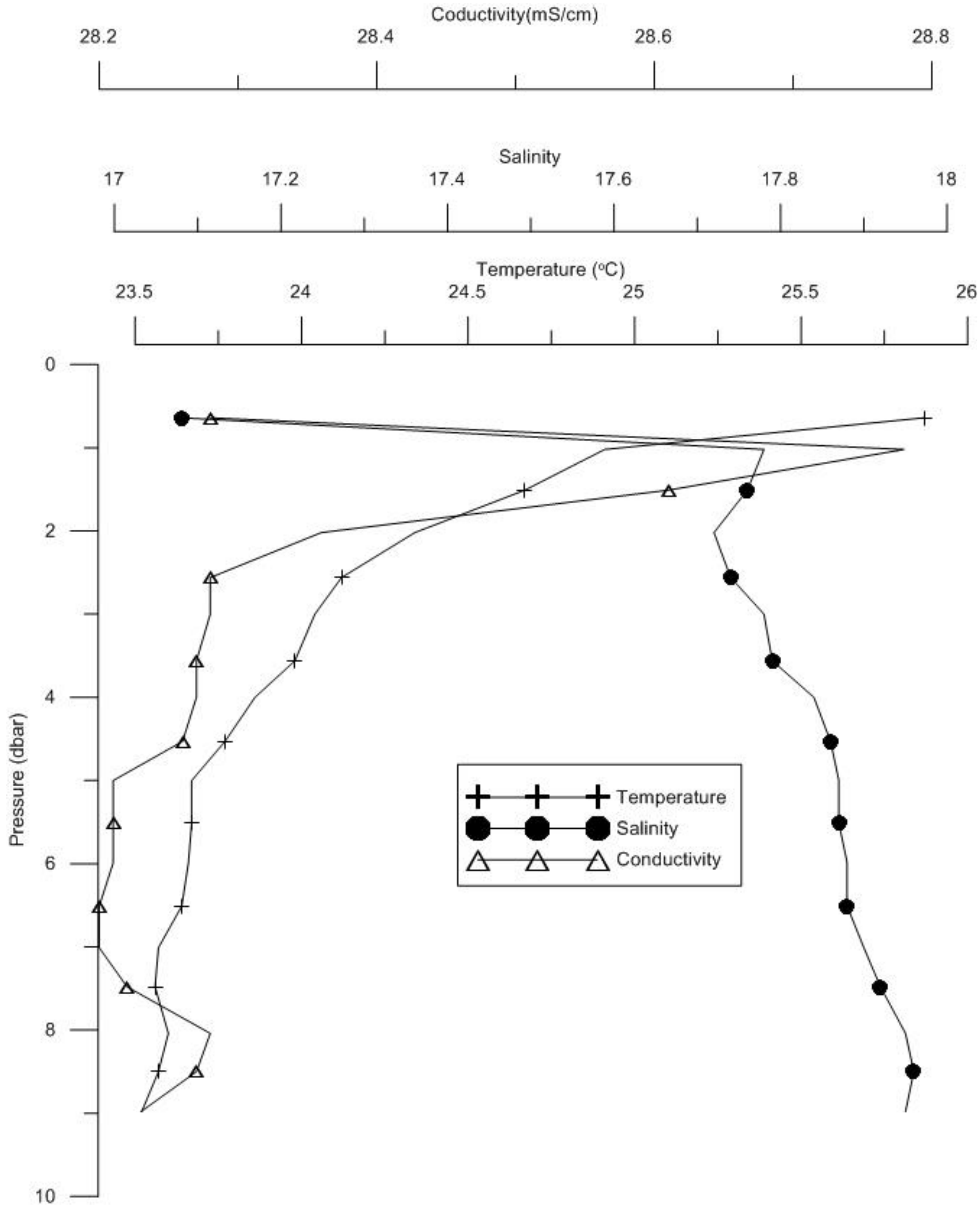

Figure 151.CTD from D11 Station for the first measurements in June 2015

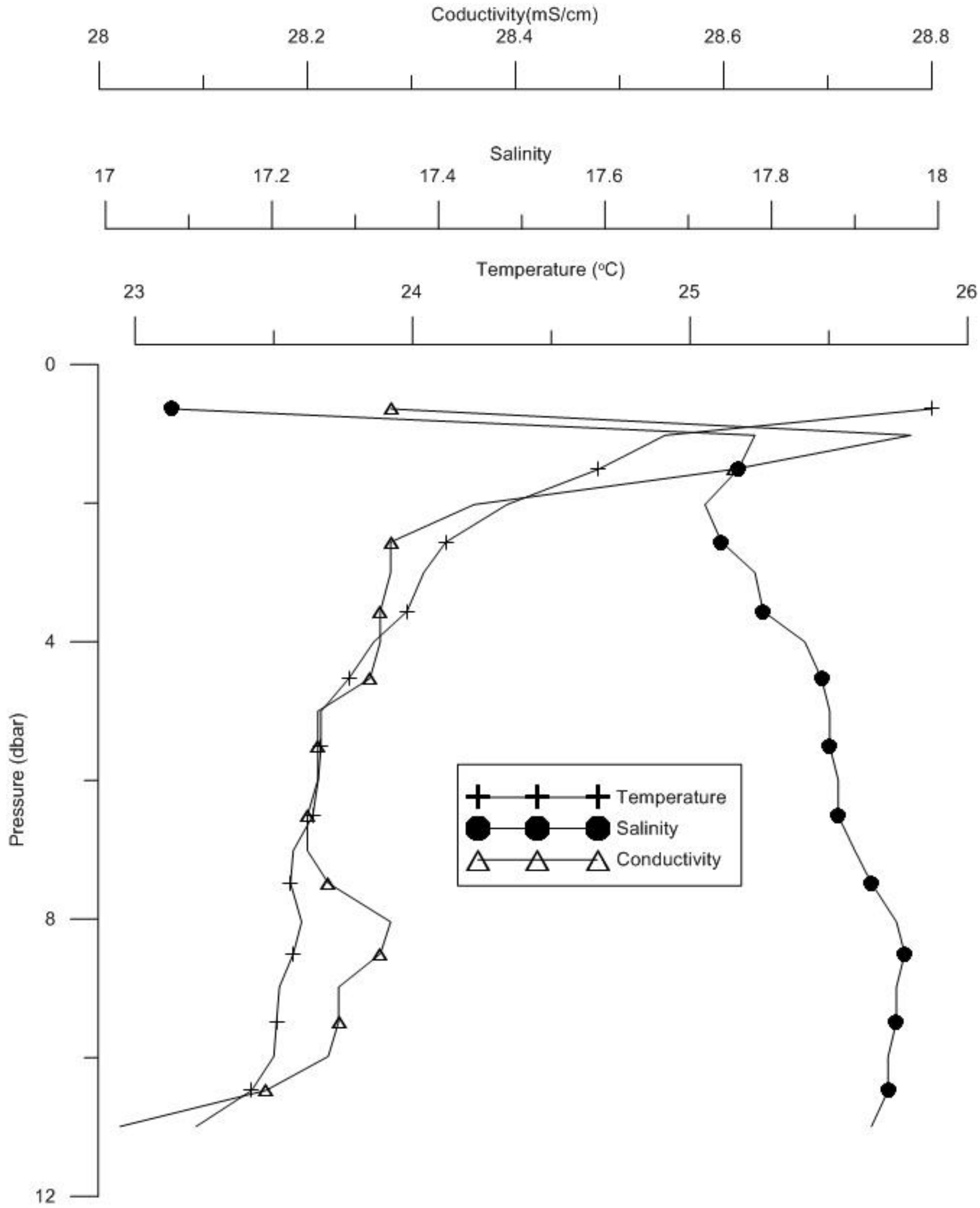

Figure 152.CTD from D12 Station for measurements in June2015

In order to cover all season data for september was obtained Project coordinator and graphs for these measurements are given in Figures 153-164.

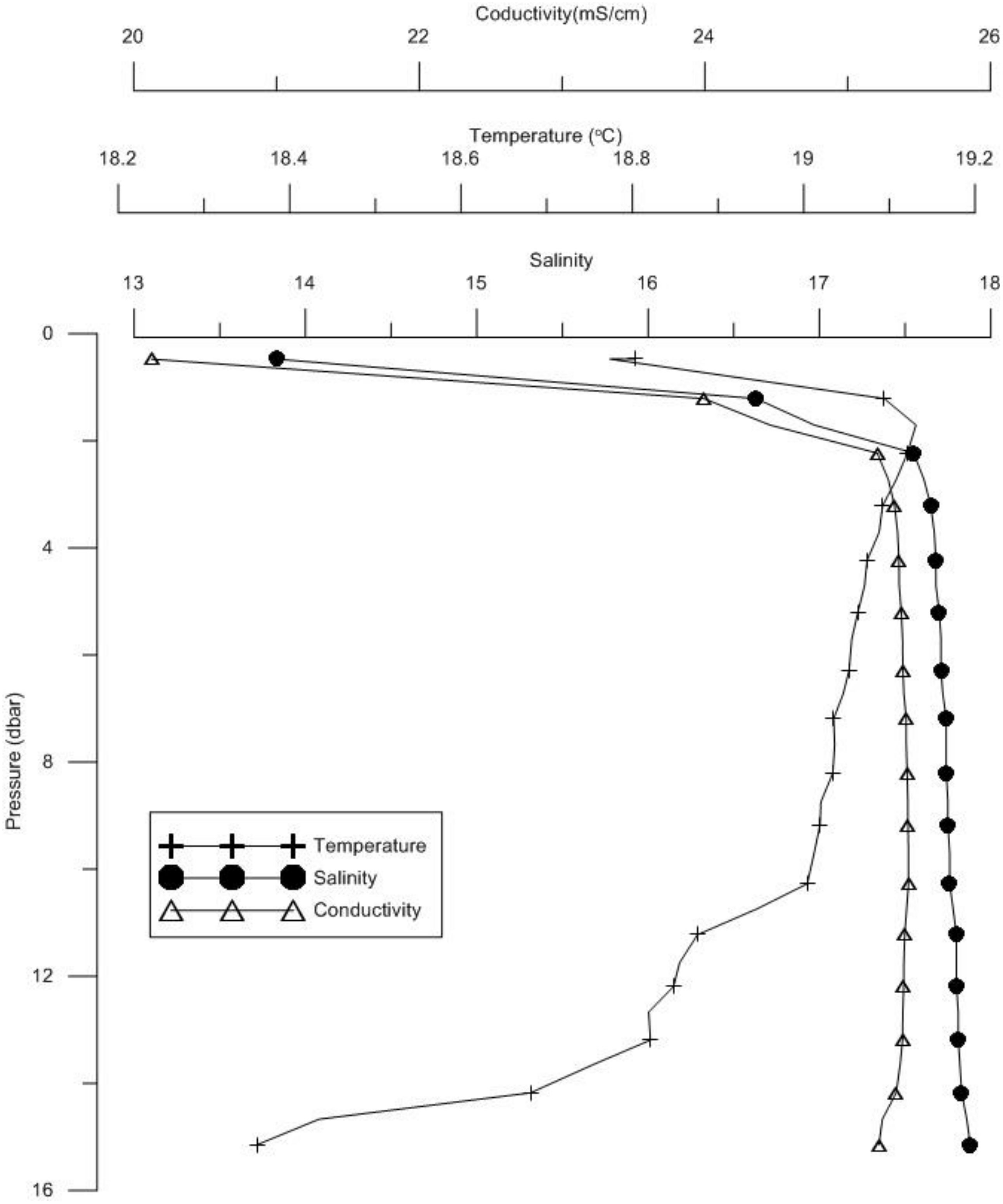

Figure 153.CTD from D1 Station for measurements in September 2014

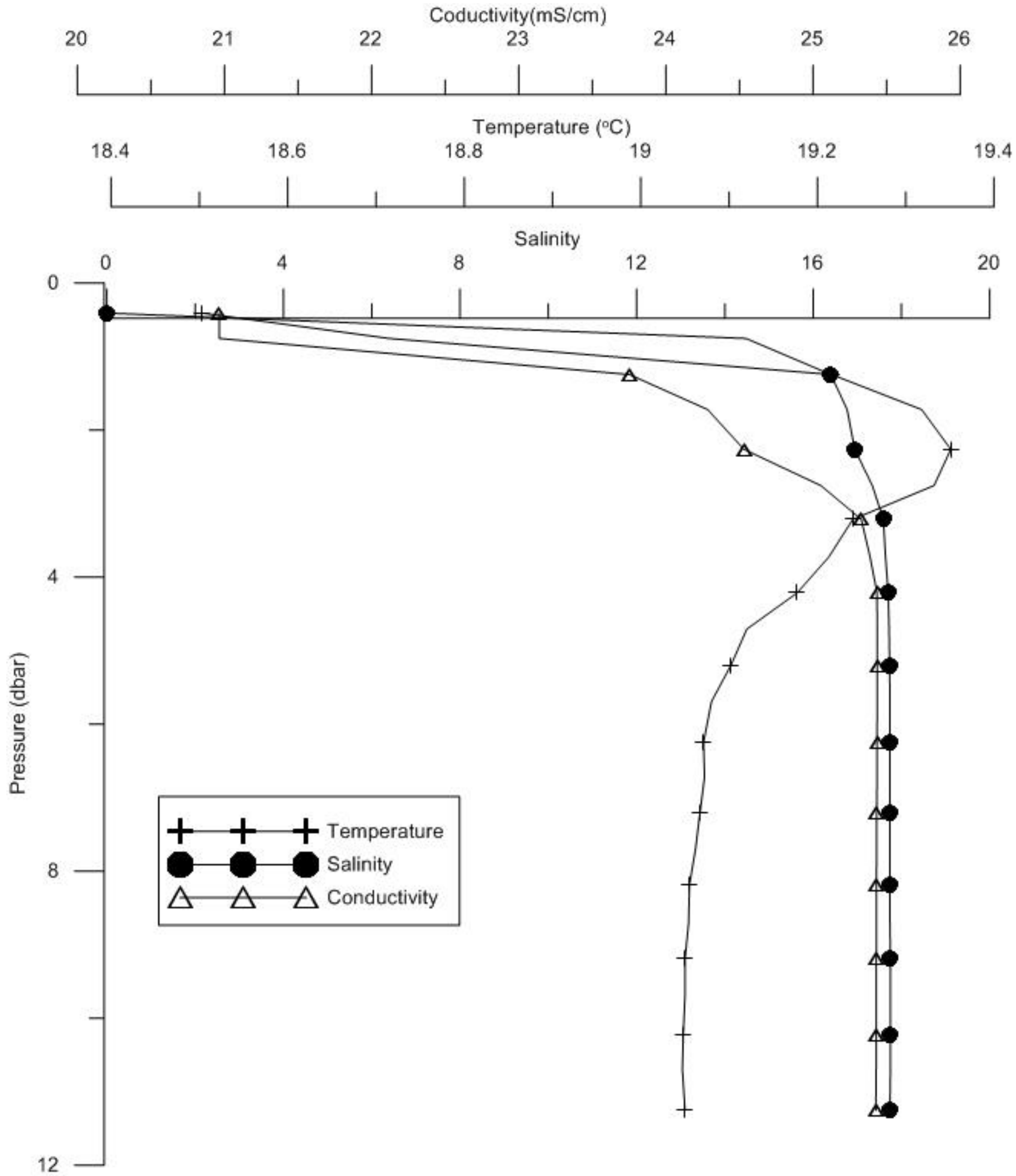

Figure 154. CTD from D2 Station for measurements in September 2014

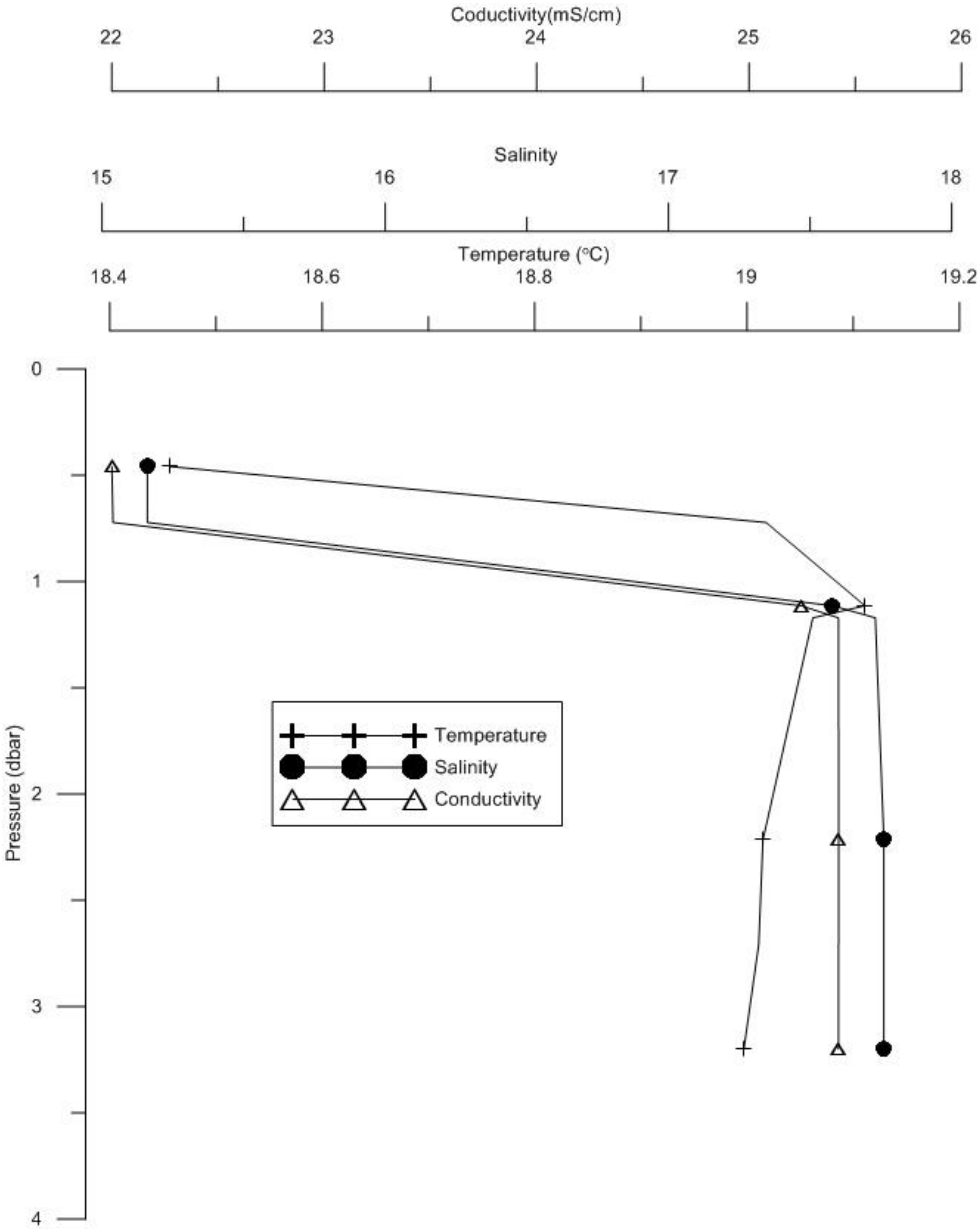

Figure 155. CTD from D3 Station for measurements in September2014

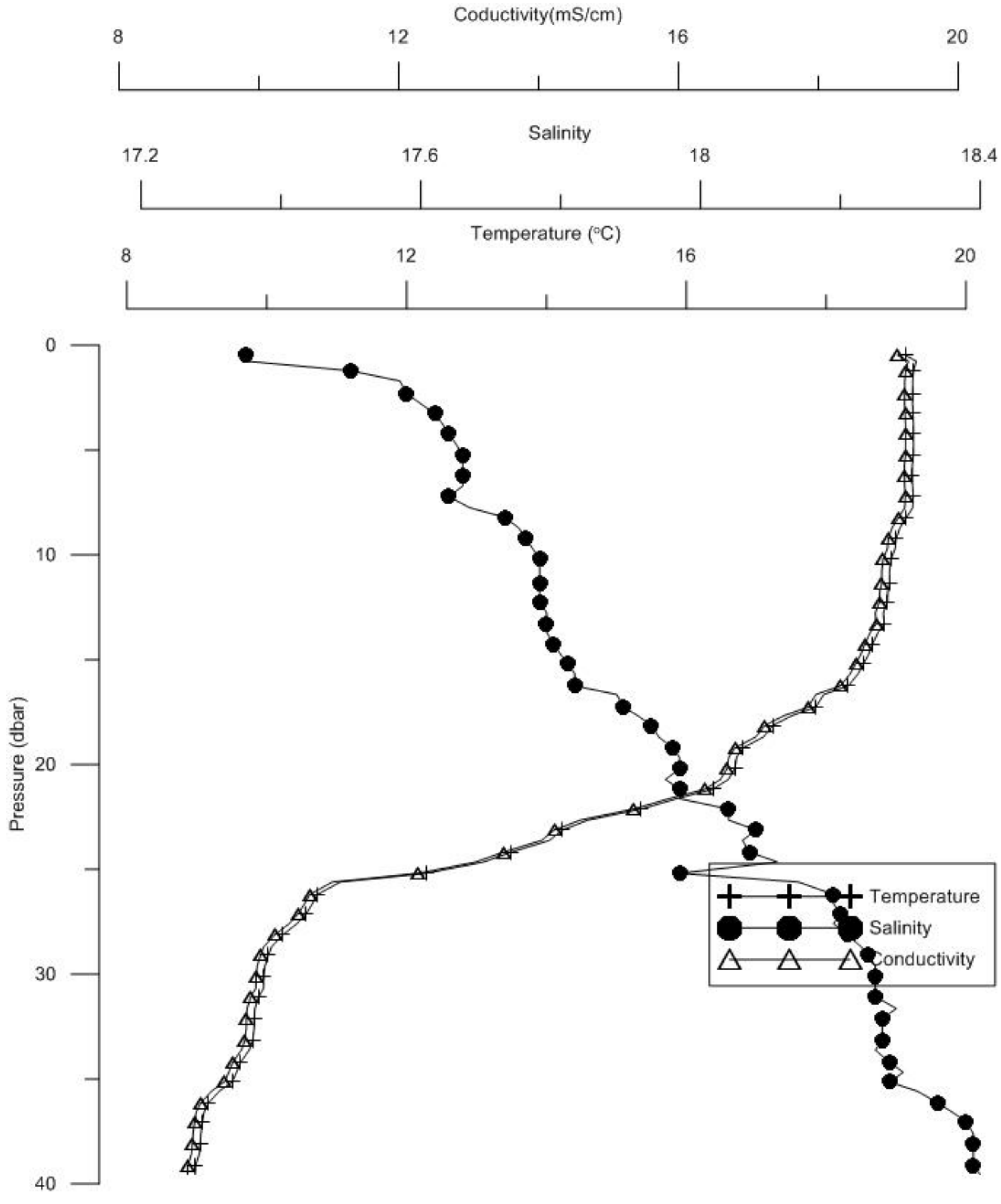

Figure 156. CTD from D4 Station for measurements in September2014

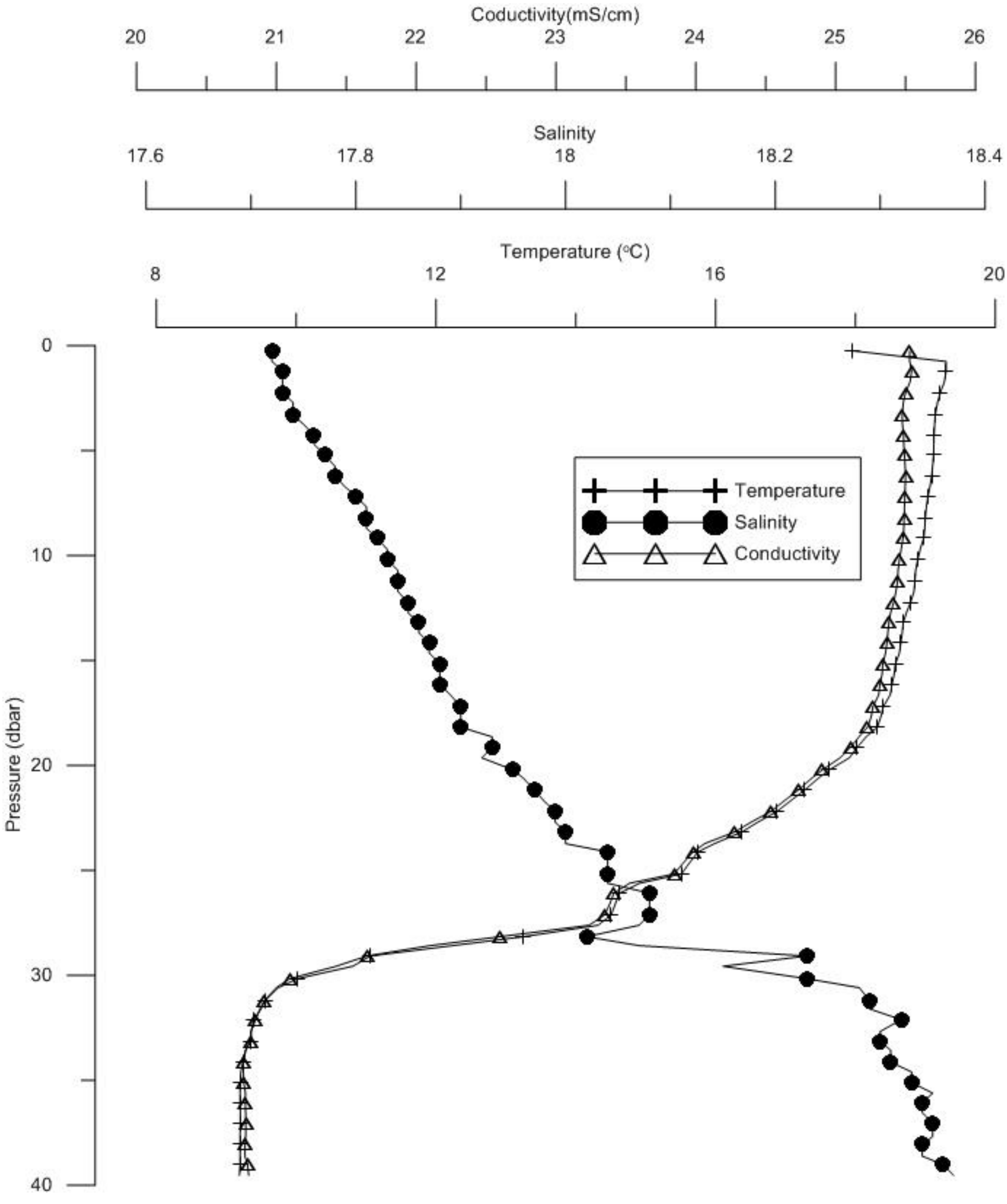

Figure 157. CTD from D5 Station for measurements in September2014

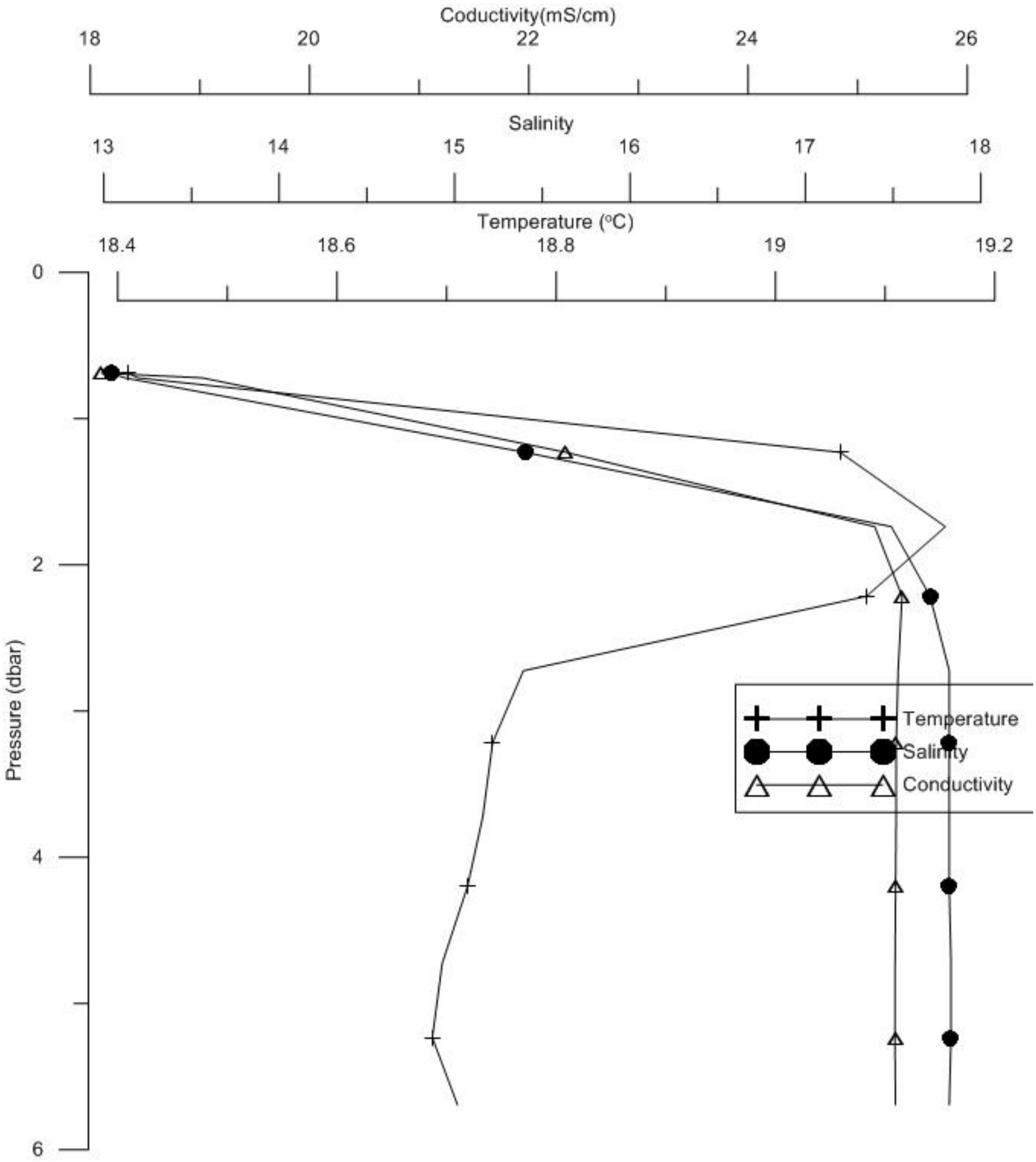

Figure 158. CTD from D6 Station for measurements in September2014

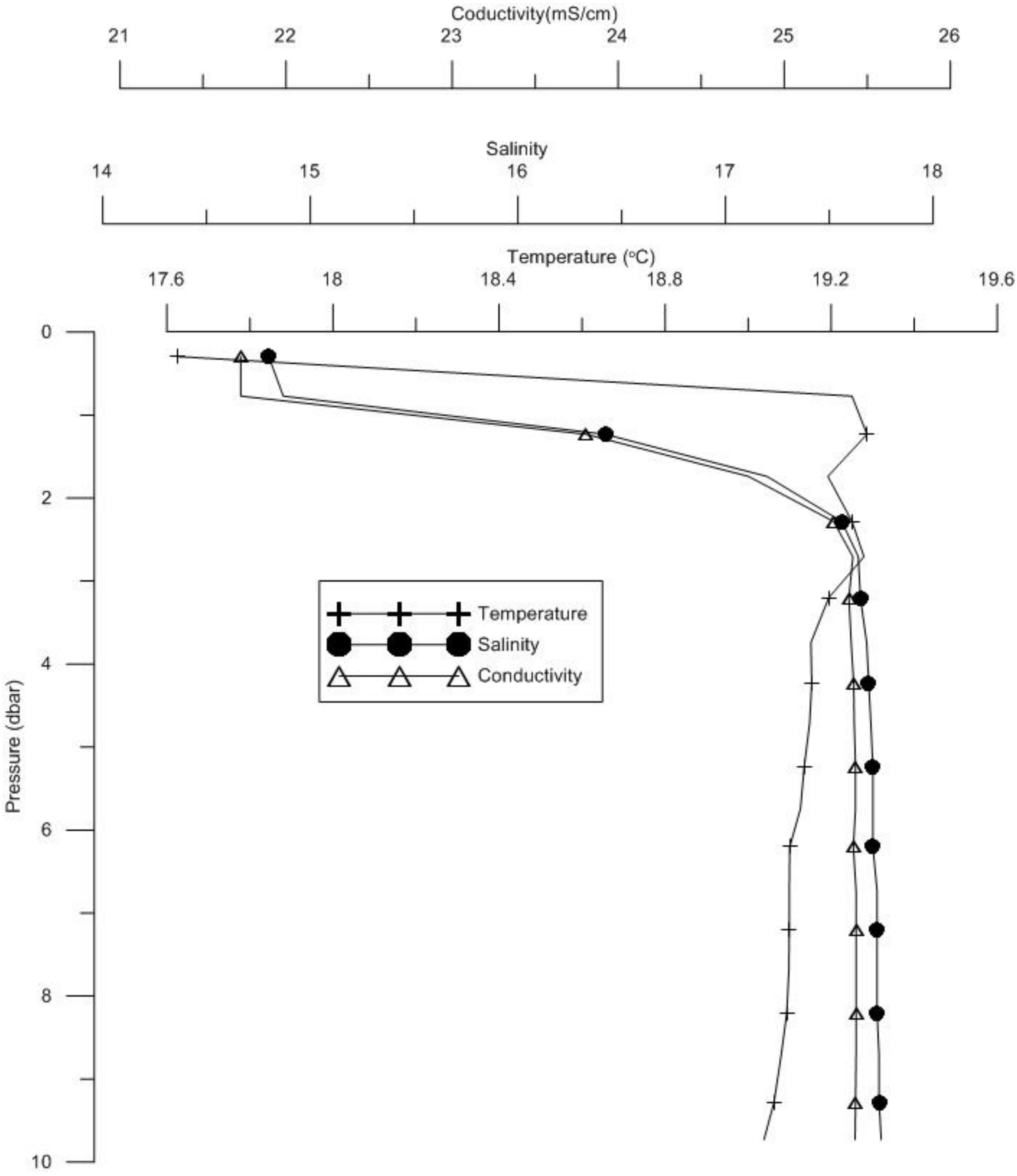

Figure 159. CTD from D7 Station for measurements in September2014

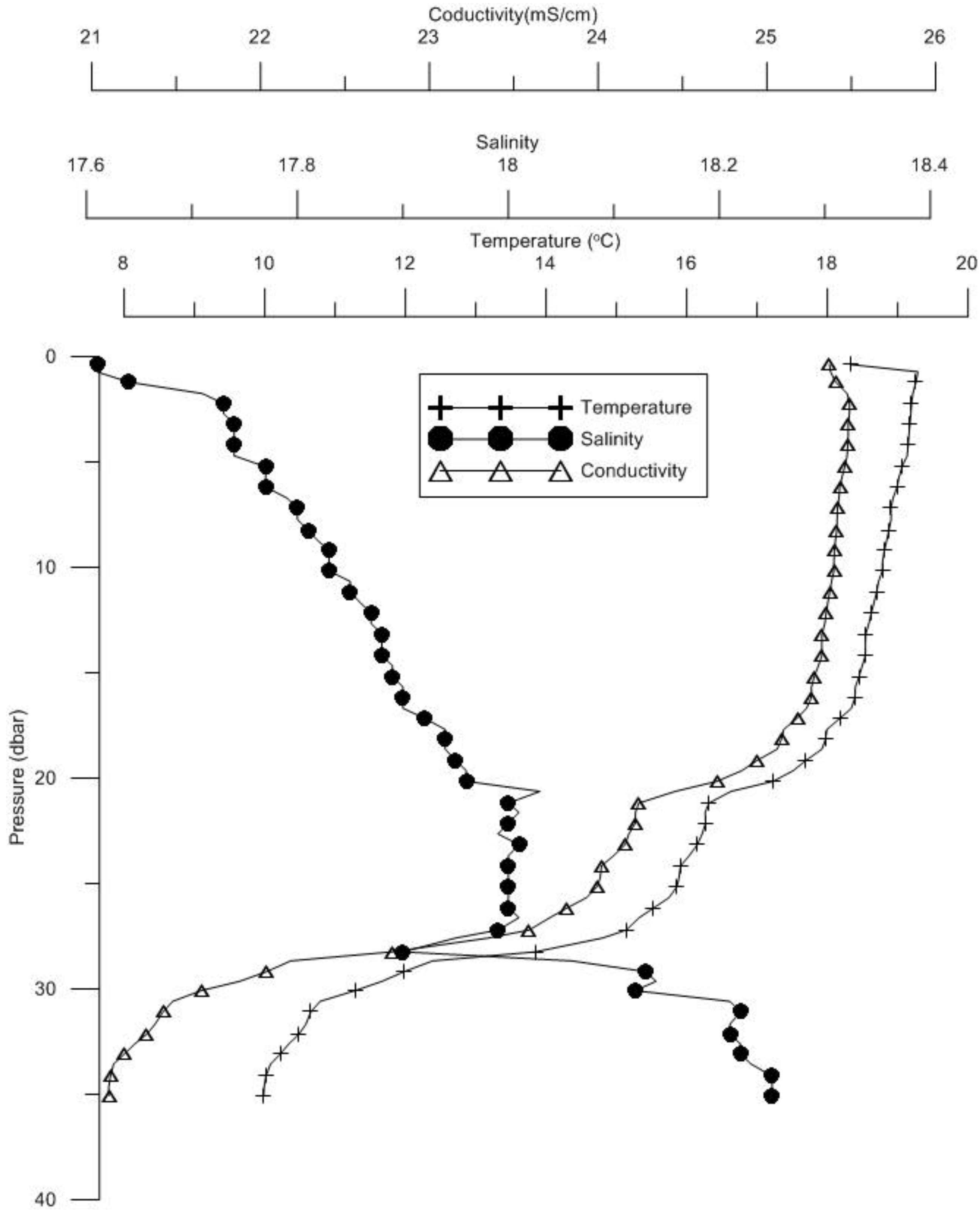

Figure 160.CTD from D8 Station for measurements in September2014

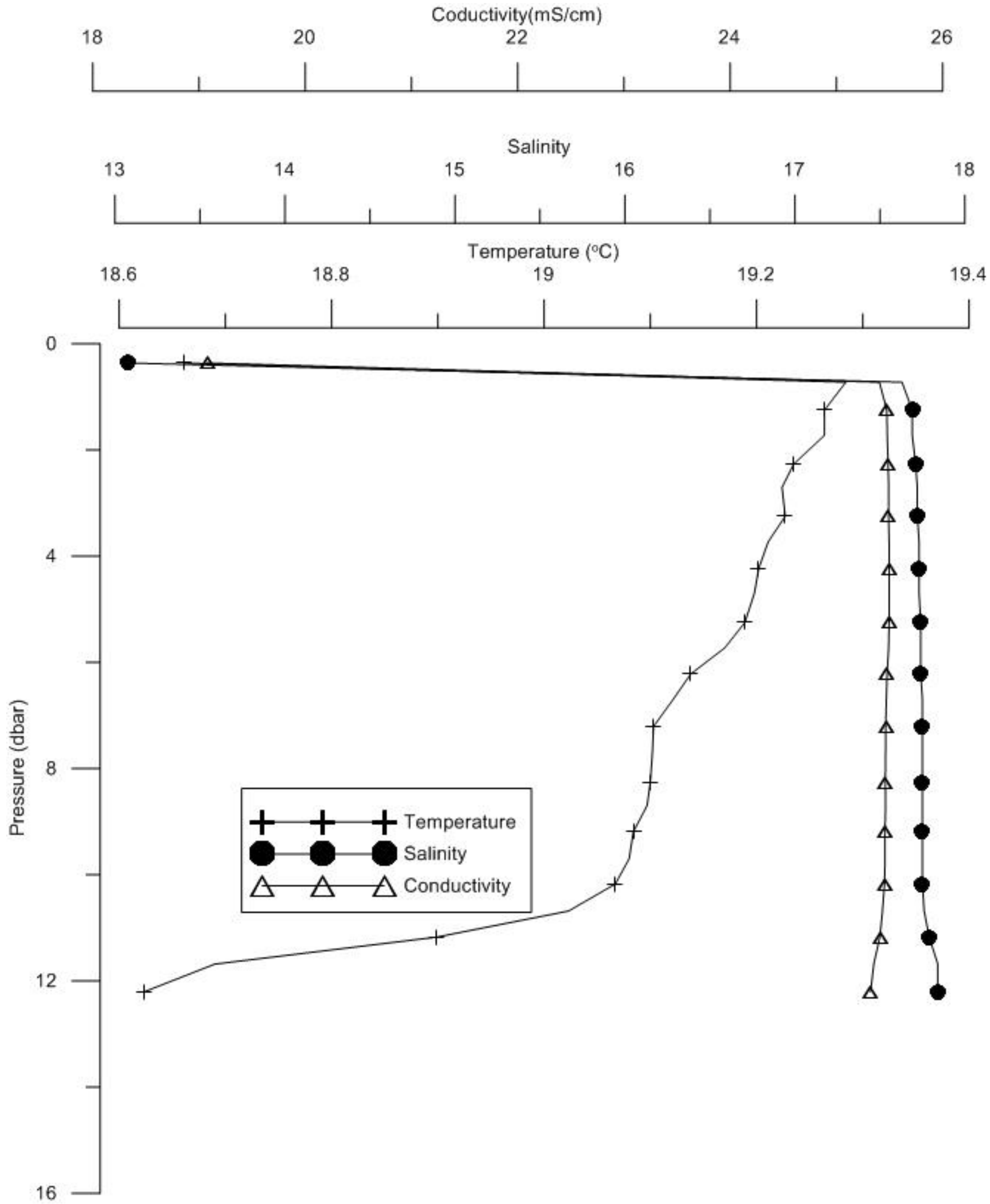

Figure 161.CTD from D9 Station for measurements in September2014

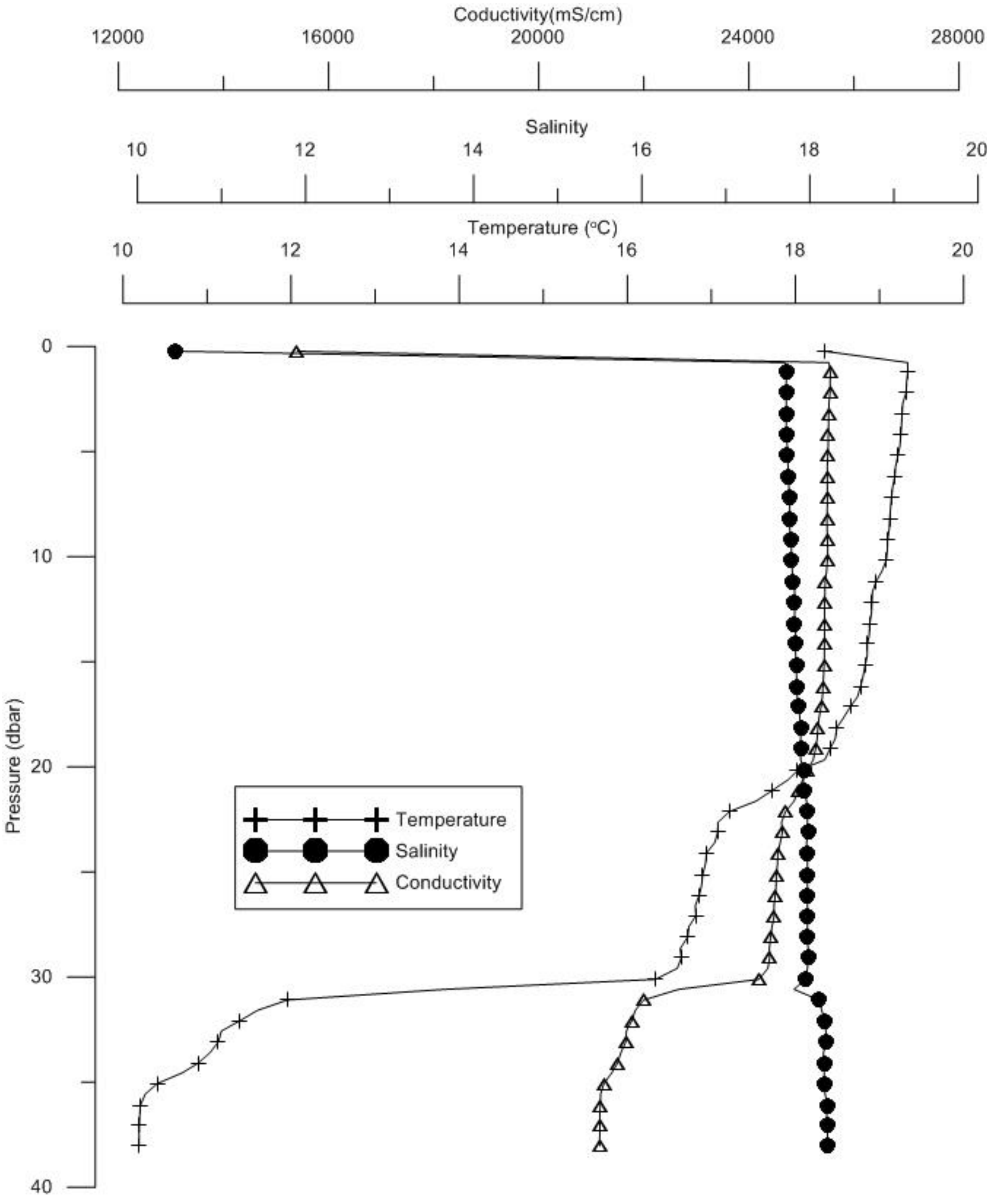

Figure 162.CTD from D10 Station for measurements in September2014

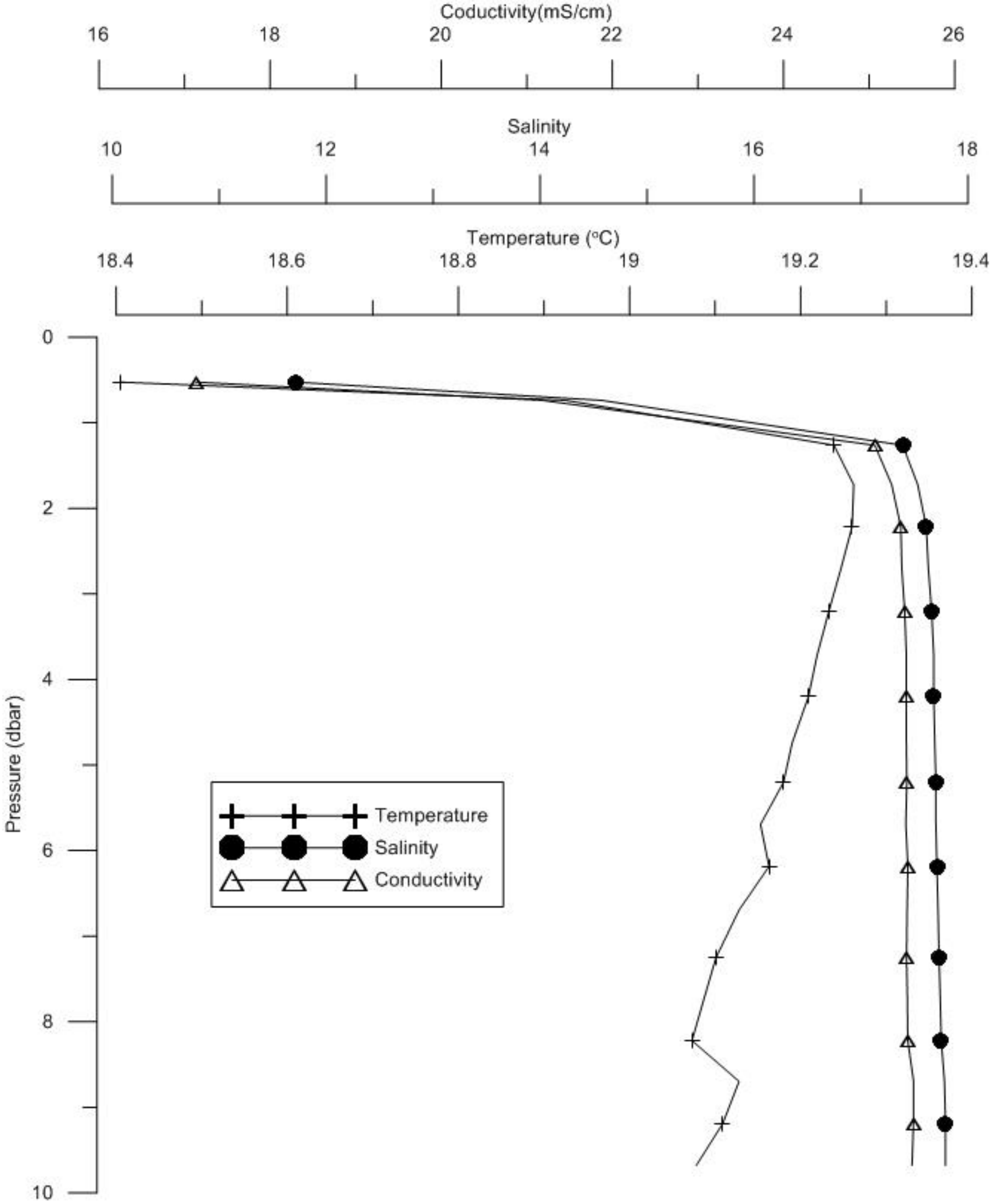

Figure 163.CTD from D11 Station for measurements in September2014

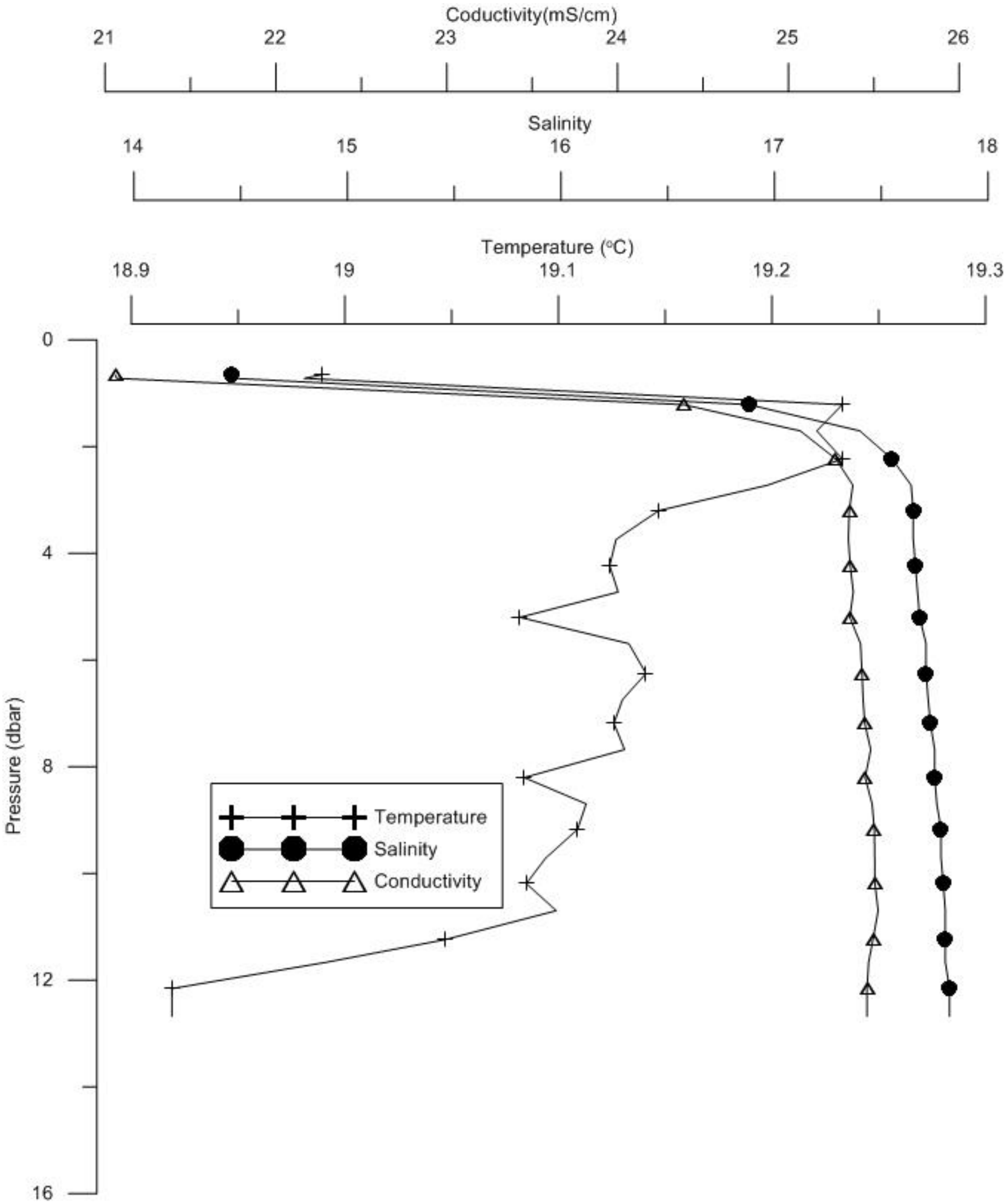

Figure 164.CTD from D12 Station for measurements in September2014

7. Heavy Metal Measurements

An orange peel bucket sampler (Picture 6) was used to collect sediment samples at stations . The stations were chosen so as to cover the metal pollution affected area. The samples were placed in polyethylene bags using a clean plastic spatula to prevent contamination. After collection, all samples were placed in refrigerator, and transported to the laboratory where they were stored at – 18 ˚C until being analyzed (Csuros and Csuros 2002). Prior to analysis, samples were dried at 45 ˚C. For general physical properties of the sediment around Trabzon harbor, sediment samples were sieved using distilled water in an AS 200 vibratory sieve shaker (Retsch, Germany). For metal analysis, sediment samples were sieved to pass <63 µm because metals exhibits usually a higher affinity to small grains (Morillo et al. 2004). Pore waters were separated from the sediment layers by centrifugation at 10,160 rcf x g for 30 min at +4 ˚C and filtered through 0.45 µm cellulose acetate membranes. Filtration and subsequent manipulation of the samples were carried out in a glove box under argon atmosphere in avoid alteration of the initial conditions (Santos-Echeandia et al. 2009). Pore water samples were acidified with suprapure HCL (pH < 2). The volume fraction of porosity (n) can be defined as the reaction of void space (V_V) relative to the apparent total bulk volume (V_T) of the sample. Porosity is described in percentage (Klobes et al. 2006).

$$n=(V_V/V_T)*100$$
(1)

Temperature, salinity, pH and oxygen were measured using a Hach Lange HQ40D multi meter. Metal concentrations were determined using an inductively coupled plasma-mass spectrometer (ICP-MS) analysis in ACME Lab., (Vancouer, BC. Canada). Results are given in Table 8.

Picture 6. Sediment grab and sediment sample

Table 8. Results of Sediment Analysis (i:Spring, k:Winter, y:Summer, s:Autum)

BUREAU VERITAS MINERAL LABORATORIES Canada

www.bureauveritas.com/um

Bureau Veritas Commodities Canada Ltd.
9050 Shaughnessy St Vancouver BC V6P 6E5 CANADA
PHONE (604) 253-3158

Client: **Karadeniz Teknik Universitesi**
Surmene Deniz Bilimleri Fakultesi
Camburnu TRABZON 61530 TURKEY

Project: TR09C1.01-02/298
Report Date: July 27, 2015

Page: 2 of 2 Part: 1 of 2

CERTIFICATE OF ANALYSIS ANK15000545.1

	Method	AQ201	AQ201	AQ201	AQ201	AQ201	AQ201	AQ201	AQ201	AQ201	AQ201	AQ201	AQ201	AQ201	AQ201	AQ201	AQ201	AQ201	AQ201	AQ201	AQ201
	Analyte	Mo	Cu	Pb	Zn	Ag	Ni	Co	Mn	Fe	As	Au	Th	Sr	Cd	Sb	Bi	V	Ca	P	La
	Unit	ppm	ppm	ppm	ppm	ppm	ppm	ppm	ppm	%	ppm	ppb	ppm	ppm	ppm	ppm	ppm	ppm	%	%	ppm
	MDL	0.1	0.1	0.1	1	0.1	0.1	0.1	1	0.01	0.5	0.5	0.1	1	0.1	0.1	0.1	2	0.01	0.001	1
D1i	Rock Chip	1.0	112.4	160.5	335	0.4	30.4	18.4	868	4.21	12.1	21.3	6.4	160	1.4	0.7	0.9	85	3.51	0.132	32
D3i	Rock Chip	0.9	115.2	163.4	331	0.4	29.9	18.2	871	4.19	12.6	20.9	6.5	157	1.4	0.7	1.0	84	3.50	0.129	32
D5i	Rock Chip	1.0	61.8	43.2	129	0.1	22.7	17.7	997	4.28	10.7	25.8	5.0	95	0.4	0.5	0.6	94	3.72	0.104	23
D6i	Rock Chip	1.0	112.0	148.3	330	0.3	29.2	18.0	868	4.24	12.3	18.4	6.4	156	1.4	0.6	1.0	85	3.54	0.128	30
D10i	Rock Chip	0.9	105.5	140.1	302	0.4	31.5	19.2	893	4.25	11.9	16.5	6.4	159	1.6	0.6	0.9	90	3.38	0.130	31
D12i	Rock Chip	0.8	125.7	195.7	456	0.4	36.8	21.9	805	4.64	13.2	20.7	6.0	143	2.3	0.7	1.0	101	3.23	0.123	28
D1k	Rock Chip	1.0	67.5	47.0	135	0.2	26.4	19.1	977	4.38	12.7	17.1	5.4	129	0.5	0.4	0.6	94	3.50	0.120	27
D3k	Rock Chip	1.0	69.0	44.3	139	0.1	25.8	17.7	826	4.06	11.4	12.8	5.3	125	0.4	0.4	0.6	84	3.06	0.112	26
D5k	Rock Chip	0.9	67.4	42.3	129	0.1	26.2	18.9	965	4.25	12.7	15.4	5.1	124	0.4	0.4	0.5	87	3.52	0.108	27
D6k	Rock Chip	1.2	58.8	47.4	152	0.1	20.4	16.5	835	4.28	10.1	5.0	5.7	135	0.4	0.5	0.7	106	3.73	0.160	27
D10k	Rock Chip	1.1	98.1	111.2	293	0.3	31.6	19.9	852	4.38	12.3	14.8	5.9	136	1.3	0.4	0.8	91	3.05	0.119	28
D12k	Rock Chip	0.8	128.4	169.1	434	0.4	34.2	20.5	855	4.48	12.6	14.7	6.0	143	2.0	0.5	0.9	90	3.05	0.115	29
D1y	Rock Chip	1.2	76.6	65.9	224	0.2	29.6	20.3	871	4.87	10.8	12.2	5.8	164	0.8	0.4	0.7	124	3.69	0.180	31
D3y	Rock Chip	1.3	66.8	45.2	164	0.2	28.7	18.6	805	4.65	9.8	14.6	6.5	180	0.9	0.4	0.5	121	3.67	0.187	34
D5y	Rock Chip	0.8	76.2	42.7	143	0.2	33.3	19.3	707	4.50	9.6	26.1	7.2	179	0.5	0.3	0.5	114	3.12	0.171	36
D6y	Rock Chip	0.9	67.3	42.6	138	0.2	30.4	19.1	766	4.40	9.3	32.7	6.1	155	0.4	0.4	0.5	103	3.28	0.144	30
D10y	Rock Chip	0.9	73.4	43.0	141	0.2	33.5	20.4	707	4.46	9.7	37.1	6.8	178	0.4	0.3	0.5	111	3.12	0.160	34
D12y	Rock Chip	0.7	86.5	74.0	180	0.2	35.9	21.5	799	4.31	11.3	7.7	5.5	146	0.6	0.4	0.6	96	3.13	0.116	26
D1s	Rock Chip	1.0	60.5	42.9	121	0.2	28.6	17.7	697	3.91	11.1	13.7	5.0	124	0.4	0.4	0.5	86	3.27	0.108	24
D3s	Rock Chip	1.5	82.6	55.3	199	0.2	30.6	21.3	1154	5.58	13.8	3.7	5.8	130	0.6	0.6	0.7	137	3.59	0.135	29
D5s	Rock Chip	0.9	62.6	38.8	128	0.1	22.7	17.8	1024	4.08	11.9	2.8	4.4	109	0.4	0.3	0.5	83	3.50	0.107	24
D6s	Rock Chip	1.4	71.2	50.7	168	0.2	26.9	20.1	1050	5.29	12.7	1.5	5.5	121	0.4	0.6	0.8	128	3.59	0.148	29
D10s	Rock Chip	1.0	68.2	43.6	156	0.1	25.1	19.9	1081	4.26	13.4	113.3	4.6	122	0.4	0.6	0.6	89	3.57	0.112	26
D12s	Rock Chip	0.8	109.8	100.4	272	0.3	33.5	19.5	808	4.35	11.4	14.5	5.6	134	1.0	0.4	0.8	88	2.98	0.125	28

Clean ports - open doors

BUREAU VERITAS MINERAL LABORATORIES Canada

www.bureauveritas.com/um

Bureau Veritas Commodities Canada Ltd.

9050 Shaughnessy St Vancouver BC V6P 6E5 CANADA
PHONE (604) 253-3158

Client: Karadeniz Teknik Universitesi
Surmene Deniz Bilimleri Fakultesi
Camburnu TRABZON 61530 TURKEY

Project: TR09C1.01-02/298
Report Date: July 27, 2015

CERTIFICATE OF ANALYSIS ANK15000545.1

	Method	AQ201	AQ201	AQ201	AQ201	AQ201	AQ201	AQ201	AQ201	AQ201	AQ201	AQ201	AQ201	AQ201	AQ201	AQ201	AQ201
	Analyte	Cr	Mg	Ba	Ti	B	Al	Na	K	W	Hg	Sc	Tl	S	Ga	Se	Te
	Unit	ppm	%	ppm	%	ppm	%	%	%	ppm	ppm	ppm	ppm	%	ppm	ppm	ppm
	MDL	1	0.01	1	0.001	1	0.01	0.001	0.01	0.1	0.01	0.1	0.1	0.05	1	0.5	0.2
D1i	Rock Chip	37	1.66	318	0.093	13	3.49	0.798	0.40	<0.1	0.16	10.8	0.1	0.20	8	<0.5	<0.2
D3i	Rock Chip	35	1.65	334	0.090	11	3.43	0.733	0.40	<0.1	0.22	10.8	0.1	0.19	8	<0.5	<0.2
D5i	Rock Chip	28	1.67	119	0.096	9	3.06	0.490	0.31	<0.1	0.16	10.7	<0.1	0.08	8	<0.5	<0.2
D6i	Rock Chip	35	1.67	348	0.094	16	3.51	1.001	0.43	<0.1	0.16	11.1	0.1	0.23	8	<0.5	<0.2
D10i	Rock Chip	41	1.67	320	0.100	18	3.44	1.249	0.43	<0.1	0.12	10.8	0.1	0.22	9	0.5	<0.2
D12i	Rock Chip	46	1.83	180	0.113	16	3.45	0.846	0.40	<0.1	0.15	11.8	0.1	0.25	9	0.7	<0.2
D1k	Rock Chip	30	1.62	140	0.091	14	3.23	1.138	0.37	<0.1	0.11	11.1	<0.1	0.15	8	0.5	<0.2
D3k	Rock Chip	28	1.61	134	0.086	11	3.32	0.726	0.34	<0.1	0.07	11.0	0.1	0.16	8	<0.5	<0.2
D5k	Rock Chip	28	1.62	131	0.079	10	3.35	0.891	0.37	<0.1	0.05	11.4	<0.1	0.14	8	0.7	<0.2
D6k	Rock Chip	29	1.48	153	0.115	10	2.70	0.642	0.29	0.1	0.05	8.9	<0.1	0.14	7	<0.5	<0.2
D10k	Rock Chip	38	1.73	157	0.095	21	3.47	1.279	0.41	<0.1	0.10	11.4	0.1	0.21	8	0.6	<0.2
D12k	Rock Chip	40	1.80	167	0.096	19	3.50	1.386	0.44	<0.1	0.10	11.9	0.2	0.27	9	0.5	<0.2
D1y	Rock Chip	40	1.55	191	0.131	11	2.85	0.724	0.31	0.1	0.07	9.4	0.1	0.21	8	<0.5	<0.2
D3y	Rock Chip	43	1.50	179	0.130	12	3.04	0.965	0.36	<0.1	0.08	10.0	<0.1	0.17	8	<0.5	<0.2
D5y	Rock Chip	49	1.58	174	0.117	12	3.52	0.827	0.42	<0.1	0.08	11.5	<0.1	0.15	9	0.5	<0.2
D6y	Rock Chip	43	1.58	153	0.111	13	3.25	0.860	0.38	<0.1	0.08	11.4	<0.1	0.14	8	0.5	<0.2
D10y	Rock Chip	48	1.61	164	0.118	15	3.54	1.152	0.43	<0.1	0.07	11.5	<0.1	0.16	9	<0.5	<0.2
D12y	Rock Chip	39	1.71	177	0.115	11	3.20	0.644	0.36	<0.1	0.08	11.2	0.2	0.25	8	<0.5	<0.2
D1s	Rock Chip	34	1.67	120	0.098	15	3.04	1.245	0.35	<0.1	0.07	10.6	<0.1	0.29	8	<0.5	<0.2
D3s	Rock Chip	40	1.57	178	0.149	14	3.07	0.663	0.36	0.2	0.16	11.3	0.1	0.16	10	<0.5	<0.2
D5s	Rock Chip	25	1.62	116	0.077	11	3.11	1.196	0.34	<0.1	0.04	10.7	<0.1	0.14	9	<0.5	<0.2
D6s	Rock Chip	36	1.58	161	0.139	14	2.96	0.856	0.34	0.1	0.10	11.2	0.1	0.16	9	<0.5	<0.2
D10s	Rock Chip	30	1.63	139	0.103	21	3.11	2.011	0.44	0.1	0.17	11.4	<0.1	0.18	9	<0.5	<0.2
D12s	Rock Chip	39	1.76	142	0.093	14	3.38	0.987	0.39	<0.1	0.12	11.3	0.1	0.22	8	<0.5	<0.2

MINERAL LABORATORIES Canada

www.bureauveritas.com/um

Bureau Veritas Commodities Canada Ltd.

9050 Shaughnessy St Vancouver BC V6P 6E5 CANADA
PHONE (604) 253-3158

Client: Karadeniz Teknik Universitesi
Surmene Deniz Bilimleri Fakultesi
Camburnu TRABZON 61530 TURKEY

Project: TR09C1.01-02/298
Report Date: July 27, 2015

QUALITY CONTROL REPORT ANK15000545.1

	Method	AQ201	AQ201	AQ201	AQ201	AQ201	AQ201	AQ201	AQ201	AQ201	AQ201	AQ201	AQ201	AQ201	AQ201	AQ201	AQ201	AQ201	AQ201	AQ201	AQ201
	Analyte	Mo	Cu	Pb	Zn	Ag	Ni	Co	Mn	Fe	As	Au	Th	Sr	Cd	Sb	Bi	V	Ca	P	La
	Unit	ppm	ppm	ppm	ppm	ppm	ppm	ppm	ppm	%	ppm	ppb	ppm	ppm	ppm	ppm	ppm	ppm	%	%	ppm
	MDL	0.1	0.1	0.1	1	0.1	0.1	0.1	1	0.01	0.5	0.5	0.1	1	0.1	0.1	0.1	2	0.01	0.001	1
Reference Materials																					
STD DS10	Standard	15.0	158.7	144.9	373	2.0	75.7	13.9	891	2.87	46.6	99.2	7.7	68	3.0	9.3	12.6	45	1.10	0.078	19
STD OXC129	Standard	1.4	30.8	6.3	44	<0.1	80.3	21.7	436	3.18	0.6	175.1	1.9	193	<0.1	<0.1	<0.1	55	0.74	0.104	13
STD DS10 Expected		14.69	154.61	150.55	370	2.02	74.6	12.9	875	2.7188	43.7	91.9	7.5	67.1	2.49	8.23	11.65	43	1.0625	0.073	17.5
STD OXC129 Expected		1.3	28	6.3	42.9		79.5	20.3	421	3.065	0.6	195	1.9					51	0.665	0.102	13
BLK	Blank	<0.1	<0.1	<0.1	<1	<0.1	<0.1	<0.1	<1	<0.01	<0.5	<0.5	<0.1	<1	<0.1	<0.1	<0.1	<2	<0.01	<0.001	<1
Prep Wash																					
QUARTZ_ANK	Prep Blank	5.7	14.1	0.4	2	<0.1	5.7	0.6	33	0.38	0.6	0.9	0.2	<1	<0.1	0.2	<0.1	<2	<0.01	0.002	<1
QUARTZ_ANK	Prep Blank	5.8	14.0	0.3	1	<0.1	5.5	0.5	31	0.40	0.5	<0.5	0.2	<1	<0.1	0.1	<0.1	<2	<0.01	0.002	<1

Programme co-funded by the EUROPEAN UNION

Clean ports - open doors

Black Sea CROSS BORDER COOPERATION

BUREAU VERITAS MINERAL LABORATORIES Canada

www.bureauveritas.com/um

Bureau Veritas Commodities Canada Ltd.
9050 Shaughnessy St Vancouver BC V6P 6E5 CANADA
PHONE (604) 253-3158

Client: Karadeniz Teknik Universitesi
Surmene Deniz Bilimleri Fakultesi
Camburnu TRABZON 61530 TURKEY

Project: TR09C1.01-02/298
Report Date: July 27, 2015

QUALITY CONTROL REPORT ANK15000545.1

	Method	AQ201	AQ201	AQ201	AQ201	AQ201	AQ201	AQ201	AQ201	AQ201	AQ201	AQ201	AQ201	AQ201	AQ201	AQ201	AQ201
	Analyte	Cr	Mg	Ba	Ti	B	Al	Na	K	W	Hg	Sc	Tl	S	Ga	Se	Te
	Unit	ppm	%	ppm	%	ppm	%	%	%	ppm	ppm	ppm	ppm	%	ppm	ppm	ppm
	MDL	1	0.01	1	0.001	1	0.01	0.001	0.01	0.1	0.01	0.1	0.1	0.05	1	0.5	0.2
Reference Materials																	
STD DS10	Standard	58	0.79	352	0.091	7	1.10	0.073	0.35	3.2	0.28	3.3	5.1	0.28	5	2.3	4.9
STD OXC129	Standard	53	1.62	53	0.407	1	1.66	0.605	0.36	<0.1	<0.01	1.1	<0.1	<0.05	6	<0.5	<0.2
STD DS10 Expected		54.6	0.775	359	0.0817		1.0259	0.067	0.338	3.32	0.3	2.8	5.1	0.29	4.3	2.3	5.01
STD OXC129 Expected		52	1.545	50	0.4	1	1.58	0.6	0.37			1.1			5.6		
BLK	Blank	<1	<0.01	<1	<0.001	<1	<0.01	<0.001	<0.01	<0.1	<0.01	<0.1	<0.1	<0.05	<1	<0.5	<0.2
Prep Wash																	
QUARTZ_ANK	Prep Blank	37	0.01	5	0.001	<1	0.03	0.003	<0.01	0.1	0.05	0.2	<0.1	<0.05	<1	<0.5	<0.2
QUARTZ_ANK	Prep Blank	36	0.01	5	<0.001	<1	0.03	0.002	<0.01	0.1	0.01	0.2	<0.1	<0.05	<1	<0.5	<0.2

The sand fractions were generally dominant (>60 %) in the surface sediments. Also, values of porosity, pH, temperature, salinity and oxygen were ranged from 35.5 to 53 %, from 7.11 to 8.10, from 10.1 to 15.1 ˚C, from 14.46 to 17.64 ‰, from 6.08 to 8.50 mg/L, respectively (Table 9).

Table 9.General properties of sediment and pore water around Trabzon harbor

Physical properties							Chemical properties			
Area	Deepth (m)	Gravel (%)	Sand (%)	Clay (%)	Porosity (%)	Temperature (˚C)	Salinity (‰)	pH	Oxygen (%)	Oxygen (mg/L)
D1	34	1.3	75.59	23.11	41	13.4	17.62	7.57	68.4	7.05
D2	1.5	8.5	79.29	12.21	42	10.1	14.46	8.1	74.3	8.5
D3	15	2.7	88.40	8.90	35.5	14.2	17.57	7.45	72.6	7.38
D4	47	0.65	60.66	38.69	53	13.2	17.64	7.38	62.4	6.45
D5	10	1.1	84.75	14.15	36	14.8	17.54	7.34	73.3	7.35
D6	12	0.87	66.98	32.15	51	14.8	17.55	7.11	65.1	6.11
D7	11	0.95	64.89	34.16	51.5	15.1	17.55	7.12	64.3	6.08
D8	18	6.4	84.19	9.41	36.5	14.1	17.58	7.82	74.2	7.46
D9	24	7.1	84.20	8.70	36.5	13.8	17.6	7.74	73.8	7.44

Metal concentrations in sediments were varied from 22.3 to 83.7 µg g^{-1} for Cr, 54.3 to 246.8 µg g^{-1} for Cu, 67.2 to 253 µg g^{-1} for Zn, 50.1 to 117.3 µg g^{-1} for Pb, 23.4 to 98.7 µg g^{-1} for Ni, 12.3 to 52.6 µg g^{-1} for As. Metal concentrations in sediment pore water were varied from 4.14 to 12.41 µg kg^{-1} for Cr, 13.21 to 32.1 µg kg^{-1} for Cu, 22 to 44.75 µg kg^{-1} for Zn, 10.72 to 36.51 µg kg^{-1} for Pb, 3.72 to 14.1 µg kg^{-1} for Ni, 3.12 to 7.78 µg kg^{-1} for As. The highest metal concentrations were determined in D6 and D7 stations. Harbors are enclosed and low-energy water bodies. It was reported in the literature that accumulation is enhanced in enclosed and semi-enclosed areas (Pekey et al. 2004). Stations of D6 and D7 were in the inner harbor, water circulation was not well enough. Mean values of Cu, Zn, Pb and As in sediments were higher than the reference values (WASW, CCV, TRV), whereas the mean values of Cr and Ni were less than reference values (Turekian and Wedepohl 1961; Taylor 1964; US EPA 1999). Mean values of Cu and Pb in sediment pore water were higher than reference value (WQC), whereas the mean values of Cr, Zn, Ni and As less than reference value (US EPA 2006) (Table 10).

According to the Sediment Quality Guideline (SQG) proposed by US EPA, sediment was classified into three classes, non-polluted, moderately polluted and heavily polluted (Pekey et al. 2004). The average metal values of stations were compared with the SQG (Table 10). According to this classification, Cr, Zn and Ni were determined as moderately polluted. But, Cu, Pb and As were determined as heavily polluted. Metal concentrations in sediment were evaluated by comparing to numerical SOG which is known as the effect range low (ERL) and effect range median (ERM), the threshold effect level (TEL) and probable effect level (PEL) values (Long et al. 1998). Low-range values (i.e., ERL or TEL) are concentrations less than those expected not to cause adverse effects in sediment dwelling fauna. In contrast, the ERM and PEL represent chemical concentrations above which adverse effects are likely to occur (Pekey et al. 2004). Concentrations of Cu, Pb, Ni and As were over TEL and ERL value in the investigated region. But, Concentrations of

Cu, Pb, Ni and As were below ERM and PEL value in investigated region. Concentration of Cr was below TEL, ERL, ERM and PEL value in the investigated region (Table 10).

Table 10.Metal content of surface sediments (μg g^{-1}) and pore water (μg kg^{-1}) around Trabzon harbor and its comparisons with reference values

Present study			Referance value				SQG[e]			
Metal	Pore water	Sediment	WQC[a]	WASV[b]	CCV[c]	TRV[d]	ERL	ERM	TEL	PEL
Cr	7.48±2.85	40.12±24.00	74.0	90.0	100	26.0	81.0	370.0	52.3	160.0
Cu	17.92±6.44	104.17±80.03	9.0	45.0	55	16.0	34.0	270.0	18.7	108.2
Zn	30.92±7.99	145.24±67.20	120.0	95.0	70	110.0	150.0	410.0	124.0	271.0
Pb	22.28±7.05	70.58±27.41	2.5	20.0	12.5	31.0	46.7	218.0	30.2	112.2
Ni	8.96±3.37	42.23±29.98	52.0	68.0	75	16.0	20.9	51.6	15.9	42.8
As	4.93±1.44	24.19±17.32	150.0	13.0	1.8	6.0	8.2	70.0	7.2	41.6

SQG (US EPA)

	Cr	Cu	Zn	Pb	Ni	As
Non-polluted	< 25	< 25	< 90	< 40	< 20	< 3
Moderately polluted	25-75	25-50	90-200	40-60	20-50	3-8
Heavily polluted	> 75	> 50	> 200	> 60	> 50	> 8

WQC Pore water chemistry, WASV worldwide average shale value, CCV continental crust values, TRV toxicity reference values, SOG sediment quality guideline, ERL effect range low, ERM effect range median, TEL threshold effect level
PEL probable effect level, [a]US EPA (2006), [b]Turekian and Wedepohl (1961), [c]Taylor (1964), [d]US EPA (1999), [e]Long et al. (1998)

Spearman's rank correlation was used to determine relationship between the metal values in sediment and sediment pore water. As a result of Spearman's rank correlation, there is a meaningful correlation between Cr, Zn and Pb variables for $p<0.05$, but there is no meaningful correlation with the other variables. Factor analysis used to varimax rotation method was performed on metal values (sediment and sediment pore water) and environmental parameters. In this analysis, three components were extracted which explained about 93.5 % of the total variance, with the first component accounting for 53.7 %, the second component for 21.2 % and the third component for 18.7 %. The first component, except for Ni in sediment pore water, includes eleven variables for metal both sediment (Cr, Cu, Zn, Pb, Ni and As) and sediment pore water (Cr, Cu, Zn, Pb and As). These eleven metals in the first component may represent anthropogenic sources, because waste water of mining has a high amount of metals. The first factor's elements (Zn and Pb) have been associated with motor vehicle emissions. Besides, Cu, Pb and Zn are probably associated discharge of sewage, industrial inputs, and surface runoff in the urban environment (Tang et al. 2008). The second component has been associated with oxygen and the third component has been associated with temperature and salinity. Environmental parameters such as temperature, salinity, dissolved oxygen and pH may influence water chemistry and metal solubility (Fritioff et al. 2005).

When the stations were examined according to potential ecological risk index, the highest values were found stations of D6 and D7 (Table 11). But, according to Indices and classification of potential ecological metals contamination, the results of metal values were determined as low risk at all study area.

Table 11. Potential ecological risk of metal values according to stations

Metal	E_r^1	E_r^2	E_r^3	E_r^4	E_r^5	E_r^6	E_r^7	E_r^8	E_r^9	RI
Cr	0.50	0.60	0.54	0.75	0.74	1.68	1.86	0.63	0.73	8.03
Cu	5.43	6.24	6.57	7.12	7.30	24.68	23.43	7.52	5.46	93.75
Zn	0.64	0.38	0.71	0.77	0.81	1.45	1.42	0.62	0.66	7.46
Pb	3.60	3.58	4.10	4.65	4.92	8.26	8.38	4.00	3.88	45.37
Ni	3.14	2.92	3.21	3.90	4.23	12.33	10.59	3.66	3.56	47.54
As	9.40	8.20	11.13	13.40	12.60	36.33	35.10	10.10	8.93	145.19

8. Current Measurements and Modelling

8.1. Current measurements

Current measurement results were given for 4 different levels: Surface, maximum depth and two intermediate levels. Current speeds and directions for the first measurements were given as an example in the following graphs.

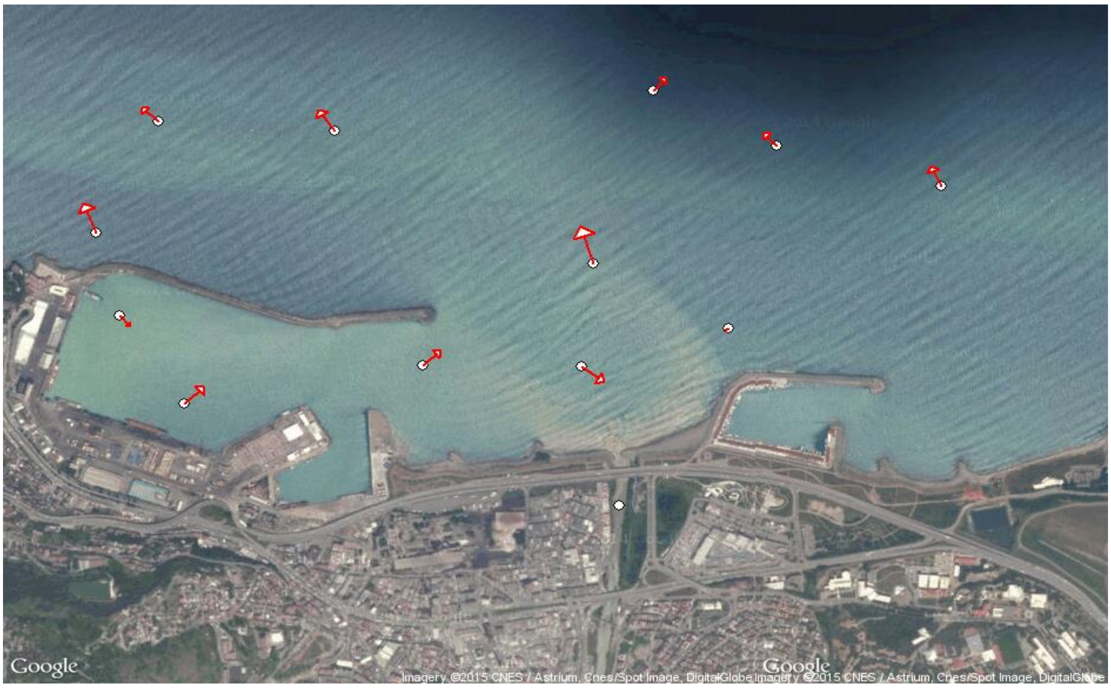

Figure 165. Surface current speed and directions for the first measurements

Figure 166. Level 1 current speed and directions for the first measurements

Figure 167. Level 2 current speed and directions for the first measurements

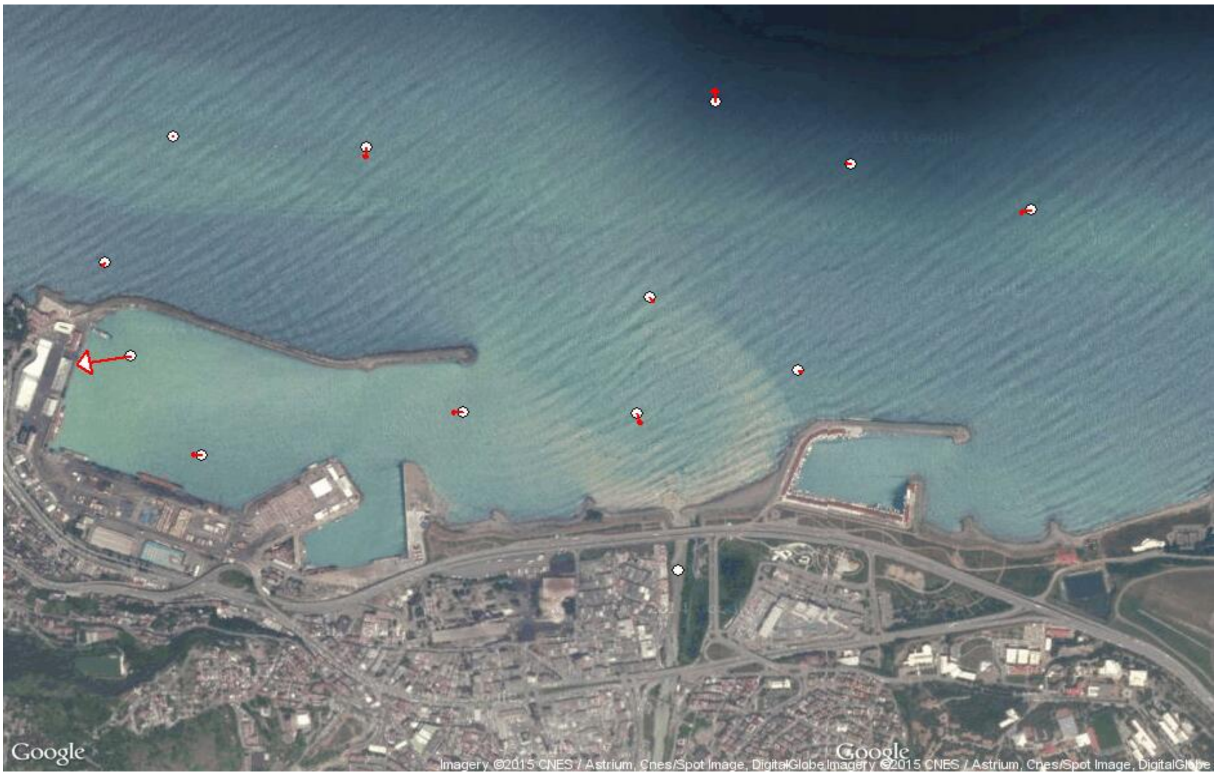

Figure 168. Deep current speed and directions for the first measurements

8.2. Hydrodynamic Modelling

The hydrodynamic modeling was developed based on POMSED model Princeton Ocean Model to simulate current speed, direction and sediment distribution by using. The principal attributes of the model are as follows:

- ✓ It contains an imbedded second momentturbulence closure sub-model to provide vertical mixing coefficients.
- ✓ It is a sigma coordinate model in that the vertical coordinate is scaled on the water column depth.
- ✓ The horizontal grid uses curvilinear orthogonal coordinates and an "Arakawa C" differencing scheme.
- ✓ The horizontal time differencing is explicit whereas the vertical differencing is implicit. The latter eliminates time constraints for the vertical coordinate and permits the use of fine vertical resolution in the surface and bottom boundary layers.
- ✓ The model has a free surface and a split time step. The external mode portion of the model is two dimensional and uses a short time step based on the CFL condition and the external wave speed. The internal mode isthree-dimensional and uses a long time step based on the CFL condition and the internal wave speed.
- ✓ Complete thermodynamics have been implemented.

The turbulence closure sub-model is introduced by Mellor, 1973 and then was significantly advanced in collaboration with Tetsuji Yamada (Mellor and Yamada,1974; Mellor and Yamada,1982).

8.2.1. The Basic Equations

Sigma coordinate system has been used for the basic equation. This coordinate system is a bottom following Phillips (1957) or Blumberg and Mellor (1980,1987),

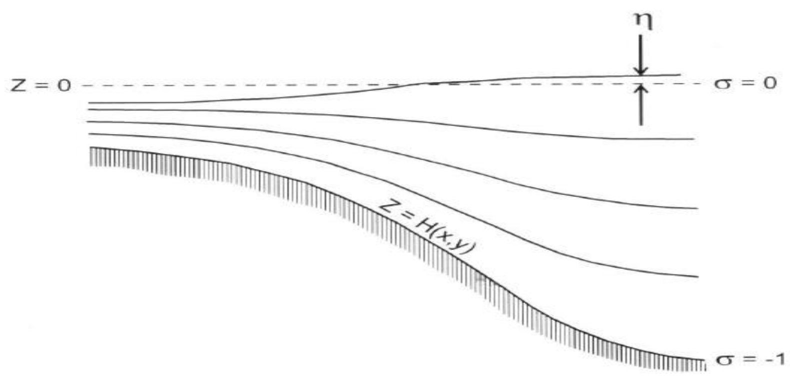

Figure 169. Sigma coordinate sistem

If internaland external conservative equations is translated from (x,y,z,t) coordinate system to (x^*,y^*, σ,t^*) coordinate system,

$x^* = x\ ,\ y^* = y\ ,\ \sigma = \frac{z-\eta}{H+\eta}\ ,\ t^* = t\ , D \equiv H + \eta$ and chain rule implemented ,

where

x,y,z are the conventional Cartesian coordinates;

D = *H* + *n* where *H* (x, *y*) is the bottom topography

n(x, y, t) is the surface elevation.

Thus, arranges from σ = 0 at z = *n* to σ = -1 at z = -H. After conversion to sigma coordinates and delete of the asterisks, the basic equations may be written (in horizontal Cartesian coordinates),

$$\frac{\partial G}{\partial x} = \frac{\partial G}{\partial x^*} - \frac{\partial G}{\partial \sigma}\left(\frac{\sigma}{D}\frac{\partial D}{\partial x^*} + \frac{1}{D}\frac{\partial \eta}{\partial x^*}\right)$$

$$\frac{\partial G}{\partial y} = \frac{\partial G}{\partial y^*} - \frac{\partial G}{\partial \sigma}\left(\frac{\sigma}{D}\frac{\partial D}{\partial y^*} + \frac{1}{D}\frac{\partial \eta}{\partial y^*}\right)$$

$$\frac{\partial G}{\partial z} = \frac{1}{D}\frac{\partial G}{\partial \sigma}$$

$$\frac{\partial G}{\partial t} = \frac{\partial G}{\partial t^*} - \frac{\partial G}{\partial \sigma}(\frac{\sigma}{D}\frac{\partial D}{\partial t^*} + \frac{1}{D}\frac{\partial \eta}{\partial t^*})$$

where$G$ is an arbitrary area and $z = \eta$ for $\sigma = 0$and $z = -H$ for $\sigma = -1$

vertical speed**:** $\omega \equiv w - U\omega\sigma\frac{\partial D}{\partial x^*} + \frac{\partial \eta}{\partial x^*} - V\sigma\frac{\partial D}{\partial y^*} + \frac{\partial \eta}{\partial y^*} - (\sigma\frac{\partial D}{\partial t^*} + \frac{\partial \eta}{\partial t^*})$

.Boundary conditions **:**

$$\omega(x^*, y^*, 0, t^*) = 0 \ , \qquad \omega(x^*, y^*, -1, t^*) = 0$$

8.2.2. 3-D Advection-Dispersion Equation for Sediment Transportation

$$\frac{\partial C_k}{\partial t} + \frac{\partial U C_K}{\partial x} + \frac{\partial V C_K}{\partial y} + \frac{\partial (W - W_{S,K}) C_K}{\partial z} = \frac{\partial}{\partial x}\left(A_H \frac{\partial C_k}{\partial x}\right) + \frac{\partial}{\partial y}\left(A_H \frac{\partial C_k}{\partial y}\right) + \frac{\partial}{\partial z}\left(K_H \frac{\partial C_k}{\partial z}\right)$$

Where,

U, V, W : 3-D velocity vectors

C_K : Sediment consantration

$W_{S,K}$: Settlement speed

A_H :Horizontal diffusion

K_H : Vertical vorteksdiffusion

Boundary conditions :

$$K_H \frac{\partial C_k}{\partial z} = 0 \ , z \rightarrow \eta$$

$$K_H \frac{\partial C_k}{\partial z} = E_k - D_K \ , z \rightarrow -H$$

E_k: Suspended sediment flux (resuspension)

D_K:Settling flux rate

η : Depth (distance from sea surface)

H :Distance from sea bed

8.2.3. Settlement of Cohesive Sediments

Settlement rate of cohesive sediments depends on the settlement flux rate and their size. According to KRONE, settlement of sediments are as follows**:**

$$D_{1=-W_{s,1}C_1P_1}$$

$$P_1 = 1 - \frac{1}{\sqrt{2\pi}}\int_{-\infty}^{Y} e^{-\frac{\omega^2}{2}} d\omega$$

$$Y = 2.04\log\left[0.25\left(\frac{\tau_b}{\tau_{b,min}} - 1\right)e^{1.07\tau_{b,min}}\right]$$

where,

D_1 : Settlement flux rate

$W_{s,1}$:Settlement speed of the cohesive sediment

C_1 : Concentration of cohesive suspended sediment

P_1 :Probability of settlement

8.2.4. Re-suspension of Cohesive Sediment

Amount of sediment re-suspends are given with the following formula

$$\varepsilon = \frac{a_0}{T_d^m}\left(\frac{\tau_b - \tau_c}{\tau_c}\right)^n$$

where,

ε:re-suspension potential

a_0:constant depends on source

T_d:time after deposition

τ_b:shear stress of the bed

τ_c:critical shear stress

m, n :constants depends on environment

8.2.5. Calculation of critical speed

D_*:Non dimensional parameter for motion

$$D_* = \left[\frac{(s-1)g}{\nu^2}\right]^{\frac{1}{3}} D_{50}$$

where,

s:specific gravity

g:acceleration of gravity

ν: Kinematic viscosity

D_{50}:diameter of sediment

According to Shields criteria, critical sliding speed for resuspension is calculated as follows:

$$U_{*,crbed} = [(s-1)gD_{50}\theta_{cr}]^{\frac{1}{2}}$$

θ_{cr}can be calculated as follows;

$$\theta = 0.24\ D_*^{-1} D_* \leq 4$$

$$\theta_{cr} = 0.14 D_*^{-0.64} 40 < D_* \leq 10$$

$$\theta_{cr} = 0.04 D_*^{-0.10} 10 < D_* \leq 20$$

$$\theta_{cr} = 0.13 D_*^{-0.29} 20 < D_* \leq 150$$

$$\theta_{cr} = 0.055 D_* > 150$$

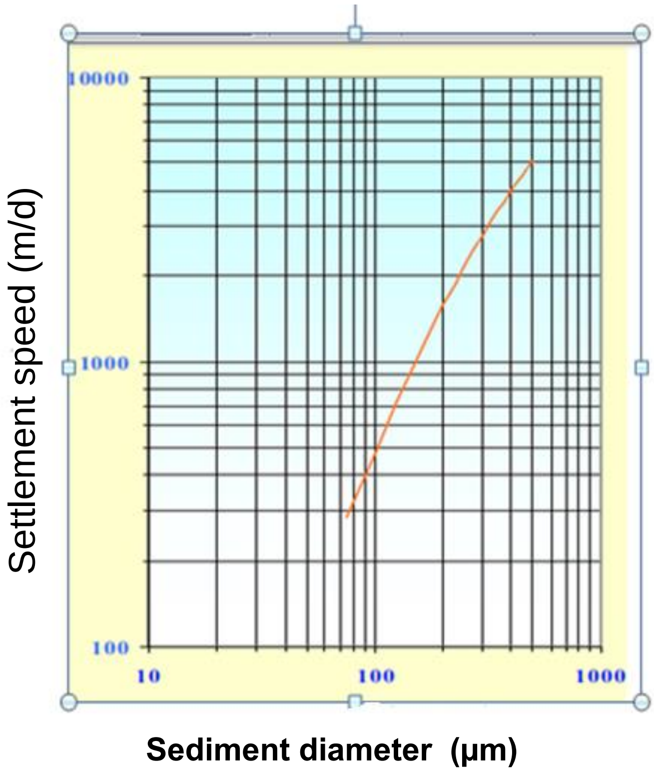

Figure 170. Sediment diameter and settlement speed

8.2.6. Re-suspension of Non- Cohesive Sediment

$$E = \frac{(sq_s - qzC_z)\Delta t}{\Delta x \Delta y}$$

where,

C_z: Sediment concentration at minimum sigma level

Δt:time step

$\Delta x \Delta y$:Surface area

$$D_2 = W_{s,2} C_2$$

where,

D_2:Settlement flux rate of non-cohesive sediments

$W_{s,2}$:Settlement speed

C_2:suspended sediment concentrationnear-bed

8.3. Results of Current Measurements and Hydrodynamic Model

Insitu current measurements for each measurements were given for 4 different depths (Surface, bottom, and 2 intermediate levels) and hydrodynamic model results for the same depths are calculated and results were given in the following graphs.

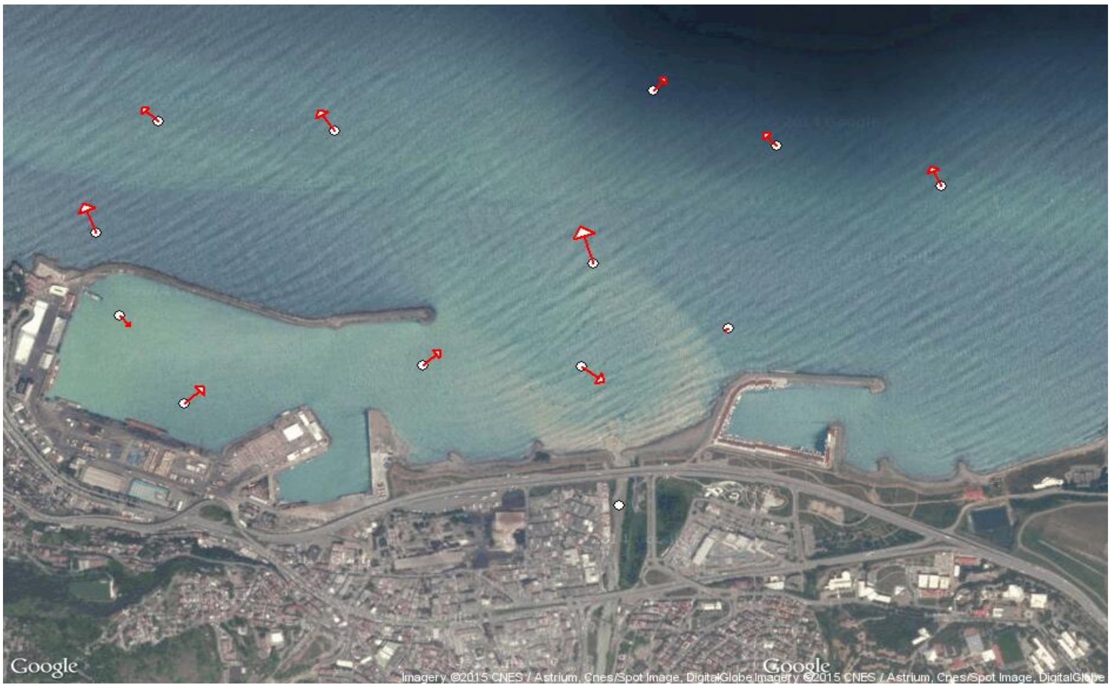

Figure 171. Surface current speed and directions for December2014 measurements

Figure 172. Level 1 current speed and directions for December2014 measurements

Figure 173. Level 2 current speed and directions for December2014 measurements

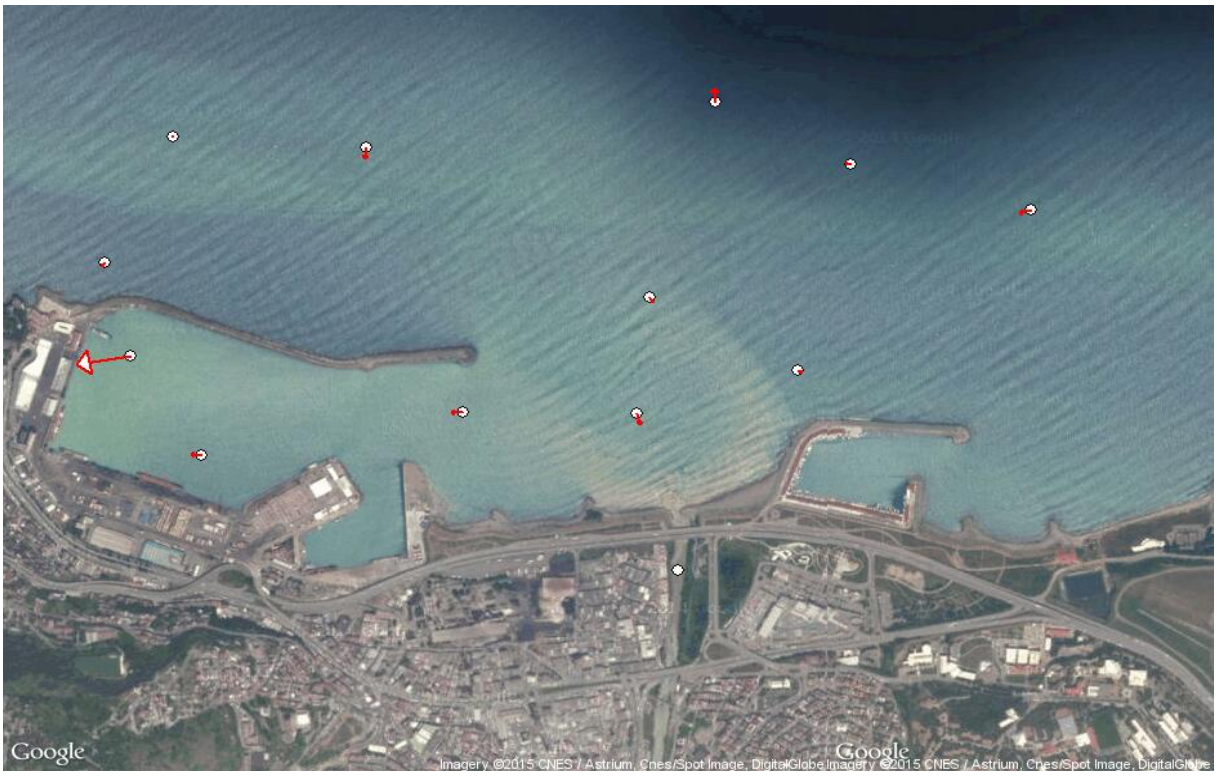

Figure 174. Bottom current speed and directions for December2014 measurements

Current speed and direction modelling results of these modellings for December 2014are given in the following graphs.

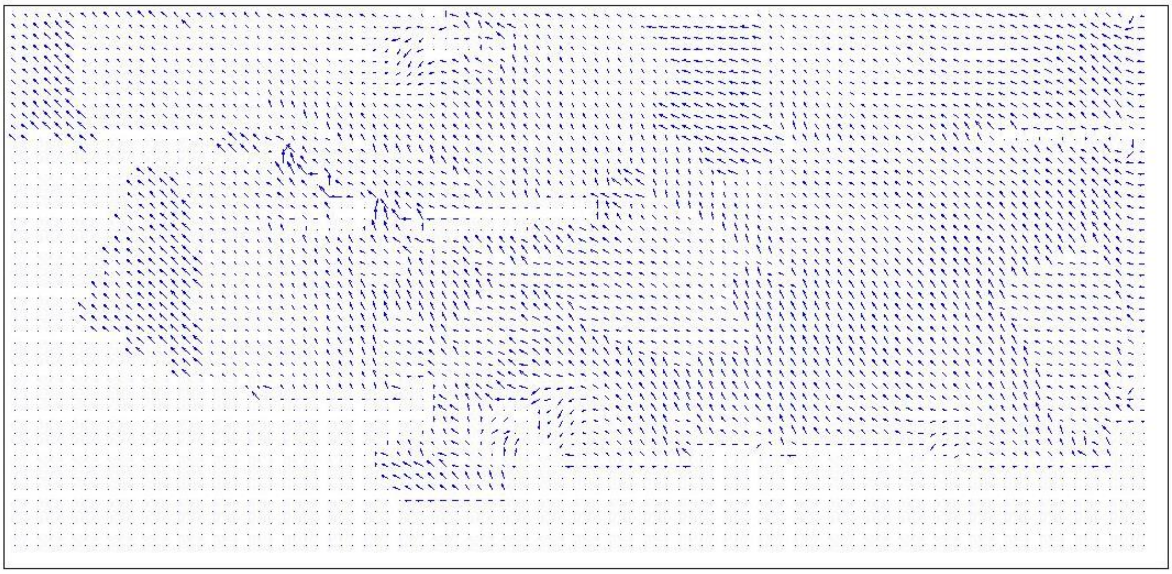

Figure 175. Modelling of the Current speed and direction at surface for December 2014

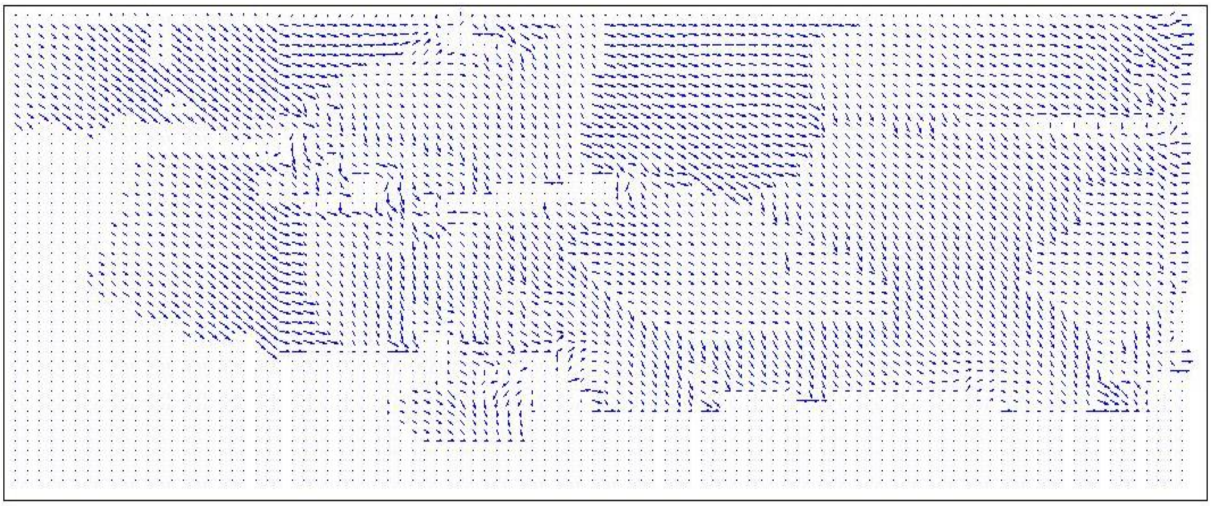

Figure 176. Modelling of the Current speed and direction at level 1for December 2014

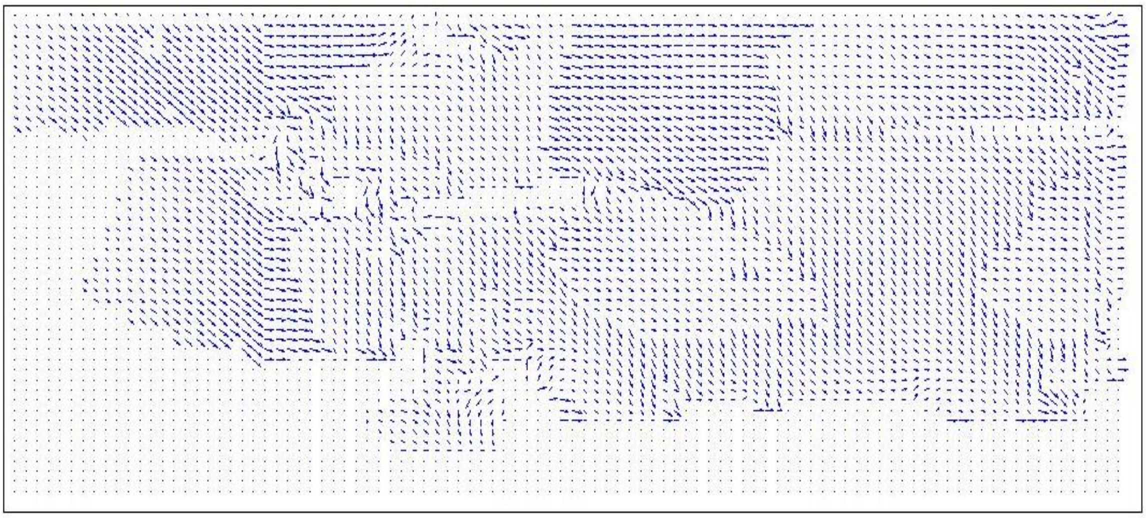

Figure 177. Modelling of the Current speed and direction at level 2 for December 2014

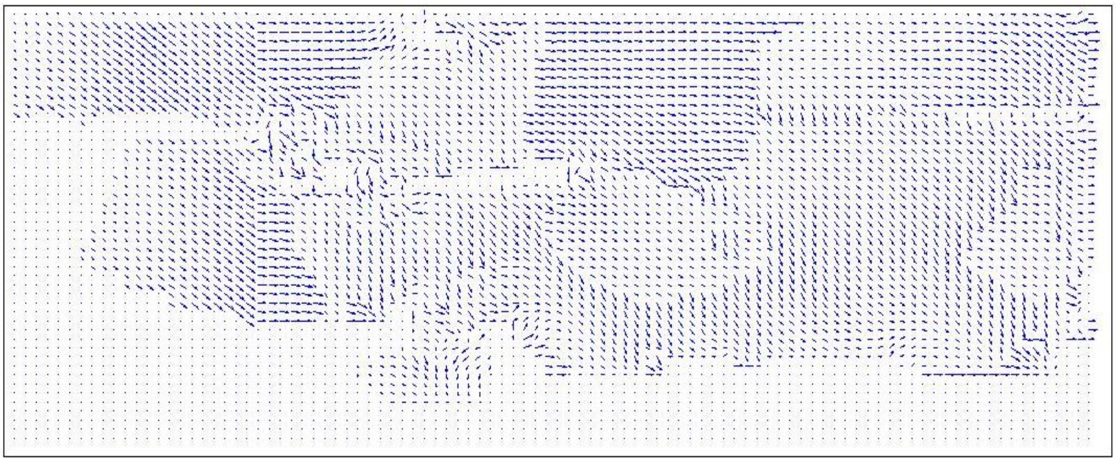

Figure 178. Modelling of the Current speed and direction at level 4 for December 2014

After hydrodynamic modelling of current speed and direction, sediment distribution was modelled.

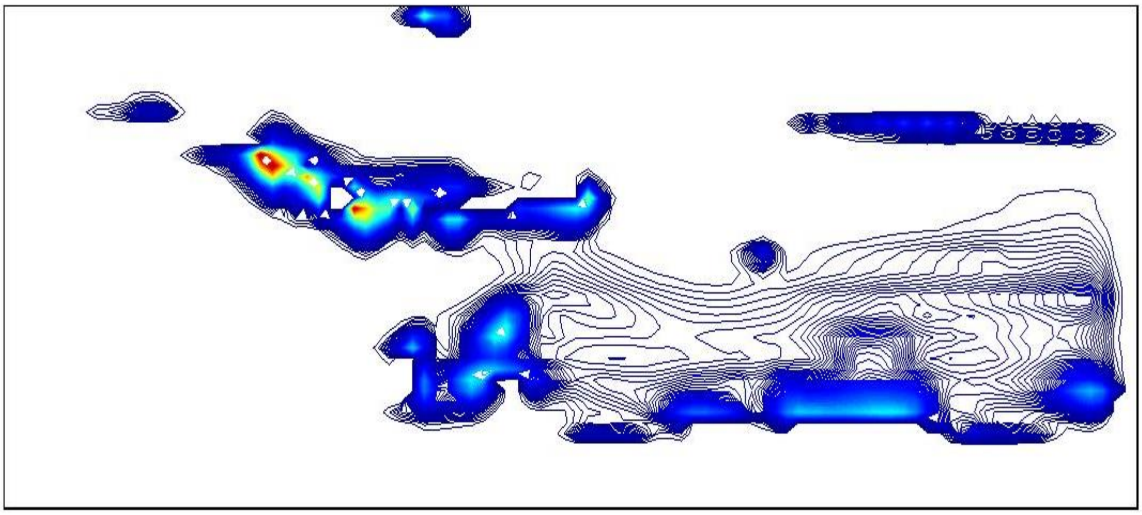

Figure 179. Sediment Distribution in Trabzon port area for December 2014

Current speed and direction modelling results of these modellings for December are given in the following graphs.

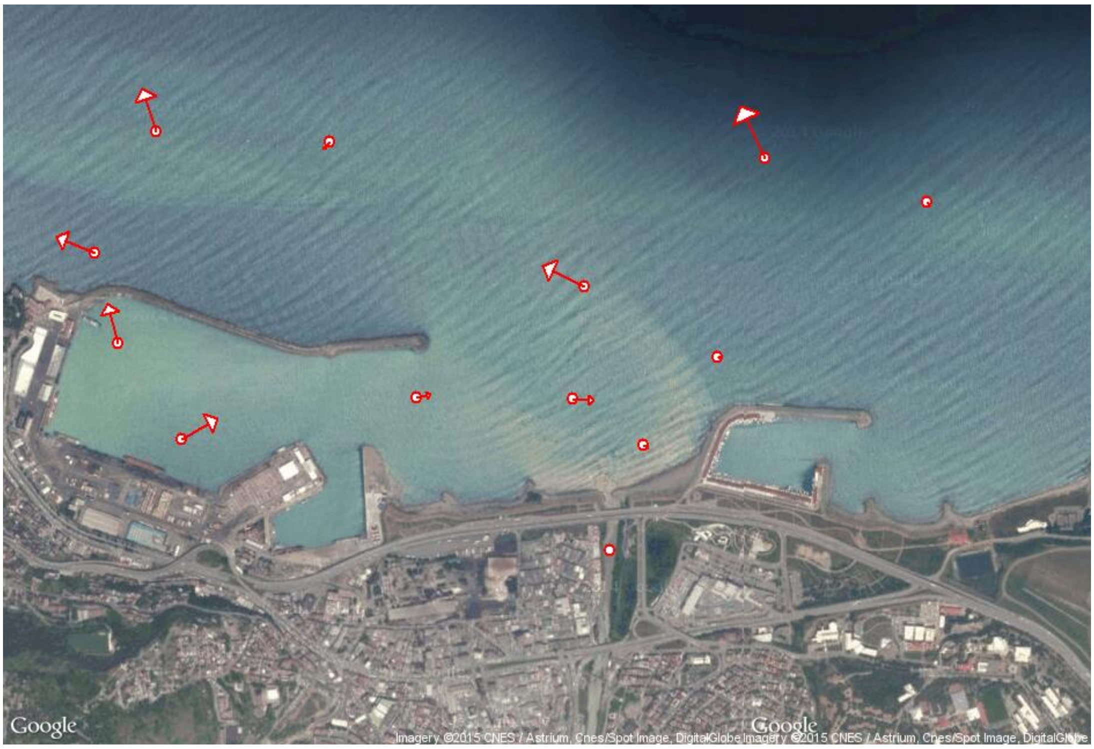

Figure 180. SurfaceCurrent measurements for January2015,

Figure 181. Level 1 Current measurements for January2015 ,

Figure 182. Level 2 Current measurements for January 2015

Figure 183. Bottomcurrent measurements for January 2015

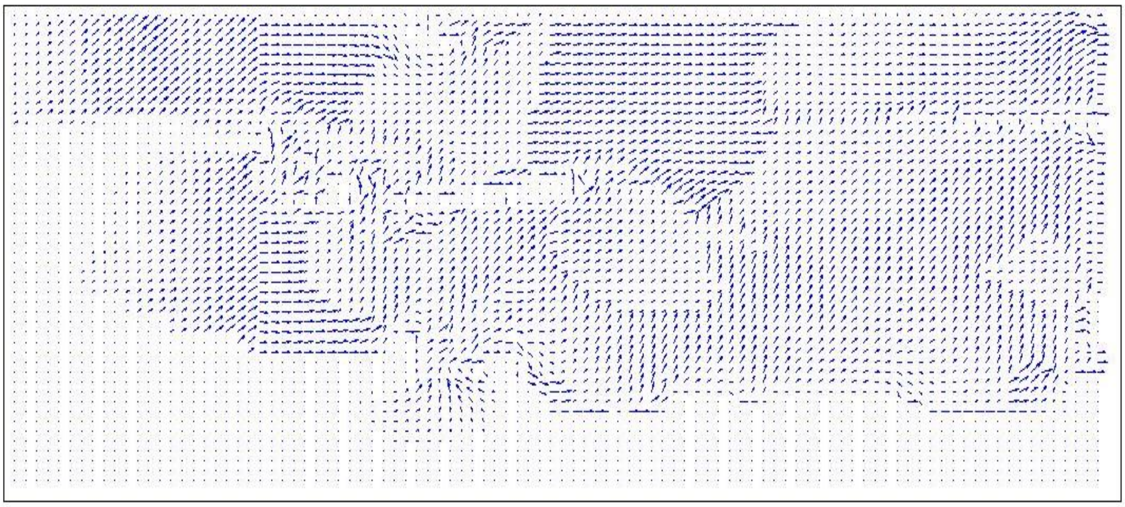

Figure 184. Modelling of the currents speed and direction for surface current for January 2015

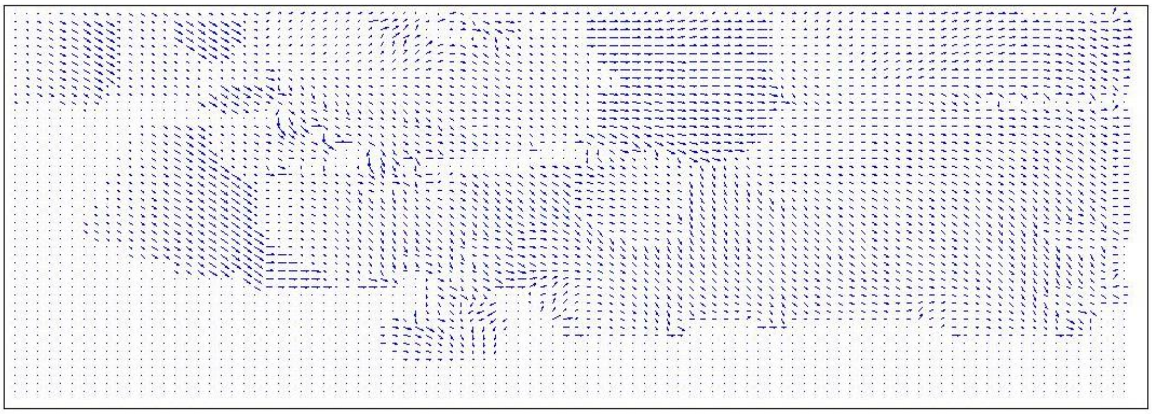

Figure 185.Modelling of the currents speed and direction for level 1 for January 2015

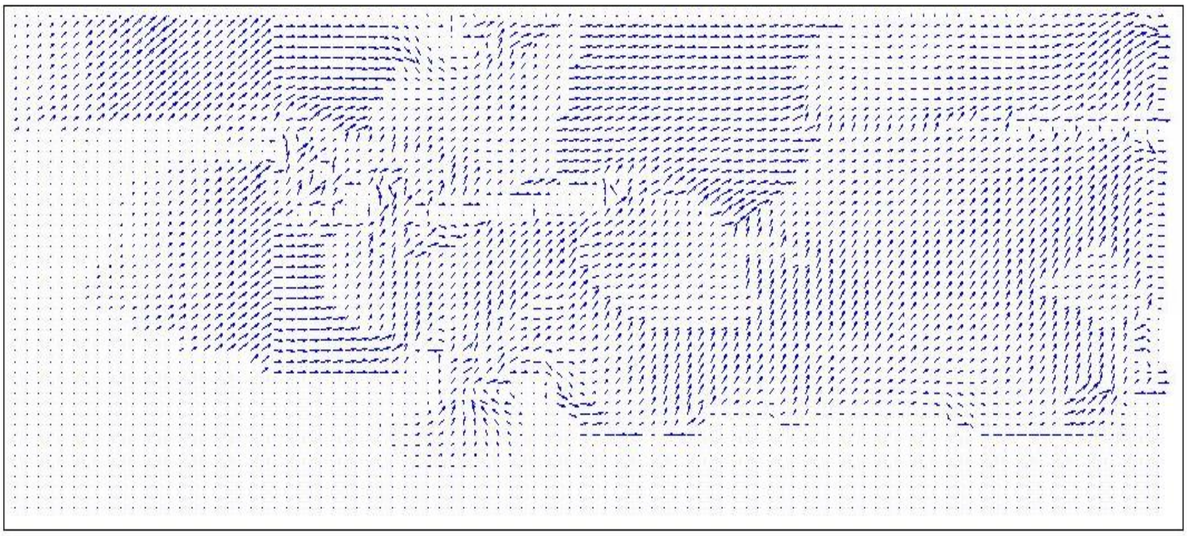

Figure 186.Modelling of the currents speed and direction for level 2 for January 2015

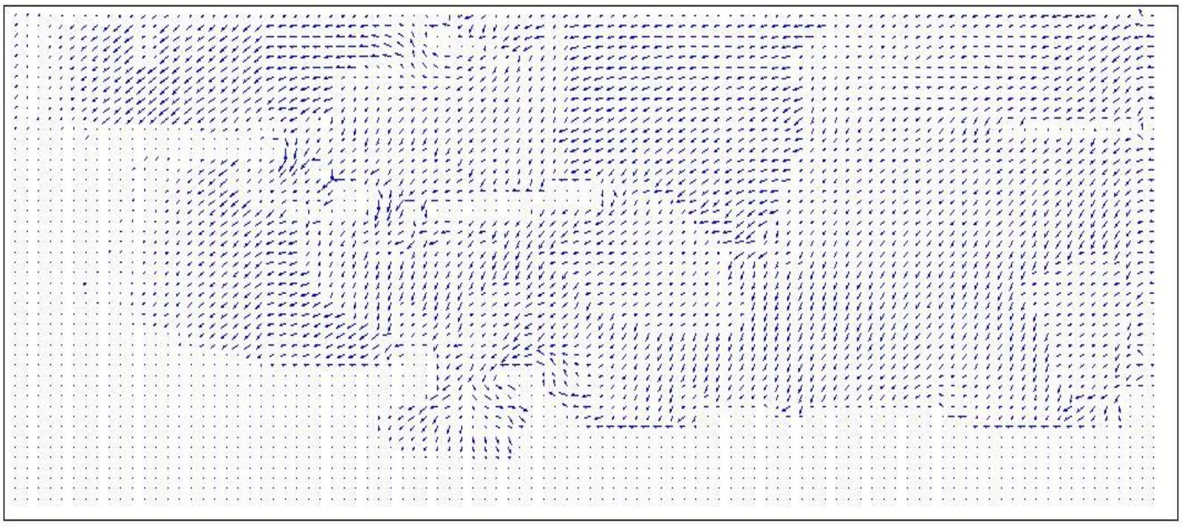

Figure 187.Modelling of the currents speed and direction for depth for January 2015

Modelled sediment distribution for january 2015 is given at Figure 188.

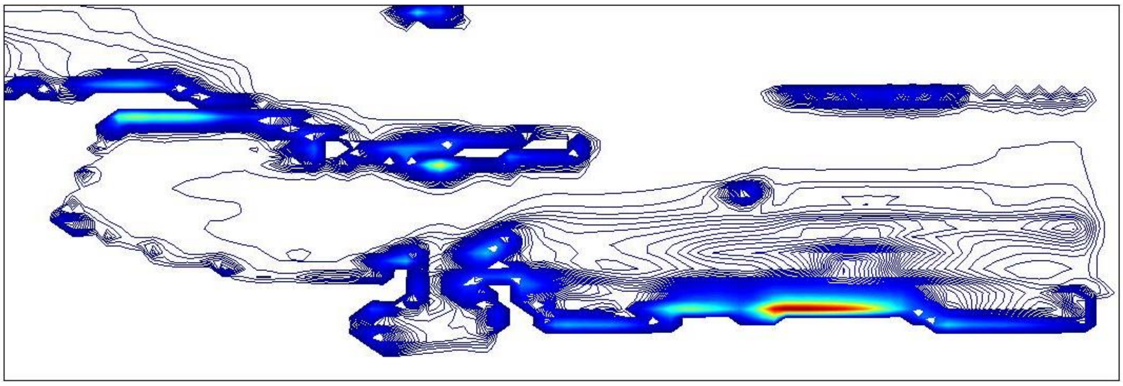

Figure 188. Sediment distribution for january 2015

Figure 189. Surface Current measurements the first measurements in February 2015,

Figure 190. Level 1 Current measurements the first measurements in February 2015,

Figure 191. Level 2 Current measurements the first measurements in February 2015

Figure 192. Bottom current measurements the first measurements in February 2015

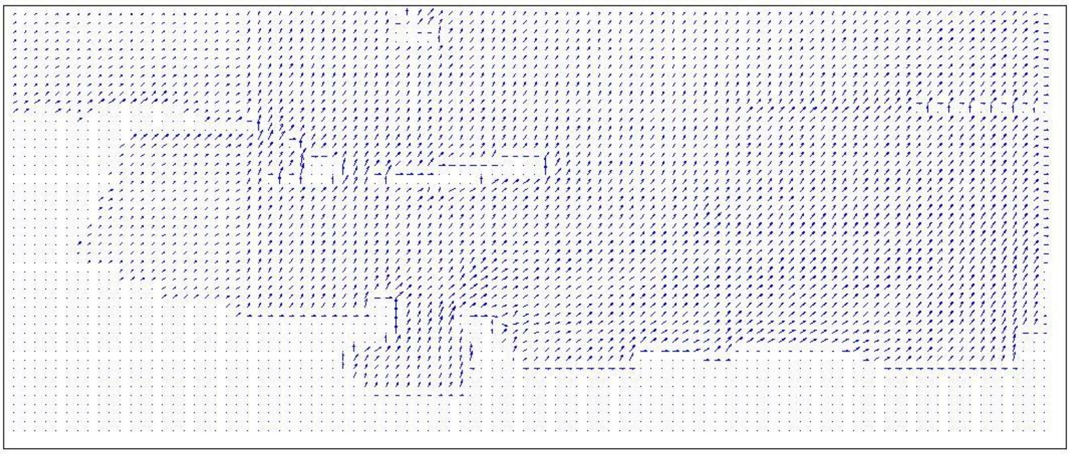

Figure 193. Modelling of the currents speed and direction for surface current

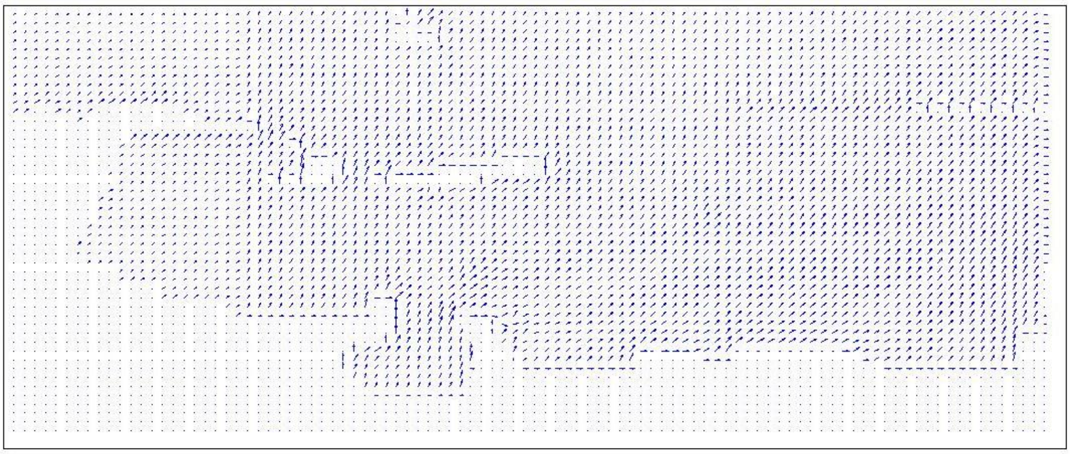

Figure 194.Modelling of the currents speed and direction for level 1

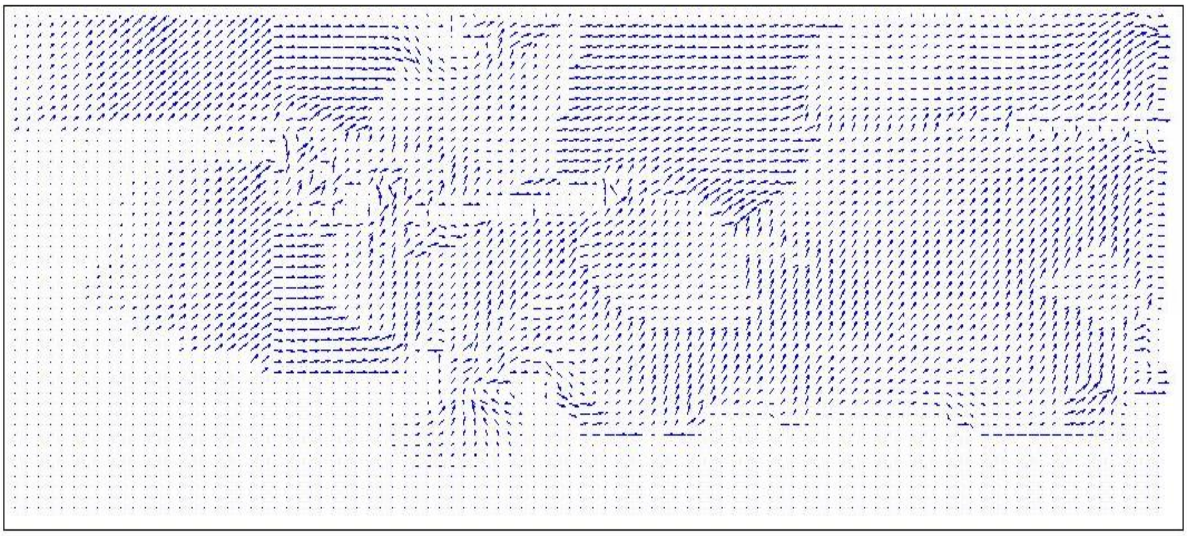

Figure 195.Modelling of the currents speed and direction for level 2

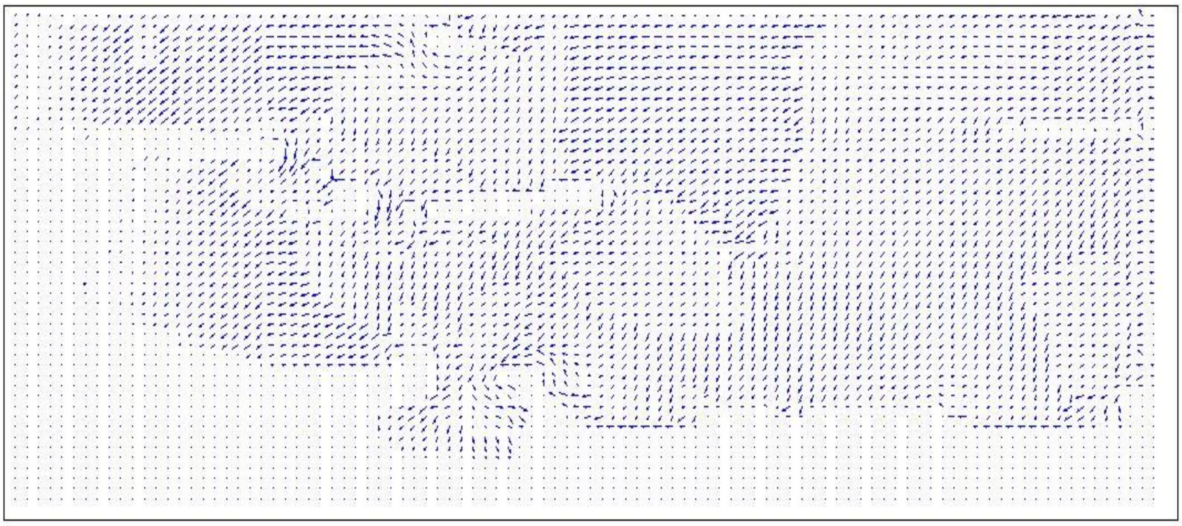

Figure 196. Modelling of the currents speed and direction for depth

Modelled sediment distribution for february is given at Figure 207.

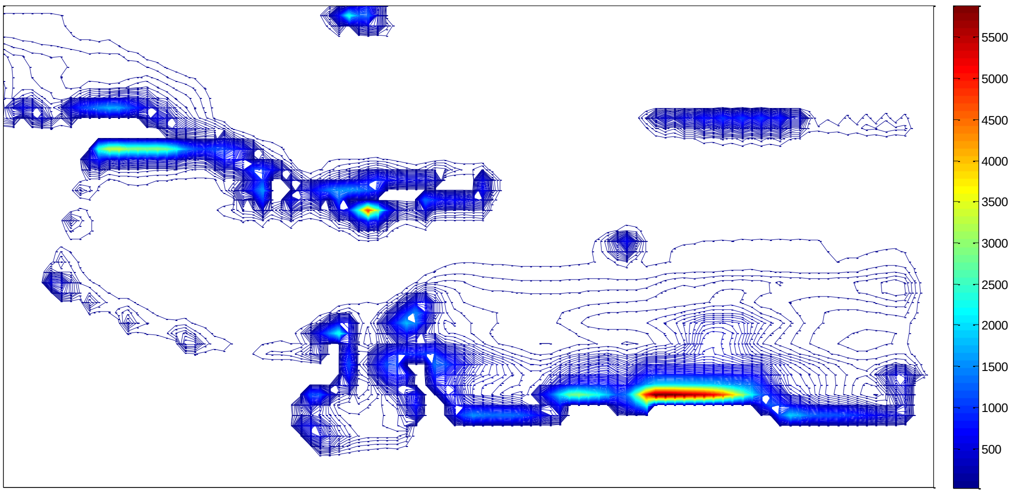

Figure 197. Sediment distribution for February 2015

Current measurements and modelling for the second measurements in Februrary 2015 are given in the Figures 198 -206.

Figure 198. Surface Current measurements for the second measurements in February2015,

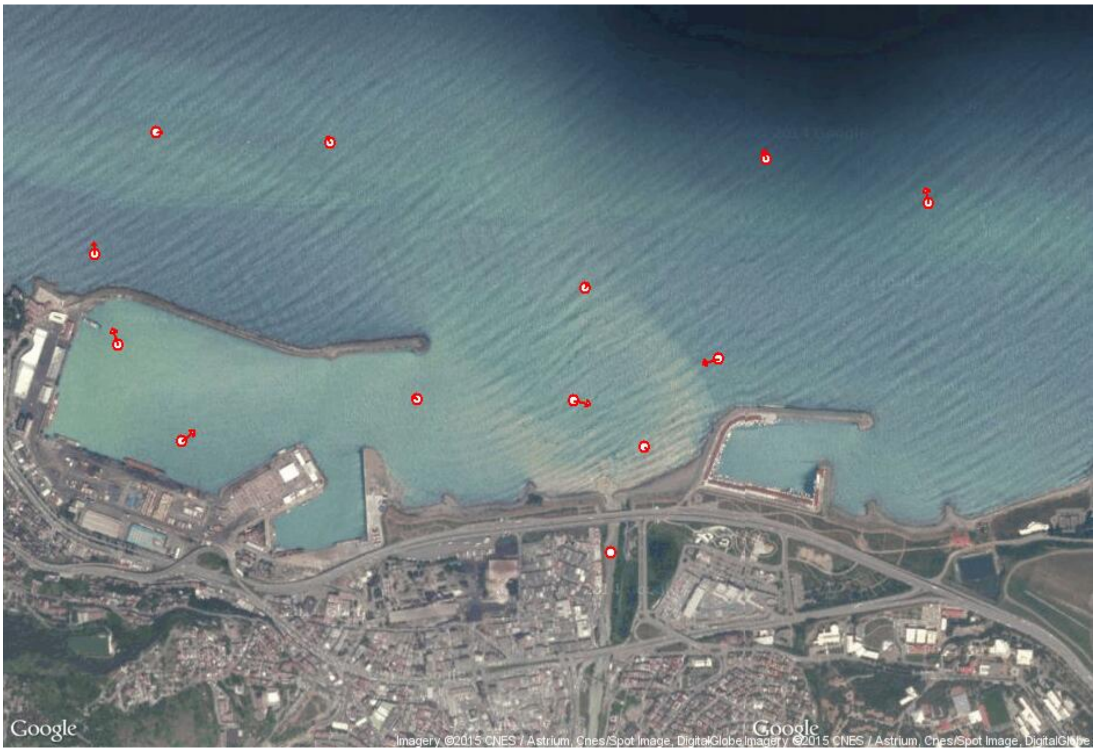

Figure 199. Level 1 Current measurements for the second measurements in February 2015,

Figure 200. Level 2 Current measurements for the second measurements in February 2015

Figure 201. Bottomcurrent measurements for the second measurements in February 2015

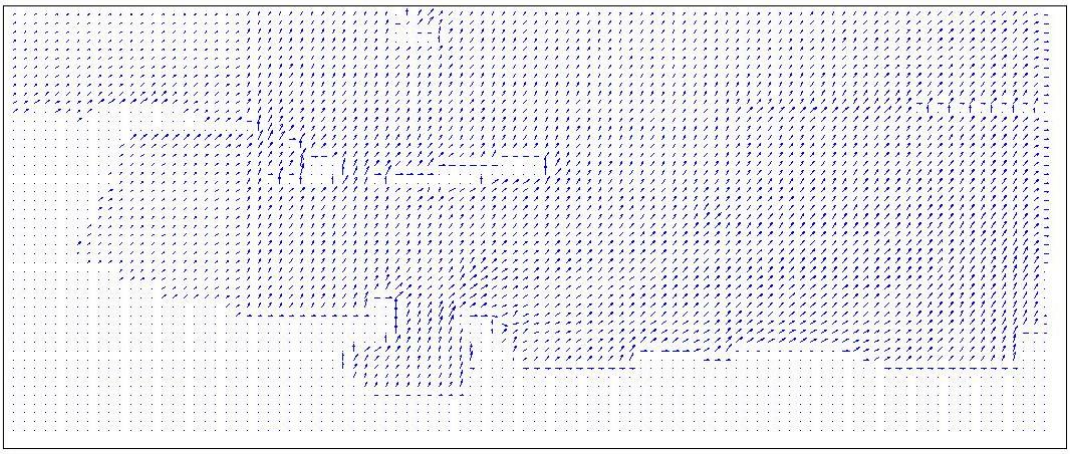

Figure 202. Modelling of the currents speed and direction for surface current

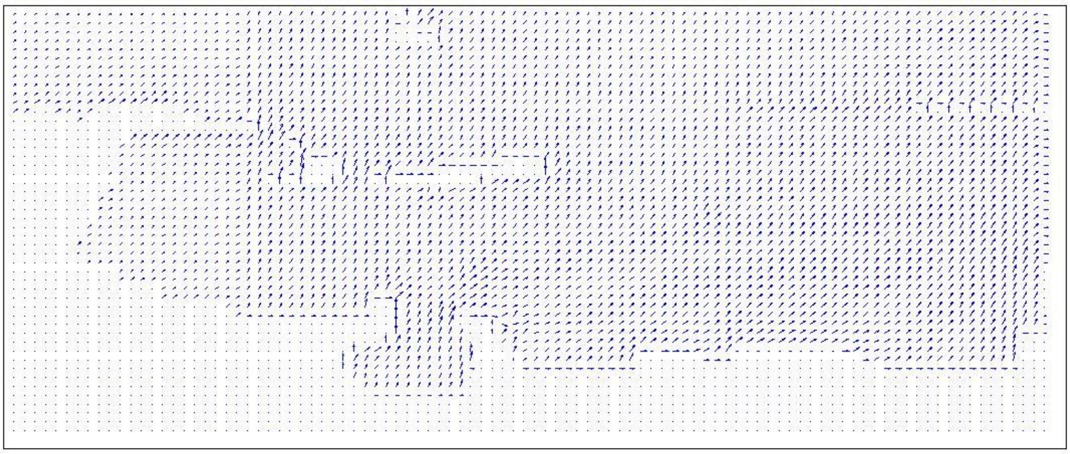

Figure 203.Modelling of the currents speed and direction for level 1

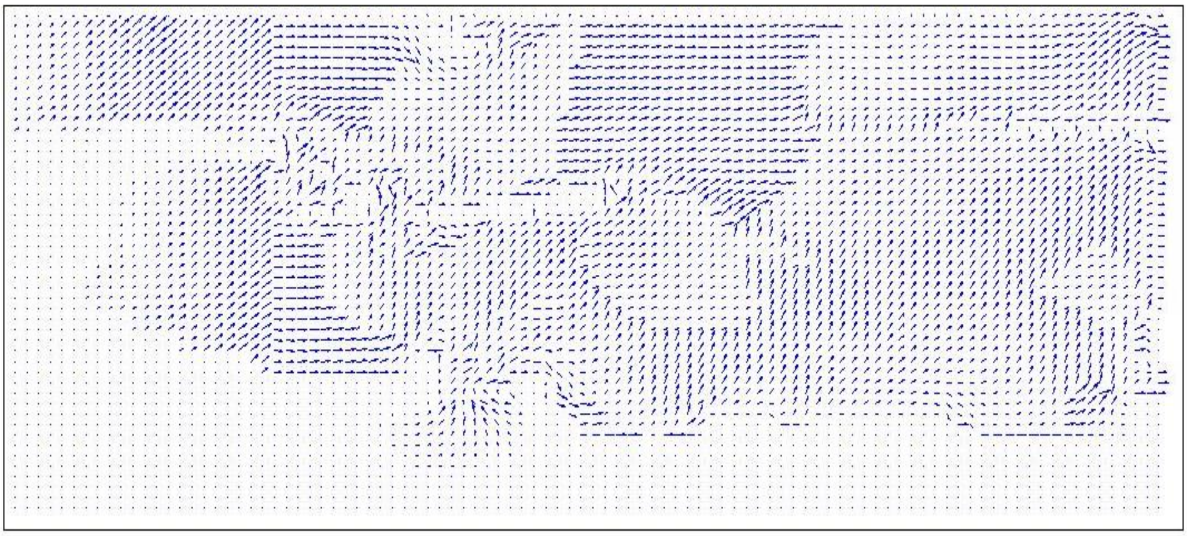

Figure 204. Modelling of the currents speed and direction for level 2

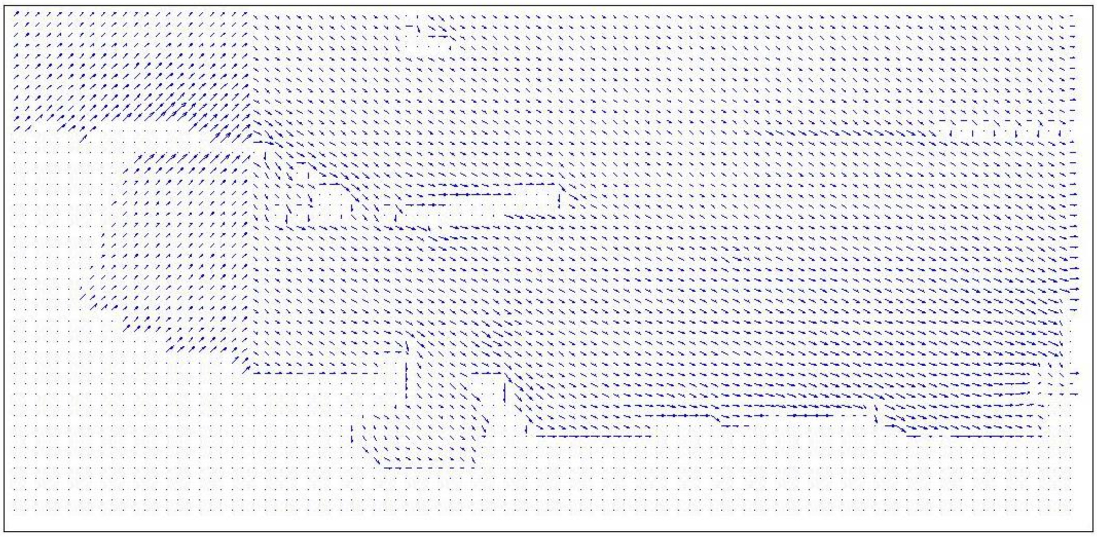

Figure 205. Modelling of the currents speed and direction for depth

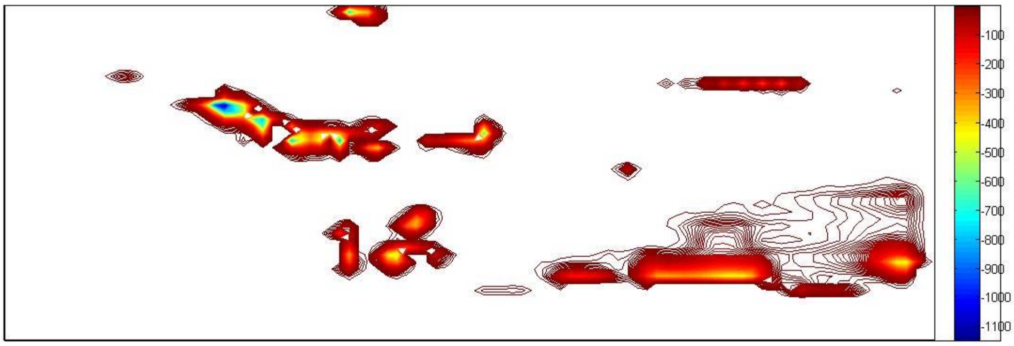

Figure 206. Modelled sediment distribution fort he second measurements fort he February 2015

Current measurements and modelling for the first measurements in March are given in the Figures 207 -215.

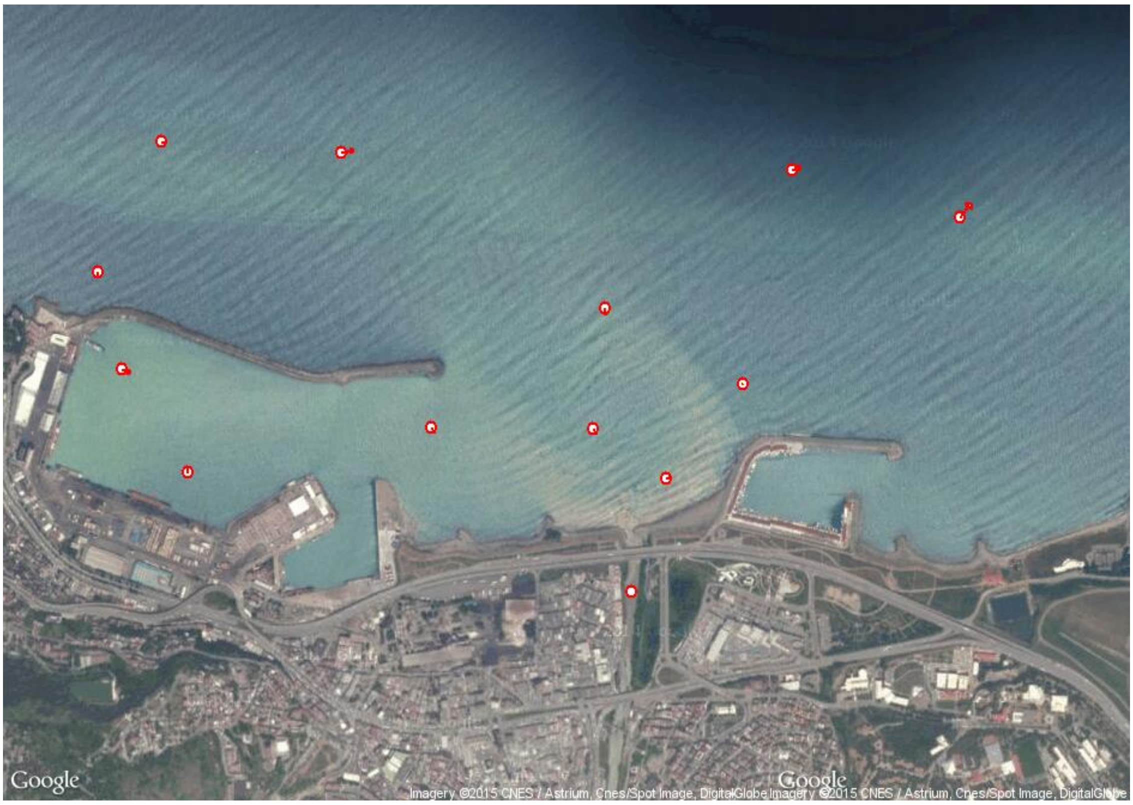

Figure 207. Surface Current measurements for first measurements in March2015,

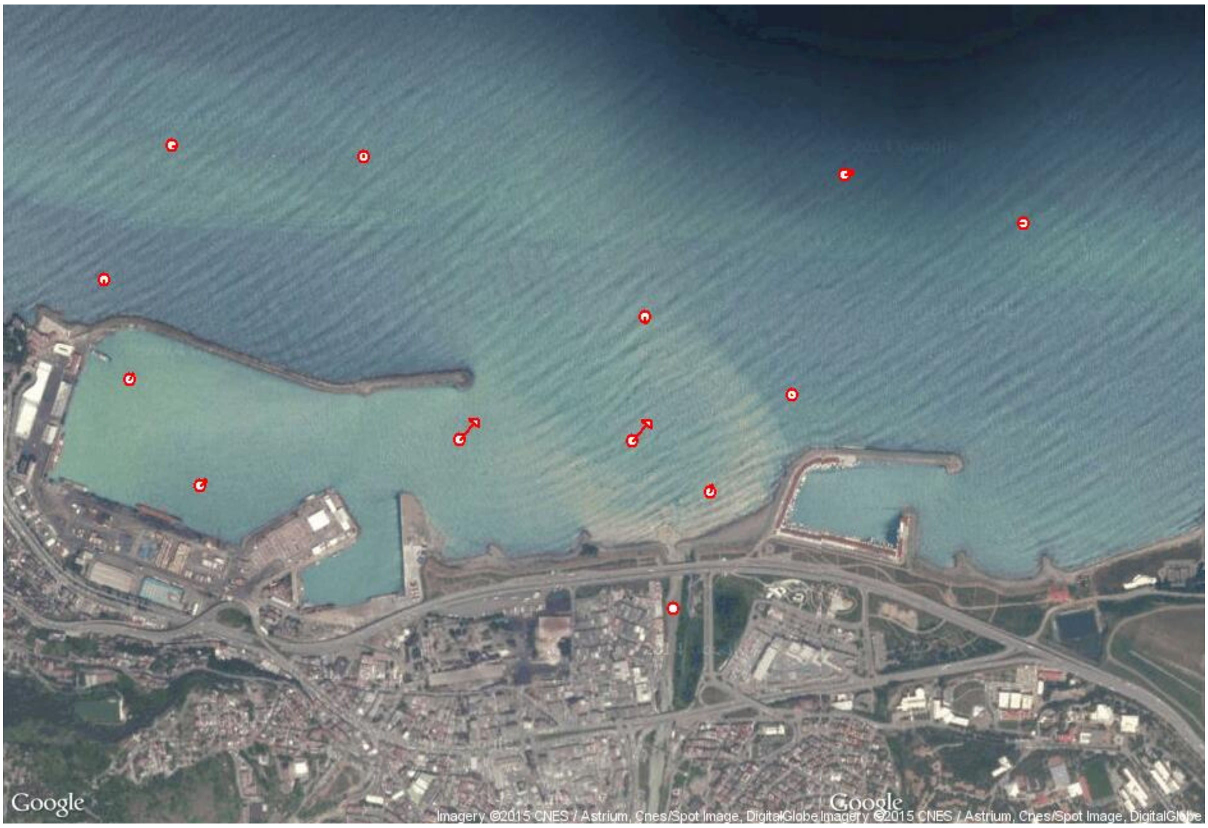

Figure 208. Level 1 Current measurements for first measurements inMarch2015 ,

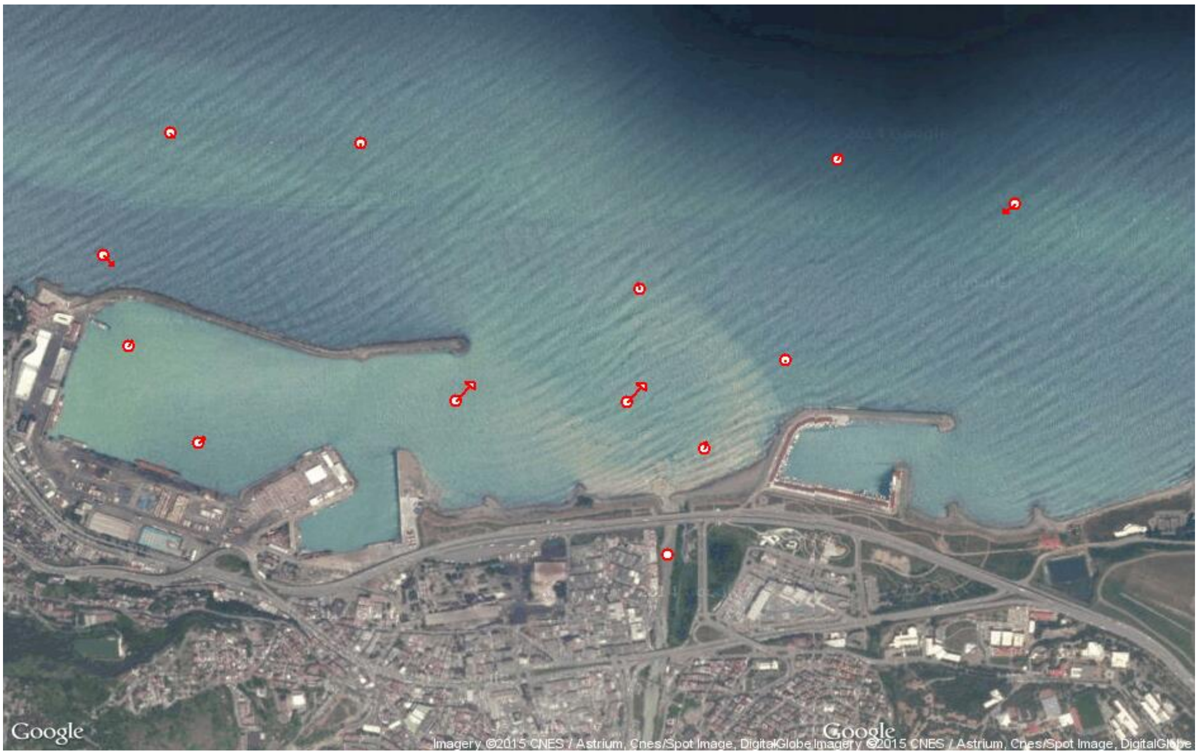

Figure 209. Level 2 Current measurements for first measurements in March2015

Figure 210. Bottom current measurements for first measurements in March 2015

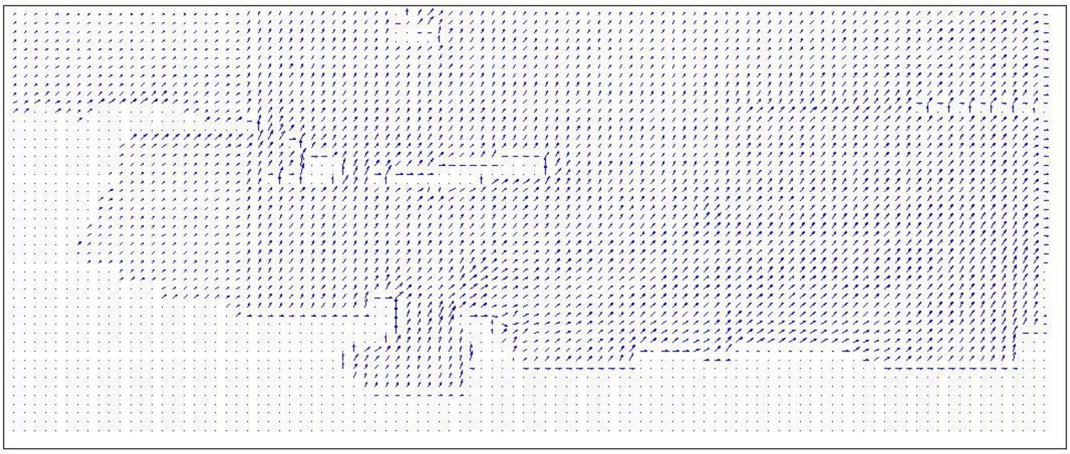

Figure 211. Modelling of the currents speed and direction for surface current

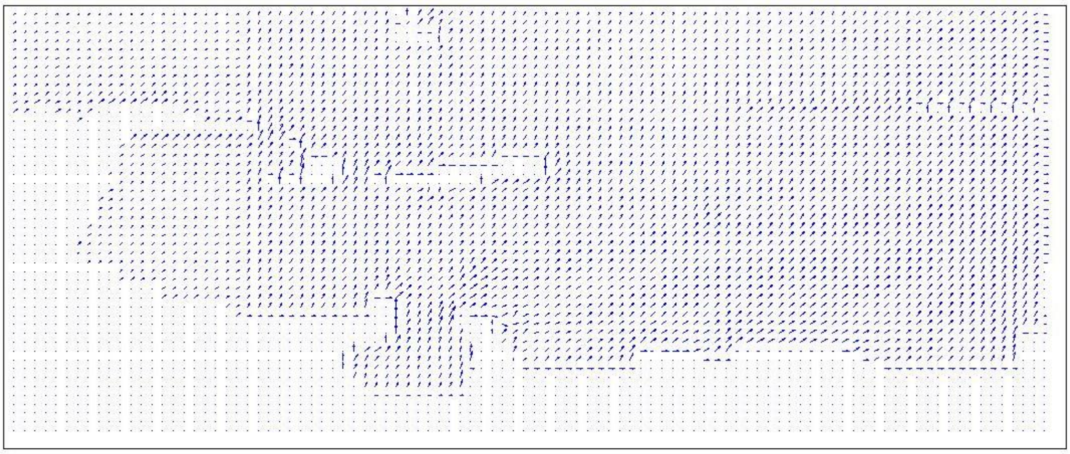

Figure 212.Modelling of the currents speed and direction for level 1

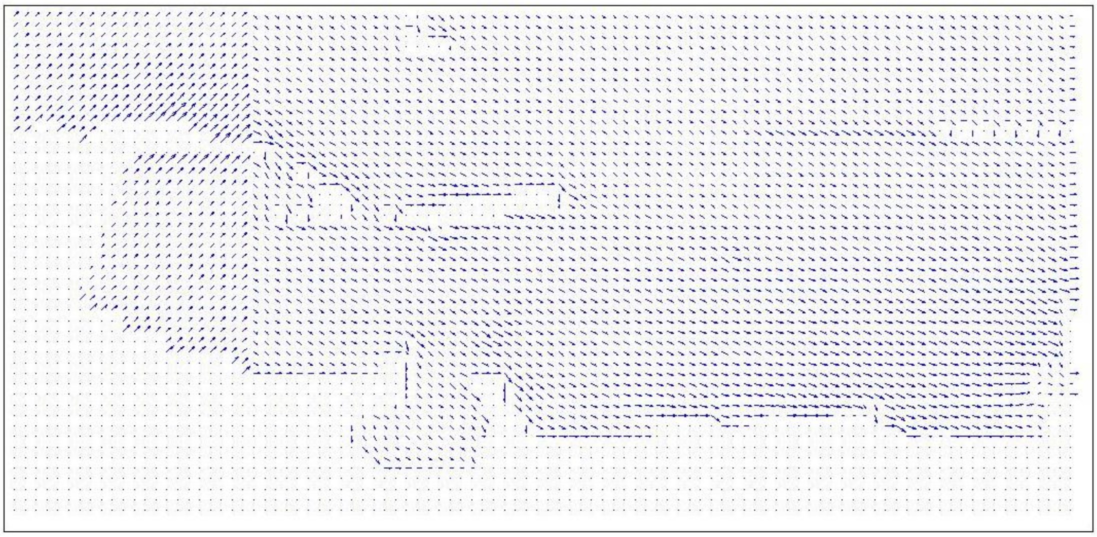

Figure 213.Modelling of the currents speed and direction for level 2

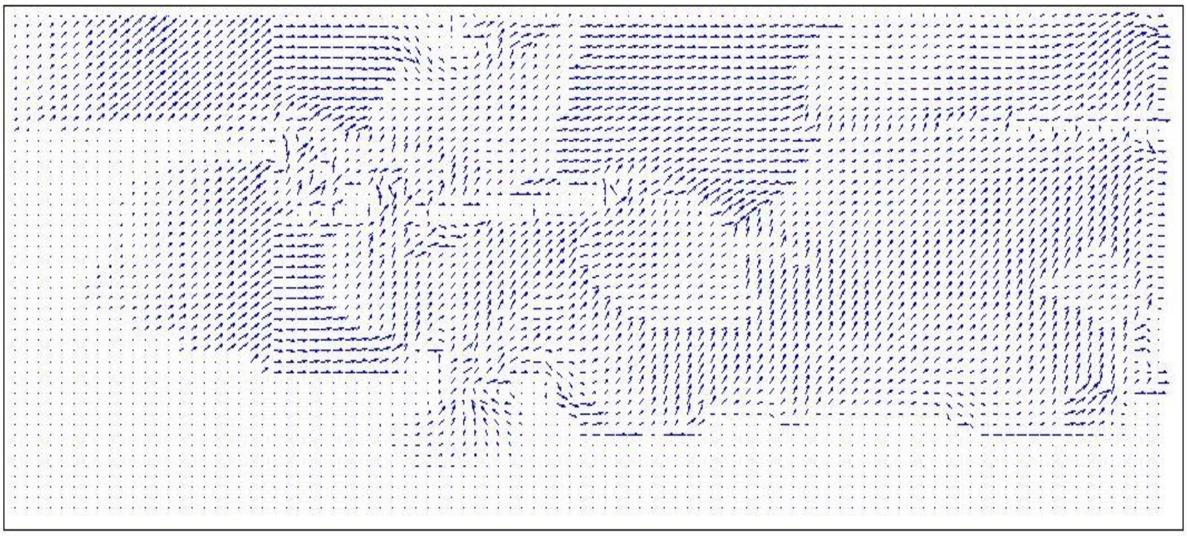

Figure 214.Modelling of the currents speed and direction for depth

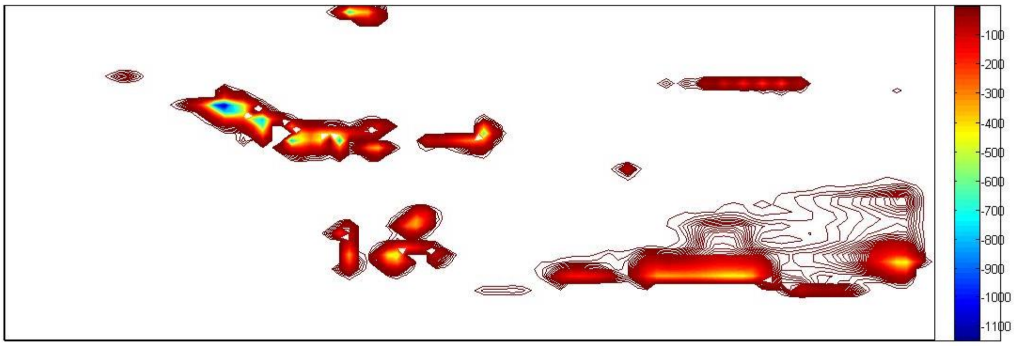

Figure 215. Sediment distribution for March 2015

Current measurements and modelling for the second measurements in March are given in the Figures 226 -234

Figure 216. Surface Current measurements for the second measurement in March 2015,

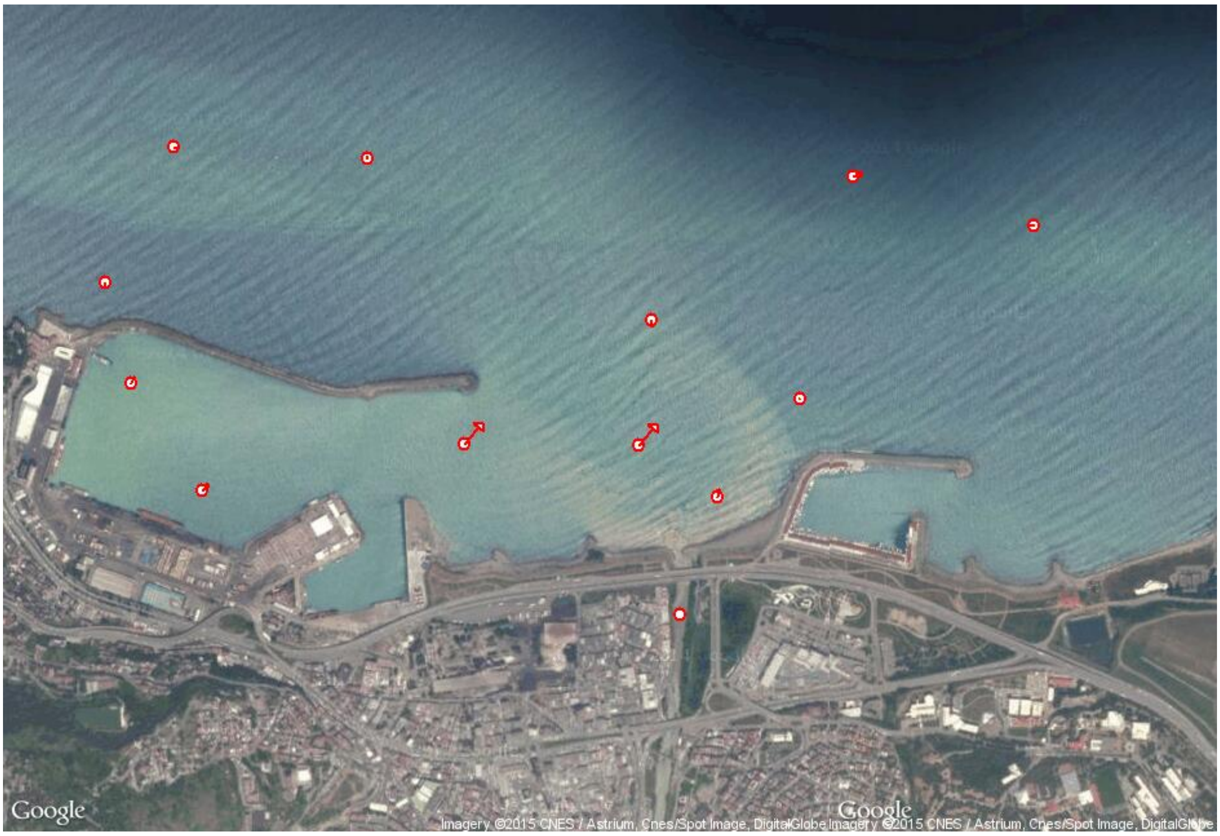

Figure 217. Level 1 Current measurements for the second measurement in March2015 ,

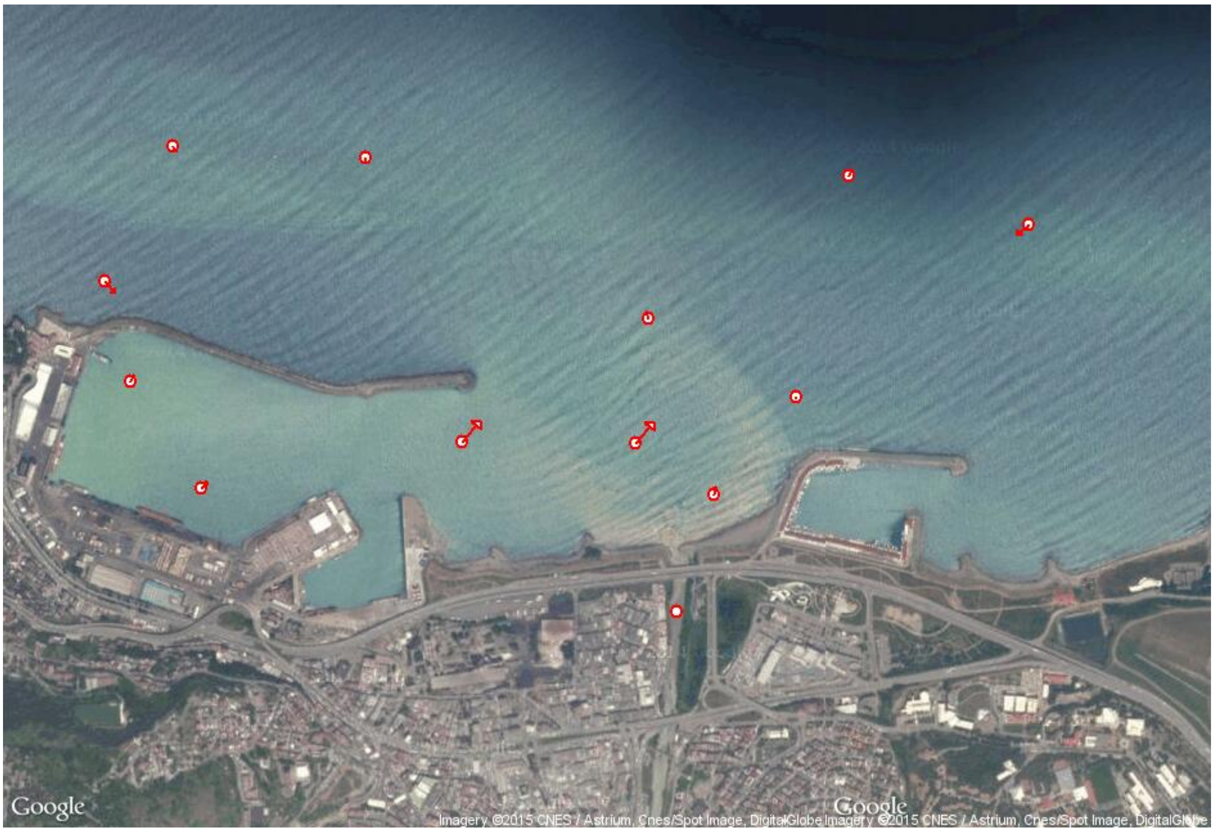

Figure 218. Level 2 Current measurements for the second measurement in March 2015

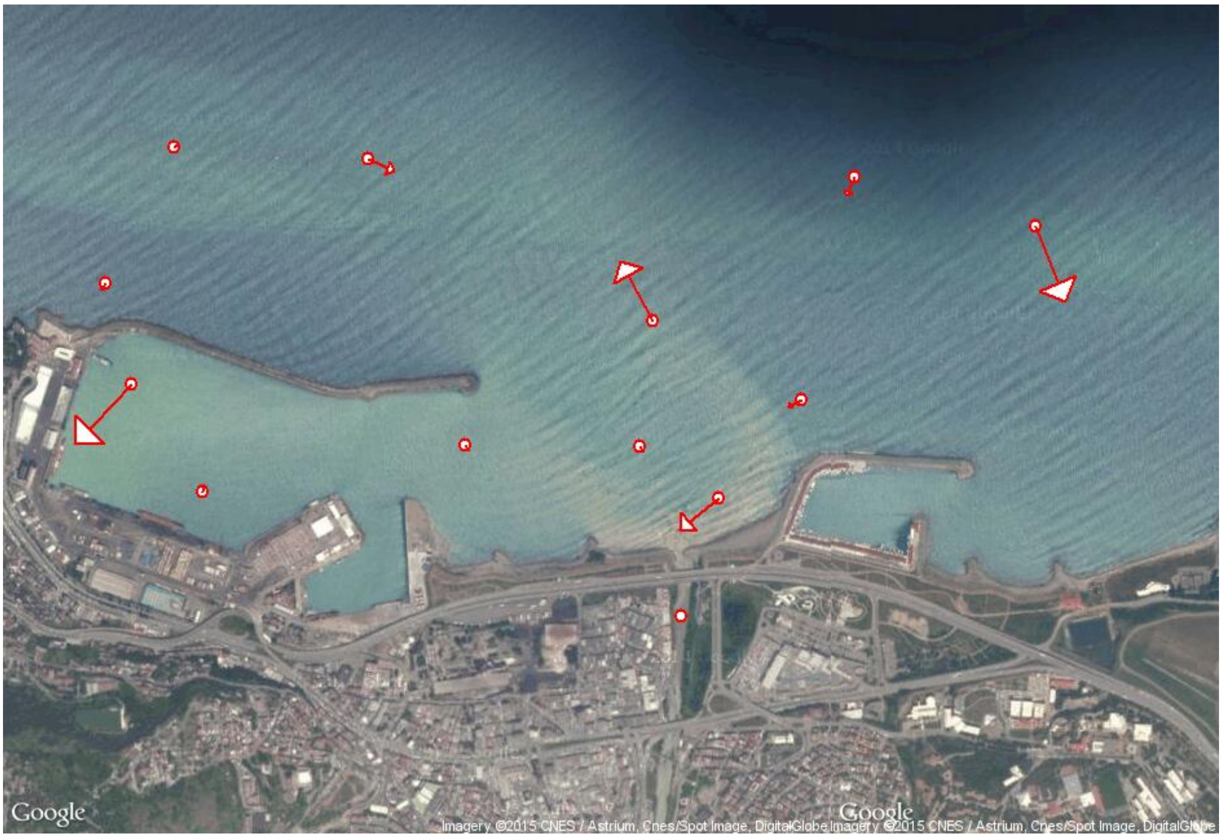

Figure 219. Bottom current measurements for the second measurement in March 2015

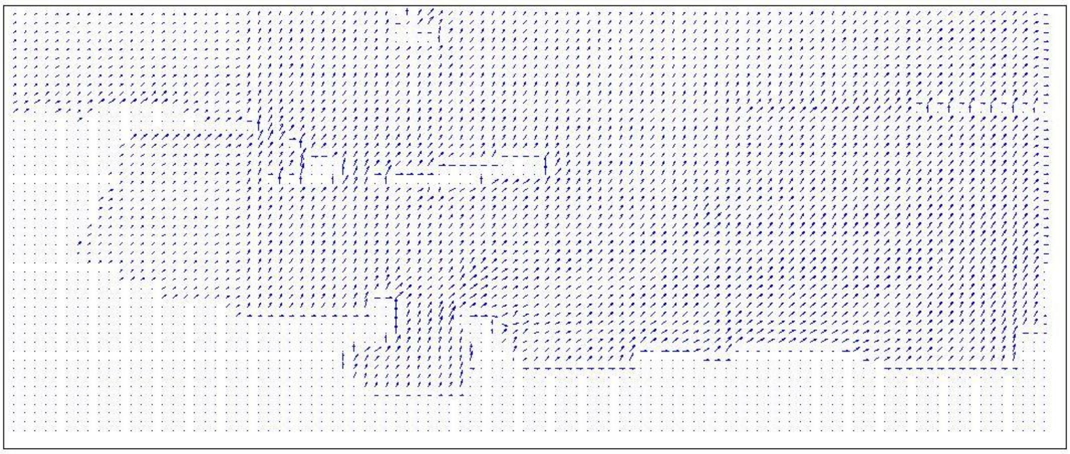

Figure 220. Modelling of the currents speed and direction for surface current

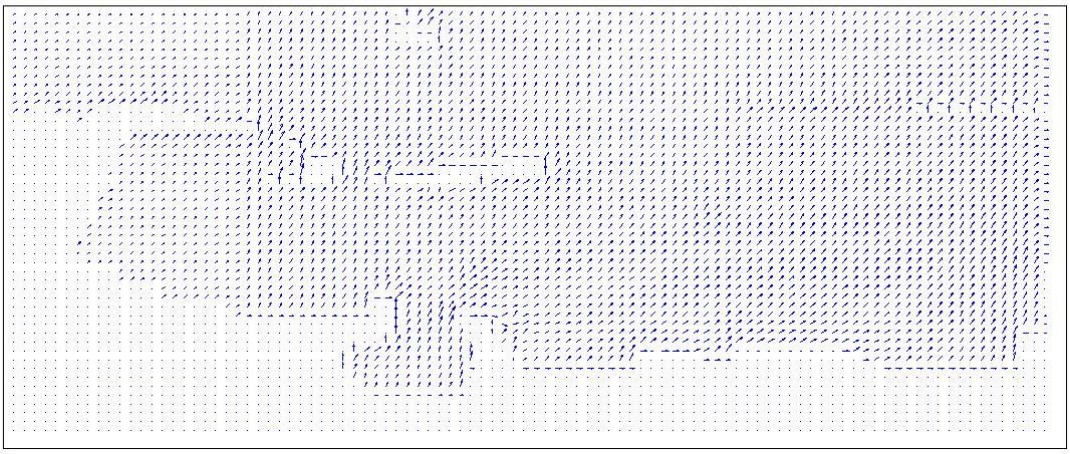

Figure 221.Modelling of the currents speed and direction for level 1

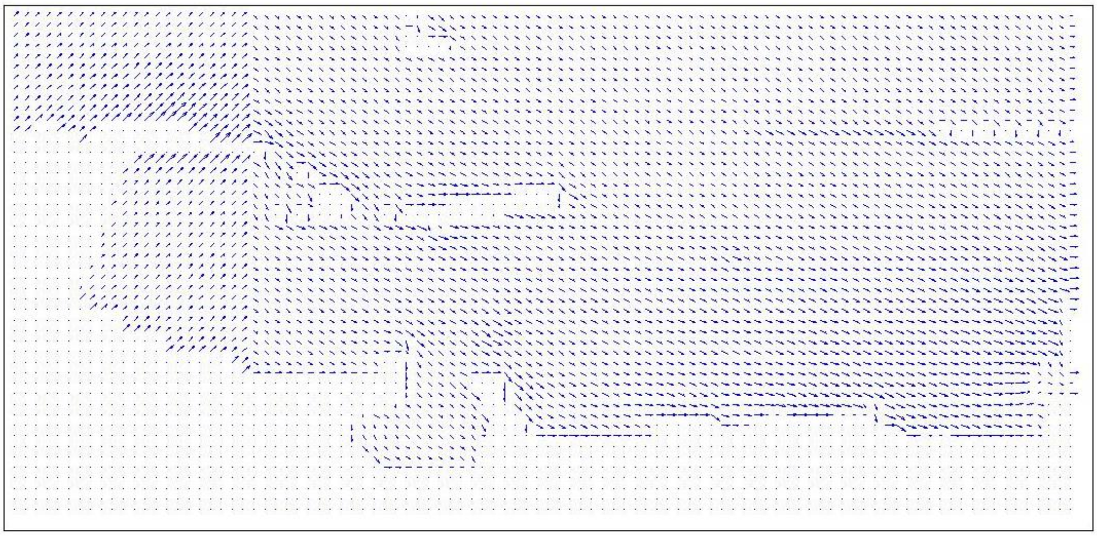

Figure 222.Modelling of the currents speed and direction for level 2

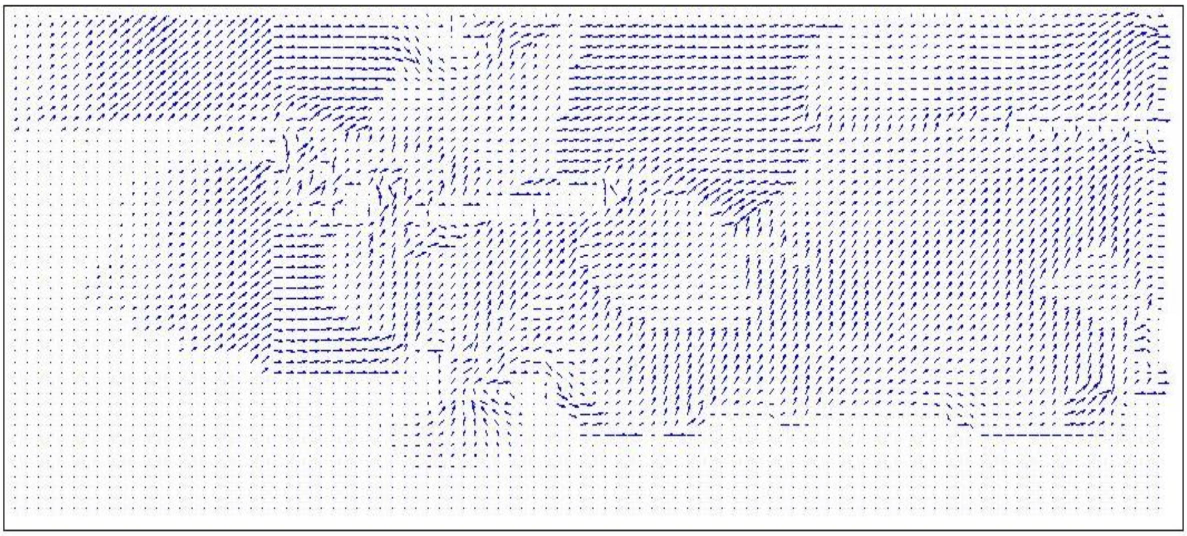

Figure 223. Modelling of the currents speed and direction for depth

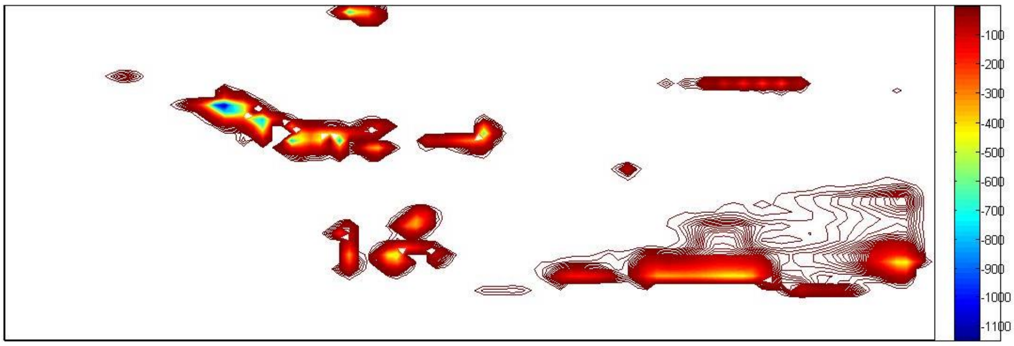

Figure 224. Sediment distribution for March 2015

Current measurements and modelling for the first measurements in April 2015 are given in the Figures 235 -243.

Figure 225. Surface Current measurements for the first measurements in April 2015,

Figure 226. Level 1 Current measurements for the first measurements in April 2015,

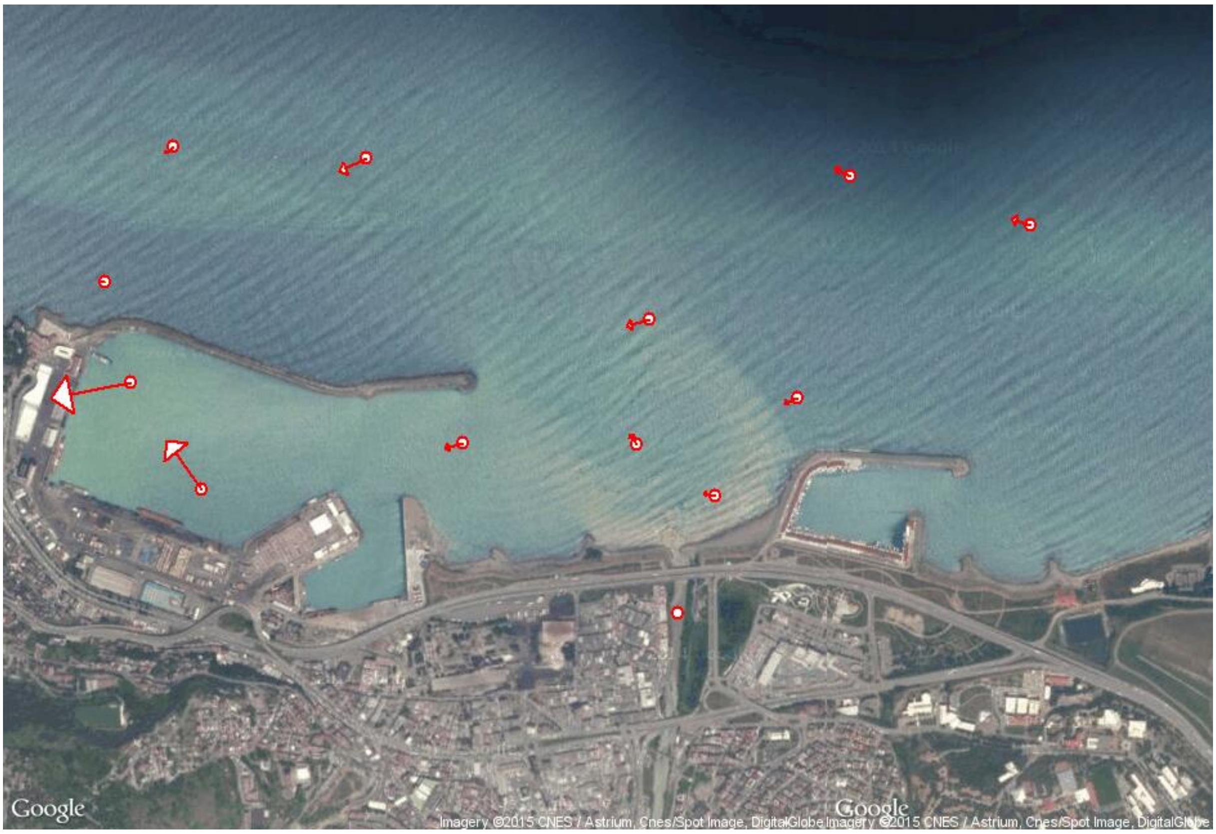

Figure 227. Level 2 Current measurements for the first measurements in April2015

Figure 228. Bottomcurrent measurements for the first measurements in April 2015

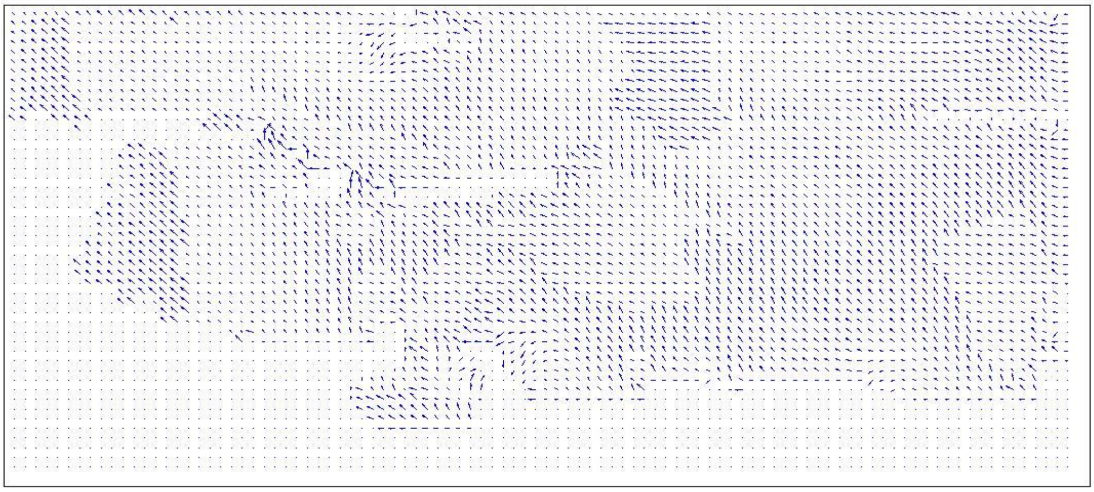

Figure 229. Modelling of the currents speed and direction for surface current

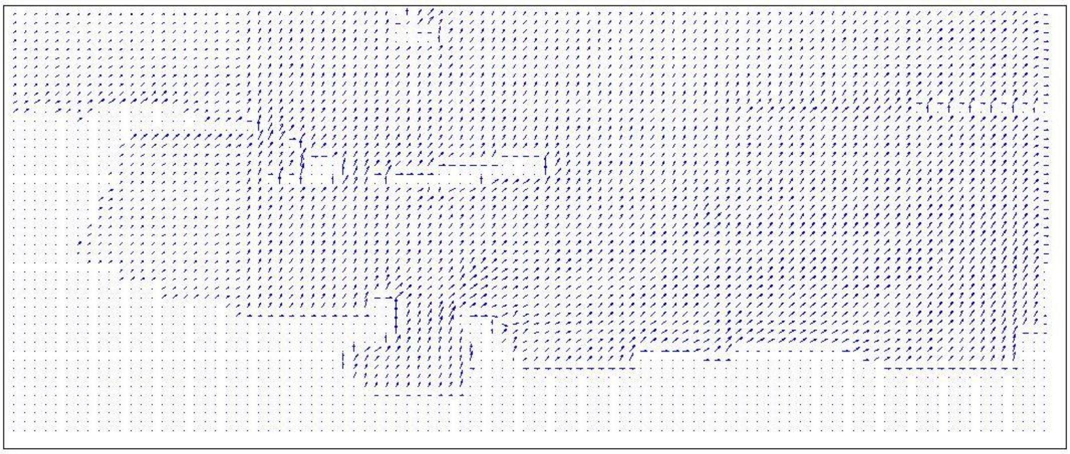

Figure 230.Modelling of the currents speed and direction for level 1

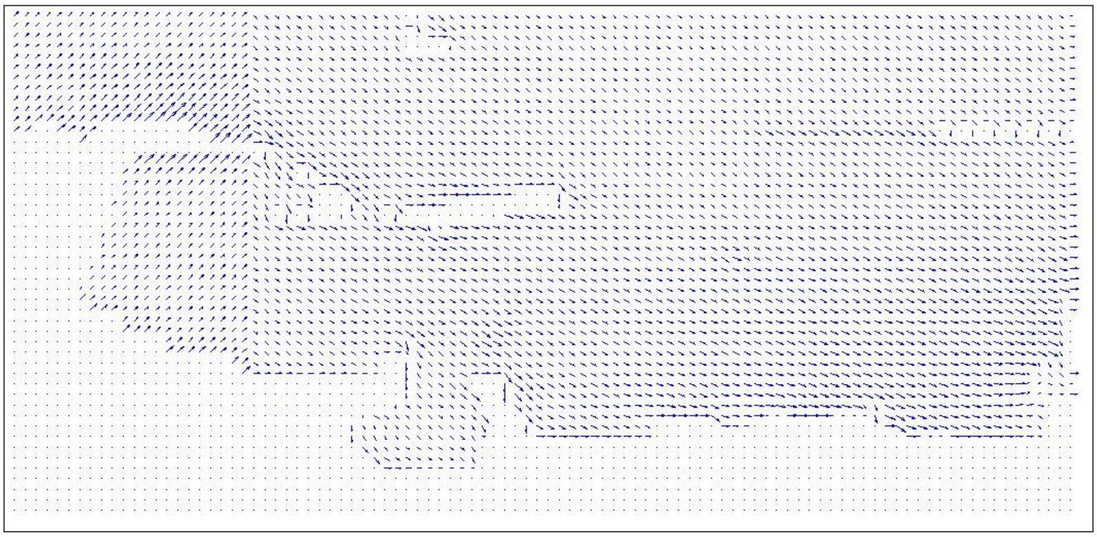

Figure 231.Modelling of the currents speed and direction for level 2

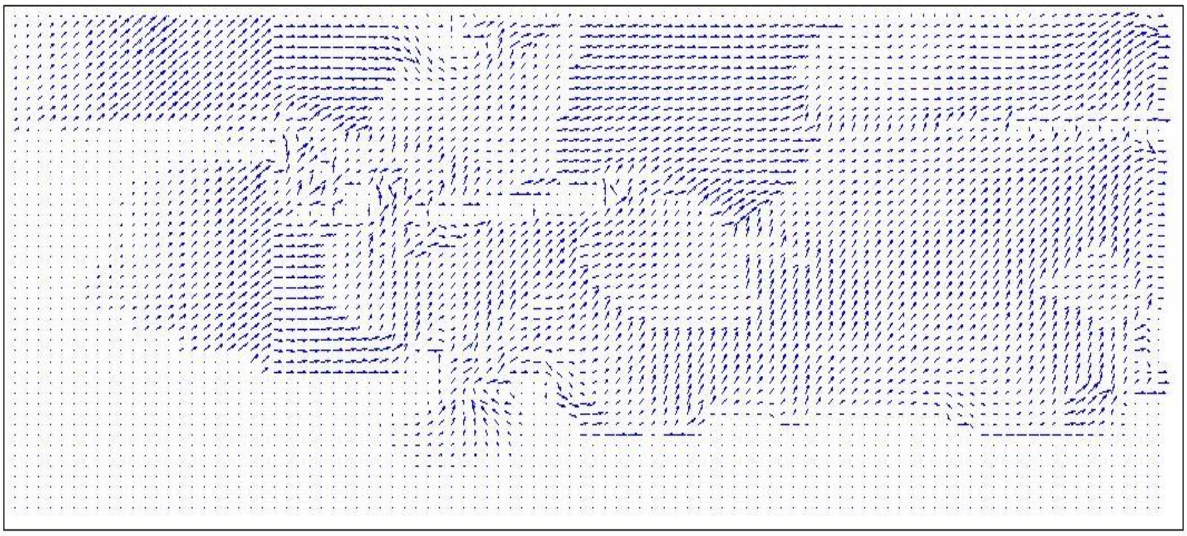

Figure 232. Modelling of the currents speed and direction for depth

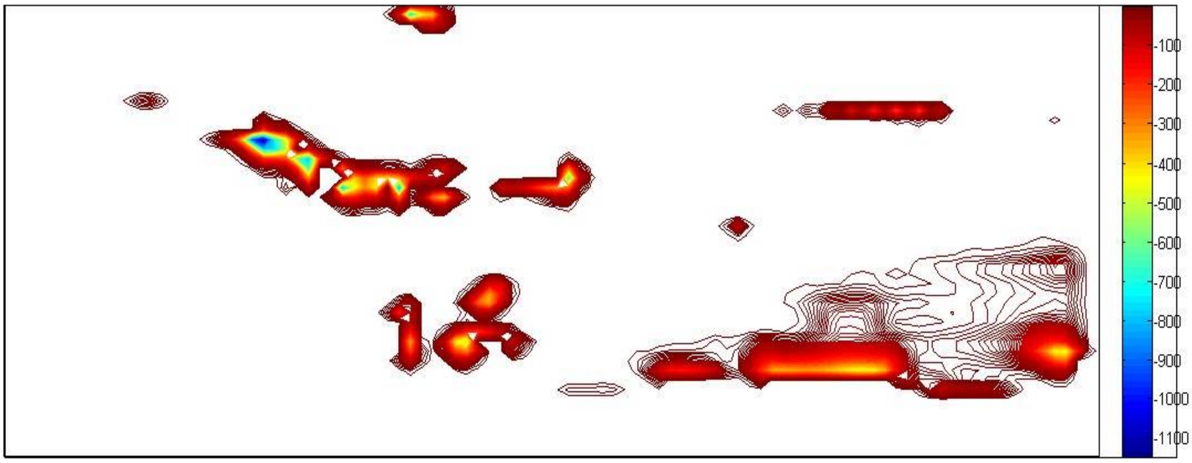

Figure 233. Sediment distribution for the first measurements in April 2015

Current measurements and modelling for the second measurements in April are given in the Figures 244 -252.

Figure 234. Surface Current measurements for the second measurements in April 2015,

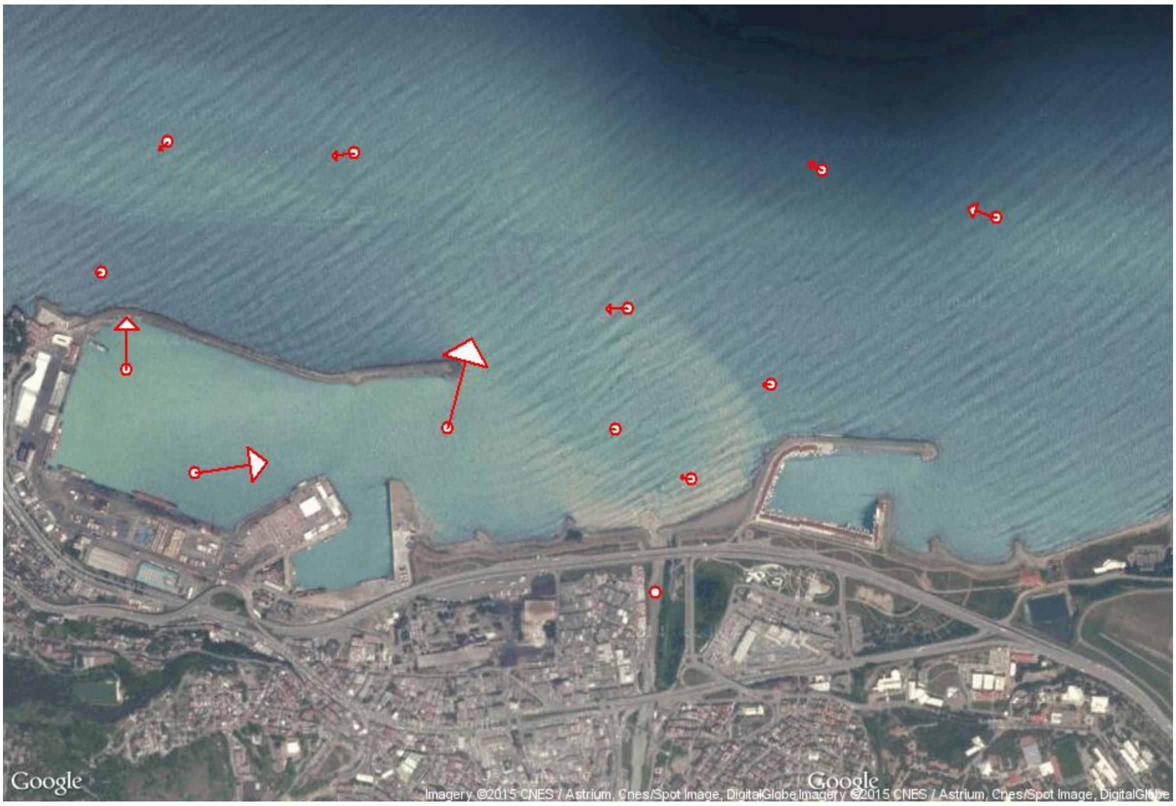

Figure 235. Level 1 Current measurements for the second measurements April2015,

Figure 236. Level 2 Current measurements for the second measurements in April 2015

Figure 237. Bottom current measurements for January for the second measurements in April 2015

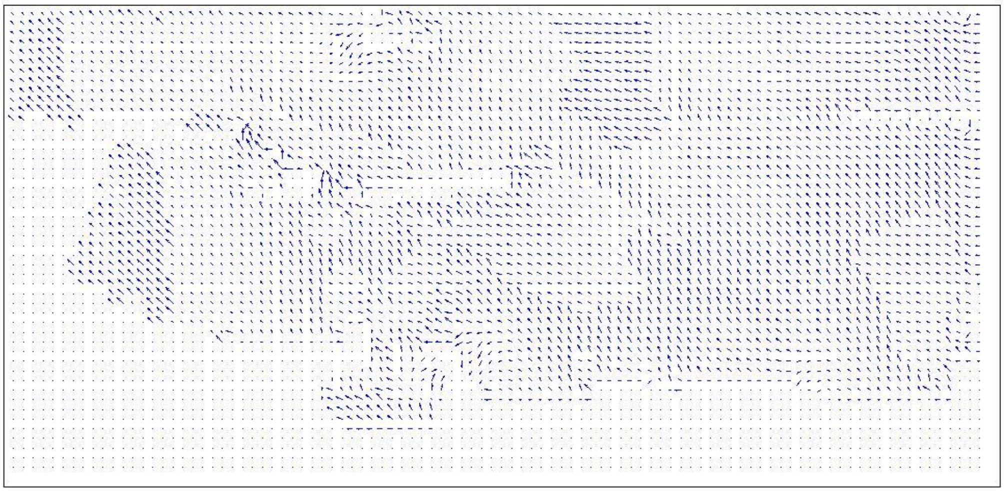

Figure 238. Modelling of the currents speed and direction for surface current

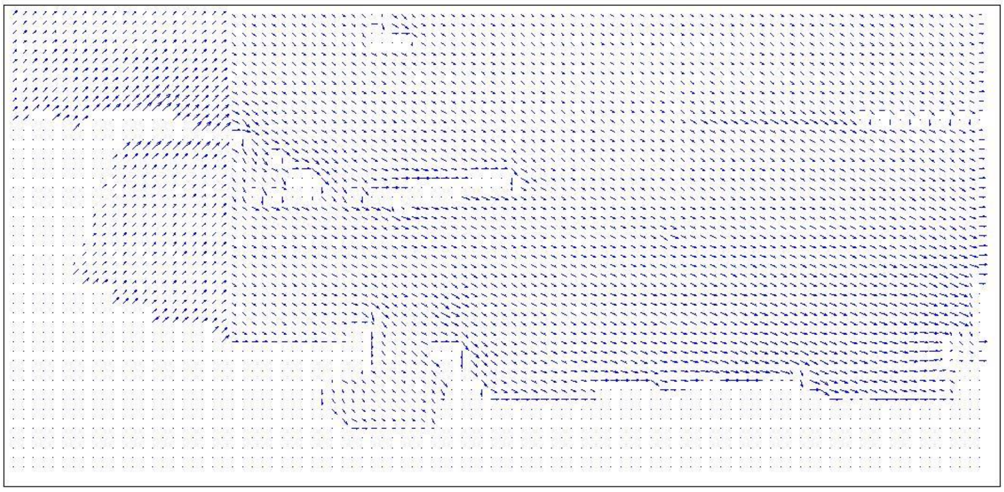

Figure 239. Modelling of the currents speed and direction for level 1

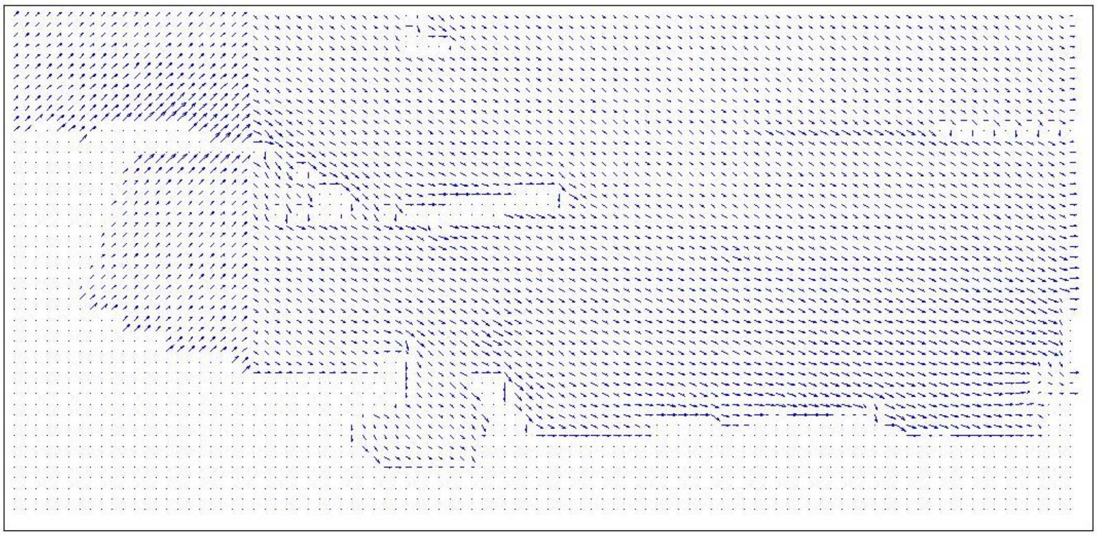

Figure 240. Modelling of the currents speed and direction for level 2

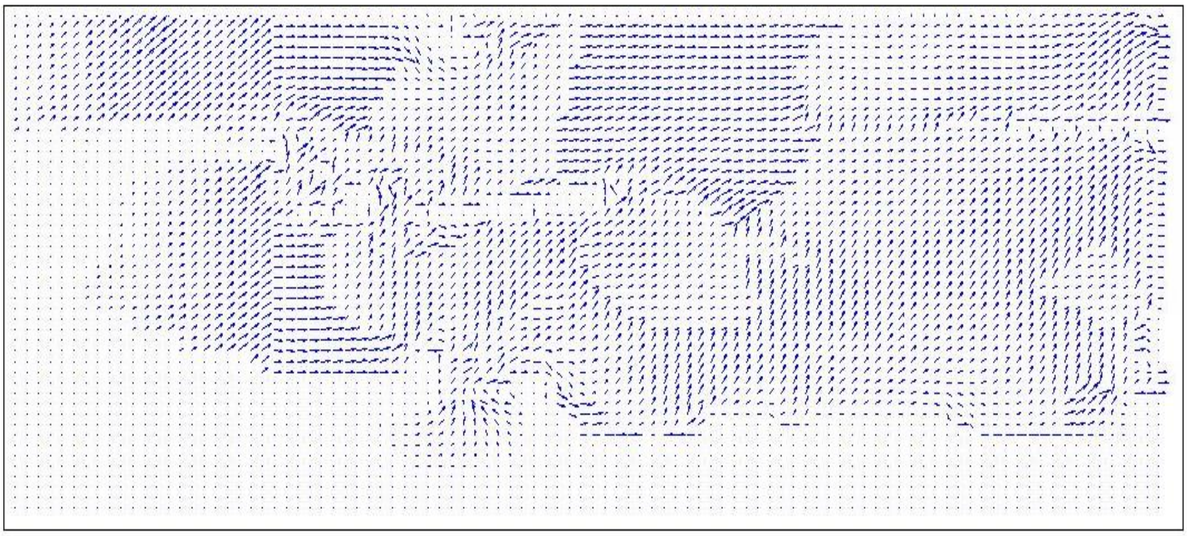

Figure 241. Modelling of the currents speed and direction for maximum depth

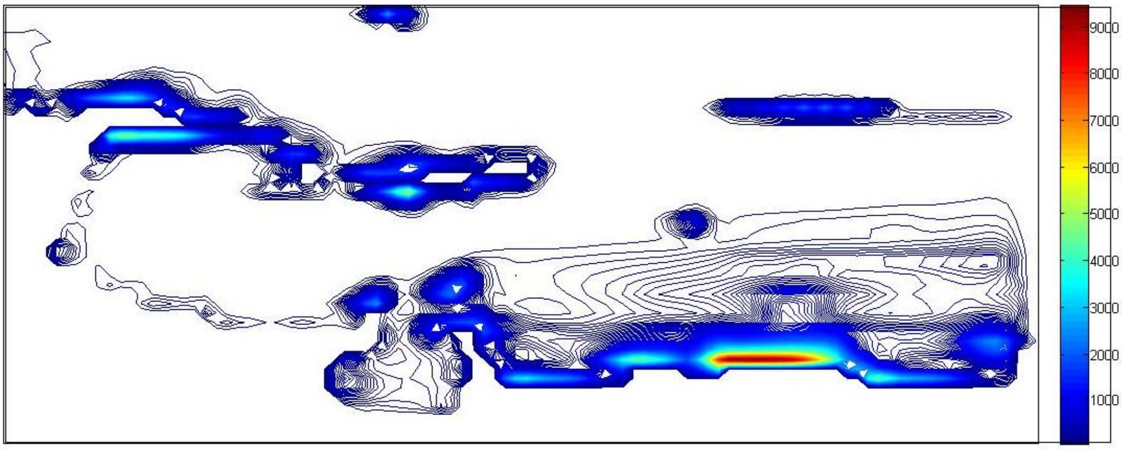

Figure 242. Sediment distribution for April

Current measurements and modelling for the first measurements in May are given in the Figures 243 -251.

Figure 243. Surface Current measurements for the first measurement in May2015,

Figure 244. Level 1 Current measurements for the first measurement in May2015 ,

Figure 245. Level 2 Current measurements for the first measurement in May 2015

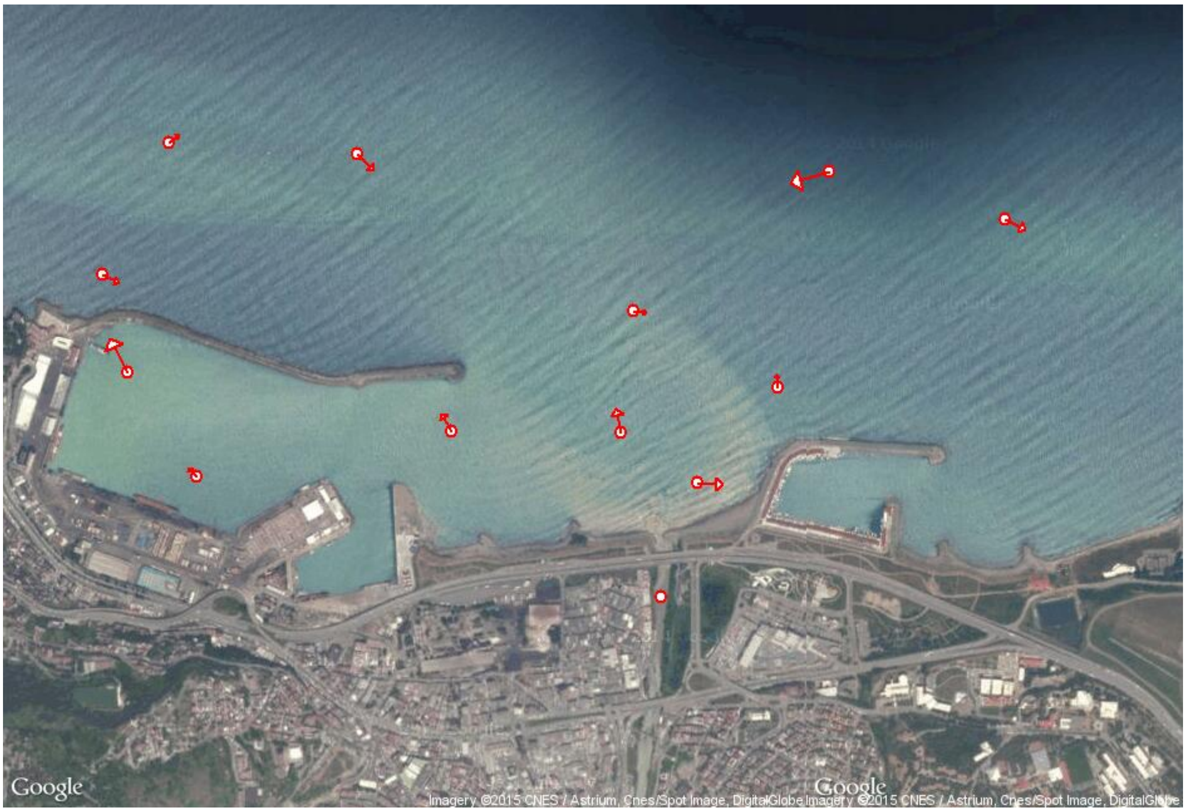

Figure 246. Bottom current measurements for the first measurement in May2015

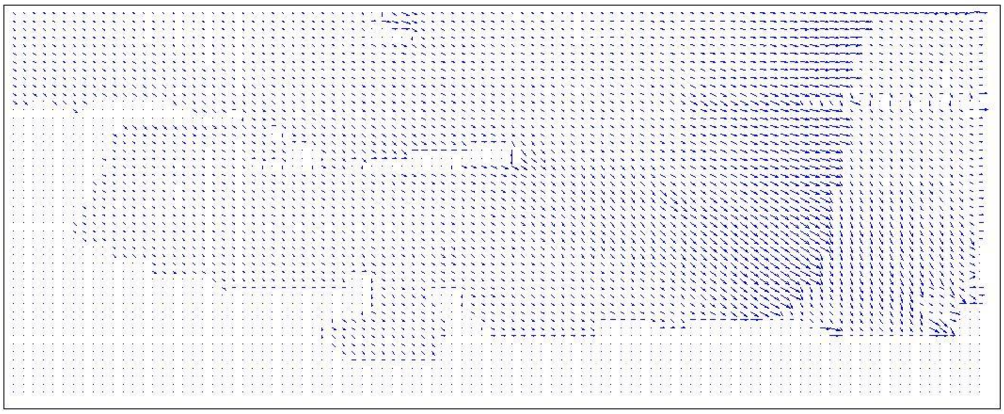

Figure 247. Modelling of the currents speed and direction for surface current

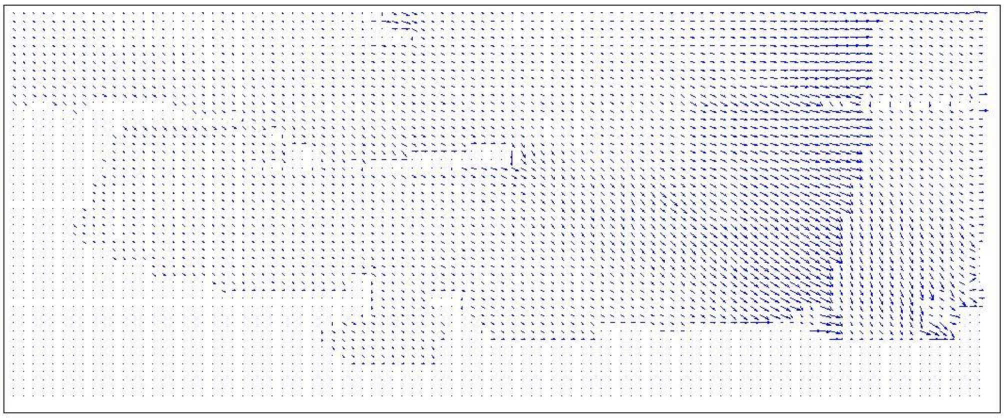

Figure 248.Modelling of the currents speed and direction for level 1

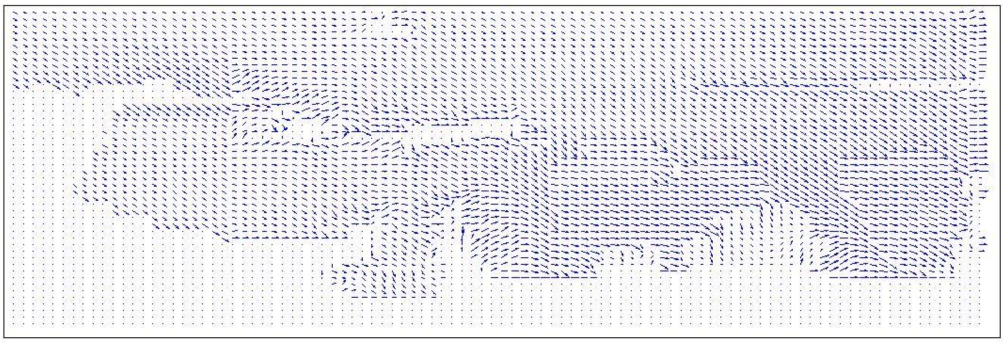

Figure 249. Modelling of the currents speed and direction for level 2

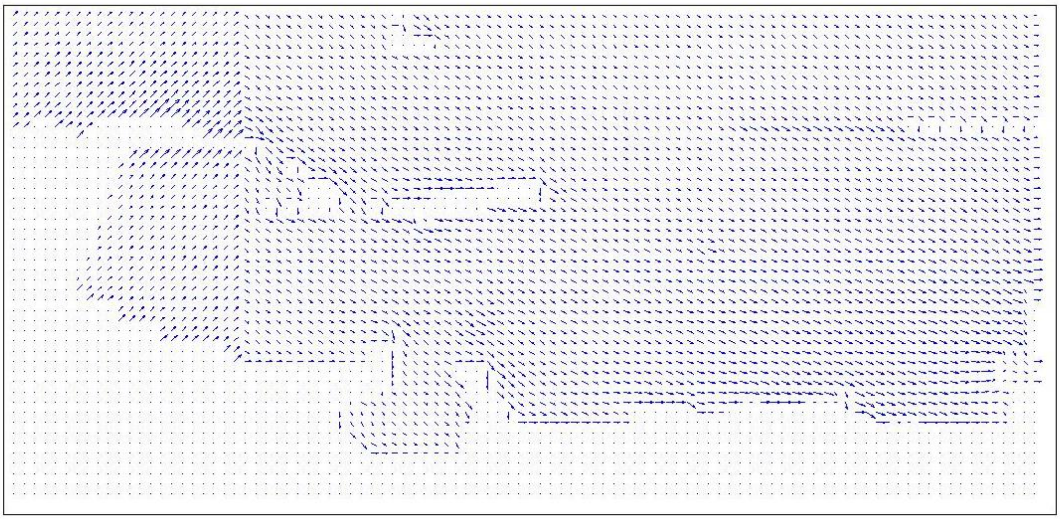

Figure 250. Modelling of the currents speed and direction for depth

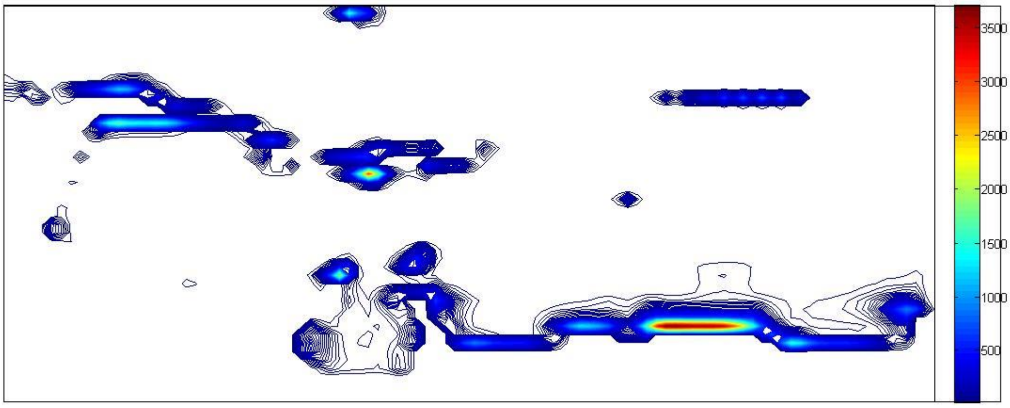

Figure 251. Sediment distribution for the first measurement in May 2015

Current measurements and modelling for the second measurements in May are given in the Figures 252 -260.

Figure 252. Surface Current measurements for the second measurements in May 2015,

Figure 253. Level 1 Current measurements for the second measurements in May2015 ,

Figure 254. Level 2 Current measurements for the second measurements in May 2015

Figure 255. Bottom current measurements for the second measurements in May 2015

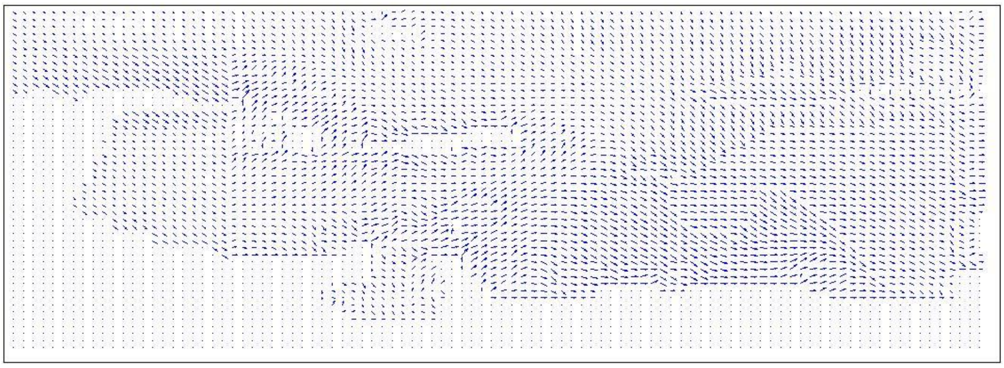

Figure 256. Modelling of the currents speed and direction for surface current

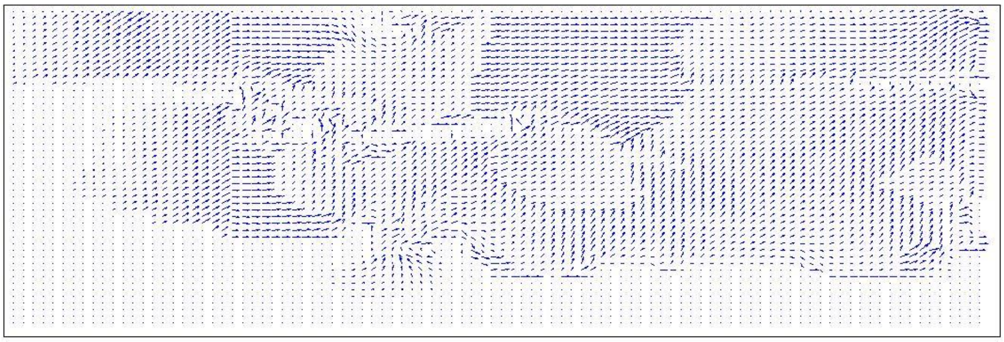

Figure 257.Modelling of the currents speed and direction for level 1

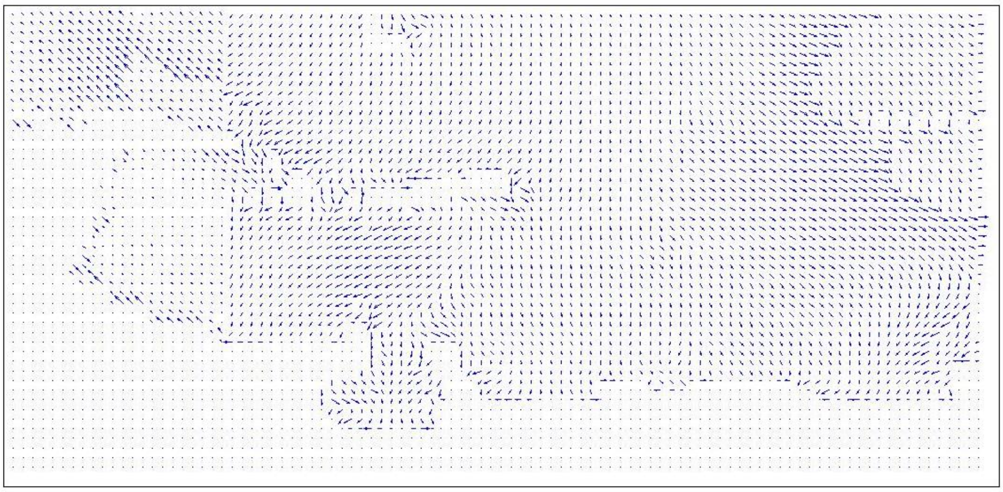

Figure 258. Modelling of the currents speed and direction for level 2

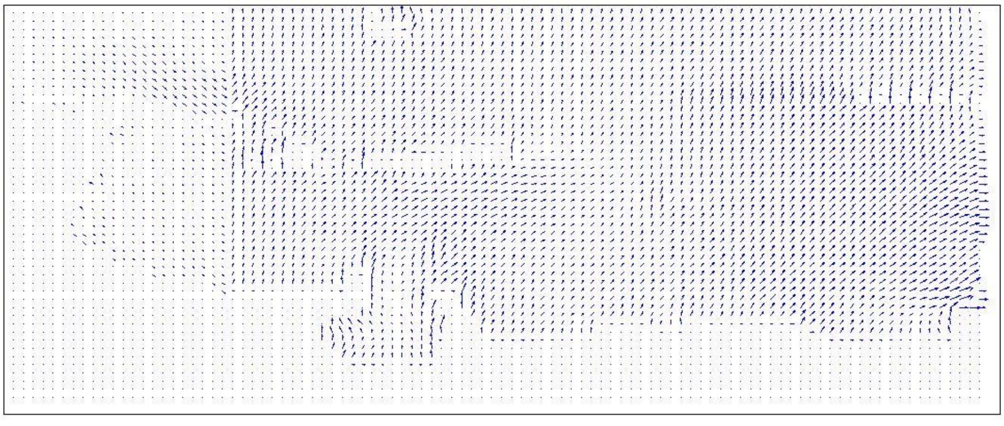

Figure 259. Modelling of the currents speed and direction for depth

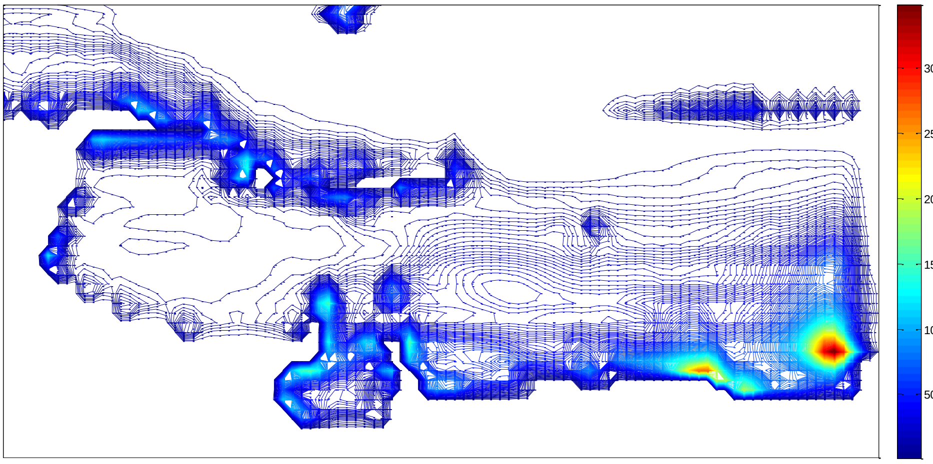

Figure 260. Sediment Distribution

Current measurements and modelling for the first measurements in June are given in the Figures 261 -269.

Figure 261. Surface Current measurements for June 2015,

Figure 262. Level 1 Current measurements for June 2015,

Figure 263. Level 2 Current measurements for June 2015

Figure 264. Bottom current measurements for June 2015

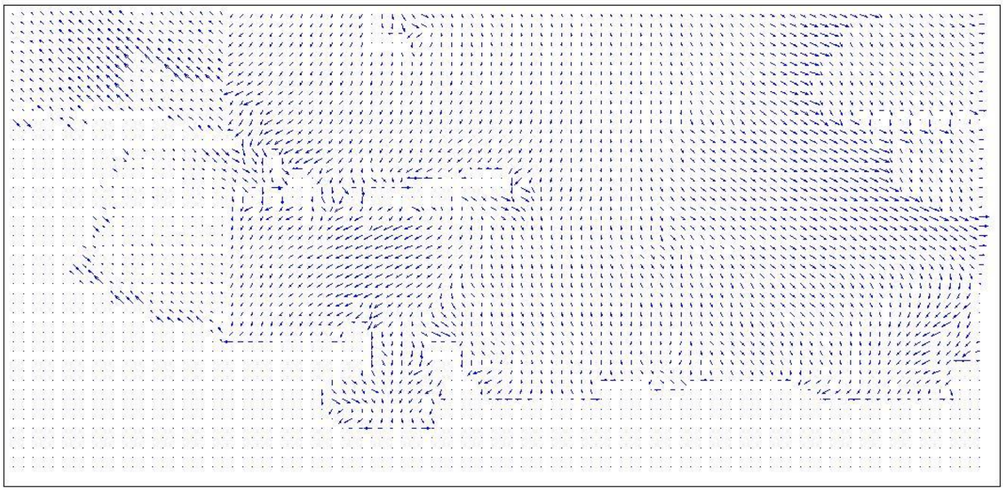

Figure 265. Modelling of the currents speed and direction for surface current

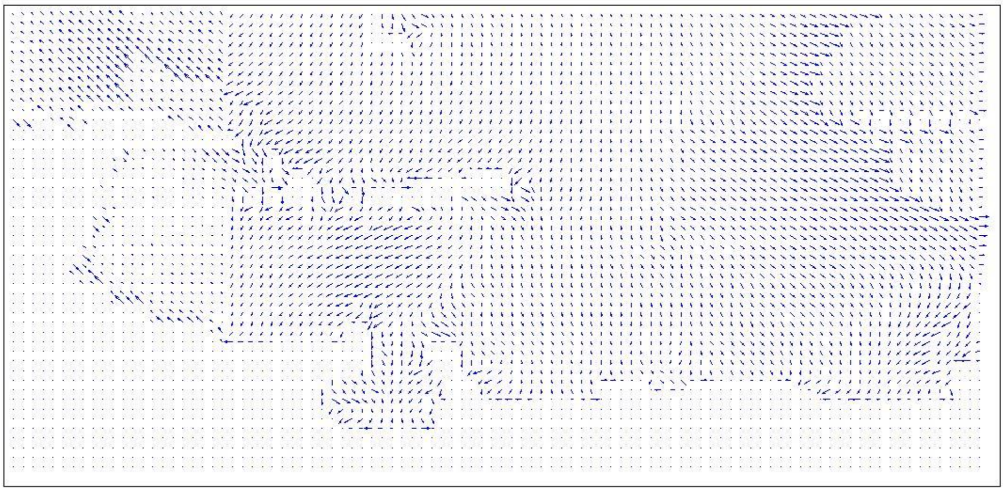

Figure 266.Modelling of the currents speed and direction for level 1

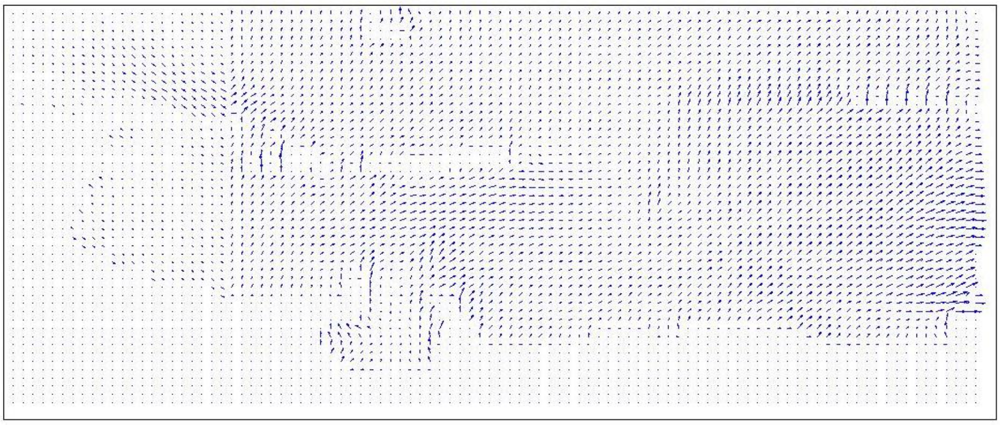

Figure 267.Modelling of the currents speed and direction for level 2

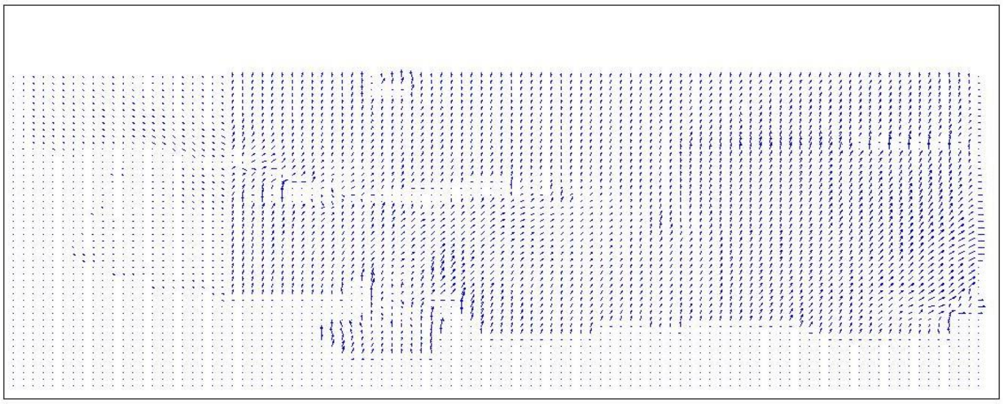

Figure 268.Modelling of the currents speed and direction for depth

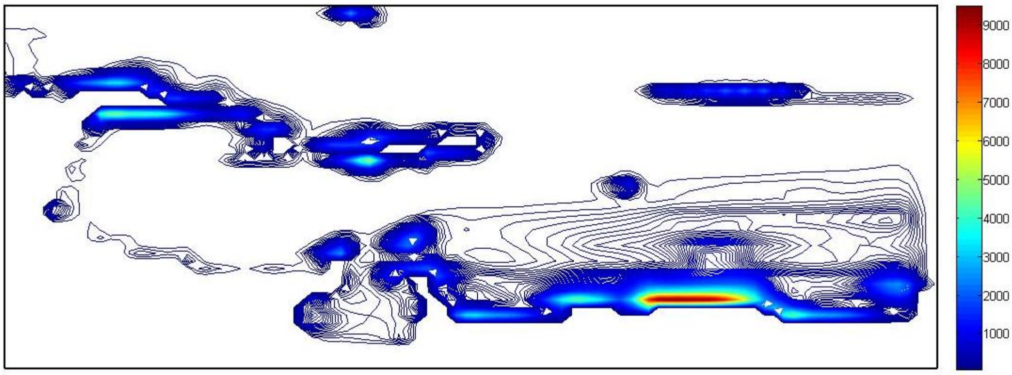

Figure 269. Sediment distribution for June 2015

9. Scenarios

As agreed on the contract, 5 different scenarios were developed.First of all, maximum sediment amount (maximum 489 mg/l measured in May 500 mg/l used in scenarieos) and measured maximum flux rate (41 m^3/s) for Değirmendere were taken into account in the modelling and result for this calculation is given in the following graph.

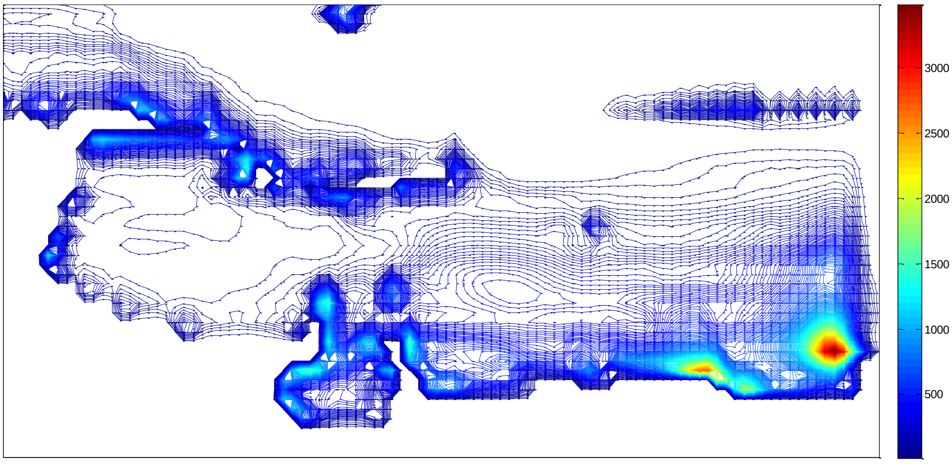

Figure 270. Modelling results maximum flux rate and sediment amount for Degirmendere river

As seen in the figure above although the sediment were found to be distributed scattered in front of the river and Trabzon Harbor mouth, mostly accumulated on the eastern side of the river. This result was compared with the pictures taken after a heavy rainy day in the region; pictures for this day are as follows.

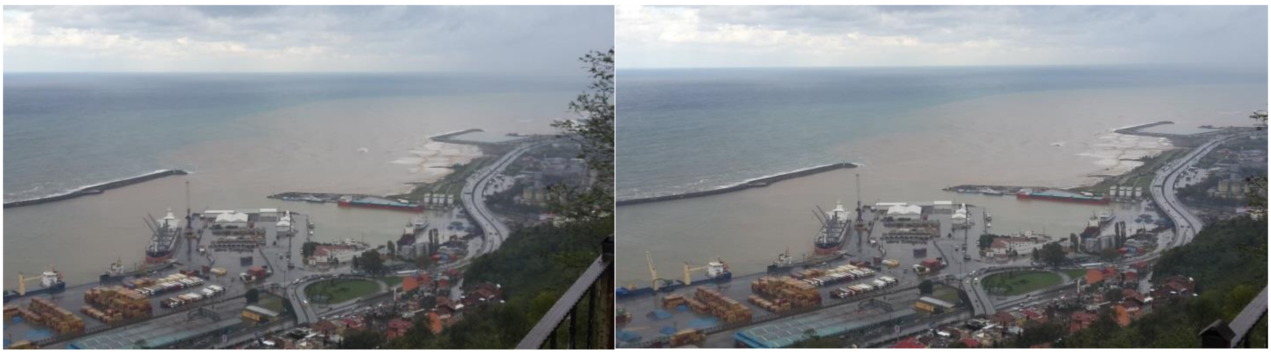

Picture 7. Trabzon port after a heavy rainy day

As clearly seen in the pictures, sediment distribution calculated by the model is in good agreement with the pictures. Especially, the first two pictures show the general sediment distribution, sediment reaches half way of the port inside (until the bow side of the first ship at the pier), modeling result at the figure 271 gives similar sediment distribution. Having received this result from the modeling studies conducted, sediment amount was increased 10%, 25%, 50% and %100 according to the stated conditions, results for these modellings are also given at the following graphs.

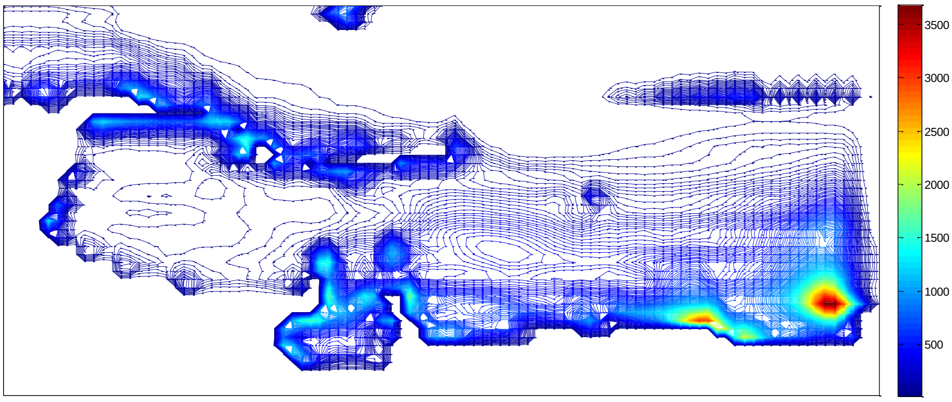

Figure 271. 10% increase in sediment amount

As seen from figure, sediment distribution remains the same but, amount increases resulted a rapid fillings of harbor when 10 % increase in sediment amount implemented in the model in the area.

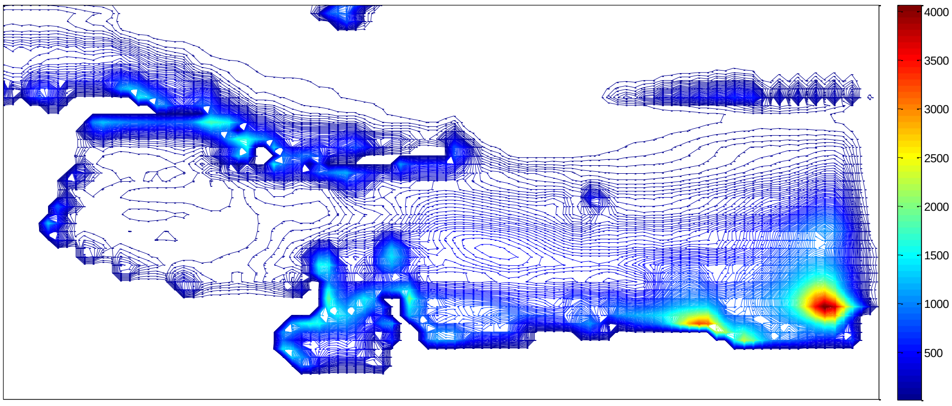

Figure 272. 25% increase in sediment amount

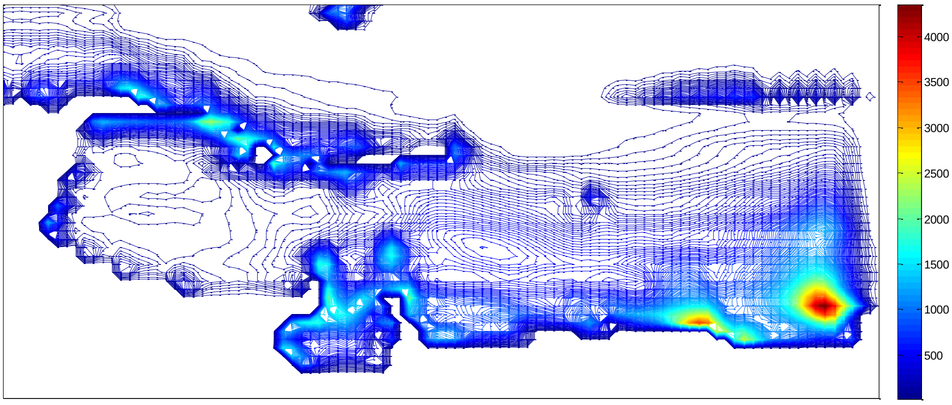

Figure 273. 50% increase in sediment amount

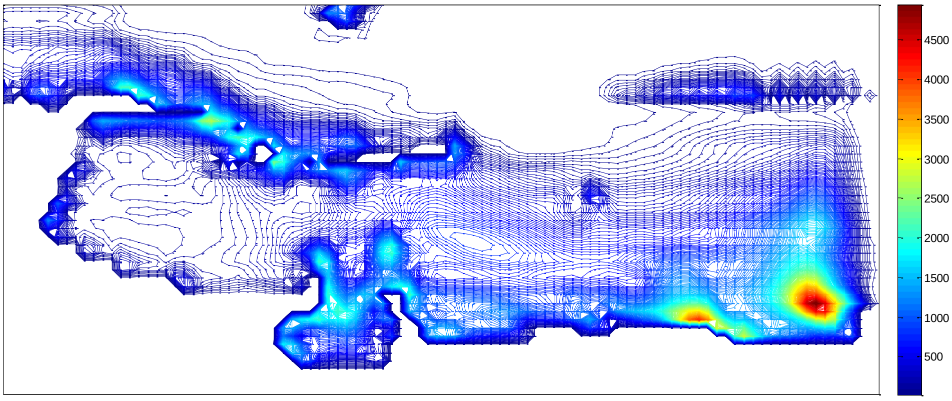

Figure 274. 100% increase in sediment amount

As hydrodynamic conditions for all runs (10, 25, 50 and 100 % increase in the sediment amount) are kept the same, only sediment amount were seen changed, general distribution remains the same, but the amount of sediment accumulated at the region increased as the increment in the sediment amount goes up.

In order to model different sediment distribution, river flux rate and sediment amount kept at maximum and wind directions were changed to see wind effect. Wind directions are shown in Table 12.Results of these runs are also in Figures275-281.

Table 12. Wind directions

Wind Direction	Abbriviation	
West	W	→
Southeast	SE	↖
Southwest	SW	↗
Northwest	NW	↘
Northeast	NE	↙
East	E	←
North	N	↓

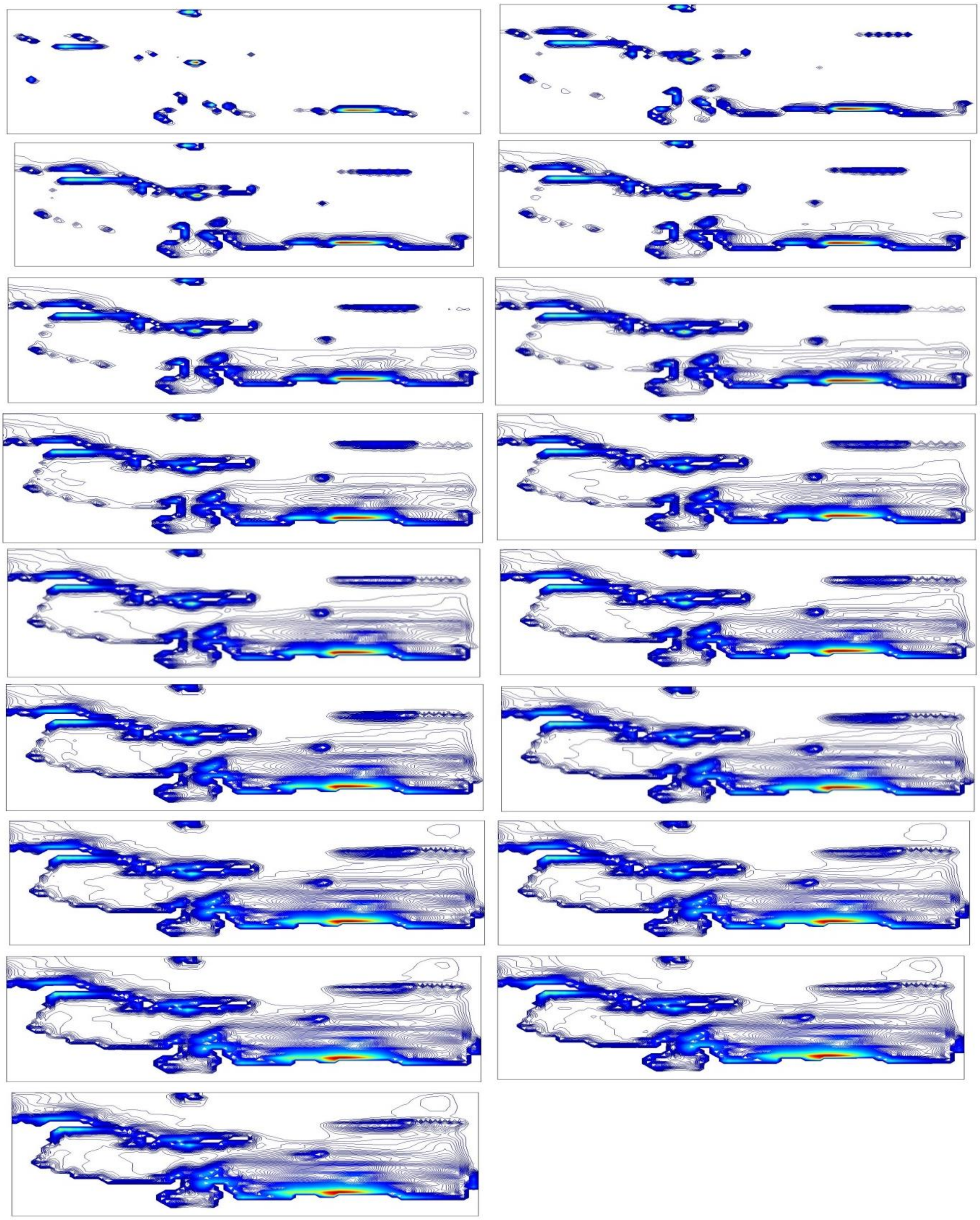

Figure 275. Sediment distribution changes with time under W (West) wind direction

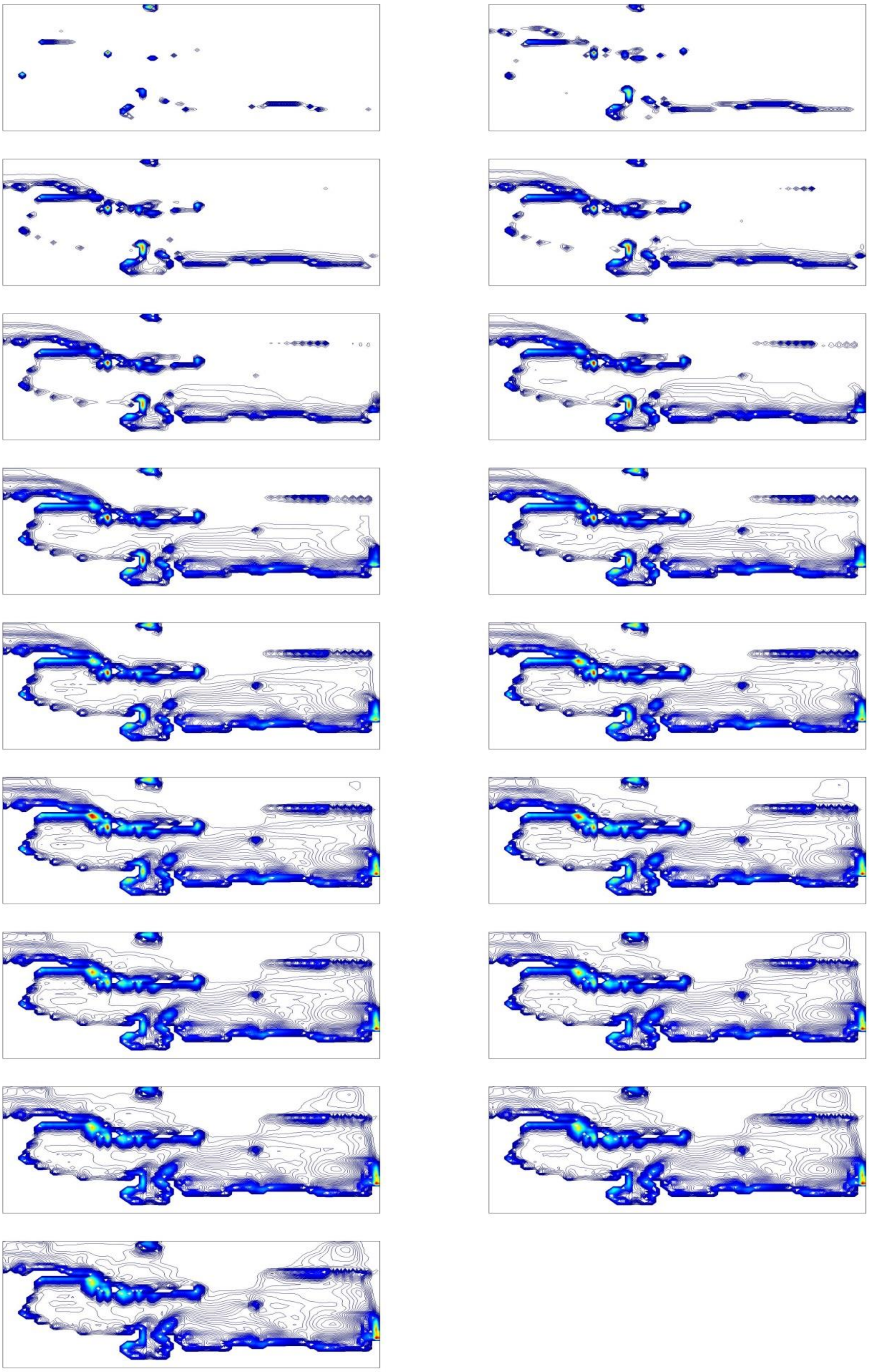

Figure 276. Sediment distribution changes with time under SE (Southeast) wind direction

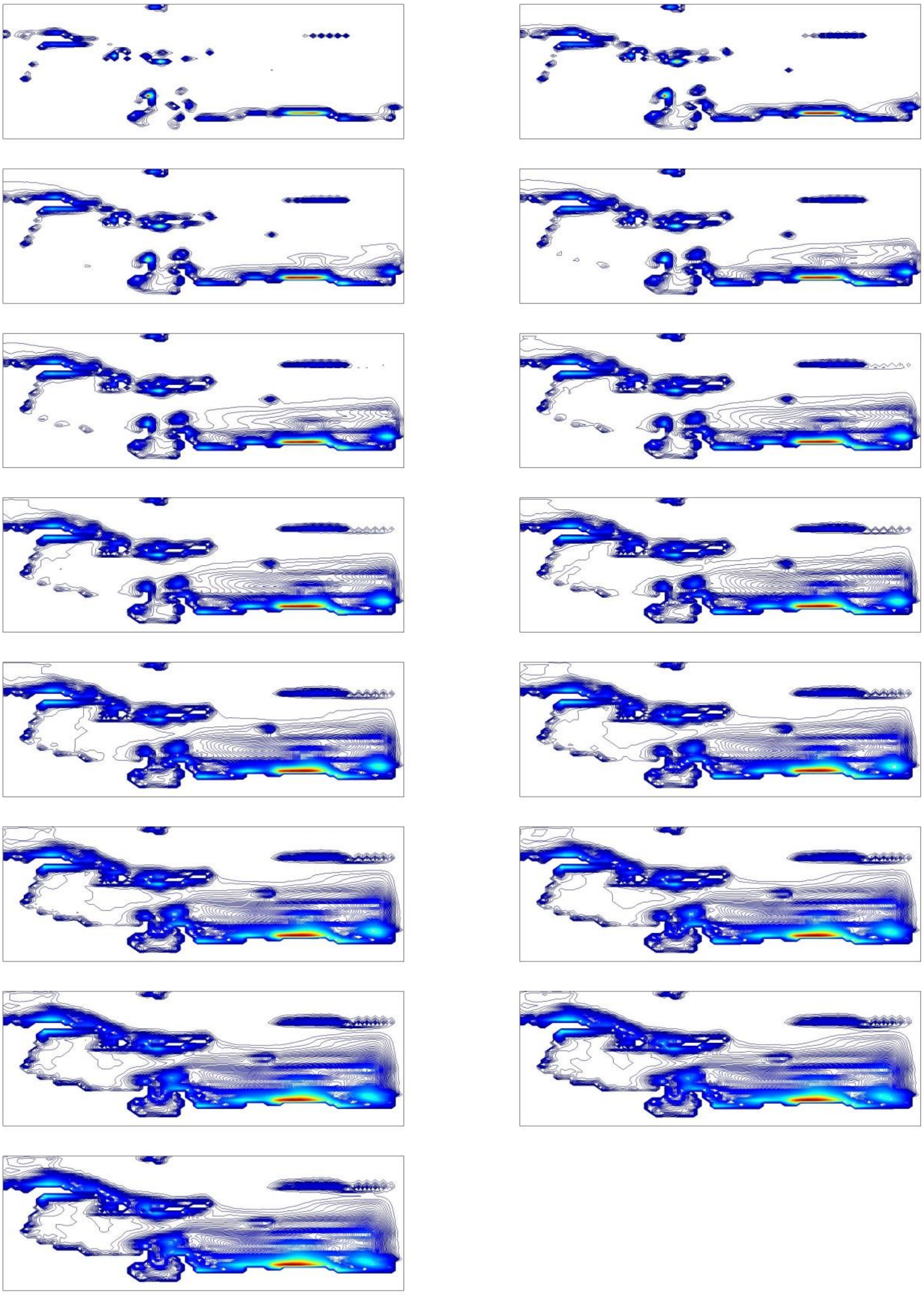

Figure 277.Sediment distribution changes with time under SW (Southwest) wind direction

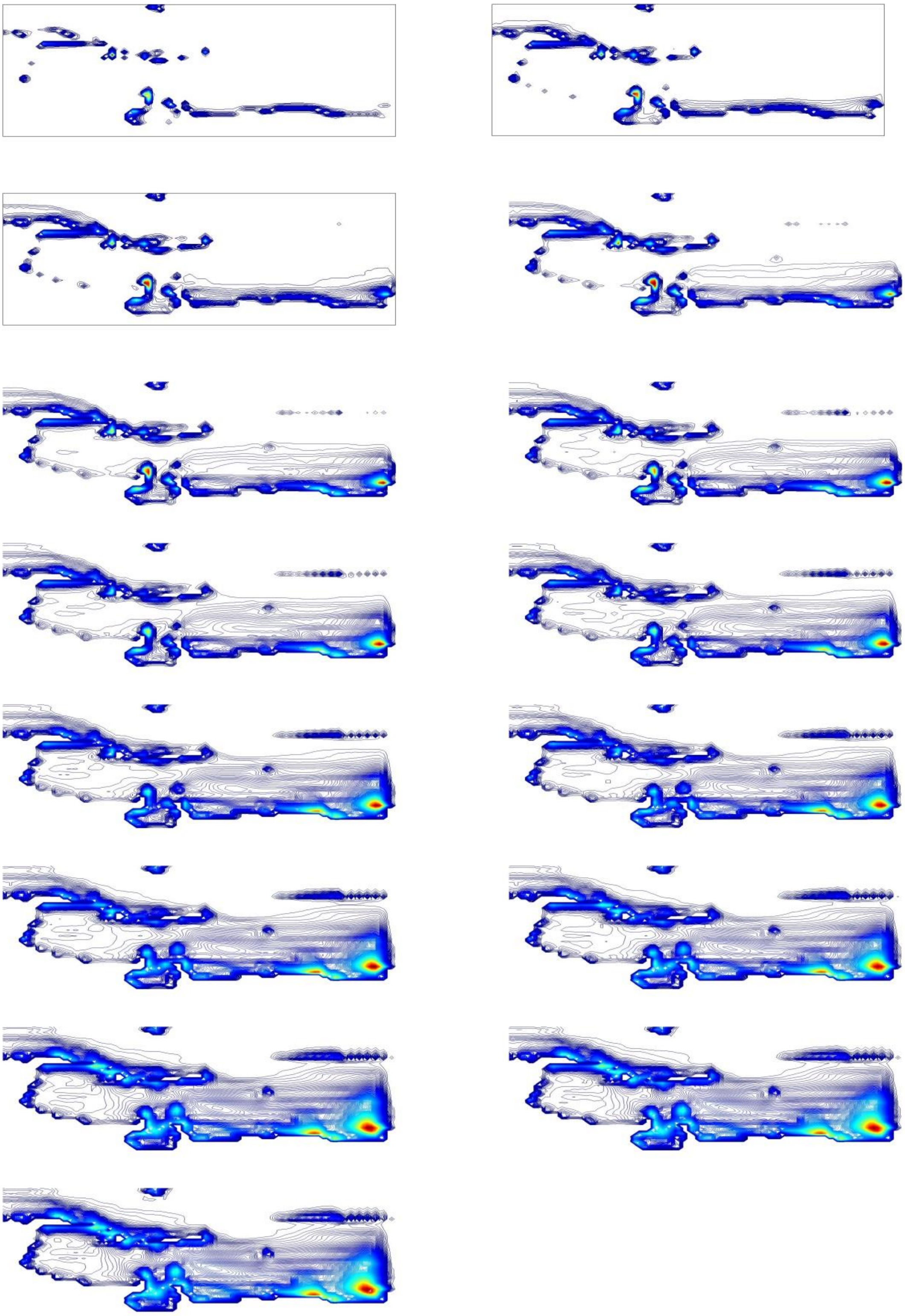

Figure 278.Sediment distribution changes with time under NW (North west) wind direction

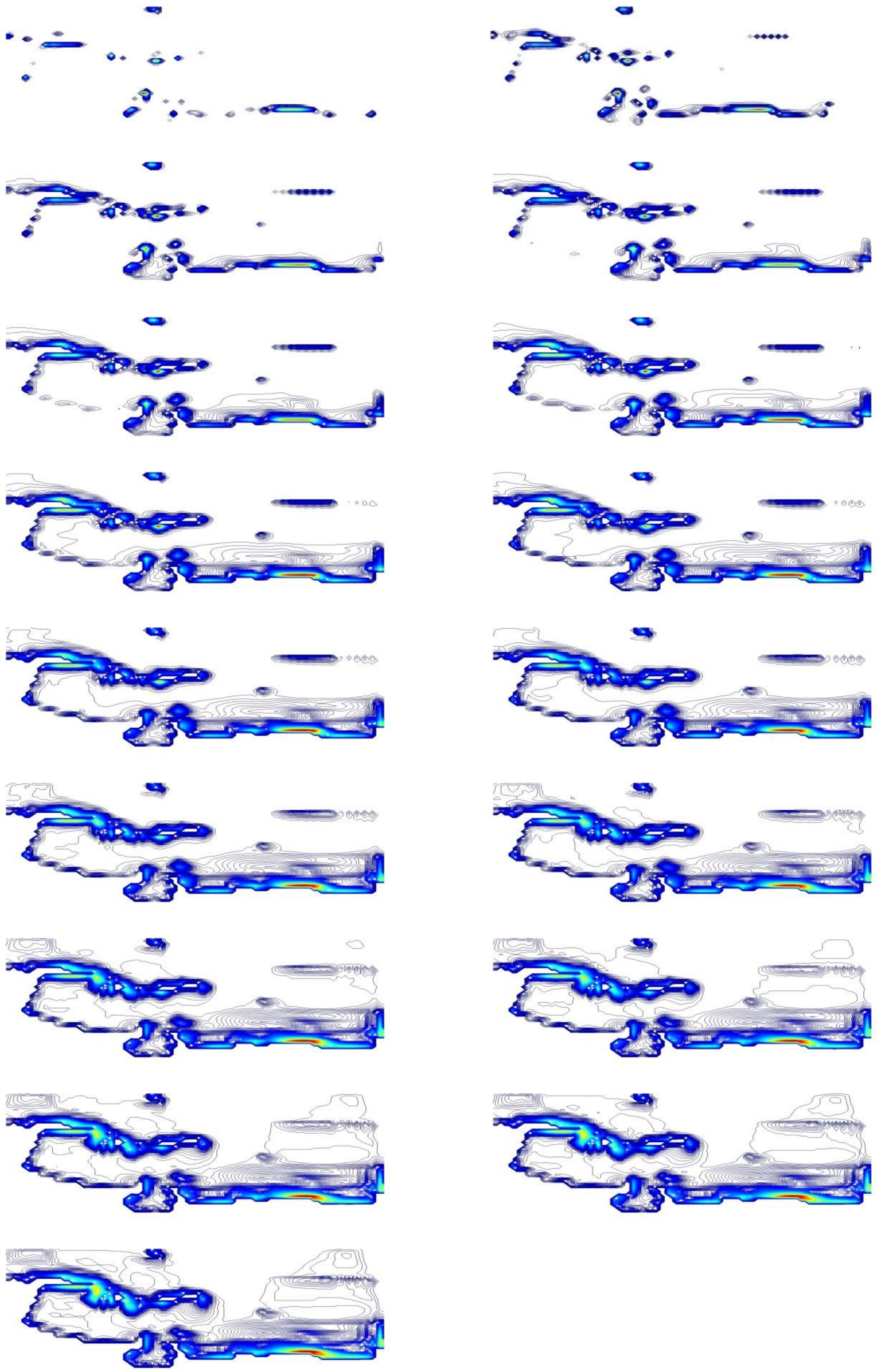

Figure 279.Sediment distribution changes with time under NE (Northeast) wind direction

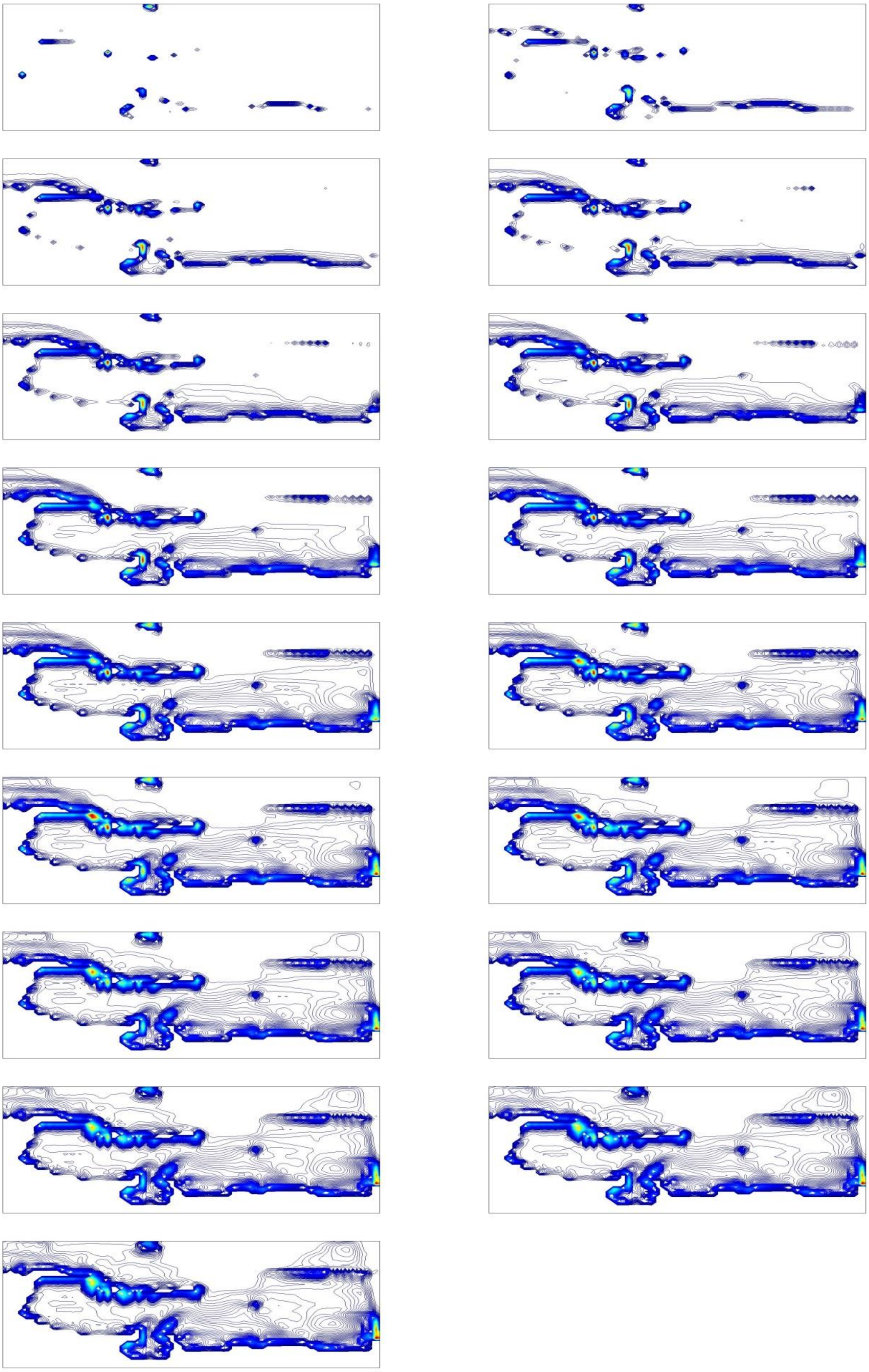

Figure 280.Sediment distribution changes with time under E (East) wind direction

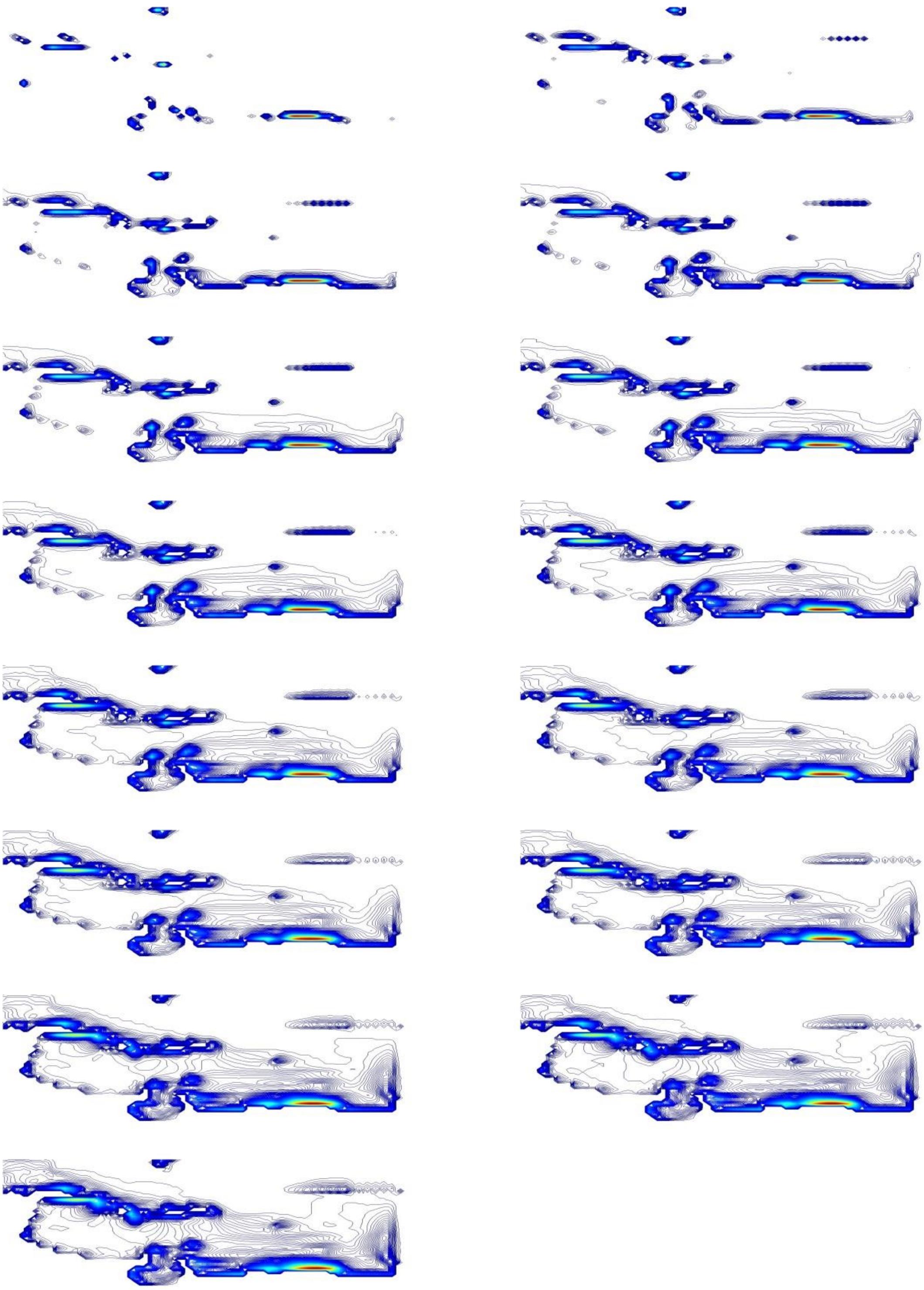

Figure 281.Sediment distribution changes with time under N (North) wind direction

10. Conclusions

The aims of this project was to investigate the effects of sediment brought by Değirmendere on the port of Trabzonand its surroundings. In order to observe this effect, All oceanographic parameters given in the contract were measured with supplied quipments (the equipment supplied by the Contracting Authority) for stated time duration.

Firstly, water and sediment analysis were done. According to the results obtained, the SEF of metals in the sediments around Trabzon harbor was: Pb > Cu > As > Zn > Ni > Cr. The highest SEF, PLI and I_{GEO} values were determined for stations of D6 and D7 (Table 13). The SEF contamination categories were described by Ozseker et al. 2013 in more comprehensive way. From this classification, SEF values of **Cr and Ni** were greater than the threshold value of 1, none exceed 3, suggesting that level of pollution enrichment was minor. SEF values of **Zn and As** were greater than the threshold value of 3, none exceed 5, suggesting that level of pollution enrichment was moderate. SEF values of **Cu and Pb** were greater than the threshold value of 5, none exceed 10, suggesting that level of pollution enrichment was moderately severe. Trabzon harbor and coast are contaminated by **Cu, Pb, Zn and As** as showed by enrichment factor greater than 4 (Table 13). Enrichment factor of Cr and Ni were classified minimal enrichment at all stations, suggesting that Cr and Ni contamination do not seem to have a major impact regarding pollution in the area nowdays.

Table 13. Values of SEF, I_{GEO} and PLI of sediment around Trabzon harbor

Stations	Value of SEF						Value of I_{GEO}						PLI
	Cr	Cu	Zn	Pb	Ni	As	Cr	Cu	Zn	Pb	Ni	As	
D1	0.89	4.33	4.23	9.04	1.23	3.89	-2.60	-0.31	-0.35	0.75	-2.02	-0.47	0.84
D2	0.99	4.55	2.32	8.21	1.13	3.10	-2.32	-0.11	-1.08	0.74	-2.12	-0.66	0.79
D3	0.83	4.92	4.05	8.83	1.16	3.95	-2.47	-0.04	-0.19	0.94	-1.99	-0.22	0.94
D4	1.09	4.60	4.16	9.45	1.33	4.50	-1.99	0.08	-0.06	1.12	-1.71	0.04	1.12
D5	1.13	4.97	4.55	10.56	1.52	4.45	-2.03	0.11	-0.02	1.20	-1.59	-0.05	1.14
D6	2.27	14.82	7.20	15.62	3.92	11.33	-0.84	1.87	0.83	1.95	-0.05	1.48	2.75
D7	2.57	14.41	7.23	16.24	3.45	11.20	-0.69	1.80	0.80	1.97	-0.27	1.43	0.97
D8	0.92	4.84	3.33	8.13	1.25	3.37	-2.24	0.16	-0.39	0.90	-1.80	-0.37	0.97
D9	1.10	3.68	3.70	8.23	1.27	3.12	-2.05	-0.30	-0.30	0.86	-1.84	-0.54	0.92

Metal concentrations in sediments and pore water of Trabzon harbor were also compared with harbor sediments reported from different areas of the world. Concentration of Cu was higher than Tolo, Guam and Sardinia harbors but lower than the Naples and Rijeka harbors. The concentrations of Zn were higher than Tolo and Sardinia harbor but lower than Naples harbors (Schintu and Degetto 1999; Owen and Sandhu 2000; Adoma et al. 2005; Cukrov et al. 2011). Results of this study compared with Rize harbor which is Southeastern Black Sea region, metal concentrations of this study were higher than Rize harbor sediments (Gedik and Boran 2013). In this study, the highest metal concentrations were determined in D6 and D7 stations which were in the inner harbor and water circulation was not well enough. Metal concentrations in sampling area decrease in the order D6 > D7 > D5 > D4 > D8 > D3 > D9 > D2 > D1, respectively, for sediment and sediment pore water. Except for the element of Ni, it was determined that there was a meaningful relationship between concentrations of sediment and pore water. Besides, it was found that temperature, salinity and dissolved oxygen, which are the environmental parameters, had an effect on metal concentrations. Based upon the results from this study, according to SQG, Cu, Pb, Zn and As can be considered as contributor to toxicity around the Trabzon harbor.

Then, a mathematical model was developed to investigate the hydrodynamic flow around Trabzon port and surroundings.According to the the contract, 5 different scenarios and their effects were investigated by using mathematical hydrodynamic model.
As seen in the Figures 272 to 275, after a heavy rain and NW wind,sediment accumulations were seen on the entrance of harbor, on the breakwater and inside of small harbor. As graphics shows that there is no change in sediment distribution with the amount of sediment. Then, wind direction were changedaccordingly (Table 9). Results of these runs illustrates that in all wind conditions, sediment reaches the middle of the port and fills the small harbor.

The following assumptions are made to calculate when unfilling operation could became necessary.

- Sediment amount transferred by the Değirmendere is constant and 489 mg/l.
- Total rainy day is 140 days in a year, and all rains assumed to be heavy rain.
- Accumulation rate is constant (Sediment size and settlement speed are unchanged)
- The maximum draft of a ship comes to Trabzon port assumed to 9 m. and minimum 1 m clearance.

- Unfilling operation is necessary when depth at any point decreases 10m.

Under the assumptions made, from the results of simulations approximately 2.4 cm of sediment accumulates at the entrance of the Trabzon portin a year. As a result of this calculation and depth contours of Trabzon port (Figure 282) , it can be concluded that unfilling operation for the main entrance has to be carried out in every 25 years taking into account the maximum draft of the possible incoming ships. Additionally, simulations results showed that small harbor will be filled in a shorter time period approximately in 15 years.

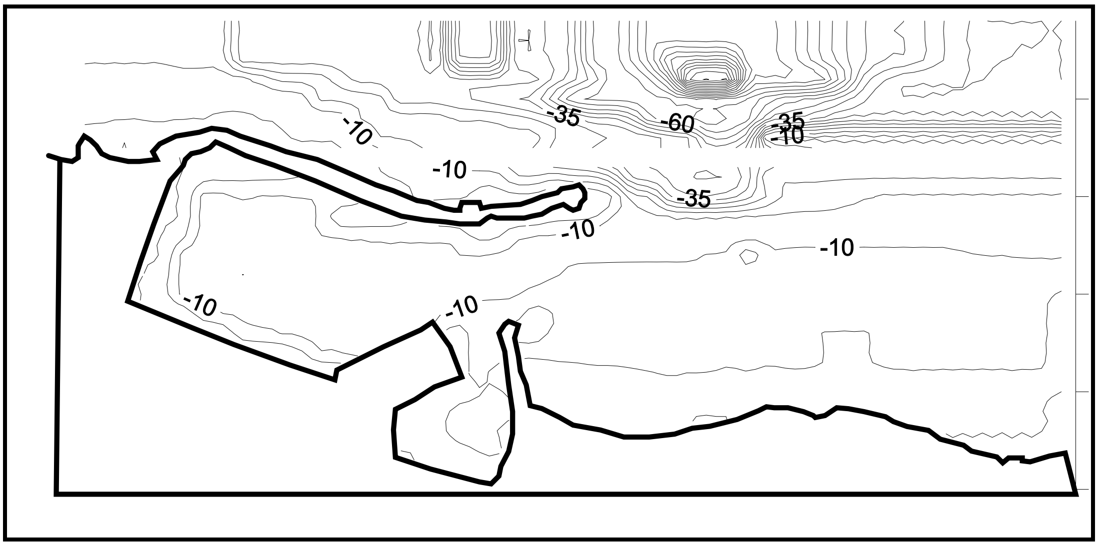

Figure 282. Depth contours of Trabzon port

A 10% increase resulted 2.6 cm decrement in a year at the depth of the mouth of the Harbor concerned, which makes unfillings operations necessary in the area approximately in 22 years. However, 25 % increment in sediment amount makes 2.84 cm decrement at the depth resulting unfillments operation necessary in 21 years. When a 50% increase is the case, decreased in depth calculated as 3.22 cm per year,

The minimum required depth for the incoming ships will be 18.5 years approximately that means for the ships with maximum allowed draft will not be possible to enter into the harbor .Finally, when the sediment is increased 100%, calculations showed that 4.2 cm sediment accumulates at the enterance of the port, this would make unfilling operation necessary in every 13.9 years.

When the fishing port taken into the consideration, sediment distribution can only reach the mouth of the port and enter into the area depending on the wind conditions, eg., E and NE directions. For the stated assumptions on which all the scenarios developed it can be concluded that fishing port is not under severe risk of sediment fillings.

11. References :

Akpınar A, Evaluation of wind energy potentiality at coastal locations along the north eastern coasts of Turkey, Energy 50 (2013)

Blumberg, A. F.,and G. L. Mellor, A coastal ocean numerical model, in MathematicalModelling of Estuarine Physics, Proc. Int. Symp., Hamburg, Aug. 1978, edited by J.

Sunderman and K.-P.Holtz, pp.203-214, Springer-Verlag, Berlin, 1980.

Blumberg, A.F., and G.L. Mellor, Diagnostic and prognostic numerical circulation studies of the South Atlantic Bight, J. Geophys.Res., 88, 4579-4592, 1983.

Blumberg, A.F., and G.L. Mellor, A description of a three-dimensional coastal ocean circulation model, in Three-Dimensional Coastal Ocean Models, Vol. 4, edited by N.Heaps, pp. 208, American Geophysical Union, Washington, D.C., 1987.

Bryden, H. L., New polynomials for thermal expansion, adiabatic temperature gradient, and potential temperature of sea water, Deep-Sea Res., 20, 401-408, 1973.

Csuros M, Csuros C, (2002) Environmental sampling and analysis for metals. Lewis, Boca Raton

DSI, The General Directorate of State Hydraulic Worksof Turkey, www.rasatlar.dsi.gov.tr, Statistics.

DMI, State Meteorological Organization of Turkey, Statistics

Ezer, T., H. Arango and A. F. Shchepetkin, Developments in terrain-following ocean models: intercomparison of numerical aspects, *Ocean Modelling,* 4, 249-267.

Fritioff A, Kautsky L, Greger M, (2005) Influence of temperature and salinity on heavy metal uptake by submersed plants. Environmental pollution, 133: 265-274

Galperin, B., L. H. Kantha, S. Hassid, and A. Rosati, A quasi-equilibrium turbulent energy model for geophysical flows, J. Atmos. Sci., 45, 55-62, 1988.

Gill, A.E., Atmosphere-Ocean Dynamics, 662 pp., Academic Press, New York, 1982.

Klein, P., A simulation of the effects of air-sea transfer variability on the structure of the marine upper layers, *J. Phys. Oceanogr*., 10, 1824-1841, 1980.

Klobes P, Meyer K, Munro R.G, (2006) Porosity and specific surface area measurements for solid materials. NIST Recommended Practice Guide

Knudsen, M., Hydrographical Tables. G.E.C. Gad, Copenhagen, pp., Williams and Norgate, London, 19010.

Köse, E**.,** B. Sönmez, Ş. Özçoban, A Preliminary Investigation On The Pollutant Distribution In The South Eastern Black Sea Cast, International Symposiom On ECOLOGY 97, Varna, 1997

Köse E**.**, Özer, F., Y. Malkoç, Box Model To Investigate Effects Of Bottom Topography On Coastal Currents, Proccedings Of The First International Conference On Fisheries And Ecology, Trabzon,1998.

Köse, E**.** C. Erüz, Ve , F. Özer, N. Sivri Seawater And Riverine Suspended Matter Distribution In Coastal Water Of Trabzon, *T. Journal Of Marine Science*. 2000.

Long ER, Field LJ, MacDonald DD (1998) Predicting toxicity in marine sediments with numerical sediment quality guidelines. Environ Toxicol Chem 17:714–727

Madala, R. V., and S. A. Piacsek, A semi-implicit numerical model for baroclinic oceans, *J. Comput.Phys,* 23, 167-178, 1977.

Martin, P.J., Simulation of the mixed layer at OWS November and Papa with several models, *J. Geophys.Res.,* 90, 903-916, 1985.

Mellor, G.L., and T. Yamada, Development of a turbulence closure model for geophysical fluid problems, *Rev. Geophys. Space Phys.,* 20, 851-875, 1982.

Mellor, G. L., Retrospect on oceanic boundary layer modeling an second moment closure, Hawaiian Winter Workshop on *"Parameterization of Small-Scale Processes*", January 1989, University of Hawaii, Honolulu, Hawaii, 1989.

Mellor, G.L., Analytic prediction of the properties of stratified planetary surface layers.,*J. Atmos. Sci,* 30, 1061-1069, 1973.

Mellor, G.L., and A.F. Blumberg, Modeling vertical and horizontal diffusivities with the sigma coordinate system, *Mon. Wea.Rev,* 113, 1380-1383, 1985.

Mellor, G.L., and T. Yamada, A hierarchy of turbulence closure models for planetary boundary layers, *J. Atmos. Sci.,* 31, 1791-1806, 1974.

Mellor, G. L., L. H. Kantha, and H. J. Herring, On Gulf Stream frontal eddies. A numerical experiment, *Ocean Modelling,* 68, 7-11, 1986.

Mellor, G.L., An equation of state for numerical models of oceans and estuaries. J_ *Atmos. Oceanic Tech*. 8, 609-611, 1991.

Mellor, G. L., T. Ezer and L. Y. Oey, The pressure gradient conundrum of sigma coordinate ocean models, *J. Atmos. Oceanic. Technol.,*, 11, 1126-1134, 1994.

Mellor, G. L. and T. Ezer, Sea level variations induced by heating and cooling: An evaluation of the Boussinesq approximation in ocean model, *J. Geophys. Res.,*100(C10), 20,565-20,577, 1995.

Mellor, G. L., and X. H. Wang, Pressure compensation and the bottom boundary layer, *J. Phys. Oceanogr*. in press, 1996.

Mellor, G. L., L.-Y. Oey and T. Ezer, Sigma coordinate gradient errors and the seamount problem.*J. Atmos. Oceanic. Technol.,* 12, 1122-1131, 1998.

Mellor, G. L., One-dimensional, ocean surface modeling, a problem and a solution. *J. Phys. Oceanogr.,* 31, 790-809, 2001.

Oey, L.-Y., G.L. Mellor, and R.I. Hires, A three-dimensional simulation of the Hudson- Raritan estuary. Part I: Description of the model and model simulations, *J. Phys. Oceanogr.,* 15, 1676-1692, 1985a.

Oey, L.-Y., G.L. Mellor, and R.I. Hires, A three-dimensional simulation of the Hudson- Raritan estuary. Part II: Comparison with observation, *J. Phys. Oceanogr.,* 15, 16931709, 1985b.

Oey, L.-Y., G.L. Mellor, and R.I. Hires, A three-dimensional simulation of the Hudson- Raritan estuary. Part III: Salt flux analyses, *J. Phys. Oceanogr.,* 15, 1711-1720, 1985c.

Ozseker K, Eruz C, Cılız S, (2013) Determination of Copper Pollution and Associated Ecological Risk in Coastal Sediments of Southeastern Black Sea Region, Turkey, Bulletin of Environmental Contamination and Toxicology, 91:661-666

Ozseker K, Eruz C, Cılız S, Mani F, (2014) Assessment of Heavy Metal Contribution and Associated Ecological Risk in the Coastal Zone Sediments of Black Sea; Case study of Trabzon,CLEAN – Soil, Air, Water, DOI: 10.1002/clen.201300785

Pekey H, Karakas D, Ayberk S, Tolun L, Bakoglu M (2004) Ecological risk assessment using trace elements from surfacesediments of Izmit Bay (Northeastern Marmara Sea) Turkey. Mar Pollut Bull 48:946–953

Paulson, C. A., and J. Simpson, Irradiance measurements in the upper ocean.*J. Phys. Oceanogr.,* 7, 952-956, 1977.

Phillips, N. A., A coordinate system having some special advantages for numerical forecasting, *J. Meteorol.,* 14, 184-185, 1957.

Richtmyer, R. D., and K. W. Morton, *Difference Methods for Initial-Value Problems,* 2nd Ed., 405pp., Interscience, New York, 1967.

Simons, T. J., Verification of numerical models of Lake Ontario. Part I, circulation in spring and early summer, *J. Phys. Oceanogr.,* 4, 507-523, 1974.

Tang CWY, Ip CCM, Zhang G, Shin PKS, Qian PY, Li XD (2008) The spatial and temporal distribution of heavy metals in sediments of Victoria Harbour, Hong Kong. Mar Pollut Bull 57: 816–825

Taylor SR, (1964) Abundances of chemical elements in the continental crust: A new table. Geochimica et Cosmochimica Acta, 28: 1273-1285

Turekian KK, Wedephol KH, (1961) Distribution of the Elements in Some Major Units of the Earth's Crust. Geol. Soc. Am. Bull, 72: 175–192

US EPA, (1999) U.S. Environmental Protection Agency, Screening level ecological risk assessment protocol for hazardous waste combustion facilities, vol. 3, Appendix E: Toxicity reference values. EPA 530-D99-001C

US EPA, (2006) Ambient water quality criteria. Office of water. Washington, D.C.

Zavatarelli, M., and G. L. Mellor, A numerical study of the Mediterranean Sea Circulation, *J. Phys. Oceanogr.,* 25, 1384-1414, 1995.